Validation of Lymphoma-Associated Antigens Identified Using Autoantibody Profiling and Protein Arrays

DPhil Thesis

November 2010

Kah-Keng Wong, Linacre College

Nuffield Department of Clinical Laboratory Sciences

University of Oxford

Preface

Declaration of originality

This dissertation is the result of research carried out between October 2007 and June 2010 (2 years and 9 months) at the Nuffield Department of Clinical Laboratory Sciences in Oxford. The following parts of my thesis were not my own work:

1) Protein array screening in collaboration with Centre for Human Proteomics in Dublin (Dr Derek Murphy) (Table 3.1 in Chapter 3)

2) cDNAs of B- and T-cell populations purified from peripheral blood (Fig 4.3 in Chapter 4), and cDNAs of DLBCL cases and their subtyping data (Fig 5.6 in Chapter 5) were provided by Dr Charles Lawrie

3) *FOXP1* mRNA expression in a panel of cell lines (Fig 5.15 in Chapter 5) and depletion of FOXP1 expression were carried out by Dr Philip Brown (Fig 5.16 in Chapter 5). Subsequent microarray experiments of the FOXP1-depleted samples were conducted by Oxford Gene Technology (Oxford) (Fig 5.17A in Chapter 5).

Kah-Keng Wong
DPhil in Clinical Laboratory Sciences candidate
Linacre College
University of Oxford
November 2010

Abstract

Diffuse large B-cell lymphoma (DLBCL) is an aggressive lymphoma subtype with heterogeneous clinical outcome and a significant number of patients still die of their disease. Characterising lymphoma patients' autoantibody repertoires represents one approach to improve the understanding of their disease biology. Our hypothesis was that characterisation of antigens eliciting humoural immune responses in lymphoma patients may provide insights into mechanisms of lymphomagenesis and identify novel diagnostic/therapeutic targets.

HIP1R was validated as a novel B-NHL autoantigen by immunoblotting with patients' sera. No response was identified to the related HIP1 protein. Consistent with this finding, more widespread expression of HIP1R, compared to HIP1, was observed in lymphoma cell lines. Expression studies, at both transcript (qRT-PCR and analysis of microarray datasets) and protein levels (blotting and immunolabelling), identified abundant HIP1R in normal B cells and low level expression in a poor prognosis activated B-cell (ABC)-like DLBCL subtype. Upregulation of HIP1R expression was observed in activated non-malignant B cells at both transcript and protein levels, suggesting that downregulation of HIP1R expression in ABC-DLBCL might be a disease-related process. Despite its potential for DLBCL subtyping, HIP1R protein expression was not statistically significantly associated with patients' survival in a series of 256 DLBCL. Short FOXP1 isoforms were identified as one mechanism repressing *HIP1R* transcription in an ABC-DLBCL cell line. Phenotypic analysis of HIP1R-depleted B-cell lymphoma cells indicated that HIP1R silencing could increase the surface levels of B-cell receptor (BCR) components such as IgM and CD79b.

HIP1R represents a novel lymphoma autoantigen and cell-of-origin marker for distinguishing germinal centre- versus ABC-DLBCL subtypes. As ABC-DLBCL survival is dependent on chronic BCR signalling, future studies will address whether HIP1R silencing plays a fundamental role in disease pathogenesis by promoting BCR signalling.

Acknowledgements

I would like to extend my deepest gratitude to my supervisor Alison Banham. It was mainly her vast knowledge, guidance and thorough discussions that got this project to where it is today, and taught me the ways of critically evaluating scientific data. I would also like to extend my gratitude to my co-supervisor Karen Pulford to initiate this project and subsequent gentle guidance, advice and help.

I am very grateful to other members of the laboratory and Department: Philip Brown, Amanda Anderson, Demin Li, Duncan Gascoyne, Andrew Graham, Andrew Campbell, Massimo Massiero, Paola Bignone, Linden, Hayley, Jenny, Carol, Charlie, Bridget, Tasneem, Panote, Margaret, Jackie, Graham, Russell, Kingsley, Lisa and all others in the Department for their assistance and for sharing numerous light moments.

I would also like to thank the Public Service Department, Malaysia for initiating this opportunity by awarding me a King's Scholarship, University Science Malaysia and Chang Da Wan for their efforts in securing me a fellowship. I am also grateful to my undergraduate lecturer Nurhayati Abidin. Special thanks to Andrew Chan and all fellow friends who have made the years in Oxford enjoyable, they will be cherished and missed.

Finally, this work is dedicated to my parents, Kit Ling and Yow Hoh, and sisters, Yin Lai, Yin Ching and Yin May.

Table of Contents

List of Figures

CHAPTER 1

CHAPTER 2

CHAPTER 3

CHAPTER 4

CHAPTER 5

CHAPTER 6

CHAPTER 7

List of Tables

CHAPTER 1

CHAPTER 2

CHAPTER 3

CHAPTER 4

CHAPTER 5

APPENDIX

Abbreviations

ABC-DLBCL	Activated B-cell-like diffuse large B-cell lymphoma
AKAP12	A-kinase anchor protein 12
ALCL	Anaplastic large cell lymphoma
ALK	Anaplastic lymphoma kinase
AML	Acute myeloid leukaemia
ANTH	AP180 N-terminal homology
ARACNe	Algorithm for the Reconstruction of Accurate Cellular Networks
ARGHEF1	Rho guanine nucleotide exchange factor 1
BCL2	B-cell CLL/lymphoma 2
BCL6	B-cell CLL/lymphoma 6
BCL7A	B-cell CLL/lymphoma 7A
BCL10	B-cell CLL/lymphoma 10
BCR	B-cell receptor
BLIMP1	B-lymphocyte-induced maturation protein 1
CARD11	Caspase recruitment domain family, member 11
CCND1	Cyclin-D1
CCV	Clathrin-coated vesicles
CD79a	CD79a molecule, immunoglobulin-associated alpha
CD79b	CD79b molecule, immunoglobulin-associated beta
cDNA	Complementary DNA
CHOP	Cyclophosphamide, doxorubicin, vincristine, prednisolone
CLL	Chronic lymphocytic leukaemia
CME	Clathrin-mediated endocytosis
CML	Chronic myeloid leukaemia
COO	Cell-of-origin
DA-EPOCH	Dose-adjusted EPOCH (etoposide, prednisone, vincristine, cyclophosphamide and doxorubicin)
DAB	Diaminobenzidine
DLBCL	Diffuse large B-cell lymphoma
DMSO	Dimethylsulfoxide
E. coli	*Escherichia coli*
ERK	Extracellular-signal regulated kinase
EZH2	Enhancer of zeste homolog 2
FACS	Fluorescence-activated cell sorting
FCS	Foetal calf serum
FFPE	Formalin-fixed paraffin-embedded

FL	Follicular lymphoma
FLIPI	Follicular Lymphoma International Prognostic Index
FOXP1	Forkhead box P1
$FOXP1_S$	Forkhead box P1 short isoforms
$FOXP1_{FL}$	Full-length forkhead box P1
GAPDH	Glyceraldehyde-3-phosphate-dehydrogenase
GC-DLBCL	Germinal centre-like diffuse large B-cell lymphoma
GEP	Gene expression profiling
GFP	Green fluorescent protein
H3K27	Lysine 27 on histone H3
H3K27me3	Trimethylated lysine 27 on histone H3
HCL	Hairy cell leukaemia
HIP1	Huntingtin-interacting protein 1
HIP1R	Huntingtin-interacting protein 1-related
His-tag	Polyhistidine-tag
HL	Hodgkin's lymphoma
IgM	Immunoglobulin M
IL2	Interleukin 2
IPI	International Prognostic Index
IRF4	Interferon regulatory factor 4
ITAM	Immunoreceptor tyrosine based activation motif
JmjC	Jumonji C
JMJD3	Jumonji domain containing 3
LPL	Lymphoplasmacytic lymphoma
MALT	Mucosa-associated lymphoid tissue
MALT1	Mucosa associated lymphoid tissue lymphoma translocation gene 1
MAPK	Mitogen-activated protein kinase
MCL	Mantle cell lymphoma
MFI	Mean fluorescent intensity
MHC	Major histocompatibility complex
MINDy	Modulator Inference by Network Dynamics
miRNA	MicroRNA
MLL	Mixed-lineage leukaemia
MM	Multiple myeloma
mTOR	Mammalian target of rapamycin
MYC	V-myc myelocytomatosis viral oncogene homolog (avian)
MZL	Marginal zone B-cell lymphomas
NF-κB	Nuclear factor-kappa B

NFAT	Nuclear factor of activated T cells
NGC-DLBCL	Non-germinal centre-like diffuse large B-cell lymphoma
NHL	Non-Hodgkin's lymphoma
NOLC1	Nucleolar and coiled-body phosphoprotein 1
p16INK4A	Cyclin-dependent kinase inhibitor 2A
PASD1	PAS domain containing 1
PCR	Polymerase chain reaction
PI3K	Phosphatidylinositol 3-kinases
PIM2	Pim-2 oncogene
PM-DLBCL	Primary mediastinal diffuse large B-cell lymphoma
PRDM1	PR domain containing 1, with ZNF domain
PRDX4	Peroxiredoxin 4
qRT-PCR	Quantitative real-time polymerase chain reaction
PTCL	Peripheral T-cell lymphoma
PTK	Protein tyrosine kinase
PTP	Protein tyrosine phosphatise
R-CHOP	Rituximab, cyclophosphamide, doxorubicin, vincristine, prednisolone
R-DHAP	Rituximab, dexamethasone, ara-C, cisplatin
R-ICE	Rituximab, ifosfamide, carboplatin, etoposide
R-IPI	Revised international prognostic index
SAC	*Staphylococcus aureus,* Cowan
SDS	Sodium dodecyl sulphate
SDS-PAGE	Sodium dodecyl sulphate polyacrylamide gel electrophoresis
siRNA	Small interfering RNA
SNP	Single-nucleotide polymorphism
SYK	Spleen tyrosine kinase
t-FL	Transformed follicular lymphoma
TBP	TATA-box binding protein
TMA	Tissue microarray
TP53	Tumour protein p53
TRAF6	Tumour necrosis factor receptor-associated factor 6
UTX	Ubiquitously transcribed tetratricopeptide repeat, X chromosome
UTY	Ubiquitously transcribed tetratricopeptide repeat, Y chromosome
XBP1	X-box binding protein 1

CHAPTER 1

INTRODUCTION

1.1 HUMAN LYMPHOID TISSUES AND NORMAL B-CELL DEVELOPMENT

1.1.1 Human lymphoid tissues

Lymphoid tissues are divided into primary and secondary lymphoid organs. The primary lymphoid tissues, comprised of bone marrow and thymus, represent the sites where progenitor cells develop into mature and functional blood cells of myeloid and lymphoid lineages. The secondary lymphoid organs include the lymph nodes, spleen and mucosa-associated lymphoid tissues (MALT). In these tissues, lymphoid and non-lymphoid cell interactions occur to generate immune responses against antigens (Lichtman *et al*., 2007).

Lymphocytes (of lymphoid lineage) consist of B cells, T cells and natural killer (NK) cells, and their precursors develop from a population of haematopoietic stem cells in the bone marrow. The precursor lymphocytes then migrate into secondary lymphoid organs where maturation into functional lymphocytes occurs (Lichtman *et al*., 2007). Studies on B-cell malignancies are the focus of this thesis and therefore, the development of normal B cells is first introduced before its malignant counterparts are discussed in the following sections.

1.1.2 Normal B-cell development

Early B-cell development occurs in the bone marrow and concludes with the precursor B-cell successfully acquiring a functional B-cell receptor (BCR) consisting of immunoglobulin (Ig) and proximal BCR subunits (CD79a and CD79b). Cells that express a functional BCR then differentiate into mature naïve B cells which leave the bone marrow and

migrate into secondary lymphoid organs, the cells that fail to express a functional non-auto-reactive BCR undergo apoptosis (Rajewsky, 1996).

In the follicles of secondary lymphoid tissues, precursor B cells move into the primary lymphoid follicle consisting of recirculating IgM^+IgD^+ B cells. The naïve B cells initiate a humoural immune response to exogenous antigens by migrating to T-cell-rich areas, where they become activated by interacting with antigen presenting cells such as dendritic cells and $CD4^+$ T cells. The B cells then proliferate rapidly and push the IgM^+IgD^+ B cells aside to form the mantle zone surrounding a structure named the "germinal centre" (GC). The mantle zone and GC collectively form the secondary lymphoid follicle (Hardie *et al*., 1993; Klein and Dalla-Favera, 2008).

A GC is the structure containing B cells in which the immunoglobulin genes are modified by somatic hypermutation (SHM) to generate a huge diversity of high affinity receptors used to recognise different antigens. The GC comprises the "dark zone" containing densely packed proliferating B cells or centroblasts. The "light zone" consists of non-proliferating centrocytes and resident T cells, follicular dendritic cells (FDCs) and macrophages (Klein and Dalla-Favera, 2008). Some centrocytes further differentiate into antibody secreting plasma cells, after undergoing class switch recombination (CSR) that mediates Ig isotype switching (from IgM and IgD to IgG, IgA or IgE), or differentiate into long-lived memory B cells (Küppers, 2005; Klein and Dalla-Favera, 2008).

1.2 LYMPHOMA AND DEVELOPMENT OF B-CELL NHL

1.2.1 Lymphoma

Lymphoma is a primary neoplasm of lymphoid tissues that also occurs in extranodal sites such as the orbit, skin, gastrointestinal tract, muscle, and genitourinary tract (Gurney and Cartwright, 2002). Lymphomas are heterogeneous disease entities. The latest World Health Organization (WHO) classification of lymphoid neoplasms identifies three major categories of lymphoid malignancies: B-cell neoplasms, T-cell and NK-cell neoplasms, and Hodgkin's lymphoma (HL), with the first two categories being designated as non-Hodgkin's lymphoma (NHL) (Harris *et al*., 1999). HL is characterised by the presence of Hodgkin/Reed-Sternberg (HRS) cells as the hallmark of the disease (Küppers, 2009). Fig 1.1 summarises information on human lymphoid tissues, their main functions, and the common lymphomas that could arise from the specific site with the focus on NHLs.

NHLs are the fifth and seventh most common type of cancer diagnosed in men and women, respectively, in the United Kingdom (Westlake, 2008), and the sixth most common type of malignancy diagnosed in the United States (Ries *et al*., 2003). The incidence rates for NHL in the United States increased nearly 80% between 1973 and 2000, one of the largest surges observed among all cancers (Ries *et al*., 2003).

There are more than 20 subtypes of NHL that have been defined based on their B- or T-cell origin (Harris *et al*., 1999; Halliday and Baxter, 2003), each differs with respect to histopathologic, cytogenetic, molecular genetics, and clinical features. Therefore, studies focussing on a specific or a handful of NHL subtypes are the major concern in most modern-day research projects.

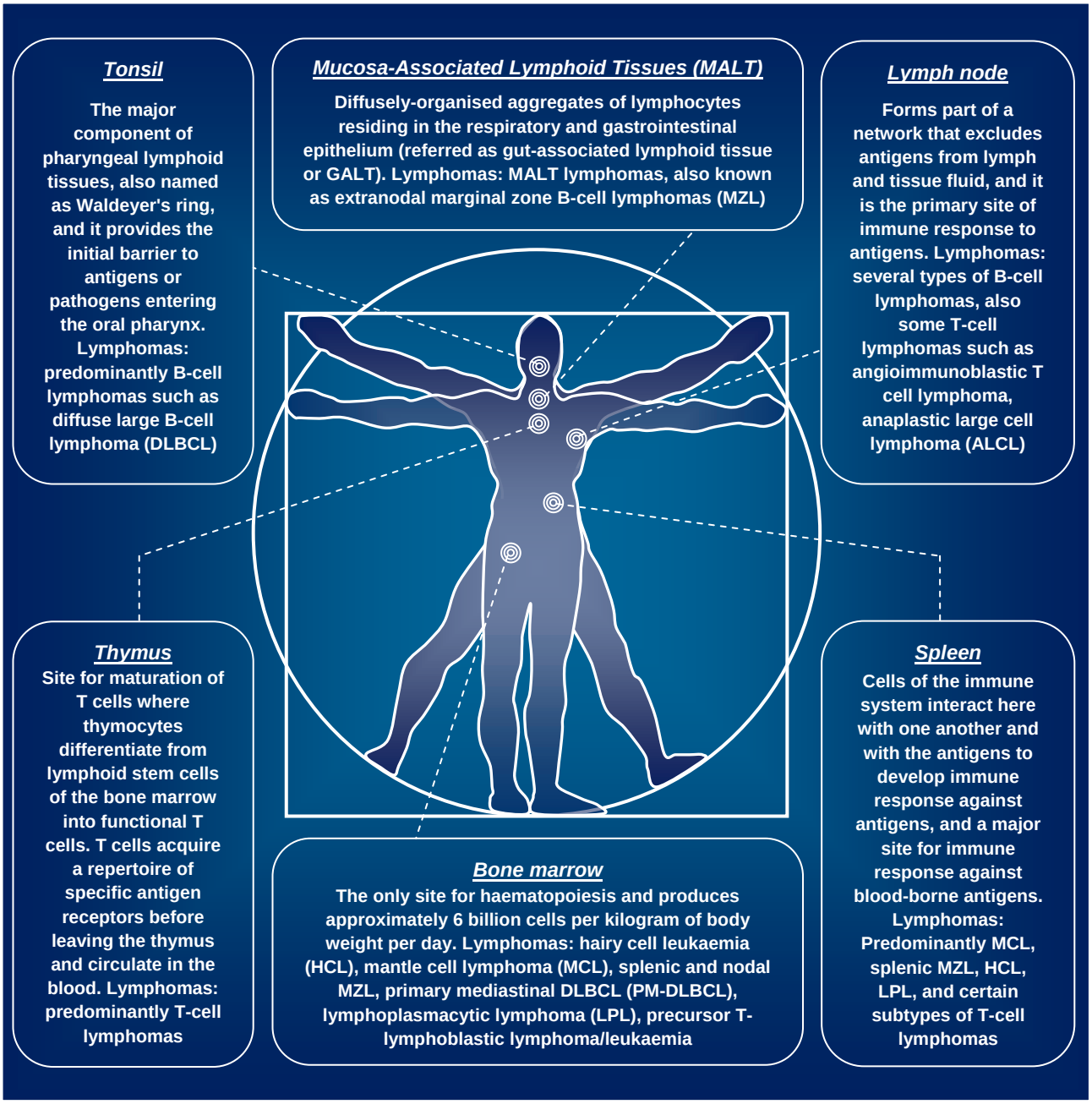

Fig 1.1 The main human lymphoid tissues' functions and types of non-Hodgkin's lymphomas arising from the tissues

Another type of lymphoma based on the site of human organs occurs in the brain, termed as primary central nervous system lymphoma (PCNSL) that often arises in immunocompromised patients. Description modified from Lichtman et al. (2007).

This DPhil project has focused on specific subtypes of B-cell NHL (B-NHL). Hence, the following sections explore the development of B-NHL in lymph nodes, the major lymphoid organs where B-NHLs arise (Lichtman *et al*., 2007).

1.2.2 Development of B-NHL

The GC is the "factory" for generating immune response against foreign antigens and is also the "Achilles heel" that is implicated in lymphoma pathogenesis. Almost all B-NHL demonstrate somatically mutated *IgV* (immunoglobulin variable) genes, indicating that the malignant cells are derived from or have passed through the GC SHM process. Many seem to be "trapped" at a specific differentiation stage that is commonly thought to reflect their cell-of-origin (COO) (Küppers *et al*., 1999).

The hallmark of most B-NHL is a chromosomal translocation involving an active *Ig* locus that confers constitutive expression of a proto-oncogene. Examples of common *Ig* locus translocations include the t(14;18) driving expression of *BCL2* in follicular lymphoma (FL) and the t(11;14) involving *CCND1* in mantle cell lymphoma (MCL). Abnormalities can also involve the chromosomal translocation of non-*Ig* genes such as the *BCL6* gene, which contains a 5' region involved in SHM that also serves as the point where chromosomal translocation breakpoints occur with various translocation partners in diffuse large B-cell lymphoma (DLBCL) (Baron *et al*., 1993; Ye *et al*., 1993).

Other transforming events or genetic lesions not involving chromosomal translocations also contribute to B-NHL pathogenesis. Examples include genomic amplifications of the *REL* NF-κB subunit (Bea *et al*., 2005), deletions of *A20* in mucosal associated lymphoid tissue (MALT) lymphoma and DLBCL (Kato *et al*., 2009), and mutation of *CARD11* (Ngo *et al*., 2006) or *CD79a/b* (Davis *et al*., 2010) in DLBCL. Aberrant somatic hypermutation targeting multiple proto-oncogene loci in DLBCL has also been reported (Pasqualucci *et al*., 2001). Fig 1.2 summarises the maturation stages of B cells and the lymphomas that could arise from these specific stages.

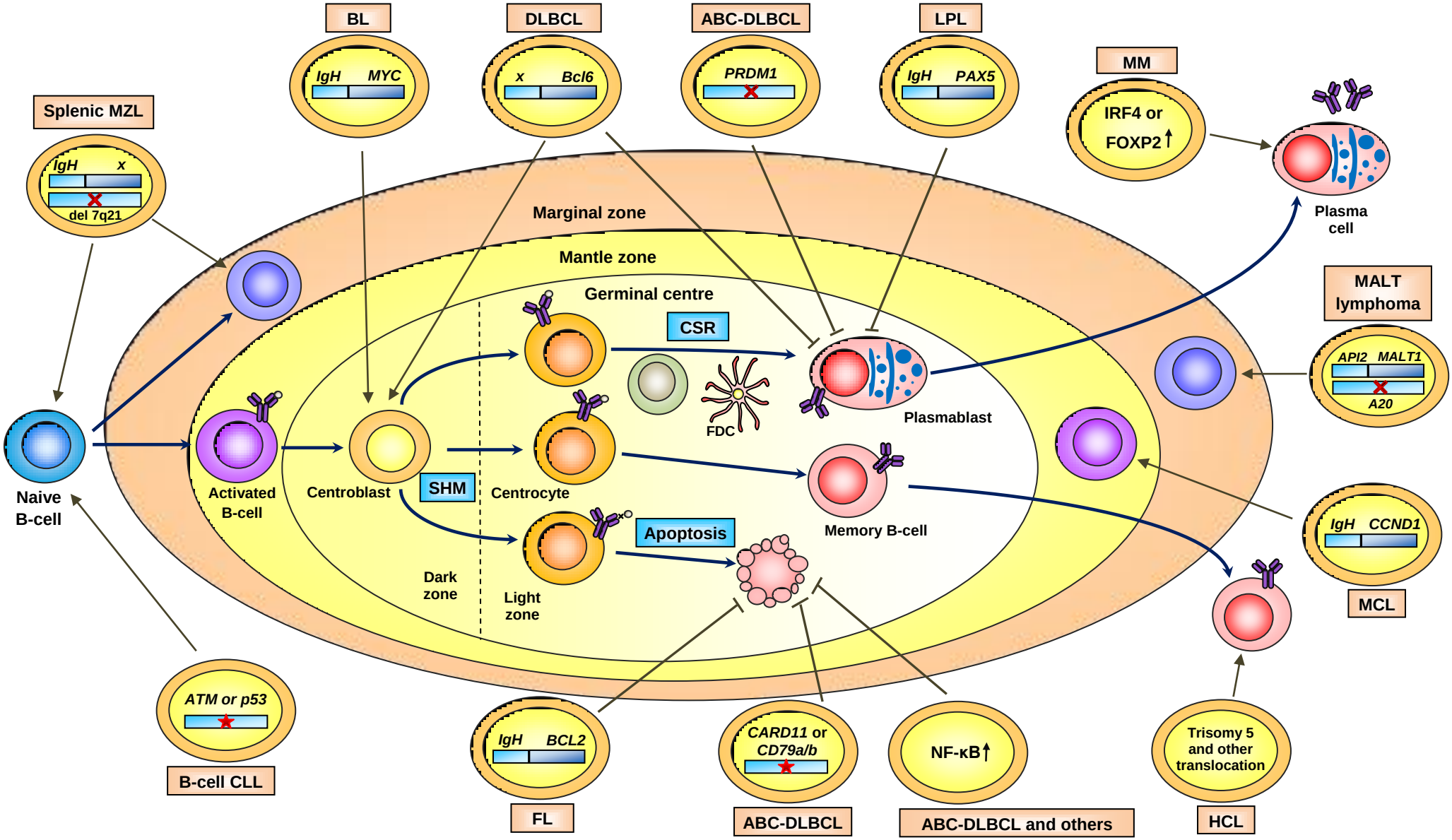

Fig 1.2 Normal B-cell differentiation stages and B-cell lymphomagenesis

The genetic lesions or transforming events not otherwise specified in the main texts body are the dysregulation of proto-oncogenes

PRDM1 (encoding the protein BLIMP1) in activated B-cell-like DLBCL (ABC-DLBCL), IgH translocation events involving MYC in BL, PAX5 in LPL, CCND1 in MCL, BCL2 in FL, and various other partners in splenic MZL and MALT lymphoma. In addition, API2-MALT1 fusion gene in MALT lymphoma, mutation of ATM or p53 in B-cell chronic lymphocytic leukaemia (CLL), trisomy 5 and other translocation in HCL. Aberrant expression of FOXP2 (Campbell et al., 2010) or abnormal function of IRF4 (Shaffer et al., 2008) occurs in multiple myeloma (MM).

The inhibitory arrows directed at "Plasmablast" denote the signalling events that prevent plasmablast differentiation into plasma cells by inhibiting PRDM1 to encode BLIMP1, the protein essential for terminal differentiation of B cells into plasma cells (Shapiro-Shelef et al., 2003), thereby keeping the cell in the GC stage of development.

Marginal zone: the interface surrounding mantle zone that primarily exists in spleen and lymph nodes, and contains antigen presenting cells and marginal zone B cells, providing the first line of defence against blood-borne antigens. Original diagram constructed from Klein and Dalla-Favera (2008).

Key: → *promotes lymphomagenesis;* ⊣ *inhibits plasmablast differentiation or apoptosis;* ★ *mutation;* ✖ *deletion or dysregulation;* ↑ *upregulation*

As shown in Fig 1.2, there is a wide spectrum of B-NHL subtypes that can arise from the various B-cell maturation stages. Studies on DLBCL and FL are the main focus of this project and thus, they are introduced in more detail in the following sections.

1.3 DIFFUSE LARGE B-CELL LYMPHOMA

1.3.1 Epidemiology and morphologic variants of DLBCL

DLBCL is the most common subtype of NHL worldwide and accounts for nearly 40% of all NHLs in the United States (Armitage and Weisenburger, 1998), 47% in Thailand (Sukpanichnant, 2004), 59% in United Arab Emirates (Castella *et al*., 2001) and 65% in Malaysia (Peh *et al*., 2003). Many subtypes of NHL have a characteristic chromosomal anomaly such as t(14;18) in FL and t(2;5) in ALK-positive ALCL. However, there is no convincing evidence of any "primary" molecular cytogenetic defect of diagnostic significance being present in DLBCL. Furthermore, defining the diverse spectrum of DLBCL morphologic variants (Fig 1.3) has not been instrumental in predicting outcome and response to chemotherapy (Hunt and Reichard, 2008) suggesting that it is the underlying heterogeneity of this disease that causes difficulties for treatment with a largely homogenous approach.

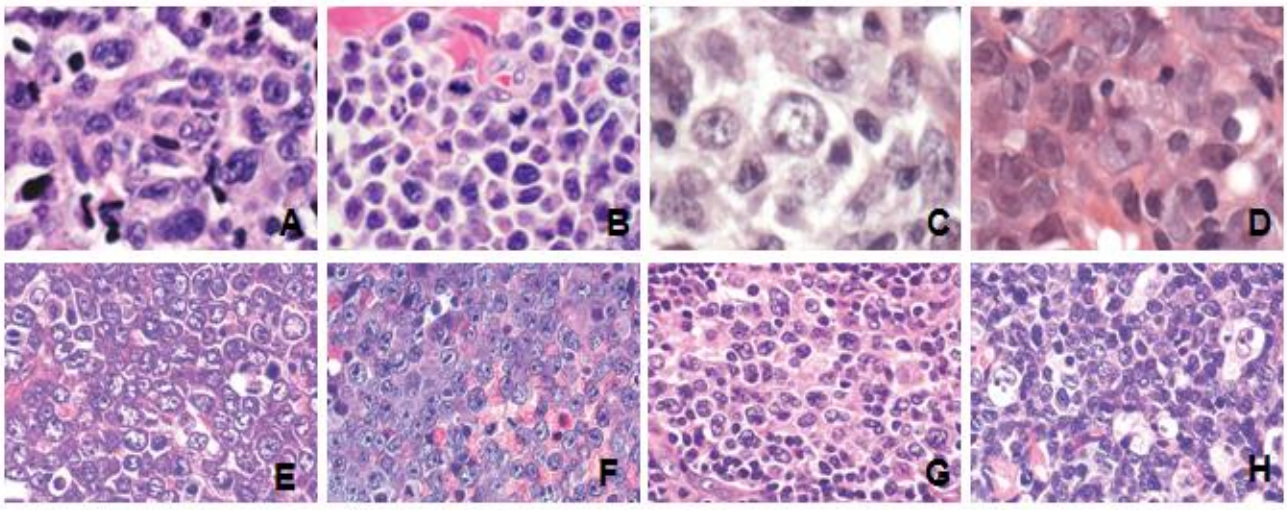

Fig 1.3 The wide morphological variants of DLBCL

A: anaplastic; B: plasmablastic; C: centroblastic; D: immunoblastic; E: predominantly centroblastic; F: predominantly immunoblastic; G: polylobated; H: unclassifiable. Adapted from Hunt and Reichard (2008), and Gatter and Pezzella (2009).

1.3.2 Subtypes of DLBCL

The application of microarray technology has led to the discovery of at least two clinically and biologically distinct DLBCL subtypes: GC B-cell-like DLBCL and activated B-cell-like (ABC) DLBCL subtypes characterised by expression of genes normally expressed in GC B cells and induced during *in vitro* activation of B cells, respectively. Patients who have GC-DLBCL demonstrated a significantly better survival, in response to CHOP chemotherapy, than those with ABC-DLBCL: 62% (GC-DLBCL) versus 26% (ABC-DLBCL) 5-year overall survival (OS) (Alizadeh *et al*., 2000; Wright *et al*., 2003). There is also a third group, type-3 DLBCL, that is unclassifiable which also has a poor prognosis (Rosenwald *et al*., 2002).

The data generated by gene expression profiling (GEP) studies have been used to develop prediction models for routine clinical use. Hans *et al*. (2004) subclassified DLBCL into GC- and non-GC (NGC)-DLBCL by IHC based on 3 markers: CD10, BCL6 and MUM1. This algorithm has approximately 80% concordance with GEP subclassification of DLBCL, and a study by Choi *et al*. (2009) has improved the accuracy of the algorithm by applying less weighting to BCL6 staining and through the addition of two novel antibodies: anti-FOXP1 and anti-GCET1. The new algorithm has 93% concordance with GEP subclassification of DLBCL. Fig 1.4 summarises the chronology of selected expression profiling and prognostic markers studies in DLBCL.

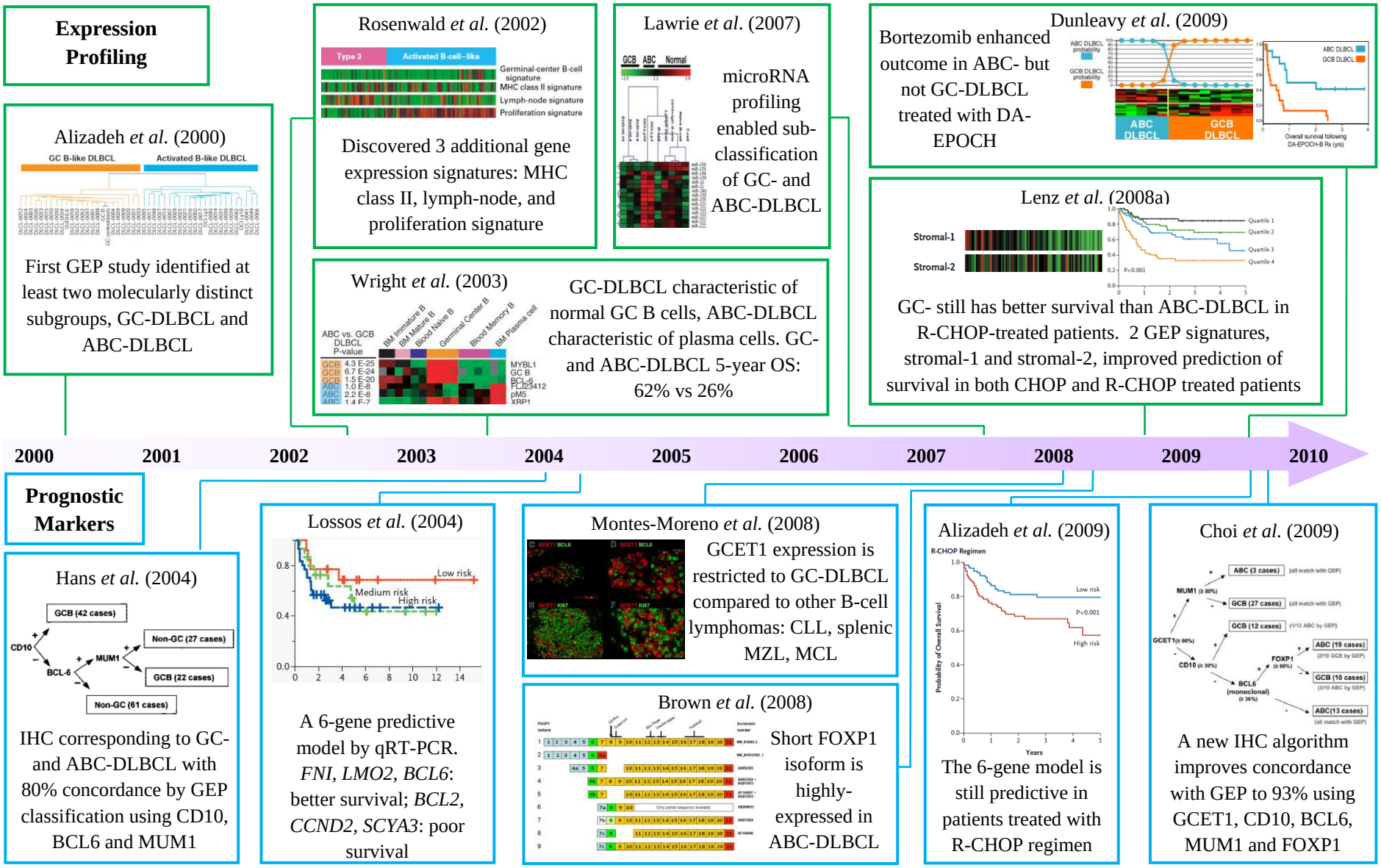

Fig 1.4 Chronology of selected expression profiling and prognostic markers studies in DLBCL since the year 2000

1.3.3 Therapeutic significance of DLBCL subtyping

DLBCL patients receive combination chemotherapy, the most commonly used being CHOP (cyclophosphamide, adriamycin, vincristine, prednisone) based regimens. In 2006, the US Food and Drug Administration (FDA) approved the use of an anti-CD20 monoclonal antibody (rituximab), for first-line treatment in DLBCL. The addition of rituximab to conventional CHOP therapy (CHOP-R or R-CHOP) has become the "gold standard" therapy, which has sparked the re-validation of survival differences between DLBCL subgroups.

Lenz *et al*. (2007a) reported that the GEP defined GC-subgroup still had superior survival than the ABC-subgroup in 233 patients treated with R-CHOP. However, two studies using the Hans *et al*. algorithm to define DLBCL subtypes by immunohistochemistry (IHC) produced conflicting results. An investigation of 90 and 104 DLBCL patients treated with R-CHOP and CHOP, respectively, found that IHC-defined GC-DLBCL subgroup lost its predictive outcome (Nyman *et al*., 2007). In contrast, another study including 112 R-CHOP- and 131 CHOP-treated DLBCL patients showed that the GC-subgroup still had significantly better survival than the NGC-DLBCL subgroup (Fu *et al*., 2008). Despite inconsistent results using the Hans *et al*. algorithm, there are several reports that combinations of ABC-DLBCL markers can be used to define DLBCL patients that have a poor response to R-CHOP (Choi *et al*., 2009; Copie-Bergman *et al*., 2009; Nyman *et al*., 2009).

Biological studies have investigated fundamental pathogenic mechanisms in ABC-DLBCL that might be amenable to therapeutic targeting. Of particular importance to the survival of ABC-DLBCL are constitutive activation of the NF-κB transcription factor (Davis *et al*., 2001) and chronic BCR signalling (Davis *et al*., 2010). A recent study by Dunleavy *et al*. (2009) demonstrated that the combination of bortezomib, a proteasome inhibitor, with

DA-EPOCH chemotherapy regimen improved the median overall survival (p = 0.003) of ABC-DLBCL patients by blocking the degradation of phosphorylated IκBα, an inhibitor of NF-κB transcription factor activity. This showed that DLBCL subtyping into ABC- or GC-DLBCL subgroups may become relevant as a predictive marker for selecting patients for personalised targeted therapy rather than a prognostic marker for response to CHOP or R-CHOP therapy.

Taken together, these results continue to justify two avenues of further research in DLBCL subtyping: 1) Discovery of novel markers that might improve or yield better prognostic data in DLBCL patients treated with R-CHOP chemotherapy regimens and/or help select patient groups for molecular-guided therapy; 2) Identification of novel survival or biological pathways in DLBCL that might uncover additional pathways for therapeutic intervention.

1.4 FOLLICULAR LYMPHOMA

1.4.1 Epidemiology and prognosis of FL

FL is the most common form of indolent lymphoma and the second most common subtype of B-NHL accounting for about 25% of all NHL cases (The Non-Hodgkin's Lymphoma Classification Project, 1997). FL patients have a relatively long median survival of 8-10 years but it is an incurable disease, and the clinical outcome of the patients is heterogeneous with 10-15% of patients having an accelerated disease course that proves fatal in 2-3 years (Carreras *et al*., 2006).

Cytogenetically, about 85-95% of FL cases are characterised by the t(14;18)(q32;q21) translocation between the *Ig* locus and the *BCL2* gene (Rowley, 1988; Horsman *et al*., 1995).

However, studies using murine models to recapitulate the abnormality have demonstrated that this alone is not adequate for lymphomagenesis and that clinical heterogeneity is a result of secondary genetic events in the tumour and alterations within the tumour microenvironment (Bende *et al*., 2007). Secondary genetic events contributing to poor survival in FL include gene mutations such as the mutations of *TNFRSF14* gene that occurs in about 18% of FL patients (Cheung *et al*., 2010).

In addition, microarray GEP has identified 2 prognostic signatures. The "immune-response 1" signature includes genes highly expressed in macrophages and T cells and confers a good prognosis, while the "immune-response 2" signature including genes preferentially expressed in macrophages and dendritic cells that confers a poor prognosis (Dave *et al*., 2004). This is distinctly different from other lymphomas where the tumour derived GEP signature commonly predicts outcome. In terms of the tumour microenvironment, high number of macrophages or tumour-infiltrating FOXP3-positive regulatory T cells in FL correlate with poor (Farinha *et al*., 2005) or improved (Carreras *et al*., 2006) survival, respectively. Thus, evidence indicates that both the tumour and the microenvironment have important roles in the biology of this disease.

Despite these attempts, there is still a lack of reliable prognostic markers or utilisation of less invasive methods to identify high-risk patients who will experience rapid disease progression. The clinical outcome of FL could be predicted by the Follicular Lymphoma International Prognostic Index (FLIPI) (Solal-Celigny *et al*., 2004) and FLIPI2 (an update on the original FLIPI) that utilise clinical parameters such as bone marrow involvement and size of the largest involved lymph node at FL diagnosis (Federico *et al*., 2009). However, the parameters used to define FLIPI and FLIPI2 represent surrogate markers of disease biology,

while the identification of prognostic markers closely relating to the biologic mechanisms involved in the development or progression of FL could also enable the design of more targeted therapeutic strategies.

1.4.2 Transformation of FL

About 30% of FL cases transform to high-grade lymphoma, often to DLBCL or rarely to BL (Al-Tourah *et al*., 2008). There are two mechanisms leading to transformation of FL that have been proposed: 1) Transformed FL (t-FL) emerges from an aggressive subclone of cells within the FL; 2) Both FL and t-FL arise by divergence from a common progenitor cell (CPC) (Matolcsy *et al*., 1999). The latter mechanism is a more accurate explanation of the transformation and is supported by several studies utilising different methodologies that suggest transformation may begin from more undifferentiated cells, for example: 1) Single-nucleotide polymorphism (SNP) array analysis uncovered that homozygosity of 9p and 17p occurred predominantly in t-FL, and the cells harboured a pre-existing mutation of either *CDKN2A* or *TP53* (Fitzgibbon *et al*., 2007); 2) Somatic hypermutation (SHM) pattern analysis demonstrated that the majority of t-FL cases originated from a CPC (Carlotti *et al*., 2009).

t-FL is a major cause of disease-associated death in FL and is frequently resistant to treatment (Wrench *et al*., 2010). t-FL has an inferior outcome with a median survival of around 1.2-1.5 years (Montoto *et al*., 2007; Al-Tourah *et al*., 2008) with a highly significant ($p < 0.0001$) shorter overall survival and a shorter survival from progression (Montoto *et al*., 2007). The 10-year overall survival of FL is 75%, while t-FL is only 36% (Al-Tourah *et al*., 2008), indicating a strong need for research to identify FL patients who will develop t-FL and novel treatments for t-FL.

1.4.3 Therapeutic approaches for FL and t-FL

The optimal or standardised therapy for FL and t-FL is not fully defined (Friedberg *et al*., 2009). Although R-CHOP regimen is the most widely adopted therapeutic strategy for FL patients, there are at least nine other initial therapeutic strategies adopted across 265 sites in the United States (Friedberg *et al*., 2009). Several approaches have also been adopted to treat t-FL patients, however R-CHOP is the recommended initial approach for t-FL patients considering the good outcome observed with this regimen for patients with *de novo* DLBCL (Bernstein and Burack, 2009). The undefined therapeutic approaches in treating FL or t-FL patients motivates studies to uncover novel molecules implicated in the disease that might contribute to tailoring targeted and novel therapeutic strategies that could potentially standardise the treatment for FL or t-FL patients.

1.5 B-CELL RECEPTOR SIGNALLING

Because of the eventual focus of this thesis on DLBCL subtyping, the next section introduces the signalling cascades in activated B cells triggered by antigen stimulation. An understanding of these processes is important to the formulation of hypotheses regarding the possible function of novel molecules in ABC-DLBCL pathogenesis.

1.5.1 BCR signalling triggers four canonical pathways

The BCR complex consists of membrane immunoglobulin (mIg) that is associated non-covalently with CD79a (or Igα) and CD79b (or Igβ) heterodimers, and all subunits contain a transmembrane domain. B-cell immune responses are initiated by the binding of foreign antigen to mIg, resulting in rapid phosphorylation of the cytoplasmic domains of CD79a/CD79b heterodimers. This triggers subsequent protein tyrosine phosphorylation events mediated by SRC-family protein tyrosine kinases (PTKs), culminating in the

activation of nuclear factor kappa-light-chain-enhancer of activated B cells (NF-κB), mitogen-activated protein kinases (MAPK), mammalian target of rapamycin (mTOR), and nuclear factor of activated T cells (NFAT) pathways (reviewed by Monroe, 2006; Lenz and Staudt, 2010) as summarised in Fig 1.5.

1.5.2 NF-κB, MAPK, mTOR and NFAT pathways

NF-κB is a family of transcription factors consisting of p50, p52, p65 (RelA), RelB and c-Rel, with the latter three members containing a transcription activation domain (TAD) necessary for regulation of gene expression. p50, p52 and p65 members are instrumental in modulating the specificity of NF-κB target gene regulation (Hayden and Ghosh, 2008).

NF-κB dimers are present in a latent protein complex that is bound to IκB proteins in the cytoplasm, and the most widely studied complex is the IκBα-p50-p65 protein complex (Gilmore, 2006; Hayden and Ghosh, 2008). NF-κB signalling is activated by the proteolytic degradation of IκBα that disintegrates p50-p65 subunit from the complex, allowing translocation of the subunit to the nucleus for transcriptional activation (Lenz and Staudt, 2010). As such, this family are "rapid-acting" transcription factors that do not require new protein synthesis to be activated. They provide the first line of B-cell response to antigens by activating the transcription of genes involved in proliferation and pro-survival such as *BCL2* and *BIRC5/Survivin* (Tracey *et al*., 2005) and differentiation into plasmablasts by activating *IRF4* (Feuerhake *et al*., 2005).

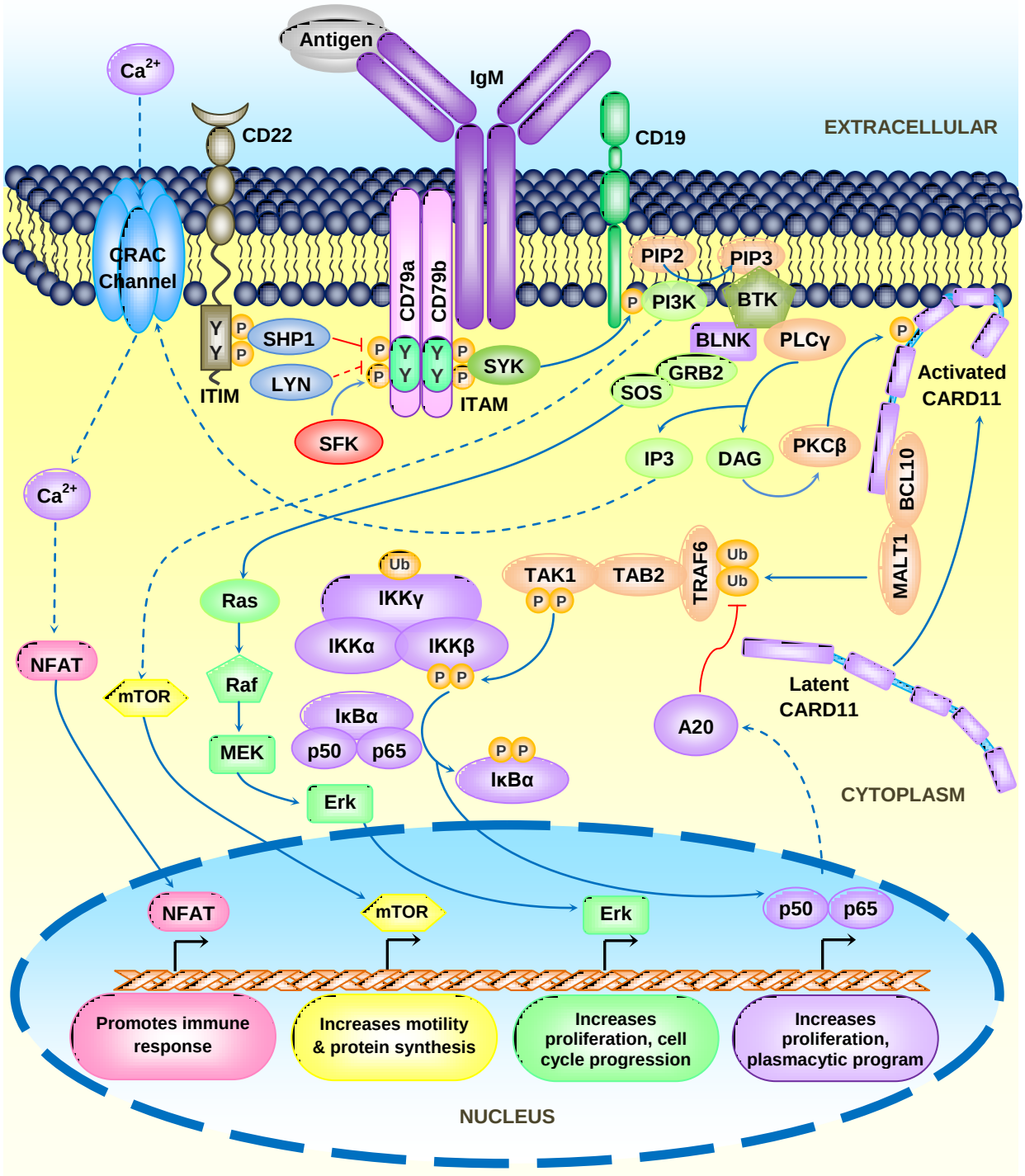

Fig 1.5 BCR signalling activates four canonical pathways in B cells

When the BCR binds to an antigen, the intracellular signalling is initiated by the phosphorylation of the immunoreceptor tyrosine-based activation motifs (ITAMs) of CD79a and CD79b mediated by SRC-family kinase (SFK). SYK, a tyrosine kinase, is subsequently recruited to the phosphorylated ITAM motifs and activated via its SH2 domains triggering the phosphorylation of CD19 and subsequent recruitment of phosphatidylinositol 3-kinase

(PI3K) that generates phosphatidylinositol 3,4,5-triphosphate (PIP3) from phosphatidylinositol 4,5-bisphosphate (PIP2) in the membrane lipid. Consequently, Bruton's tyrosine kinase (BTK) is recruited and binds to PIP3, forming a complex with PLCγ and the adapter BLNK. PLCγ generates two second messengers, IP3 that triggers calcium ions influx that triggers the opening of CRAC channel and subsequent activation of the NFAT pathway, and DAG that activates PKCβ. CARD11 in its latent state localised in the cytoplasm is phosphorylated by activated PKCβ that leads to CARD11 recruitment to the plasma membrane and forms a multiprotein complex with BCL10 and MALT1 (CBM complex). This causes the ubiquitination of IκB kinase (IKK) γ subunit and the ubiquitin ligase TRAF6, forming a complex with TAB2 and TAK1 kinase that leads to phosphorylation of the IKKβ subunit by TAK1. IKKβ in turn phosphorylates IκBα, triggering NF-κB signalling by disintegrating p50-p65 from the complex that permits p50-p65 subunit to be translocated to the nucleus for transcriptional activation. A target gene of NF-κB, A20, attenuates NF-κB signalling via deubiquitination of TRAF6 and IKKγ, forming a negative feedback loop for NF-κB signalling pathway.

The mTOR pathway is also activated by PI3K activities. The MAPK pathway is triggered by SOS homologue complex with BLNK and GRB2. LYN kinase and co-receptors such as CD22 negatively regulate BCR signalling by inhibiting the phosphorylation of ITAM. Regulation of BCR signalling by CD22 is achieved via the activity of SHP1, an inositol phosphatase, bound on its ITIM motifs. Diagram and description constructed from Monroe (2006), Lenz and Staudt (2010) and Cell Signaling Techonology (http://www.cellsignal.com/pathways/lymphocyte.jsp)

Key: ⟶ *Direct positive regulation;* ⇢ *Indirect positive regulation;* ⟙ *Direct inhibition;* ⇣ *Indirect inhibition;* ⮡ *Transcription.*

The most widely-studied MAPK subfamily of pathways is the extracellular-signal regulated kinases (ERK) MAPK pathway essential for cell proliferation and differentiation, and the activation of several key growth factors (Fang and Richardson, 2005). The ERK MAPK pathway is itself activated by PI3K (Sato *et al*., 2004) or PKC (Wang *et al*., 2004) activities. ERK MAPK promotes cell division by activating the transcription of *CCND1*

(Lavoie *et al*., 1996). This is counter-balanced by cyclin-dependent kinase inhibitor A (p21) protein, which is also activated by MAPK pathway itself (Woods *et al*., 1997), producing a negative regulatory feedback loop.

mTOR or the mammalian target of rapamycin, named due to the action of the antifungal agent rapamacyin with anticancer properties which perturbs mTOR function, is a large protein kinase that nucleates two multi-protein complexes, mTORC1 and mTORC2. mTOR pathway is activated by the activities of PI3K (Sabatini, 2006). The signalling pathways are vital in regulating cell growth by promoting ribosome biogenesis and protein synthesis (Sarbassov *et al*., 2005).

NFAT is a group of transcription factors consisting of five members, NFAT1, NFAT2, NFAT3, NFAT4 and NFAT5. The first four members are regulated by calcium signalling that causes the activation of calcineurin phosphatase via calmodulin (a calcium sensor protein) and subsequently dephosphorylates NFAT proteins, exposing their nuclear-localisation signal (NLS) to confer an ability to regulate gene transcription (Crabtree and Olson, 2002; Macian, 2005). NFAT exerts its effects of promoting immune responses after antigen activation by targeting ligases such as CBL (Loeser and Penninger, 2007).

1.5.3 Tonic BCR signalling

Apart from antigen-driven responses, the localisation of PTKs in the membrane and their basal activity is likely to initiate BCR signalling independently of ligand binding to the BCR, a process termed as “tonic” BCR signalling (Monroe, 2004). Peripheral B cells die upon induction of BCR loss in mice (Lam *et al*., 1997), and the ablation of CD79a signalling via loss of the CD79a ITAM motif leads to the loss of mature B cells (Kraus *et al*., 2004).

These studies have indicated that ongoing or tonic BCR signalling is essential in maintaining the viability of B cells in the absence of antigen-driven responses. Activation of SYK at the basal level is thought to be essential for tonic BCR signalling and its activation is, in turn, inhibited by protein tyrosine phosphatase (PTP) (Rolli *et al*., 2002). For instance, a type of lymphoid PTP called PTP receptor-type O truncated (PTPROt) controls tonic BCR signalling through a SYK-PTPROt mechanism (Chen *et al*., 2006). The abnormal BCR signalling in DLBCL via a novel "chronic active" BCR signalling pathway which contrasts with that of tonic signalling is introduced in Chapter 5.

1.6 AUTOANTIBODY PROFILING

The following sections introduce two major topics of fundamental importance to the research project pursued in this thesis. Firstly is the use of autoantibody profiling to identify novel lymphoma-associated antigens, and secondly an overview of the literature on the two molecules that were selected for further studies, HIP1R and JMJD3.

1.6.1 Autoantibodies and tumour-associated antigens

Autoimmune responses are characterised by the immune response of the body against proteins or cells that are not of exogenous or foreign origin. They have been considered to be a causative event in certain tumours e.g. there is a strong link between the autoimmune disease Sjögren's syndrome and NHL (Ekström *et al*., 2008). The characterisation of autoantigens has paved the way for exploiting serological tools for biomarker discovery to aid in the early diagnosis and management of autoimmune diseases such as serum cardiac troponin I (cTnI) for the diagnosis of myocardial infarction (Katus *et al*., 1989) or the B-type natriuretic peptide (BNP) for the diagnosis of congestive heart failure (Mukoyama *et al*., 1990).

Autoantibodies recognise tumour-associated antigens (TAAs) known to be involved in lymphoma pathogenesis. For instance, FL patients had circulating autoantibodies against BCL2 (Pulford *et al*., 2002), and translocation involving *BCL2* loci was linked to the pathogenesis of FL. Moreover, Ait-Tahar *et al*. (2010) reported that the antibody titre to the ALK oncogene was associated with clinical features and disease progression. Thus, there are possibilities to exploit the humoural immune response to identify other proteins involved in lymphoma pathogenesis which have not previously been identified.

1.6.2 Mechanisms triggering immune response against TAAs

Several mechanisms causing autoantibody responses against TAAs have been proposed. A well-studied mechanism causing cancer immunity is the aberrant expression of genes that are not normally expressed in adult tissues from non immuno-privileged sites. An example is expression of a foetal protein such as p62, an mRNA binding protein that is not normally present in adult tissue but is frequently expressed in liver cancer cells (Lu *et al*., 2001). This mechanism also includes the expression of cancer testis antigens (CTAs), a group of proteins normally expressed in the testis (an immuno-privileged site that is not normally recognised by the immune system) that trigger immune responses when aberrantly expressed in tumour cells such as NY-ESO-1 in melanoma (Stockert *et al*., 1998) and lung cancer (Türeci *et al*., 2006).

Gene overexpression also contributes to immune response against TAAs and can induce the loss of immune tolerance to these self-antigens, eliciting an autoimmune response in the process (Casciola-Rosen *et al*., 2005). For instance, HER-2/neu is overexpressed in about 20% of colorectal tumours and autoantibodies against HER-2/neu were found in 46% of the patients with overexpressed HER-2/neu. This was in contrast with only 5% in those

patients without HER-2/neu expression (Ward *et al*., 1999). Another example is GA733-2 protein which is overexpressed in more than 90% of colorectal tumours, and anti-GA733-2 antibodies were present in 14.5% of the patients (Mosolits *et al*., 1999).

An alternative mechanism leading to autoantibody production is the potential mutation of specific genes. A study utilising combinatorial DNA libraries encoding numerous random mutations in tyrosinase-related proteins found that truncations of the tyrosinase protein were adequate for eliciting an immune response and additional of amino acid substitutions in the protein increased the immune response (Engelhorn *et al*., 2006). Autoantibodies against p53 antigens have often been implicated in colorectal cancer (Scanlan *et al*., 2002; Kijanka *et al*., 2010) and the generally accepted explanation of this observation is that the expression of the mutated tumour suppressor gene *p53* leads to conformational or functional changes of the protein that are recognised by the immune system (Roth *et al*., 1996; Kijanka and Murphy, 2009).

Other mechanisms triggering autoantibody responses against TAAs include the disrupted cellular localisation of antigens in tumour cells (Kijanka *et al*., 2010) or post-translational modifications of proteins such as phosphorylation (Wu *et al*., 2001).

1.6.3 Identification of TAAs using SEREX or protein arrays

There are two approaches in the identification of TAAs that will be introduced in this section, SEREX and protein arrays, because of the established SEREX technique historically employed in our laboratory, and the alternative protein arrays chosen for the current study. Autoantibody profiling to identify new TAAs using protein arrays and SEREX technique in a range of malignancies has resulted in a large "library" of TAAs (Table 1.1).

Table 1.1 Selected autoantibody profiling studies in human malignancies

Type of cancer	Methodology	Key TAA(s)	Patients versus controls (n)	Reference
Colorectal cancer	Protein array	UCH-L3	15 vs 15	Nam *et al*. (2003)
Lung cancer	Protein array	CRP, MUC1	24 v 24	Gao *et al*. (2005)
Ovarian cancer	Protein array	LMNA, SSRP1, RALBP1	30 vs 30	Hudson *et al*. (2007)
Colorectal cancer	Protein array	ITFG3, p53	43 vs 40	Kijanka *et al*. (2010)
CTCL	SEREX	cTAGE-1	17 vs 28	Eichmüller *et al*. (2001)
CLL	SEREX	KW-1	25 vs 14	Krackhardt *et al*. (2002)
Colon cancer	SEREX	p53	74 vs 75	Scanlan *et al*. (2002)
Squamous cell lung carcinoma	SEREX	p53	20 vs 36	Diesinger *et al*. (2002)
DLBCL, AML, CML	SEREX	PASD1	10 (in each disease) vs 20	Liggins *et al*. (2004a)
Hepatocellular carcinoma	SEREX	KRT23, AHSG, FTL	30 vs 30	Wang *et al*. (2009a)

NB: Apart from SEREX, other non-array proteomics approach e.g. 2D-gel electrophoresis, mass spectrometry and serological proteome analysis (SERPA) are not included for simplicity. SEREX: serological analysis of recombinant cDNA expression libraries

SEREX is one of the early proteomics approaches developed in the mid 90s to allow unbiased and comprehensive search for autoantibodies responses against TAAs (Sahin *et al*., 1995) and has since been widely used in autoantibody profiling studies. SEREX involves the construction of cDNA expression libraries from fresh cancerous specimens (or tissues such as

testis) that are cloned into lambda phage expression vectors (Fig 1.6). Infection of *E. coli* by the phages results in recombinant protein expression and the products of these lytic plaques are transferred onto nitrocellulose membranes. The membrane containing the vast array of recombinant proteins is then incubated with diluted serum before incubation with an enzyme-conjugated (e.g. alkaline phosphatase) anti-human antibody and the final detection of immunoreactive clones is visualised with substrates such as NBT/BCIP producing blue staining (Preuss *et al*., 2002; Zhou *et al*., 2006). Tertiary screening is then performed to analyse the frequency of reactivity of each antigen with both patients' sera and sera from age- and sex-matched normal healthy donors.

An alternative array approach now utilises protein arrays for serum screening. Microspots of proteins are arrayed at high density on the planar surface of filter membranes such as PVDF (Büssow *et al*., 1998). This is initially achieved by the conventional generation of *E. coli* cDNA expression libraries derived from specific cells.

By using a picking or gridding robot, a large number of colonies (approximately 200,000) are picked into several microtitre plates (usually of 384-well) and grown overnight before gridding onto filter membranes in a duplicate pattern. The membrane is then probed with autoantibodies from sera, incubated with anti-human secondary antibody conjugated with an enzyme (e.g. alkaline-phosphatase), developed with a fluorescent substrate (e.g. Attophos) and illuminated with UV light to acquire a grey-white image with the positive signals recognised as bright, white spots and the image analysis is carried out using specific software (Fig 1.7).

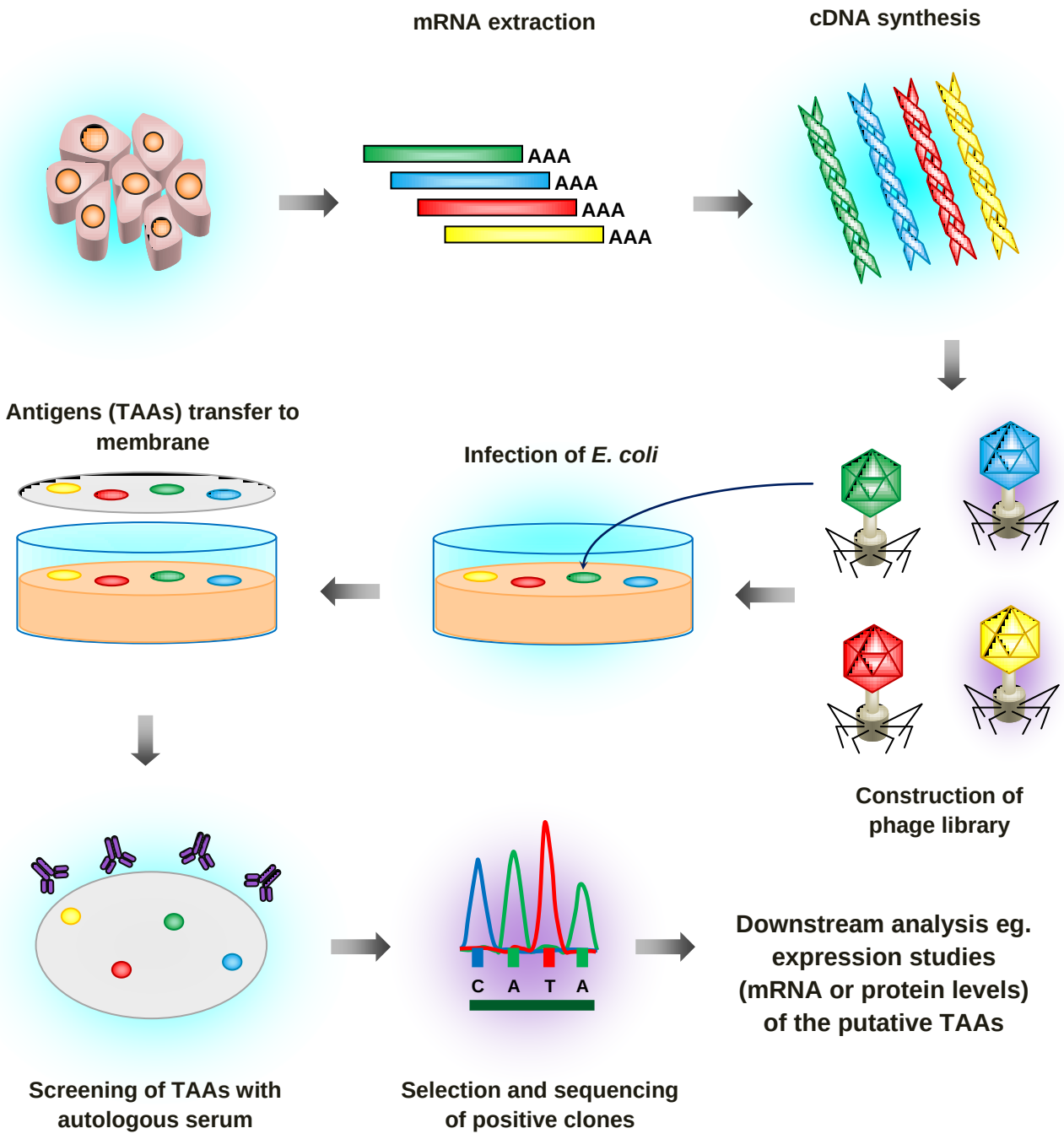

Fig 1.6 SEREX methodology in autoantibody profiling

Downstream analysis of SEREX antigens include verifications of the expression pattern of the antigen of interest in the tumour tissues versus normal counterparts to elucidate the basis in the presence of autoantibodies against the TAA.

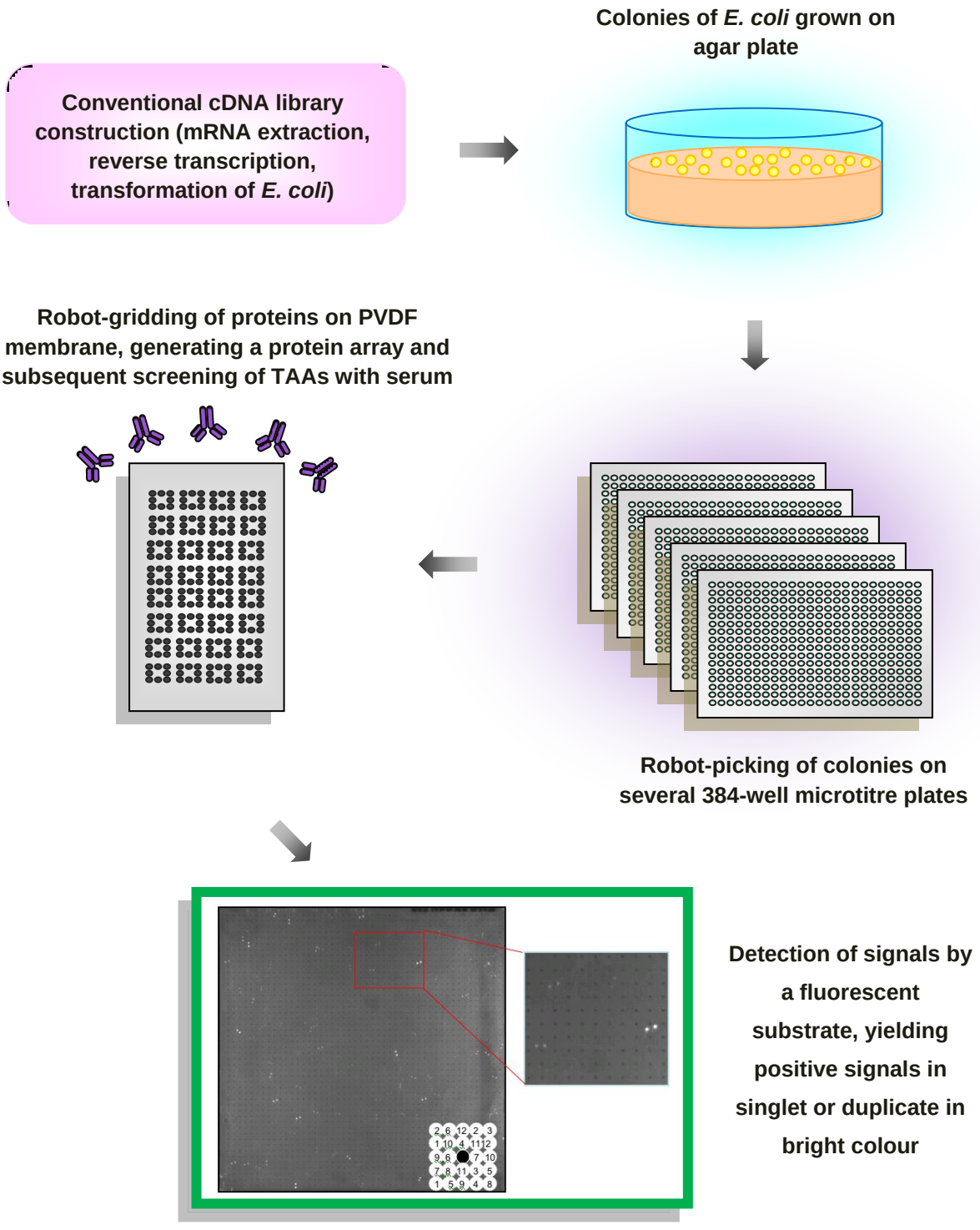

Fig 1.7 Protein array approach in autoantibody profiling

Analysis of the acquired image whether which TAA is over-represented is performed by computer software that also determines which protein is represented by the positive signals and this is further shown in Chapter 3.

1.6.4 Identification of lymphoma-associated antigens using protein arrays

Our interest in autoantibody profiling of B-NHL arose from early work in our laboratory showing that autoantibodies in lymphoma patients recognise the products of chromosomal translocations e.g. circulating autoantibodies against NPM-ALK protein were identified in ALK-positive ALCL patients (Pulford *et al*., 2000) and autoantibodies against the tumour-related antigen BCL2 in FL (Pulford *et al*., 2002). Thus, autoantibody profiling offers the opportunity to identify antigens involved in the pathogenesis of other B-NHL where there is not a single underlying genetic abnormality. In addition, the identification of PASD1 as a common DLBCL-associated CTA has paved research avenues into its use for lymphoma vaccine development and immunotherapy (Liggins *et al*., 2004b; Cooper *et al*., 2006; Joseph-Pietras *et al*., 2010).

Despite the long-standing SEREX methodology used in our laboratory for autoantibody profiling studies, the screening data obtained before the start of this project was derived from the use of protein array technology for autoantibody profiling of B-NHL patients. This approach enables a large number of serum samples to be studied within a short time interval and allows autoantibody signatures that may represent disease subgroups to be identified (Horn *et al*., 2006).

A collaboration was established with Dr Derek Murphy and colleagues (Centre for Human Proteomics, Dublin) for the purpose of identifying lymphoma-associated antigens that could be used as components in the development of a routine non-invasive diagnostic screening tool based on protein array technology. The group in Dublin had a history in the development of arrayed cDNA expression libraries and subsequent production of protein microchips, and the group was screening human sera to identify biomarkers in many different

human diseases and types of malignancy. They were keen to use the serum bank from Oxford to expand their studies and include lymphoma.

This offered our laboratory the opportunity to obtain auto-antibody profiling data (including antigen identification) from a much larger number of lymphoma patients than was achievable using SEREX, in return for supplying sera. Our group agreed to perform follow-up validation studies on interesting antigens arising from this array screening and thus this was the project selected for my DPhil. The protein array screening identified a list of many potential antigens for further validation. As described in the first results chapter, HIP1R and JMJD3 were the antigens chosen for further studies. An overview of their family members, general functions and any known association with lymphoma is introduced in the following sections.

1.7 HIP1R

1.7.1 HIP1R and its family member HIP1

Huntingtin interacting protein 1-related (HIP1R) is an endocytic protein involved in clathrin-mediated endocytosis (CME) of surface receptors such as EGFR and transferrin (Engqvist-Goldstein *et al*., 2001) and involved in vesicle trafficking at the *trans*-Golgi network for lysosome biogenesis (Carreno *et al*., 2004; Poupon *et al*., 2008). *HIP1R* maps to 12q24.31 and was identified on the basis of sequence homology with its only known mammalian relative HIP1 (Seki *et al*., 1998).

HIP1 maps to 7q11.23 (Wedemeyer *et al*., 1997) and was originally identified via its interaction with Huntingtin (Htt) (Wanker *et al*., 1997), the protein that is mutated by expansion of a polyglutamine tract in the neurodegenerative Huntington's disease. Unlike

HIP1, murine Hip1r does not bind Htt (Hyun *et al*., 2004a) suggesting that only HIP1 is directly involved in neurodegeneration.

HIP1 and HIP1R have 49% sequence homology and share three similar domains: the ANTH (AP180 N-terminal homology) domain at the N-terminus, a central coiled-coil domain, and a C-terminally localised talin-like (talin, a protein that connects integrin to the cytoskeleton) domain (Hyun *et al*., 2004b) as shown in Fig 1.8. The ANTH, central coiled-coil and talin-like domains confer on both proteins the ability to bind phosphoinositides, clathrin and actin, respectively.

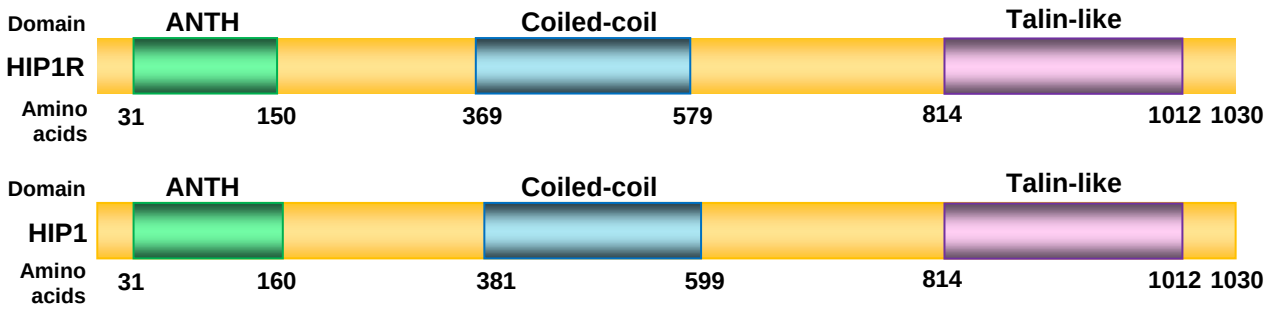

Fig 1.8 HIP1 and HIP1R domains

The ANTH and talin-like domains of HIP1R share a high homology with those of HIP1, and the coiled-coil domain shares the lowest degree of similarity. A detailed alignment of both proteins is shown in Chapter 3. Diagram modified from Bradley et al. (2007a).

HIP1R has been frequently implicated in binding the actin molecule (Engqvist-Goldstein *et al*., 1999; Engqvist-Goldstein *et al*., 2001; Poupon *et al*., 2008). However, the actin-binding capacity of HIP1 is controversial with different groups reporting HIP1 affinity for actin as being absent, far weaker or almost similar to that of HIP1R (Legendre-Guillemin *et al*., 2002; Senetar *et al*., 2004; Wilbur *et al*., 2008). The role of HIP1R in CME has been

widely documented due to the ability of HIP1R to bind both clathrin and actin (Poupon *et al*., 2008; Wilbur *et al*., 2008).

HIP1 was reported as a TAA that is expressed in B-NHL (Bradley *et al*., 2007b). Furthermore, *in vivo* studies implicate this molecule in B-NHL pathogenesis. Thus, shared biological roles of HIP1 and HIP1R could extend to lymphoma pathogenesis, although no data were available at the start of this project on HIP1R in lymphoma.

1.7.2 Functions of HIP1R

A well-documented function of HIP1R is its involvement in CME by facilitating the formation of clathrin-coated vesicles (CCV). CCVs are major carriers for proteins or surface receptors for the internalisation from plasma membrane, and the transport from *trans*-Golgi network (TGN) to lysosomes for degradation or recycling back to plasma membrane (Le Roy and Wrana, 2005; Doherty and McMahon, 2009).

HIP1R promotes the formation of CCV. This is achieved by mediating clathrin assembly through its ability to bind clathrin light chain that regulates the formation and disassembly of CCV (Engqvist-Goldstein *et al*., 2001; Chen and Brodsky, 2005; Wilbur *et al*., 2008). The ability of HIP1R to bind filamentous actin (F-actin) confers its ability to link clathrin with the actin cytoskeleton which provides mechanical force in the formation of CCV (Engqvist-Goldstein *et al*., 1999; Engqvist-Goldstein *et al*., 2004; Brett *et al*., 2006) before final pinching off from plasma membrane or TGN by dynamins, a separate family of endocytic proteins (Bonifacino and Lippincott-Schwartz, 2003; Le Roy and Wrana, 2005).

HIP1R also regulates actin polymerisation. In order to form a functional actin cytoskeleton, actin monomers need to polymerise to form F-actin, and this polymerisation is promoted by cortactin (a monomeric cytoplasmic protein), but negatively regulated by HIP1R (Carreno *et al*., 2004; Engqvist-Goldstein *et al*., 2004). HIP1R mediates the inhibition of actin polymerisation by binding to cortactin via its proline-rich domain at the far C-terminus of HIP1R protein, disrupting the actin polymerisation capabilities of cortactin (Le Clainche *et al*., 2007). This ensures actin polymerisation is tightly regulated for CCV formation and release.

Due to the involvement of HIP1R in CCV formation, the next issue to be addressed was which surface receptors are affected by HIP1R. EGFR is the most widely-studied receptor in the context of depleted or overexpressed HIP1R. Overexpression of HIP1R stabilised EGFR in 293T cells (Hyun *et al*., 2004b), but EGF uptake was not lost in siRNA-mediated downregulation of HIP1R in HeLa cells (Engqvist-Goldstein *et al*., 2004) and no abnormalities were observed in EGF uptake in *Hip1r* $^{-/-}$ mouse embryonic fibroblasts (MEFs) and spleen cells (Hyun *et al*., 2004a). These inconclusive observations suggest that regulation of surface receptors by HIP1R might be dependent on the type of cells investigated.

Hip1r $^{-/-}$ mice were viable, fertile, without any noticeable abnormalities and had similar lifespan to wild-type mice (Hyun *et al*., 2004a). No abnormalities were observed in EGF or transferrin uptake, and no changes in the Akt/PI3K signalling pathways were found in the MEFs and spleen cells investigated. Hyun *et al*. then went on to generate the double-knockout *Hip1r*$^{-/-}$;*Hip1*$^{null/null}$ mice that showed an accelerated phenotype which was already present in *Hip1*$^{-/-}$ mice: accelerated spinal deformity and dwarfism. This suggests that Hip1r and Hip1 might have overlapping roles in some tissues. By using the same *Hip1r*$^{-/-}$ mice from

Hyun *et al*. (2004a), Jain and colleagues (2008) demonstrated that *Hip1r*$^{-/-}$ gastric parietal cells decreased in number, and exhibited disrupted acid secretion with much slower acid release and glandular hypertrophy. The *in vivo* model suggests that phenotypical changes upon depletion of Hip1r are dependent on the specific cell type investigated.

Hip1$^{-/-}$ mice have been generated by three independent research groups and display a significant number of phenotype discrepancies. The first *Hip1*$^{-/-}$ mice model was generated by Rao *et al*. (2001) (these mice were used to generate the *Hip1r*$^{-/-}$;*Hip1*$^{null/null}$ double knockout discussed previously). The *Hip1*$^{-/-}$ mice developed normally and were viable except for testicular degeneration and increased apoptosis of post-meiotic spermatids in adult male mice, indicating a sex-biased phenotype. *Hip1*$^{-/-}$ mice developed by Metzler *et al*. (2003) demonstrated a more severe phenotype with the mice developing tremors, spinal and reproductive defects, and growth retardation culminating in premature death. Oravecz-Wilson *et al*. (2004) generated the final *Hip1*$^{-/-}$ mouse model and in addition to spinal defects, these mice also developed haematopoietic and ophthalmic abnormalities. The authors suggested that the phenotypical discrepancies observed from *Hip1*$^{-/-}$ mice developed by independent groups might be due to different mouse strains used and generation of hypomorphic alleles.

Apart from the generated double-knockout *Hip1r*$^{-/-}$;*Hip1*$^{null/null}$ mice, the phenotypical changes observed in *Hip1*$^{-/-}$ mice were largely different from those observed in *Hip1r* $^{-/-}$ mice. This indicates that both proteins have distinct functions and overlapping roles might be limited to the nervous system i.e. the accelerated spinal deformity observed in the double knockout mice (Hyun *et al*., 2004a). It is possible that co-expression of Hip1 and Hip1r in specific tissue types might indicate the occurrence of overlapping roles.

1.7.3 Association of HIP1R with lymphomas or leukaemias

There is relatively little data available to directly implicate HIP1R in the pathogenesis of haematological malignancies and most of this was not available at the start of this project. Trisomy 12 (+12) is one of the most frequent genetic aberrations found in CLL with intermediate-risk of disease (Quijano *et al*., 2008). Porpaczy *et al*. (2009) showed that *HIP1R* had the strongest correlation with +12 in microarray analysis of CLL patients and *HIP1R* was overexpressed in a separate set of +12 CLL patient samples by qRT-PCR. This observation is not surprising given the fact that *HIP1R* maps to chromosome 12, and they proposed that *HIP1R* expression levels could be used as a surrogate marker to diagnose CLL patients with +12.

HIP1R was chosen as one of 217 genes in a gene-expression based predictor of BL (profiled from 303 BL and DLBCL patients) discriminating BL from DLBCL (Dave *et al*., 2006). *HIP1R* is also overexpressed in E2A-PBX1^{+} ALL, a type of B-cell leukaemia arising from various genetic abnormalities such as the *E2A-PBX1* fusion gene, from three independent studies (Yeoh *et al*., 2002; Ross *et al*., 2003; Li *et al*., 2009). These findings indicate that HIP1R has interesting potential associations with haematological malignancies, a link that has been largely overlooked probably due to more research focus on transcription factors in diseases than endocytic proteins. Moreover, HIP1 is a lymphoma autoantigen that might be functionally able to contribute to disease pathogenesis (Bradley *et al*., 2007b). It is plausible that HIP family of proteins might be associated with lymphomagenesis.

1.8 JMJD3

1.8.1 JMJD3 and its family members UTX and UTY

Jumonji domain containing 3 (*JMJD3*) maps to 17p13.1 and is a histone H3K27 (the lysine 27 residue of histone H3) demethylase that reverses the transcriptional repressive effect of a di- or tri-methylated epigenetic mark on H3K27 (Hong *et al*., 2007; Agger *et al*., 2007). Trimethylated H3K27 (or H3K27me3) is instrumental for maintaining embryonic stem cell pluripotency and plasticity that regulates stem cell differentiation, and X chromosome inactivation (Boyer *et al*., 2006; Schuettengruber *et al*., 2007).

JMJD3, ubiquitously transcribed tetratricopeptide repeat, X chromosome (UTX) and UTY belong to a subfamily of JmjC domain-containing proteins. UTY is the Y-linked homolog of UTX sharing 88% homology with UTX (Hong *et al*., 2007). JMJD3 shares a 32% and 31% homology with UTX and UTY, respectively. JMJD3 differs from UTX and UTY in that it does not have the tetratricopeptide repeat (TPR) domain shared by UTX and UTY (Fig 1.9) (Klose *et al*., 2006). The detailed sequence alignment of all 3 proteins is demonstrated in Chapter 6. Both JMJD3 and UTX (but not UTY) are crucial demethylases that erase the epigenetic mark of di- or tri-methylated H3K27 to activate gene transcription (Agger *et al*. 2007; De Santa *et al*. 2007).

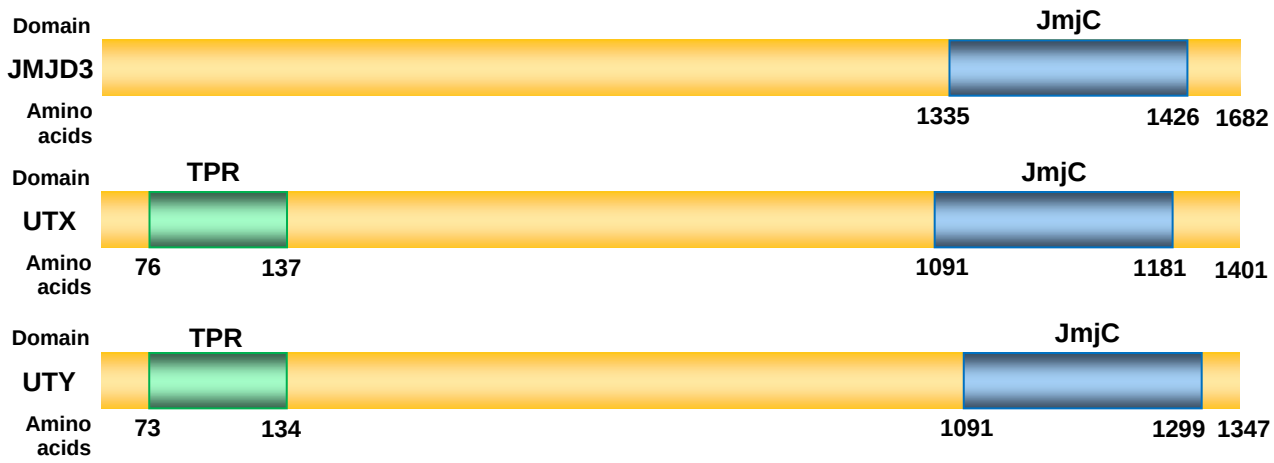

Fig 1.9 JMJD3, UTX and UTY domains

JMJD3 lacks the TPR domain but shares an extensive (more than 30%) homology with UTX and UTY, and all three proteins have a JmjC domain at the C-terminus (Klose et al., 2006). A detailed alignment of the proteins is shown in Chapter 6.

1.8.2 Functions of JMJD3

Epigenetic regulation of transcription via lifting di- or tri-methylation epigenetic marks is the hallmark mechanism of JMJD3 function and recent studies have shed light on how JMJD3 is upregulated. NF-κB induces *Jmjd3* expression and it links inflammation to the control of histone modification involved in lineage determination, differentiation and tissue homeostasis (Boyer *et al*, 2006; De Santa *et al*., 2007). JMJD3 expression is also upregulated upon activation by the MAPK pathway, and its subsequent recruitment and direct binding to the *INK4A-ARF* locus contributes to transcriptional activation of *INK4A-ARF* by demethylating H3K27me3 (Agger *et al*., 2009; Barradas *et al*., 2009).

The roles of JMJD3 in macrophages have been frequently reported. De Santa *et al*. (2006) demonstrated that Jmjd3 is highly induced in activated macrophages in response to inflammation and it functions as a transcriptional activator during cell differentiation. 70% of the genes activated by Jmjd3 in macrophages are lipopolysaccharide (LPS)-inducible genes (De Santa *et al*., 2009), suggesting that JMJD3 plays a role in eliciting the human immune

response. Jmjd3 is upregulated in alternative activated (M2) macrophages (one of two polarised macrophage types that has roles in parasite infection and tumour progression) to remove the H3K27 methylation epigenetic silencing (Ishii *et al*., 2009), indicating that JMJD3 is vital in the acquisition of M2 macrophage phenotype. Recent findings showed that Jmjd3 is essential for M2 macrophage polarisation by transcriptional activation of *Irf4* in response to helminth infection, triggering anti-helminth host responses (Satoh *et al*., 2010).

On the other hand, EZH2 is a histone lysine methyltransferase that trimethylates H3K27 (Völkel and Angrand, 2007), having the mode of action that opposes JMJD3. Expression of EZH2 is activated by the E2F transcription factor (Bracken *et al*., 2003) and together with EED and SUZ12, EZH2 forms the Polycomb repressor complex 2 (PRC2) that trimethylates H3K27 (Völkel and Angrand, 2007). Depletion of JMJD3 increases EZH2 but decreases $p16^{INK4A}$ expression, the protein encoded by *INK4A-IRF* locus (Agger *et al*., 2009), indicating that $p16^{INK4A}$ expression is regulated by both JMJD3 and EZH2. Fig 1.10 shows the mechanism of actions of EZH2 and JMJD3 on chromatin modifications and *INK4A-IRF* transcriptional activation.

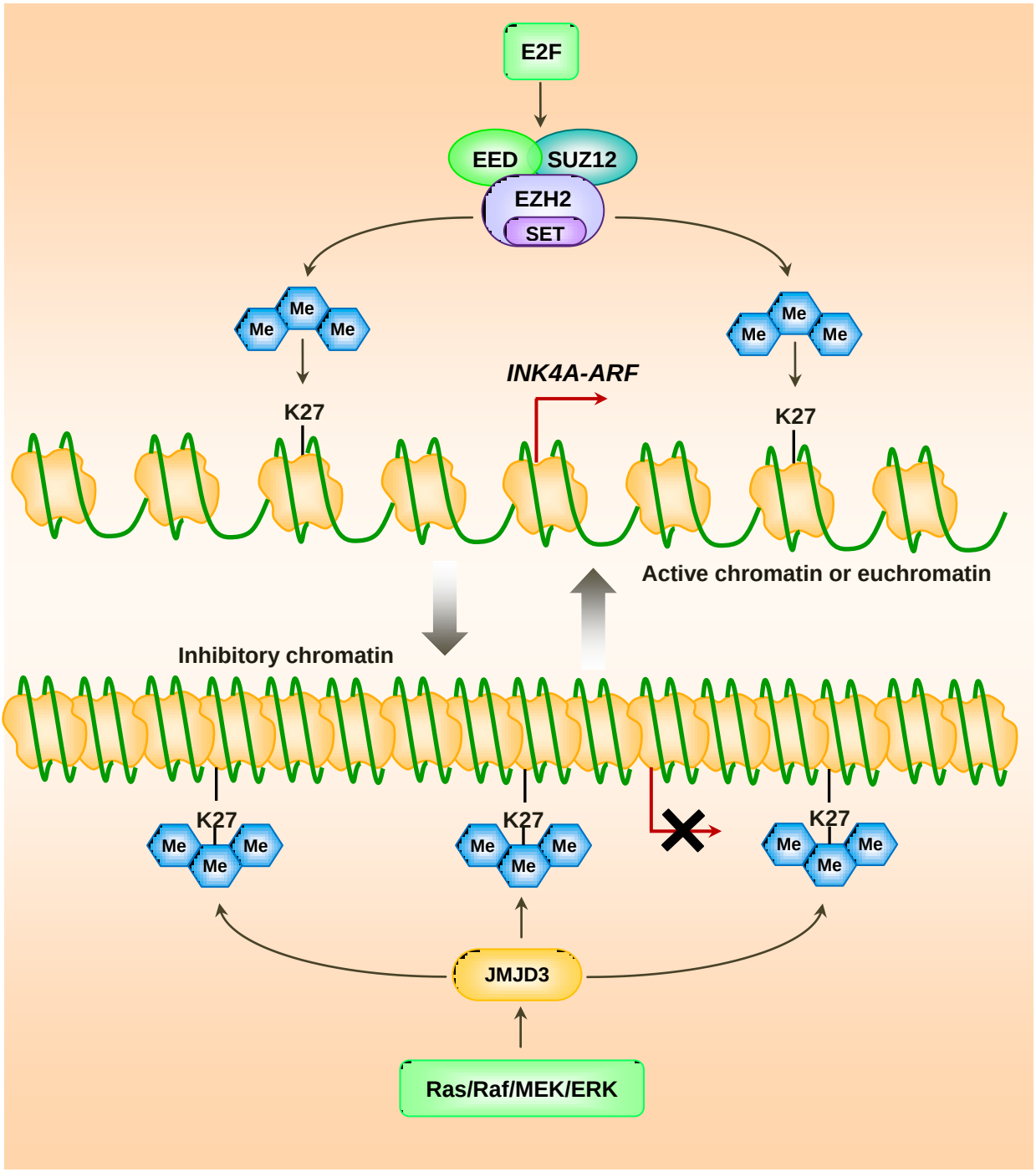

Fig 1.10 Signalling pathways affecting histone modifications by JMJD3 and EZH2

Mutation of tyrosine-641 in the SET domain of EZH2 might inhibit its methylation capability on H3K27 (Morin et al., 2010) while no somatic mutation of JMJD3 has been documented.

1.8.3 Possible association of JMJD3 with lymphomas

JMJD3 has not been implicated in haematological malignancies. However, it has been frequently linked to positive association with blood cell activation: 1) JMJD3 is upregulated by NF-κB in macrophages during inflammatory responses (De Santa *et al*., 2007); 2) Upregulated by MAPK pathway in human embryonic fibroblasts upon senescence (Agger *et al*., 2009); 3) Jmjd3 upregulates *Irf4* expression [IRF4 is also important in differentiation of mature B cells into plasma cells (Shaffer *et al*., 2009)] in M2 macrophages (Satoh *et al*., 2010). This evidence suggests that JMJD3 might have an association with B-cell activation, and possibly with B-NHL, particularly ABC-DLBCL.

In addition, induction of JMJD3 by the MAPK pathway contributes to the transcriptional activation of $p16^{INK4A}$ (Agger *et al*., 2009; Barradas *et al*., 2009). $p16^{INK4A}$ is downregulated in B-NHL including DLBCL and FL transformation into DLBCL (Villuendas *et al*., 1998). This suggests that JMJD3 could act as a tumour suppressor in B-NHL.

Recent interest on methylation profiling of FL cases was motivated by previous studies suggesting that FL might be more susceptible to methylation than other B-NHL (Rahmatpanah *et al*., 2006; Taylor *et al*., 2007). Widespread hypermethylation was identified in FL samples with over half of the methylated genes being targets for epigenetic repression in stem cells by the PRC2 complex (O'Riain *et al*., 2009). This complex contains EZH2, suggesting that JMJD3 expression might be silenced via unknown mechanisms to allow the hypermethylation of FL to occur.

Another possible association of JMJD3 with B-NHL is the observed mutation of *UTX* and *EZH2* in B-NHL or myelomas. Homozygous deletion of different exons of *UTX* occurs

in both HL and myelomas (van Haaften *et al*., 2009). *EZH2* mutation, on the other hand, occurs within its catalytic SET domain in 21.7% of GC DLBCL, 7% of FL cases but none in ABC DLBCL (Morin *et al*., 2010), suggesting that ABC DLBCL may require frequent methylation of H3K27, a mechanism antagonised by demethylation activities of JMJD3.

1.9 BIOINFORMATICS PREDICTION OF GENE REGULATION

One of the eventual observations in this project was high expression of HIP1R in BL cell lines. HIP1R was one of 662 putative MYC modulators identified by a bioinformatics algorithm affecting the transcription of a subset of MYC targets in both normal and malignant human B cells (Wang *et al*., 2009b). Thus, we were interested to investigate the putative role of HIP1R might have in BL as well as elucidating the HIP1R interactome in B cells by using bioinformatics software. The bioinformatics algorithms used are further introduced in the next section.

1.9.1 ARACNe and MINDy algorithms

Gene expression profiling (GEP) by clustering genes with similar expression patterns among distinct groups of patients has enabled classification of disease-related phenotypes. However, this avenue generates a limited number of transcriptional networks that rely on the most differentially expressed genes, without suggesting direct or indirect physical interactions between pairs of genes or proteins. These challenges have sparked the refinement of approaches in reconstructing transcriptional networks from microarray data taking into account both pairwise interaction and indirectly interacting genes, computationally-calculated and theorised from a wide expression spectrum (Margolin *et al*., 2006).

One such computational and mathematical algorithm is called ARACNe (Algorithm for the Reconstruction of Accurate Cellular Networks). This generates a network of gene-

gene interactions relying on a statistical calculation used to maximise information, and minimise false positives inferred solely by co-expression analysis (Basso *et al.*, 2005; Margolin *et al.*, 2006). The reconstructed network is an illustration of nodes representing genes, and edges connecting the nodes representing direct or indirect regulatory interactions (Fig 1.11). ARACNe has a number of limitations: the algorithm is unable to infer the direction of the relationship between nodes, and it is based on two-way interactions only. These limitations are overcome by a novel algorithm called MINDy (Modulator Inference by Network Dynamics) allowing inference of post-translational modulators of a TF that modify its regulatory effects on a subset of known targets of the TF (Wang *et al.*, 2009b). MINDy predicts a three-way interaction between the modulator (M), TF and target of the TF (t) based on microarray data (Fig 1.11 and Fig 1.12).

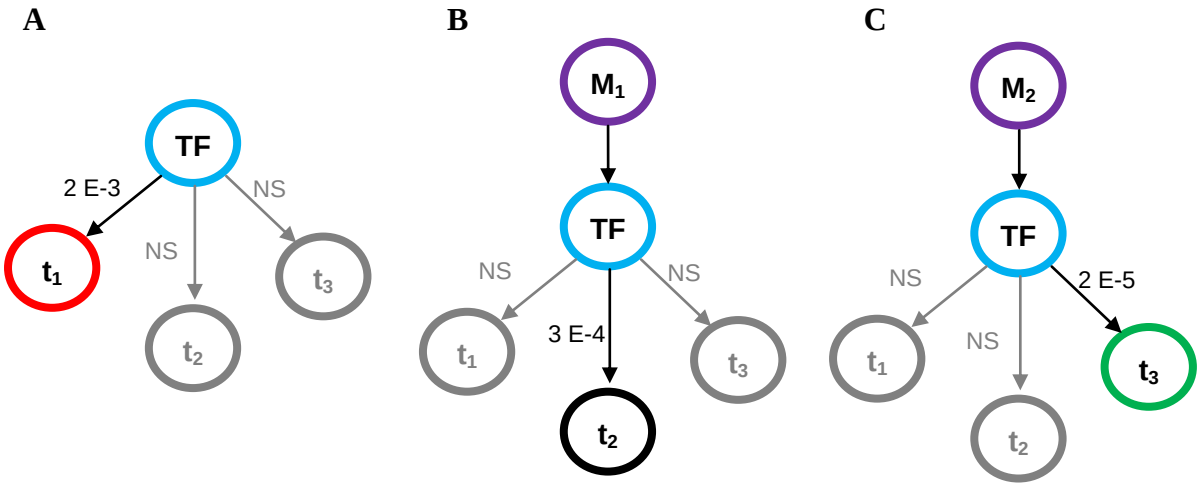

Fig 1.11 Comparison of networks generated by ARACNe (A) and MINDy (B and C)

A: ARACNe generates an unconditional, pairwise relation of the TF with its upregulated (red node) target t_1 and insignificant relation with the rest of its targets (t_2 and t_3); B: MINDy algorithm uncovers indirect regulation of target t_2 via regulation of TF by modulator M_1 that causes TF to cease regulating t_2 (black node denotes unchanged expression) in this example; C: The conditional interaction between TF and target t_3 (green node) modulated by M_2 illustrates another three-way interaction inferred by MINDy. The p values indicate significant or NS (not insignificant) relation. Modified from Wang et al. (2009b).

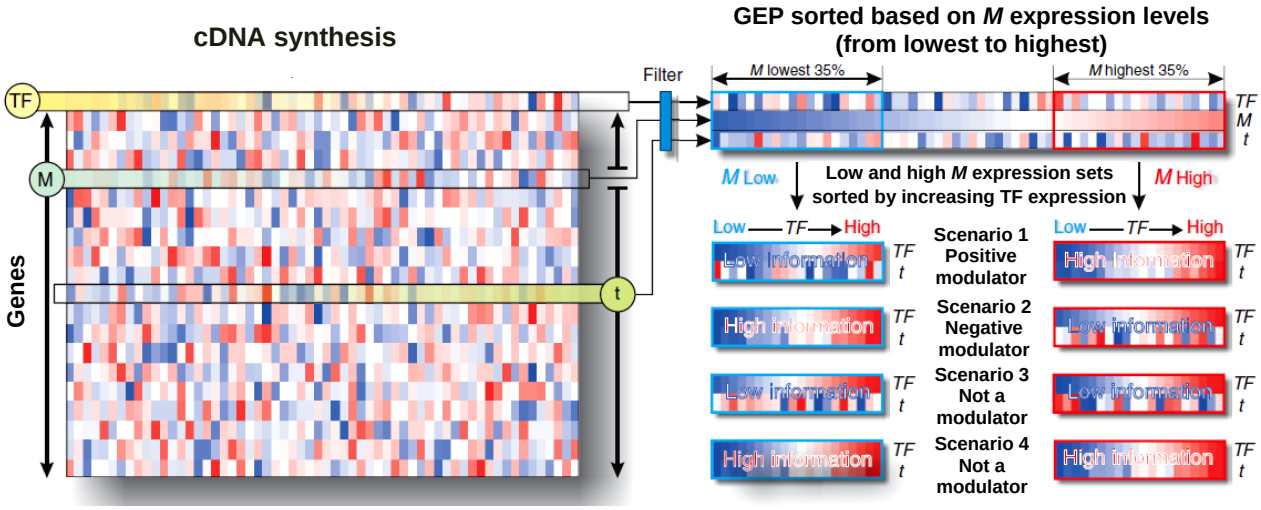

Fig 1.12 Prediction of modulator of transcription factor based on MINDy algorithm

A TF of interest is chosen along with a potential modulator M and a target (t) to be tested. The samples are sorted according to the increasing expression of the modulator M, and two sets of expression were selected, the lowest and highest 35% M expression labelled "M low" and "M high", respectively. The samples are then sorted again according to the increasing TF expression.

In Scenario 1, there is an increase in mutual information (the presence of M expression affects the TF to upregulate the expression of its target t). In Scenario 2, there is a decrease in mutual information (the presence of M disrupts the regulation of t expression by TF). In Scenario 3 and 4, there are no significant mutual information (t expression levels regulated by TF are not affected by the presence or absence of M). Modified from Wang et al. (2009b).

1.10 DPhil PROJECT

Protein array serum screening data from 25 patients of B-NHL (GC DLBCL, NGC DLBCL, transformed DLBCL, FL, MCL) by Dr Derek Murphy (Dublin) had already generated autoantigen profiles for each subgroup of lymphomas. The hypothesis underlying this project was that a preferential or specific humoural immune response to these antigens in lymphoma patients (compared to control sera from normal individuals) might enable the identification and further characterisation of novel proteins with a role in lymphoma pathogenesis. The aims of the DPhil project are as follows:

1) The first aim was to prioritise antigens for further study based on a combination of the frequency and specificity of immunological recognition, literature review and the availability of reagents for further study.

2) The second aim was to validate the available antibody reagents to these antigens and perform an initial analysis of expression patterns at both transcript and protein levels in normal tissues and lymphomas; to determine whether the antigens had any potential diagnostic or prognostic clinical relevance. The expression of both the HIP1R and JMJD3 antigens was further investigated during this project.

3) The third aim was to study the potential biological role of at least one antigen where expression data implicated the molecule in lymphoma biology. Functional experiments in this thesis address both the potential regulators of HIP1R expression and its biological role in B-NHL cell lines.

CHAPTER 2

MATERIALS AND METHODS

2.1 MATERIALS

2.1.1 Patient samples

Sera were collected from adult patients with GC-DLBCL (n = 5), NGC-DLBCL (n = 5), transformed DLBCL (n = 4), FL (n = 6), MCL (n = 5) and age- and sex-matched controls (n = 5) who were attending the Department of Haematology, John Radcliffe Hospital, Oxford (UK). The DLBCL patients were stratified into GC- or NGC-DLBCL subtype by IHC staining of each patient's corresponding formalin-fixed, paraffin-embedded (FFPE) tissue sections, and stratification was based on Hans *et al*. (2004) algorithm. Clinical details of the DLBCL patients only are shown in Table 2.1. The median age of all patients were 58 and informed ethical consent was obtained from all patients in accordance with the Declaration of Helsinki and local ethical approval.

Table 2.1 Clinical details of DLBCL patients

Case ID	Subtype	Sex	Age	Stage	Treatment	Current status from time of diagnosis
DLBCL077	GC	F	59	1	R-CHOP	CR (22 months)
DLBCL078	GC	M	56	4	R-CHOP + RX	Died (19 months)
DLBCL081	GC	F	74	2	R-CHOP	Died (6 months)
DLBCL103	GC	M	53	3	R-CHOP	PR (24 months)
DLBCL110	GC	F	71	3	R-CHOP	PR (23 months)
DLBCL004	NGC	N/A	57	4B	PACEBOM, ESHAP	Died (N/A)
DLBCL047	NGC	M	45	1E	CODOX + IVAC/MTX	CR (72 months)
DLBCL067	NGC	F	77	2	R-CNOP	Remission (60 months)

DLBCL075	NGC	M	74	3A	R-CNOP	Died (3 months)
DLBCL087	NGC	F	76	1	R-CHOP	PR (29 months)
DLBCL005	T-DLBCL	M	51	2	R-CHOP	CR (29 months)
DLBCL045	T-DLBCL	M	54	N/A	N/A	N/A
DLBCL092	T-DLBCL	F	69	N/A	R-CHOP + chlorambucil, prednisolone	Died (72 months)
FOL012	T-DLBCL	M	72	1E	R-CHOP + MTX	Remission (N/A)

NB: DLBCL cases were subtyped according to Hans et al. (2004) algorithm.
Key: GC: GC-DLBCL; NGC: NGC-DLBCL; T-DLBCL: Transformed-DLBCL; R-CHOP: Rituximab, cyclophosphamide, doxorubicin, vincristine, prednisolon; R-CNOP: Rituximab, cyclophosphamide, mitoxantrone, vincristine, prednisolone; RX: Radiotherapy; PACEBOM: Prednisolone, adriamycin, cyclophosphamide and etoposide (PACE) with bleomycin, vincristine and methotrexate (BOM); ESHAP: Etoposide, methyprednisolone, cytarabine, cisplatin; CODOX + IVAC: Cyclophosphamide, doxorubicin, methotrexate, ifosfamide, etoposide, cytatabine; MTX: Intrathecal methotrexate; CR: Complete response; PR: Partial response; F: Female; M: Male; N/A: Data not available.

Commercial cDNA panels of normal tissue, MTC^{TM} cDNA Panel I and II (Clontech, Takara BioEurope, France) and Human Blood Fractions MTC^{TM} Panel (Clontech) were obtained for mRNA expression analysis. Additional lymphocyte subsets and cDNA of DLBCL patients were kindly provided by Dr Charles Lawrie. Collaboration with Dr Randy Gascoyne (BCCA, Canada) kindly provided us with 4 series of DLBCL tissue microarray consisting of 273 cases.

All patient samples were obtained with informed consent from the John Radcliffe Hospital, Oxford; BC Cancer Agency (BCCA), British Columbia, Canada. The ethical approval of the Oxfordshire Clinical Research Ethics Committee was obtained to conduct this work.

2.1.2 Preparation of cell lysates

Whole cell lysates were prepared using RIPA buffer (50 mM Tris HCl pH 8.0, 150 mM NaCl, 1% IGEPAL CA-640, 0.5% sodium deoxycholate, 0.1% SDS). 1-2 x 10^6 cells were washed in 1x PBS and pelleted into 100 µl of RIPA buffer supplemented with 1x complete protease inhibitor cocktail PIC (Sigma Aldrich, UK). The cells were chilled on ice for 20 min.

For equivalent gel loading, the protein concentration of samples was calculated by utilising Bradford Assay as follows: 2 µl of the protein extract in RIPA buffer was added with 1 ml of Bradford Reagent (Sigma Aldrich, UK) in a 1.5 ml eppendorf tube and mixed well. The mixture was transferred into a cuvette and the absorbance was measured at the wavelength 595 nm in a spectrophotometer. A standard curve was prepared using a serial dilution series of 0.1-1.0 mg/ml of a known protein sample concentration i.e. BSA (New England Biolabs, UK) dissolved in RIPA buffer. The standard curve was used to calculate the protein concentration of the samples.

2.1.3 Antibodies

Antibodies were used for immunohistochemistry (IHC), immunofluorescence (IF), Western blot (WB) and flow cytometry (FC) applications as listed in Table 2.2.

Table 2.2 List of antibodies used

Immunogen	Marker for	Antibody	Dilution	Species raised in	Supplier
Hip1r (mouse)	HIP1R/Hip1r	44	1/75 IHC, IF 1:300 WB 1:50 FC	Mouse (monoclonal)	BD Bioscience
HIP1R (human)	HIP1R	3E10	1/100 IHC	Mouse (monoclonal)	Abnova
HIP1 (human)	HIP1	4B10	1/5000 IHC, IF	Mouse (monoclonal)	Abcam

JMJD3 "C-term" (human)	JMJD3	Polyclonal	1/100 IHC	Rabbit (polyclonal)	Abgent
JMJD3 "N-term" (human)	JMJD3	Polyclonal	1/200 IHC	Rabbit (polyclonal)	Abgent
JMJD3 "center" (human)	JMJD3	Polyclonal	1/200 IHC	Rabbit (polyclonal)	Abgent
JMJD3 (human)	JMJD3	Polyclonal	1/500 IHC	Rabbit (polyclonal)	Abcam
JMJD3 (human)	JMJD3	Polyclonal	1/1000 WB	Rabbit (polyclonal)	Cell Signaling
Foxp1 (mouse)	FOXP1/Foxp1	JC12	1/80 IHC	Mouse (monoclonal)	"in house"
Xpress™ Tag	Xpress™ tagged recombinant proteins	R91025	1/400 IHC	Mouse (monoclonal)	Invitrogen
Actin (human)	Sample loading	AC15	1/10000 WB	Mouse (monoclonal)	Sigma Aldrich
IRF4	Activated B cells and plasma cells	M-17	1/400 IHC (D)	Mouse (monoclonal)	Santa Cruz
MUM1	Activated B cells and plasma cells	MUM1p	1/200 IHC (D)	Mouse (monoclonal)	Dako
BCL-6	Centroblasts/ centrocytes	PG-B6p	1/5 IHC (D)	Mouse (monoclonal)	Dako
PAX5	Naïve B cells	24	1/50 IHC (D)	Mouse (monoclonal)	BD Bioscience
XBP1	Plasma cells	143F	1/40 IHC (D)	Mouse (monoclonal)	Dr Giovanna
IgM	Surface IgM	G20-127	1/40 FC	Mouse (monoclonal)	BD Bioscience
CD79b	Surface CD79b	CB3-1	1/100 FC	Mouse (monoclonal)	eBioscience
CD3	T cells	Polyclonal	1/100 IF	Rabbit (polyclonal)	Dako
CD19	B cells	HD37	Undiluted	Mouse (monoclonal)	"in house"
CD20	B cells	L26	1/10 IHC, IF	Mouse (monoclonal)	"in house"
CD22	B cells	4KB128	Undiluted	Mouse (monoclonal)	"in house"
CD30	Activated B- and T cells	BerH2	Undiluted (D)	Mouse (monoclonal)	"in house"
CD68	Granulocytes	KP-1	1/10 IHC (D)	Mouse (monoclonal)	"in house"
CD38	Plasma cells	SPC32	1/100 IHC (D)	Mouse (monoclonal)	Vector laboratories
CD138	Plasma cells	MI15	1/50 IHC (D)	Mouse (monoclonal)	Dako
Immunoglobulin	Negative control antibody	MR12	Variable*	Mouse (monoclonal)	Dako

*Key: IHC (D): Double-immunoenzymatic labelling. *: Dilution factor for the mouse IgG1 negative control antibody was based on the dilution factor used for tested antibody*

2.2 CELL CULTURE

2.2.1 Cell lines and culture conditions

Cell lines were obtained commercially from DSMZ (Braunschweig, Germany) or ATCC (Rockville, USA) and after cell lines were kind gifts from various research groups (Table 2.3). Cells were maintained in RPMI 1640 media supplemented with 10% foetal calf serum (FCS), 2 mM glutamine, and antibiotics [streptomycin (50 µg/mL) and penicillin (50 U/mL)] at 37°C and 5% CO_2. For OCI-LY10, cells were grown in Iscove's Modified Dulbecco's Medium (IMDM; Invitrogen, UK) supplemented with 5% FCS, 5% fresh human plasma, 50 µM 2-beta mercaptoethanol (Sigma Aldrich, UK) and the same concentration of glutamine and antibiotics as described previously. Adherent cells were passaged by washing in PBS followed by addition of 3-5ml of trypsin/EDTA (Lonza Wokingham, UK) for 1-2 minutes to release cells from the container wall, before addition of equal volume of RPMI 1640 for downstream applications.

Counting of cells were performed by using a haemocytometer on a regular basis to maintain the cells at a desired density, and cells were harvested for analysis of mRNA and protein levels when they were in rapid growth phase. For cytospins preparation, a density of 1 x 10^6 cells/ml was required. Adherent cells required trypsinisation prior to cytospins preparation using Shandon Cytospin 2 (Shandon, Runcorn, UK). Cytospin slides were left to air dry overnight at room temperature before performing downstream experiments or for long-term storage at -20^{o}C.

Table 2.3 Sources of lymphoma cell lines

Cell lines	Type of lymphoma	Source
DB, SUDHL6, SUDHL10 OCI-LY3, OCI-LY10	DLBCL	Dr Eric Davis (Bethesda, USA)
MIEU, HLY-1	DLBCL	Dr Talal Al Saati (Toulouse, France)
SUDHL9	DLBCL	Prof. Martin Dyer (Leicester)
MEDB1	PM-DLBCL	Drs S. Brüderlein, P. Möller, T. Barth (Institute of Pathology, Ulm, Germany)

2.2.2 MTS assay

Proliferation of si*HIP1R*-treated or scramble siRNA control-treated cell lines (MIEU, SUDHL4, SUDHL6, SUDHL10, Riva, Raji) were assessed by measuring MTS [3-(4,5 dimethylthiazol-2-yl)-5-(3-carboxymethoxyphenyl-2-(4-sulfophenyl)-2H-tetrazolium] dye absorbance at 0, 24, 48, 72 and 96 hours (h) after treatment. 100 µl of cells were incubated with 20 µl of CellTiter 96 ® AQueous One Solution Reagent (Promega, USA) MTS solution in duplicate in a 96-well plate for 1 h before absorbance was recorded at 490 nm using an enzyme-linked immunosorbent assay plate reader.

2.2.3 Naïve B-cell purification and activation

Peripheral blood mononuclear cells (PBMCs) were purified from blood buffy coats by density gradient centrifugation over Ficoll Paque. Naïve B cells were purified from 60 x 10^7 PBMCs using the naïve B-cell isolation kit (Miltenyi Biotech, Bisley, UK). Purified naïve B cells were cultured for 1 h at 37°C prior to activation and then treated under the following conditions: (1) unstimulated (naïve); (2) stimulated with 50 µg/mL F(ab')2 goat anti-human IgM (Cambridge Biosciences, Cambridge, UK); or (3) stimulated with 1:20 000 wt/vol *Staphylococcus aureus*, Cowan (SAC) strain (Pansorbin cells; Merck Biosciences,

Nottingham, UK) plus 5 ng/mL recombinant interleukin-2 (rIL-2; R&D Systems, Minneapolis, MN). Cells were incubated at 37°C, 5% CO_2 for 44 h. After activation, cytospins were prepared from each sample. The total RNA and protein were extracted from the remaining cells using μMACS mRNA Isolation Kit (Miltenyi Biotech) and RIPA buffer, respectively, for subsequent qRT-PCR and immunoblotting experiments. qRT-PCR and immunoblotting procedures are detailed in section 2.3.2 and 2.4.5, respectively.

2.3 MOLECULAR BIOLOGY PROCEDURES

2.3.1 Generation of full-length HIP1R construct

Cloning: No full-length *HIP1R* cDNAs were available as IMAGE or MGC clones, thus the full-length *HIP1R* cDNA was PCR-amplified by Phusion polymerase (Finnzymes) and cloned into a eukaryotic expression vector. To construct the full-length *HIP1R* (3.2 kb), the cDNA was PCR-amplified in two-halves from Raji cell lines yielding 2 products with similar sizes (1.6 kb). The generated products were subsequently A-tailed and then TA-cloned using pGEM-T Easy (Promega, Madison, WI) and the correct inserts were verified by sequencing (MWG Eurofins, Germany). The inserts were restriction-digested by *Eco*RI and *Xho*I or *Xba*I before the fragments were ligated sequentially to a pcDNA4/His-Max^{TM} (Invitrogen) vector containing the *Eco*RI-*Xba*I site. The final construct was validated by sequencing which identified a single nucleotide difference from the reference sequence (NM_003959.1). The PCR primers used are as follows:

KKW1H-*Eco*RI: 5'-CTCGAATTCATGAACAGCATCAAGAACGTGCC-3'

KKW11H-*Xho*I: 5'-CTCCTCGAGCTGGTCGCTCTTCTCCTCTAGCTTC-3'

KKW12H-*Xho*I: 5'-CTCCTCGAGAAGCTCAAGAGGGAGCTGGAGG-3'

KKW4H-*Xba*I: 5'-CTCTCTAGACTAGTAGTTCACGAGTTGAGCTGGGT-3'

Transformation: *E. coli* XL1 blue competent cells (tetracycline resistant) were transformed with the DNA ligation or uncut plasmid (as a positive control) by mixing on ice, heat shocking for 90 seconds at 42^{o}C followed by 5 min incubation on ice and incubation at 37^{o}C on a rocker at 300 rpm for 1 h. The cells were spread out onto LB agar plates containing ampicillin before incubation overnight at 37^{o}C. Individual colonies were picked and grown in an overnight 5 ml culture. The plasmid DNA was purified from the cells using Qiagen Spin Miniprep Kit (Qiagen, UK) according to manufacturer's instructions. Restriction enzyme digest was performed to confirm the presence of an insert with the expected molecular weight. This was followed by larger scaled 100 ml overnight cultures to enable a larger scale DNA Midiprep (Qiagen, UK) the following day. Restriction enzyme digestion was conducted before validation by DNA sequencing (MWG Eurofins, Germany).

Transfection: HIP1R expression in mammalian cells was achieved by transfecting the plasmid into 293T cells containing low levels of endogenous HIP1R and HIP1. This was performed using Fugene 6 (Roche Diagnostics Boehringer, Mannheim, Germany). Cells at confluency of about 70% on day one of transfection was used in a 25 cm^2 flask, and transfection mix made up of 300 µl serum free RPMI, 9 µl of Fugene and 3 µg of DNA were mixed gently and left at room temperature for 15 min before adding into the flask and incubating for 24 h, followed by preparation of cytospins and/or cell lysates.

2.3.2 Quantitative reverse-transcription polymerase chain reaction (qRT-PCR)

mRNA was extracted from pellets of approximately 1 x 10^7 cells using the µMACS mRNA Isolation Kit according to the manufacturer's instructions (Miltenyi Biotech). Approximately 100 ng mRNA was used as a template for cDNA synthesis using Superscript III (Invitrogen) according to manufacturer's instructions. Polymerase chain reaction (PCR)

was set up using 2 µl cDNA template, 1× buffer for KOD Hot Start Polymerase, 0.2 mM dNTPs, 1 mM MgSO4, 0.3 µM each primer, and 1 U KOD Hot Start Polymerase; and the thermocycler was programmed at 94°C for 2 min, followed by 35 cycles of 94°C for 15 seconds, 60°C for 30 seconds, and 72°C for 30 seconds, and a final extension of 72°C for 10 min. The obtained cDNA was diluted in 1:8 dH_2O before mixing with SensiMix (Quantace) and 200 nM FAM/VIC-labelled TaqMan probe (Applied Biosystems Ltd). Triplicate PCR reactions were prepared for each cDNA sample. The Chromo4^{TM} continuous fluorescence detector system (MJ Research) was used in the quantification of genes expression. PCR consisted of 40 cycles of 95°C denaturation (15 s) and 60°C annealing/extension (60 s). The point at which the PCR product is first detected above a fixed threshold, termed cycle threshold (Ct), was determined for each sample.

To determine the quantity of gene-specific transcripts present in lymphomas relative to 293T cells, their respective Ct values (i.e of the gene of interest, FAM dye-labelled TaqMan probe) were first normalized by subtracting the Ct value obtained from the endogenous control (VIC dye-labelled TaqMan probe) (ΔCt = Ct FAM - Ct VIC). The concentration of gene-specific mRNA in the panel of cell lines studied relative to 293T cells was calculated by subtracting the normalized Ct values obtained with 293T from those obtained with the samples (ΔΔ Ct = ΔCt of samples - ΔCt to those of normal B cells or tonsil), and the relative concentration was determined (relative concentration = $2^{-\Delta\Delta Ct}$). The primer sets and TaqMan Gene Expression Assays (Applied Biosystems) used are listed in Table 2.4, apart from the control target gene *GAPDH* TaqMan control kit obtained from Eurogentec (UK).

Table 2.4 TaqMan probes (Applied Biosystems) used for qRT-PCR

Target	Probe
HIP1R	Hs00391321_m1
HIP1	Hs00193477_m1
JMJD3	Hs00389738_m1
IRF4	Hs00180031_m1
FOXP1	Hs00212860_m1
TBP (control gene)	4326322E
18S RNA (control gene)	4319413E

2.3.3 *HIP1R* silencing by siRNA

Silencing of suspension cell lines (MIEU, Raji, Riva, SUDHL4, SUDHL6, SUDHL10) were carried out using the Amaxa system as follows: Cells at confluency of 2 x 10^6 were resuspended in Nucleofector solution (Nucleofector kit V, C or T depending on the cell lines) with 1.8 µM of HIP1R or scramble siRNA duplexes (Invitrogen), and the cells were electroporated using the Amaxa Nucleofector apparatus and programs M-013 (for Raji cells) or O-017 (for the rest of the cell lines). Cells were harvested at 24 h, 48 h, 72 h and 96 h, and cell lysates were obtained for Western blotting or qRT-PCR analysis. *FOXP1* silencing by siRNA was performed by Dr Philip Brown (NDCLS, Oxford).

Three HIP1R Stealth Select RNAi™ (Invitrogen) siRNA oligonucleotides (Target accession no. NM_003959.1) were used for depletion of HIP1R expression, and scrambled siRNA [Stealth RNAi Negative Control (medium GC)] was used as the control siRNA. The sequences were pre-designed and synthesised by Invitrogen (Table 2.5).

Table 2.5 Details of siRNA oligonucleotides [(Stealth Select RNAi™ (Invitrogen)] used for depletion of HIP1R expression

Oligo ID	Designation	Target sequence	Target exon
HSS113327	'si1'	5'-GGATTGTGAGCTGAAGCTTTCTGAA-3'	7
HSS189770	'si2'	5'-CACCTGGCTGCGGATACCATCATCA-3'	21
HSS189771	'si3'	5'-GGGCCTGGAGGTGACAGATGAGGTA-3'	6

Fig 2.1 illustrates the exon structure of HIP1R and the exons targeted by HIP1R siRNAs, or recognised by TaqMan probe and the anti-HIP1R-44 mAb (clone 44, BD).

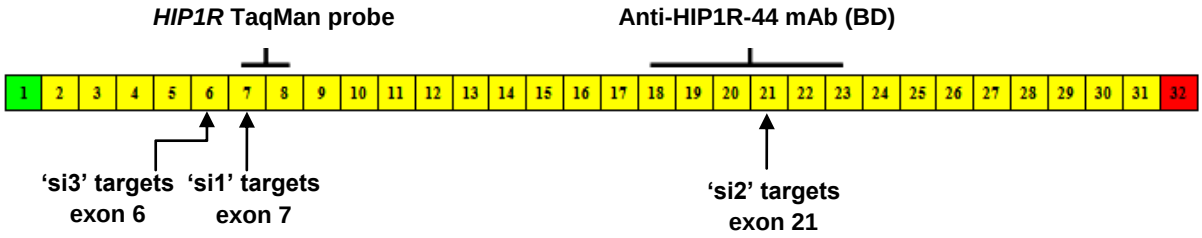

Fig 2.1 Schematic diagram illustrating the exon structure of *HIP1R* (accession number NM_003959.1)

Green shaded exon contains the translational start site, yellow shaded exons are coding exons, and red exon contains the translational stop codon. The exons detected by the HIP1R TaqMan probe (Applied Biosystems) and the exons encoding the immunogen sequence recognised by the anti-HIP1R-44 mAb (BD) are illustrated above the diagram, and the exons targeted by siRNA duplexes are illustrated below the diagram.

2.3.4 SYBR GreenER™ qRT-PCR

mRNA expression of *AKAP12*, *PRDX4* and *NOLC1* in si*HIP1R* cells versus cells treated with a scramble siRNA were quantified by using SYBR GreenER™ qPCR SuperMix Universal (Invitrogen) with the following conditions: The qPCR mix was in a final volume of 20 µL and contained 1x SYBR GreenER™ qPCR Super-Mix Universal, 200 nM each primer,

50 nM Rox dye, and 40% diluted cDNA. The Chromo4^{TM} system (MJ Research) was used to quantify the genes expression. The thermal profile included an initial uracil DNA glycosylase (UDG) incubation for 2 min at 50^{o}C followed by UDG inactivation and DNA polymerase activation for 10 min at 95^{o}C. This was followed by 40 cycles of 95^{o}C for 15 s, 56^{o}C for 35 s and 60^{o}C for 60 s.

The integrity of amplification indicated by a single melt peak for each product was verified by a dissociation curve analysis at 95^{o}C for 15 s, 60^{o}C for 1 min and 95^{o}C for 15 s. *18S RNA* (4319413E, Applied Biosystems) was used as the control gene. The primers used for the qRT-PCR reactions were designed by using OligoPerfect™ Designer (Invitrogen; http://tools.invitrogen.com/content.cfm?pageid=9716). Primers were designed to produce an amplification product which spanned at least two exons except for the amplification of *AKAP12*. Each qRT-PCR reaction was conducted in parallel with non-template water control in triplicate to rule out the possibility of genomic DNA amplification. Primer sequences, position in the coding region, exon(s) spanned by the primers and the expected qRT-PCR product size are listed in Table 2.6.

Table 2.6 Details of primers used for SYBR Green qRT-PCR

Primer	Sequence (5' → 3')	Exon(s) spanned	Product size (bp)
AKAP12 for	TGAAGTCGATGAGCAGGTTG	Within exon 3	177
AKAP12 rev	CTTTGTCGGTGGCTTTACAA		
PRDX4 for	ATTATCGCTTTTGGCGACAG	3 → 4	100
PRDX4 rev	ATGGGTAAACCGGACCTAAT		
NOLC1 for	AGACTAAAGCCCCTCCCAAA	5 →6	100
NOLC1 rev	TCGTCGTCGTCATCGTCACT		

2.3.5 Generation of HIP1R lentiviral particles and transduction

Generation of HIP1R lentiviral particles: Overexpression of HIP1R in the DB, OCI-LY3 and OCI-LY10 DLBCL cell lines were achieved by infection of the cells with a pLenti6.3 lentivirus vector (Invitrogen) expressing HIP1R or Express-tagged GFP-only control.

Initially, the full-length *HIP1R* cDNA from the pcDNA4/His-Max^{TM} (Invitrogen) vector was subcloned into pCR-Blunt II-TOPO (Invitrogen) as follows: 1 µl of construct (pcDNA4/His-Max^{TM} containing *HIP1R* cDNA) (~75 ng/µl), 1 µl salt solution (1.2 M NaCl, 0.06 M $MgCl_2$), 4 µl dH_2O, 1 µl of pCR-Blunt II-TOPO vector (10 ng/µl). The TOPO cloning reaction was mixed gently and incubated for 5 min at room temperature. The reaction was then placed on ice and transformed into One Shot Competent Cells (*E. coli*) as follows: 2 µl of the TOPO cloning reaction was added into a vial of One Shot Competent *E. coli* and incubated on ice for 5 s for 30 min. This was followed by heat shock of the cells for 30 s at 42°C without shaking; the tubes were immediately transferred to ice and mixed with 250 µl of room temperature S.O.C. medium. The tubes were incubated on a rocker (200 rpm) at 37°C for 1 h before streaking out onto LB agar plates containing kanamycin and incubated overnight at 37°C. Individual colonies were picked and grown in LB culture overnight at 37°C, and DNA was purified using Qiagen Spin Miniprep Kit (Qiagen, UK).

This was followed by subcloning of the full-length *HIP1R* cDNA into the destination vector pLenti6.3/TO/V5-DEST (Invitrogen) vector by LR recombination reaction as follows: 1 µL of 5× LR buffer, 0.5 µL of LR clonase, 1 µL of destination vector pLenti6.3/TO/V5-DEST (~75 ng/µL), 1.5 µL of entry construct (pCR-Blunt II-TOPO containing full-length *HIP1R* cDNA) mini-prep DNA (~50 µg/ml), and 1 µL TE (Tris-EDTA) buffer. The reactions were incubated at 25°C for 1 hour followed by addition of 1 µl Proteinase K solution and

incubated at 37°C for 10 minutes to terminate the reaction. 1 µl of the LR reaction was transformed into 50 µl of One Shot® OmniMAX™ 2 T1 Phage-Resistant Cells (Invitrogen). The reaction was incubated on ice for 30 min followed by heat-shock of the cells at 42°C for 30 seconds. 250 µl of S.O.C. medium was added and incubated on a rocker (200 rpm) at 37°C for 1 hour. Growing the cells on LB agar plates or medium, and DNA extraction were performed as indicated in the TOPO reaction except the use of ampicillin selection marker.

293FT producer cell lines were cultured to a confluency of 70-80%. Co-transfection of the cell line with pLenti6.3-HIP1R construct and ViraPower Packaging Mix (Invitrogen) was carried out using Fugene 6 (Roche Diagnostics Boehringer, Germany). The viral supernatant was collected after 24 h, and the cells were replenished with fresh media. Collection of the viral supernatant was repeated after another 24 h cycle for 3 days.

Transduction of cell lines: The 3 batches of viral supernatant produced every 24 h for 3 days were used separately to infect the cells without dilution in a 6-well plate at the confluency of 1 x 10^6 cells, yielding transduction experiment in triplicates. Cells were grown in the viral supernatant for 4 days, and 0.1 x 10^6 cells were harvested at 24 h, 48 h and 96 h time point for immunostaining with anti-HIP1R (clone 44, BD) or anti-Xpress™ (Invitrogen) mAb, or fluorescent imaging of GFP protein. After 96 h of transduction, the viral supernatant was replaced with fresh media containing Blasticidin (Invitrogen) to select for stably transduced cells for 12 days, and the media was changed with fresh Blasticidin-containing media every 2-3 days. Efficiency of the antibiotic selection process was examined by immunostaining with anti-HIP1R (clone 44, BD) or anti-Xpress™ (Invitrogen) mAb.

2.4 PROTEIN PROCEDURES

2.4.1 Plasma screening on high density protein arrays

These procedures were performed by Dr Derek Murphy and colleagues (Royal College of Surgeons in Ireland). Briefly, high-density protein arrays of the protein expression set of the hEx1 library were obtained from RZPD (German Resource Centre for Genome Research) and prepared as described by Büssow *et al.* (1998). Blocking of the filters were conducted in 3% non-fat milk in TBS-tween (TBS, 0.1% v/vTween 20) for 2 h, washed twice in TBS-tween followed by incubation with human plasma diluted 1/20 in 2% w/v BSA/TBS-tween for 16 h. Three 30 min of TBS-tween washes were performed and subsequent incubation with secondary antibody (mouse anti-human IgG, Sigma) in 2% w/v BSA/TBS-tween. The filters were washed in TBS-tween 3 times for 30 min each wash, followed by incubation with tertiary antibody (rabbit-antimouse-IgG-AP, Sigma) in 2% w/v BSA/TBST. The filters were washed for three times in TBS-tween for 20 min, 10 min in TBS, and 10 min in AP buffer (1 mM MgCl2, 0.1 M Tris pH 9.5). Incubation in 25 mM Attophos (JBL Scientific) was conducted in AP buffer for 5 min. Illumination of the filters with long-wave UV light was performed and images taken using high-resolution CCD detection system (Fuji) and analysis of image was done by using VisualGrid (GPC Biotech, Germany).

2.4.2 Enzyme-linked immunosorbent assay (ELISA) of recombinant proteins

Recombinant protein at 5 µg/ml diluted in dH_2O (as the antigen) was prepared and 50 µl was added into each well of an ELISA plate, and left to coat the wells overnight at room temperature. On the following day, the antigen solutions were discarded and wells were washed with 1x PBS-tween for 5 times. 200 µl of blocking solution (5% marvel in PBS-tween) was added into each well for 2 h at room temperature. The wells were washed with PBS-tween for 5 times before filling the wells with 50 µl 1x PBS. Serial dilutions of patient

sera (as the source of autoantibodies) at 1/10, 1/50, 1/100, 1/200 was performed, added into appropriate wells and incubated for 1 h at room temperature. The sera were discarded and wells were washed with PBS-tween for 5 times before incubation with 50 µl HRP-conjugated secondary antibody (rabbit anti-human antibody 1/8000, Dako) for 1 h at room temperature. The wells were washed with PBS-tween for 5 times and incubated with 50 µl of ABTS substrate solution (Roche) for 15 min at room temperature. 1% SDS in dH_2O was added to stop the developing reaction and results were obtained on a platereader at 405 nm.

2.4.3 Immunohistochemistry

Immunostaining of cytospin preparations: The sections that were kept at 4^oC were first thawed for 10 min on bench before fixation with 100% acetone for 10 min and air dried for 20 min. Hydrophobic PAP pen (Menarini Diagnostics, Wokingham, UK) was used to draw around the section and primary antibodies were added onto the sections after dilution at desired concentration in 1x PBS. After 30 min of incubation, slides were washed in 1x PBS and 1x PBS-Tween [300 µl Tween-20 (Sigma Aldrich) per litre 1x PBS] for 5 min, and horseradish peroxidase-conjugated secondary antibody anti-mouse/rabbit from Envision kit (Dako) were added and incubated for 30 min. The slides were washed as previously with 1x PBS and 1x PBS-Tween, developed in 3,3'-diaminobenzidine (DAB, supplied in the Envision kit) substrate and counterstaining in haematoxylin [Haematoxylin Solution, Gill No.2 (Sigma Aldrich)] for 5-30 seconds and rinsed in tap water for 1 min before mounting in Aquamount (VWR, Lutterworth, UK) for aqueous mounting or Aquatex (VWR) for non-aqueous mounting.

Cutting sections from FFPE blocks: The FFPE blocks were checked to ensure that the tissue was not close to exhaustion. FFPE blocks were kept chilled in 4^{o}C fridge or on ice before cutting. Sections of 4 µm thickness were cut serially on a rotation microtome (model 0325; Anglia Scientific Instruments, Cambridge, UK) using microtome blades (Thermo Fisher, Eastbourne, UK) and let sit on 37^{o}C water bath before mounting on Superfrost (VWR, Lutterworth, UK) or Snowcoat Xtra (Leica Microsystems, Eynesbury, UK) adhesive slides. The sections were incubated overnight at 37^{o}C and stored at room temperature.

Immunostaining of FFPE sections: The sections were first placed in a 60^{o}C incubator for 10 min, dewaxed in Citroclear (HD Supplies, UK) for 10 min, followed by serial rehydration for 5 min each as follows: Twice in 100% industrial methylated spirit or IMS (Oxford Radcliffe Hospital, Oxford, UK), 70% IMS, 50% IMS, 30% IMS, tap water. Antigen retrieval was performed by microwaving in 50 mM Tris/2 mM EDTA (pH 9.0) at full power for 10 min in a pre-heated pressure cooker. The slides were cooled down in 1x PBS, hydrophobic ink was applied around the section, and peroxidase block (0.3% H_2O_2 and 0.1% Na Azide in dH_2O) was applied to block endogenous peroxidase activity. Primary antibodies diluted in 1x PBS were applied for 30 min, washed in 1x PBS and 1x PBS-Tween for 5 min before applying secondary antibody from the Envision kit (Dako) for 30 min. The slides were rinsed in 1x PBS and 1x PBS-tween followed by developing, counterstaining and mounting as described for cytospin preparations.

Double immunoenzymatic labelling of FFPE sections: The same procedures were performed as immunostaining of FFPE sections described above for the application of the first primary antibody without applying the counterstain, followed by the secondary antibody and detection using Vector SG (Vector Laboratories, Peterborough, UK) blue horseradish

peroxidase substrate kit. Slides were washed in tap water, dehydrated in xylene and mounting in VectaMount (Vector Laboratories). Anti-HIP1R mAb (clone 44, BD) was used as the first antibody. Scoring of DLBCL TMA series was performed by observers (ES, AHB, KP and KKW) blinded to the clinical diagnosis.

2.4.4 Double immunofluorescent labelling of HIP1R and CD3/CD20 in reactive tonsil

The reactive tonsil sections were dewaxed in citroclear and antigen retrieval was performed by microwave pressure cooking for 3 min at full pressure in 50 mM Tris and 2 mM EDTA, pH 9. After subsequent blocking with Serum-free Protein Block (DAKO) for 10 min, slides were rinsed in PBS, then 1:75 dilutions of the primary antibodies HIP1R (IgG1) and CD3 (1:100, polyclonal, Dako) or CD20 (1:10, IgG2a, Dako), were applied together for 45 min at room temperature. After washing in PBS, the isotype-specific secondary antibodies, goat antimouse IgG2a AlexaFluor-488, and goat antimouse IgG1 AlexaFluor-568 (Molecular Probes, Eugene) were added and incubated for an additional 1 h at room temperature. The slides were rinsed thoroughly in PBS and coverslips applied with a few drops of Fluorescent Mounting Medium (DAKO). Immunostaining was run in parallel without application of primary antibodies as controls.

2.4.5 SDS polyacrylamide gel electrophoresis (SDS PAGE)

Protein samples were boiled for 5 min in gel loading buffer (0.2M Tris-HCl pH6.8, 0.28M SDS, 40% glycerol, 0.6M β-mercapthoethanol, 0.05M EDTA, 12 mM bromophenol blue) and then loaded into wells on the gel. Separation was done on the basis of size using SDS-PAGE in 7.5% gel (resolving gel: acrylamide 7.5%, 0.375M Tris pH 8.8, sterile MQ-water 42%, SDS 0.1%, APS 0.1%, TEMED 0.1%; stacking gel acrylamide 5%, 0.125M Tris pH 8.8, sterile MQ-water 72%, SDS 0.1%, APS 0.1%, TEMED 0.1%) and 1x SDS reservoir

buffer (0.192M glycine, 0.025M Tris, 0.1% SDS) at 100V for 1h. Molecular weights were determined by comparing with standard protein markers (Full range rainbow markers, GE Healthcare). Following electrophoresis, gels underwent Coomassie blue staining or Western blotting.

Coomassie blue staining: The gels were stained with Coomassie Brilliant Blue R (1.25% in fixing solution, Sigma Aldrich) and destained in methanol:acetic acid:water (1:1:8 v/v) until the background was clear.

Western blotting: The gels were transferred to Hybond ECL Nitrocellulose Membrane (GE Heatlhcare) at 10V for 1h. Membrane was then incubated in blocking buffer (5% skimmed milk powder in 1x PBS) for 1h, followed by incubation with primary antibody diluted in 2% skimmed milk powder overnight at 4^{o}C. The membrane was washed in 1x PBS-tween for 1 h followed by incubation with HRP-conjugated secondary antibody (Dako) diluted 1/5,000 in 1x PBS. Immunodetection was performed using enhanced chemiluminescence (ECL) reagent (GE Heatlhcare). Equal volumes of the ECL detection reagents 1 and 2 were mixed, and the membrane incubated in the solution for 1 min. The membrane was wrapped in Saran Wrap, exposed to X-ray film in a cassette to develop the X-ray film. Control antibody (actin: 42kDa) was used without stripping the blot as it has different molecular weights from the original protein target [HIP1R and HIP1: 120 kDa; JMJD3: 180 kDa (predicted molecular weight)].

2.4.6 Fluorescence-activated cell sorting (FACS)

0.25 x 10^6 cells were resuspended in 1ml of FACS wash in a standard FACS tube. Cells were spun down at 1500 rpm for 5 min and supernatant was discarded by decanting. Primary antibody, Phycoerythrin (PE)-conjugated anti-IgM (BD) or PE-conjugated anti-CD79b (eBioscience), was diluted in 50 µl FACS wash and applied onto cells for 20 min. Cells were spun down in 1 ml of FACS wash and subsequently resuspended in 500 µl of FACS Fix (eBioscience) and cells were analysed by using FACS Calibur flow cytometer from Becton Dickinson (Heidelberg, Germany) in the fluorescence channel FL-2 with an excitation beam of 488 nm and detection of light at 585 nm (emitted by PE conjugated to the primary antibody).

To exclude dead/dying cells and therefore non-specific antibody-binding cells, cells were gated according to forward-angle light scatter and side-angle light scatter on a dot plot, and at least 10,000 cells were counted with the flow cytometer using CellQuest (BD, Germany) software. Analysis of data, construction of flow cytometry graphs (or histograms), and acquisition of mean fluorescent intensity (MFI, relative fluorescence units) of IgM or CD79b expression were performed using FlowJo software (version 7.6.1, Tree Star Inc.). The cells were gated on the basis of their forward and side scatter before acquisition of flow cytometry histograms and MFI were obtained by using FlowJo. All FACS staining and data analysis was performed along with an isotype-matched (IgG1) negative control antibody which did not stain the cells.

2.5 BIOINFORMATICS ANALYSIS

2.5.1 Gene Ontology over-representation analysis

To identify relevant functions or biological processes of a set of genes or proteins, Gene Ontology (GO) (GO Consortium, 2004) enables the identification of the enrichment of a set of genes or proteins known to have the same biological function, and the degree of over-representation is assessed by Fisher's exact test (*p*-value) and complemented by false discovery rate (FDR or *q*-value) (Storey and Tibshirani, 1995) that estimates the proportion of false positives.

The genes encoding the antigens were first categorised to their specific annotated GO terms before sub-grouping into 2 major categories, namely "Molecular Function" (MF) and "Biological Processes" (BP) category, by using the software Expression Analysis Systematic Explorer. (Hosack *et al*., 2003) The fold enrichment of a specific GO term in MF category is then calculated as follows:

$$\text{Background } \% = \left(\frac{\text{Sum of genes assigned to MF}}{\text{Sum of genes assigned to a specific GO term in MF}} \right) \bullet 100$$

$$\text{Input } \% = \left(\frac{\text{Sum of the shortlisted lymphoma-associated antigens}}{\text{Sum of the antigens assigned to the queried GO}} \right) \bullet 100$$

$$\text{Fold enrichment} = \frac{\text{Input } \%}{\text{Background } \%}$$

2.5.2 Ingenuity Pathway Analysis, ARACNe and MINDy algorithm

Microarray data generated from si*FOXP1* studies by Dr Philip Brown (Oxford) were analysed by Ingenuity Pathways Analysis or IPA (Ingenuity Systems, http://www.ingenuity.com) in order to identify pathways affecting HIP1R. ARACNe is a computer-generated algorithm able to identify interaction between one molecule with another (Basso *et al*., 2005) and MINDy is another recent algorithm that is able to predict putative post-translational modulators of transcription factors (Wang *et al*., 2009b). Both algorithms were adopted to investigate these associations in a microarray dataset containing 100 samples of normal and malignant B cells (Table 2.7) by using the software geWorkbench version 2.0.1 (http://wiki.c2b2.columbia.edu/workbench/index.php/Home), a free open source genomic analysis platform developed at Columbia University.

Table 2.7 Breakdown of samples analysed with ARACNe and MINDy algorithm

	Genes	Abbreviation	Number (n)
Non-malignant	Centroblasts	CB*	10
	Naïve B cells	N*	5
	Memory B cells	M*	5
	Centrocytes	CC*	5
Malignant	B-cell chronic lymphocytic leukaemia	CLL	12
	Purified B-cell chronic lymphocytic leukaemia	P-CLL*	22
	Burkitt's lymphoma	BL	4
	Diffuse large B-cell lymphoma	D*	3
	Purified diffuse large B-cell lymphoma	DLCD/DLCL*	16
	Follicular lymphoma	FL	6
	Hairy cell leukaemia	HCL	7
	Primary effusion lymphoma	PEL	5

**: Abbreviations here were only used in HeatMap visualisation in Chapter 4 and not elsewhere in the thesis.*

CHAPTER 3
LYMPHOMA-ASSOCIATED ANTIGENS

INTRODUCTION

3.1 LYMPHOMA-ASSOCIATED ANTIGENS AND PROTEIN ARRAYS

3.1.1 Non-invasive cancer diagnostic

The development of non-invasive methods for cancer diagnosis could in the future prevent the need to biopsy lymph nodes for lymphoma diagnosis. This could both save patients from an invasive procedure and cuts costs to the health service by removing the need for a hospital visit. This approach potentially also excludes current sampling complications, such as inadequate biopsy size, tissue fragmentation, and intra- and inter-observer variability in interpreting immunolabelling results (Regev *et al*., 2002). Furthermore, it represents an alternative approach for the detection of early malignancy by screening asymptomatic subjects. However, the lack of sensitivity and specificity of non-invasive diagnostics using biological fluids has generally precluded their use for the primary diagnosis of cancer (Duffy, 2007).

3.1.2 Circulating proteins and nucleic acids

There are two main classes of circulating molecules that can be detected in patients' sera: circulating proteins (or peptides), and circulating nucleic acids (CNA) including miRNA, DNA and mRNA. Detection of CNA represents one approach to non-invasive diagnosis of malignancies. There has been considerable interest in detecting viral DNA, e.g. CNA from Epstein Barr Virus (EBV) has been detected in nasopharyngeal carcinoma patients (Lo *et al*., 1999) and both specific genetic and epigenetic tumour markers in sera (reviewed by Tsang and Lo, 2007). Circulating tumour-derived miRNAs (a class of small non-coding

RNAs that regulate gene expression at the post-transcriptional level) in the serum were first reported by Lawrie *et al*. (2008). The stability of these miRNAs makes them particularly attractive markers and may help to overcome some of the technical difficulties that have complicated comparisons of CNA detection between laboratories (Tsang and Lo, 2007).

To date, circulating proteins have been more frequently studied and serum protein markers have been incorporated into routine clinical cancer diagnosis, an example being CA-125 in the screening for ovarian cancer (Bell *et al*., 1998; Jacobs *et al*., 1999). However, the lack of disease specificity in the detection of circulating proteins in serum can be a disadvantage of their use in disease diagnosis, for instance the elevated prostate-specific antigen (PSA) levels are not specific for prostate cancer (Zappa *et al*., 1998; Bunting, 2002; Ford *et al*., 2005). Nonetheless, autoantibodies represent attractive markers because of their specificity for tumour markers, and their stability in the circulation, which is in part mediated by interaction with neonatal Fc receptor (FcRn) in the kidney that recycles the IgG molecules back into the serum (Ghetie and Ward, 2000; Ward *et al*., 2003). Furthermore, there are well-established techniques for their quantitation, e.g. ELISA.

3.1.3 Comparison of SEREX and protein arrays for characterising the anti-tumour humoural immune response

Both SEREX and protein array technology adopt a similar approach for identifying the antigens targeted by circulating autoantibodies in patients' sera by screening technologies using bacterially expressed recombinant protein libraries. The main differences between the approaches relate to their cost, the requirement for specialised equipment, the volume of serum required, the time and labour involved in screening and antigen identification. SEREX generally uses individual sera (Liggins *et al*., 2004), or a very small pool of sera for primary

screening. The necessary repeat screening to eliminate false positive clones and/or assess the frequency of recognition of numerous autoantigens with additional patients and control sera is laborious and time-consuming, as noted by other research groups (Koroleva *et al*., 2004; Cha *et al*., 2006; Bi *et al*., 2010). However no specialised equipment is required, making this technology widely accessible to the academic community.

Protein arrays require more specialised facilities and are still relatively expensive. However, they facilitate the screening process by avoiding the necessity for large volumes of serum and do not require the removal of antibodies reactive with bacterial antigens i.e. the serum cleaning step required in SEREX (Liggins *et al*., 2005). Importantly, the high throughput screening increases the number of antigens identified as all sera can be screened against the entire library (Lueking *et al*., 2005; Horn *et al*., 2006), rather than being used to validate a subset of antigens identified using small number of sera. Furthermore, the known location of pre-identified clones on the array means that antigen identification can be made immediately without the further gene cloning and sequencing steps needed for SEREX.

3.1.4 Lymphoma-associated antigens identified using protein arrays

Before the start of this project, a collaboration was established between the LRF Lymphoma Antigens Programmes (Dr Alison Banham and Dr Karen Pulford, Oxford) and the Centre for Human Proteomics (Dr Derek Murphy, Dublin). The aim of the collaboration was to use protein arrays to screen circulating autoantibodies (IgGs) from lymphoma patients. The collaborating group in Dublin has been involved specifically in the development of protein arrays for use as tools for detecting and identifying autoantibodies in serum, and subsequent production of protein microchips (Lueking *et al*., 2003; Horn *et al*., 2006). The primary aim of my DPhil project was to validate and characterise some of the antigens arising

from the protein array screening. Our laboratory was particularly interested in identifying and characterising new molecules that might have a role in lymphoma pathogenesis. It was hoped that this proof-of-principle data would aid in the future development of protein microchips by the group in Dublin for the diagnosis and/or prognosis of cancer patients.

The array screening was performed before the start of this project. Sera from patients with different lymphoma subtypes were used to screen a protein array containing more than 10,000 proteins to identify lymphoma-associated antigens (Fig 3.1). The individual lymphoma serum samples screened by the protein arrays were derived from patients with *de novo* GC-DLBCL (n = 5), *de novo* NGC-DLBCL (n = 5), transformed DLBCL (transformed from FL) (n = 4), FL (n = 6), MCL (n = 5) and age- and sex-matched controls (n = 5).

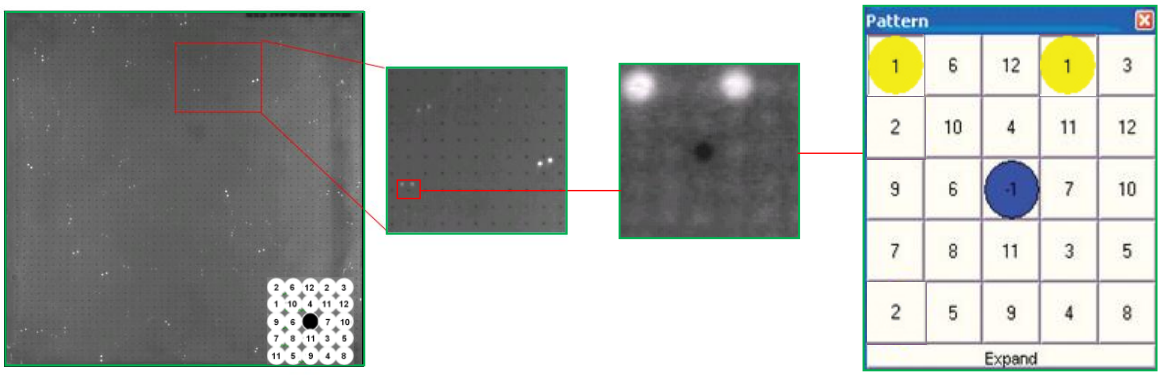

Fig 3.1 Screening of circulating antibodies in patients' sera by using protein arrays

Recombinant human proteins are arrayed in duplicate. The two positive signals shown in the enlarged pictures indicate serum IgG antibodies binding to a clone arrayed twice in a specific pattern. Positive clones were identified using the 5×5 gridding pattern surrounding an ink guide dot (lower right corner of the protein array picture, and the computerised format) which allows rapid and accurate identification of positive clones.

Diagram modified from Kijanka et al. (2010).

A large number of antigens were identified by the protein array screening approach. These underwent further shortlisting on the basis of the frequency of antigen recognition from sera across different subtypes of B-NHL or within a particular lymphoma subtype, this

being more frequent than reactivity with healthy donor sera, resulting in a 'short' list of 35 antigens as detailed in Table 3.1.

Analysis of the array data identified FL as the B-NHL subtype eliciting the immune response to the highest number of antigens [(n = 117, $p = 5.88E^{-31}$ (total number of antigens recognised by this subgroup of patients versus controls)], followed by transformed DLBCL (n = 77, $p = 4.13E^{-26}$), GC-DLBCL (n = 70, $p = 2.57E^{-17}$), MCL (n = 50, $p = 1.9E^{-10}$) and the lowest frequency of autoantibodies was detected in NGC-DLBCL (n = 23, $p = 0.004$).

Table 3.1 Frequency of serological-reactivity against 35 lymphoma-associated antigens identified using protein arrays

No	Antigen	Control (n = 5)	GC-DLBCL (n = 5)	NGC-DLBCL (n = 5)	Trans-Formed DLBCL (n = 4)	FL (n = 6)	MCL (n = 5)	All B-NHL (n = 25)
1)	PIP5K1C	1	4	1	4	6	4	19/25 (76%)
2)	CDKN2C	0	5	0	4	6	3	18/25 (72%)
3)	EXT1	1	4	2	3	5	2	12/25 (64%)
4)	PGLS	0	3	1	3	5	3	15/25 (60%)
5)	NUDT16	0	4	2	1	5	2	14/25 (56%)
6)	ZNF579	1	4	1	4	4	1	14/25 (56%)
7)	ZNF133	1	1	1	4	3	4	13/25 (52%)
8)	ARPP21	0	3	1	3	4	1	12/25 (48%)
9)	MAFF	0	3	1	1	5	2	12/25 (48%)
10)	RPL4	0	1	0	3	5	3	12/25 (48%)
11)	CDK2AP2	0	3	0	2	5	1	11/25 (44%)
12)	CKB	0	0	2	2	6	1	11/25 (44%)
13)	FADD	0	3	0	2	5	1	11/25 (44%)
14)	HDAC5	1	3	1	3	2	2	11/25 (44%)
15)	HIP1R	1	3	1	2	4	1	11/25 (44%)

No	Antigen	Control (n = 5)	GC-DLBCL (n = 5)	NGC-DLBCL (n = 5)	Trans-Formed DLBCL (n = 4)	FL (n = 6)	MCL (n = 5)	All B-NHL (n = 25)
16)	NUMA1	0	3	0	1	5	2	11/25 (44%)
17)	POLE	1	3	1	3	2	2	11/25 (44%)
18)	ZNF154	0	1	0	3	4	2	10/25 (40%)
19)	KLHL21	0	2	1	1	5	0	9/25 (36%)
20)	RPL24	0	2	0	4	3	0	9/25 (36%)
21)	SPAG7	0	2	0	3	3	1	9/25 (36%)
22)	CREBBP	0	1	0	0	5	2	8/25 (32%)
23)	DNM2	0	0	1	3	3	1	8/25 (32%)
24)	CCNL2	0	0	0	3	3	1	7/25 (28%)
25)	MLLT6	0	3	2	0	1	1	7/25 (28%)
26)	NHN1	0	0	0	1	5	1	7/25 (28%)
27)	RBM5	0	0	3	2	1	1	7/25 (28%)
28)	PRAF2	0	0	1	3	2	0	6/25 (24%)
29)	SEPT5	0	2	0	3	0	0	5/25 (20%)
30)	UBTF	0	0	0	3	2	0	5/25 (20%)
31)	ZNF638	0	3	0	1	1	0	5/25 (20%)
32)	JMJD3	0	3	0	1	0	0	4/25 (16%)
33)	ING5	0	1	0	0	0	3	4/25 (16%)
34)	SAP30BP	0	0	0	1	0	3	4/25 (16%)
35)	ZNF768	0	0	0	2	2	0	4/25 (16%)
	TOTAL	**7**	**70**	**23**	**77**	**117**	**50**	337/875 (39%)
	***p*-value of total antigens vs. those of controls**		**$2.57E^{-17}$**	**0.004**	**$4.13E^{-26}$**	**$5.88E^{-31}$**	**$1.9E^{-10}$**	$9.43E^{-15}$

NB: The p-value was generated from comparison of total antigens in a particular subgroup versus the total antigens in the normal control (n = 7). For example, in the GC-DLBCL subgroup, p value of $2.57E^{-17}$ was generated from comparison of 70 [out of a possible total of 175 (5 patients multiplied by 35 shortlisted antigens, yielding 175)] versus 7 (out of a possible total 175 in the normal controls).

3.1.5 Association of antigens with subtypes of lymphomas

Based on data from Table 3.1, 11 antigens elicited a variable frequency of immune response across all B-NHL subtypes: ARPP-21, EXT1, HDAC5, HIP1R, MAFF, NUDT16, PIP5K1C, PGLS, POLE, ZNF133 and ZNF579. No antigen was specifically recognised by a particular subgroup of lymphoma patients. However, six antigens were recognised by sera from lymphomas with a common germinal centre cell-of-origin i.e. FL, transformed-DLBCL and/or GC-DLBCL, and they are RPL24, SEPT5, UBTF, ZNF638, JMJD3 and ZNF768.

3.1.6 Gene Ontology over-representation analysis

In order to identify common relevant functions or biological processes mediated by the 35 B-cell lymphoma-associated antigens, Gene Ontology (GO) over-representation analysis was adopted (GO Consortium, 2004). This method enables the identification of the enrichment of a set of genes or proteins known to have the same biological function, and the degree of over-representation can then be assessed in a statistical manner.

Table 3.2 summarises the GO over-representation analysis for the 35 lymphoma antigens. GO "Molecular Function" category enrichment analysis showed an enrichment in classes of genes demonstrating capabilities of DNA binding (p = 0.008) or nucleic acid binding (p = 0.009), suggesting that a significant cluster of B-cell lymphoma-associated antigens are involved either directly or indirectly in the regulation of transcription. The enrichment analysis in "Biological Processes" category revealed a strong enrichment of the same set of antigens involved in cell cycle (p = 0.001) and cell proliferation (p = 0.003), with another significant cluster involved in cell cycle regulation (p = 0.011). These findings are consistent with existing data that implicates these processes in lymphomagenesis.

Table 3.2 Gene Ontology (GO) over-representation analysis in Molecular Function categories (highlighted in green) and Biological Function categories (highlighted in red) of the shortlisted 35 B-cell lymphoma-associated antigens. GO categories with significant *p*-value (< 0.05) are in bold. *p*-value: Fisher's exact test; *q*-value: false discovery rate (Storey and Tibshirani, 1995); FE: fold enrichment; Bkgd: background

Gene Ontology term	Bkgd total	Bkgd hits	Bkgd %	Input total	Input hits	Input %	FE	*p*-value	*q*-value	Genes
DNA binding	**15981**	**2385**	**14.92**	**35**	**13**	**37.14**	**2.49**	**0.008**	**0.134**	**CREBBP; MAFF; MLLT6; P28ING5; POLE; RBM5; SAP30BP; UBTF; ZNF133; ZNF154; ZNF579; ZNF638; ZNF768**
Nucleic acid binding	**15981**	**3364**	**21.05**	**35**	**17**	**48.57**	**2.31**	**0.009**	**0.134**	**ARPP21; CREBBP; MAFF; MLLT6; NHN1; P28ING5; POLE; RBM5; RPL4; SAP30BP; SPAG7; UBTF; ZNF133; ZNF154; ZNF579; ZNF638; ZNF768**
Transcription cofactor activity	15981	355	2.22	35	3	8.57	3.86	0.05	0.134	CREBBP; HDAC5; MAFF
Transcription regulator activity	15981	1540	9.64	35	8	22.86	2.37	0.051	0.134	CREBBP; HDAC5; JMJD3; MAFF; MLLT6; UBTF; ZNF133; ZNF154
Transcription factor binding	15981	500	3.13	35	3	8.57	2.74	0.108	0.171	CREBBP; HDAC5; MAFF
Structural molecule activity	15981	656	4.10	35	3	8.57	2.09	0.189	0.193	NUMA1; RPL4; SEPT5
RNA binding	15981	762	4.77	35	3	8.57	1.80	0.259	0.224	RBM5; RPL4; ZNF638
Transferase activity, transferring phosphorus-containing groups	15981	916	5.73	35	3	8.57	1.50	0.46	0.321	CKB; PIP5K1C; POLE
Transferase activity	15981	1711	10.71	35	5	14.29	1.33	0.587	0.381	CKB; CREBBP; EXT1; PIP5K1C; POLE
Cell cycle	**14934**	**965**	**6.46**	**35**	**9**	**25.71**	**3.98**	**0.001**	**0.116**	**CCNL2; CDKN2C; DNM2; EXT1; HDAC5; NUMA1; POLE; RBM5; SEPT5**
Cell proliferation	**14934**	**1099**	**7.36**	**35**	**9**	**25.71**	**3.49**	**0.003**	**0.116**	**CCNL2; CDKN2C; DNM2; EXT1; HDAC5; NUMA1; POLE; RBM5; SEPT5**
Regulation of cell cycle	**14934**	**342**	**2.29**	**35**	**4**	**11.43**	**4.99**	**0.011**	**0.116**	**CDKN2C; EXT1; HDAC5; RBM5**
Mitotic cell cycle	14934	466	3.12	35	3	8.57	2.75	0.108	0.146	DNM2; NUMA1; POLE
Regulation of transcription	14934	2665	17.85	35	10	28.57	1.60	0.208	0.211	CREBBP; HDAC5; MAFF; MLLT6; P28ING5; SAP30BP; UBTF; ZNF133; ZNF154; ZNF579
Nucleobase, nucleoside, nucleotide and nucleic acid metabolic process	14934	4189	28.05	35	14	40.00	1.43	0.298	0.264	CREBBP; HDAC5; MAFF; MLLT6; P28ING5; POLE; RBM5; SAP30BP; UBTF; ZNF133; ZNF154; ZNF579; ZNF638; ZNF768

3.1.7 Validation of antigen recognition by ELISA

Recombinant proteins were requested from Dublin for 20 antigens. These showed the highest frequency of lymphoma-specific immunological recognition and a known or potential role in lymphoma from a comprehensive literature review (e.g. antigen implicated in other cancers or from a family of proteins involved in lymphoma, see Supplementary Table 1 in Appendix). A total of 18 recombinant proteins expressed in *E. coli* were purified, in Dublin, using a His-tag affinity column and sent to our laboratory. Our initial aim was to validate the humoural immune response to these bacterially expressed recombinant proteins using an ELISA assay to confirm the protein array data.

Although different experimental parameters were used in attempts to optimise the ELISA assay, such as different protein concentration or blocking reagent [(Milk versus Ultrablock (Serotec)], this approach was not successful. Firstly, one of the normal control (N1) sera consistently showed high levels of immunoreactivity across all proteins tested, generating a high positive cut-off value (Fig 3.2). This normal control did not show immunoreactivity against any of the 35 shortlisted antigens on the protein array, and there was no acceptable scientific reason to exclude this data when generating the cut-off value. Secondly, *E. coli* proteins were also enriched by the His-tag affinity purification, as illustrated by anti-His blotting of the recombinant proteins (Fig 3.3). Critically, the protein arrays were not spotted with purified recombinant proteins and thus ELISA against the purified recombinant proteins from Dublin was not a particularly effective method for validating the protein array data.

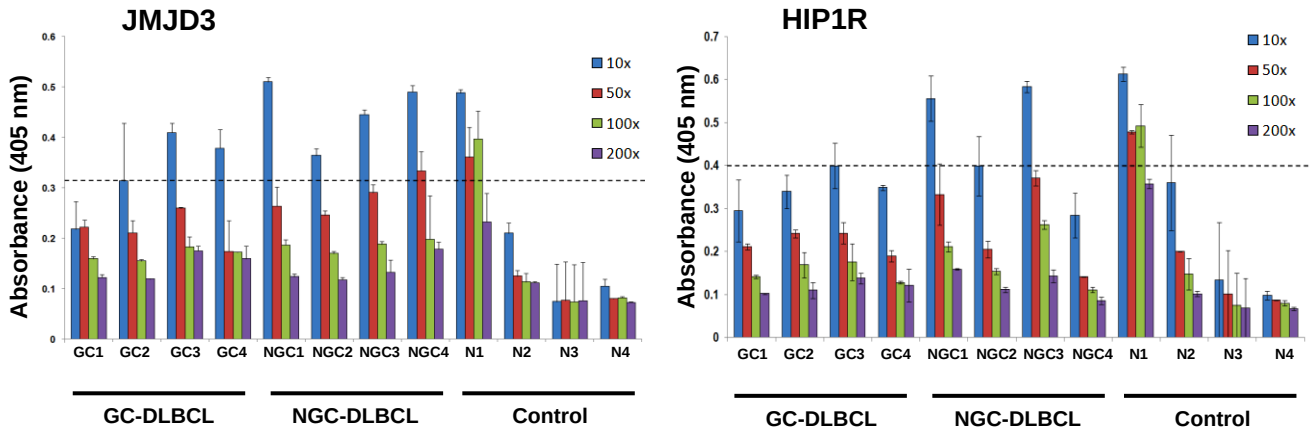

Fig 3.2 ELISA validation of patient's immunoreactivity against representative autoantigens

The line denotes positive cut-off value. Figure legend indicates the dilution factor of tested sera e.g. 10x denotes 1/10 dilution. The ELISA results did not correlate with those screened by protein arrays.

Coomassie blue staining confirmed the presence of recombinant proteins but anti-His immunoblotting showed detection of additional proteins across all the samples tested (Fig 3.3). Some may be degradation products but in many cases the proteins were of a much higher molecular weight than that predicted for the recombinant antigen (or exhibited by the main protein band labelled by Coomassie blue).

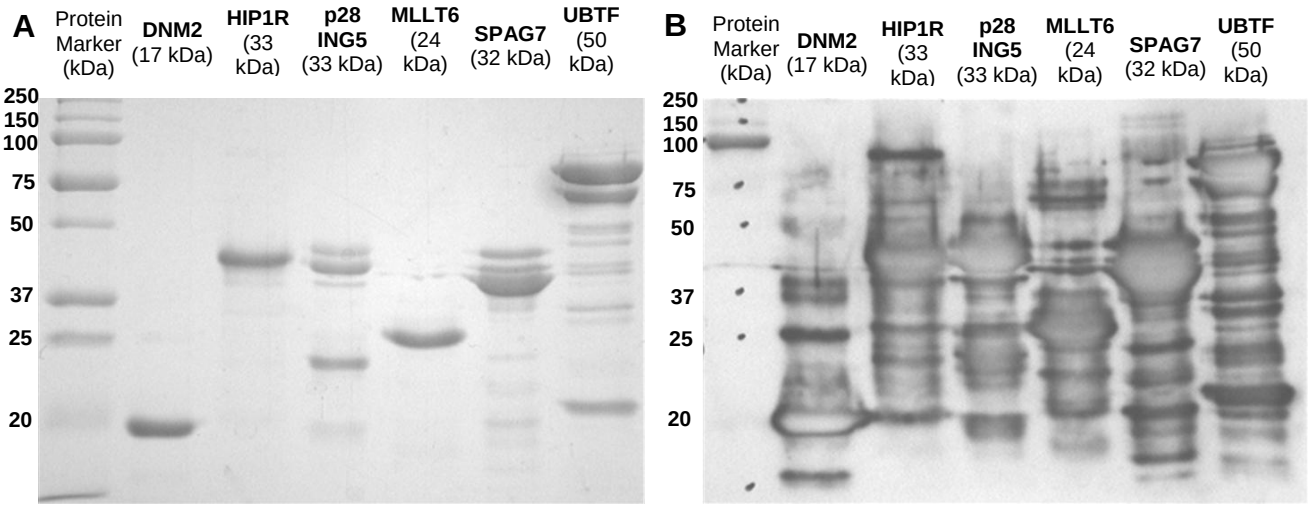

Fig 3.3 Validation of six recombinant proteins by SDS-PAGE

A: Coomassie blue staining; B: Immunoblotting of the same SDS-PAGE gel by anti-His antibody (radiographic exposure time of 15 seconds). NB: The predicted molecular weight of each recombinant protein is shown in brackets at the top of the gel.

Rather than pursuing another approach to specifically validate the array data across a panel of antigens, we decided to pursue a more focussed study of one or two antigens that had not been previously studied in lymphoma. Two candidate antigens selected for more detailed validation were HIP1R and JMJD3. This was based partly on their novelty in the field of lymphoma and also on their possible association with lymphomagenesis. HIP1R shares functionality with HIP1, which had been reported to be a lymphoma oncogene (Bradley *et al*., 2007b), and JMJD3 was topical and could play a role in lymphoma through histone modifications and epigenetic regulation of gene expression (Agger *et al*. 2007; De Santa *et al*. 2007). Other important considerations were the commercial availability of both HIP1R and JMJD3 antibodies and potentially full-length cDNAs. This chapter focuses on validating HIP1R as an autoantigen in B-NHL. The validation of JMJD3 as a potential lymphoma autoantigen is explored in the final results chapter.

RESULTS

3.2 VALIDATION OF HIP1R ANTIBODIES

3.2.1 Generation of full-length *HIP1R* plasmid construct

The commercially available HIP1R antibody had been used in published studies (Hinrichsen *et al*., 2006; Jain *et al*., 2008) but no data was available to demonstrate whether this reagent was well-validated. Thus, a HIP1R expression construct was needed to generate transfected cells for antibody characterisation. A potentially full-length *HIP1R* cDNA was available as an MGC clone (MGC ID: 71280; IMAGE: 6085487) but sequencing this clone identified it as a splice variant containing an internal deletion that affected the protein coding sequence. Thus, PCR primers were designed to amplify the full-length transcript. Several attempts were made to generate the full-length *HIP1R* cDNA (3.2 kb) from normal testis or Raji cDNA templates by PCR but the full-length transcript could not be amplified. Therefore, the *HIP1R* cDNA was PCR-amplified in two-halves from the Raji cell line, which has high levels of *HIP1R* transcript according to GNF Symatlas (http://biogps.gnf.org), and cloned sequentially into a eukaryotic expression vector pcDNA4/His-Max^{TM} (Invitrogen) as detailed in Fig 3.4.

The final construct was validated by sequencing which identified a single nucleotide difference from the reference sequence (NM_003959.1). This results in a single amino acid change of alanine to valine (position of the amino acid change: 531) in the clathrin binding domain, which was identified as a single-nucleotide polymorphism (SNP) in tissue of West African origin. The Raji cells are derived from an African Burkitt's lymphoma patient, thus explaining the presence of the SNP in this construct.

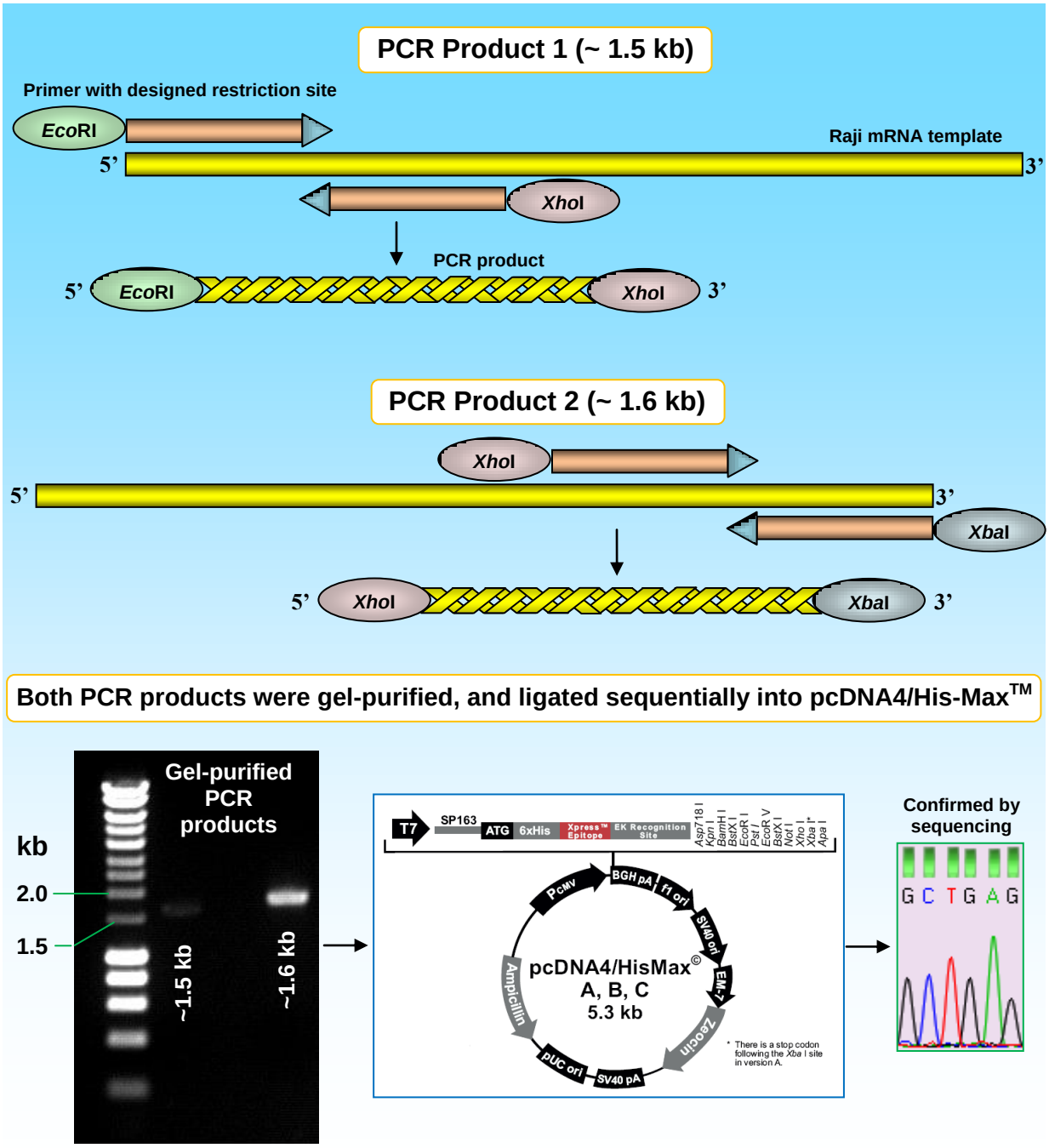

Fig 3.4 Generation of full-length *HIP1R* plasmid construct

"PCR Product 1" and "PCR Product 2" were cloned into pGEM-T Easy (Promega) vector before being excised and sequentially ligated into pcDNA4/His-Max™ (Invitrogen) vector and confirmed by sequencing.

3.2.2 Validation of HIP1R monoclonal antibodies

293T cells, that have relatively low levels of *HIP1R* and the related *HIP1* transcript (by qRT-PCR), were transfected with either the HIP1R expression construct, or the empty vector as a control. Immunolabelling with the anti-Xpress™ antibody (Invitrogen) to the epitope tag confirmed the efficiency of transfection and the subcellular localisation of HIP1R within the cytoplasm. These transfected cells enabled the validation of two commercially available HIP1R antibodies: anti-murine Hip1r monoclonal antibody (mAb) clone 44 (anti-Hip1r-44, from BD Transduction Laboratories) and anti-HIP1R mAb clone 3E10 (anti-HIP1R-3E10, from Abnova) by immunohistochemistry. The anti-murine Hip1R-44 mAb showed cross-reactivity with the human HIP1R protein (Fig 3.5). We therefore refer to the Hip1r-44 reagent as the HIP1R antibody throughout the remainder of the thesis to avoid confusion as to human/murine nomenclature.

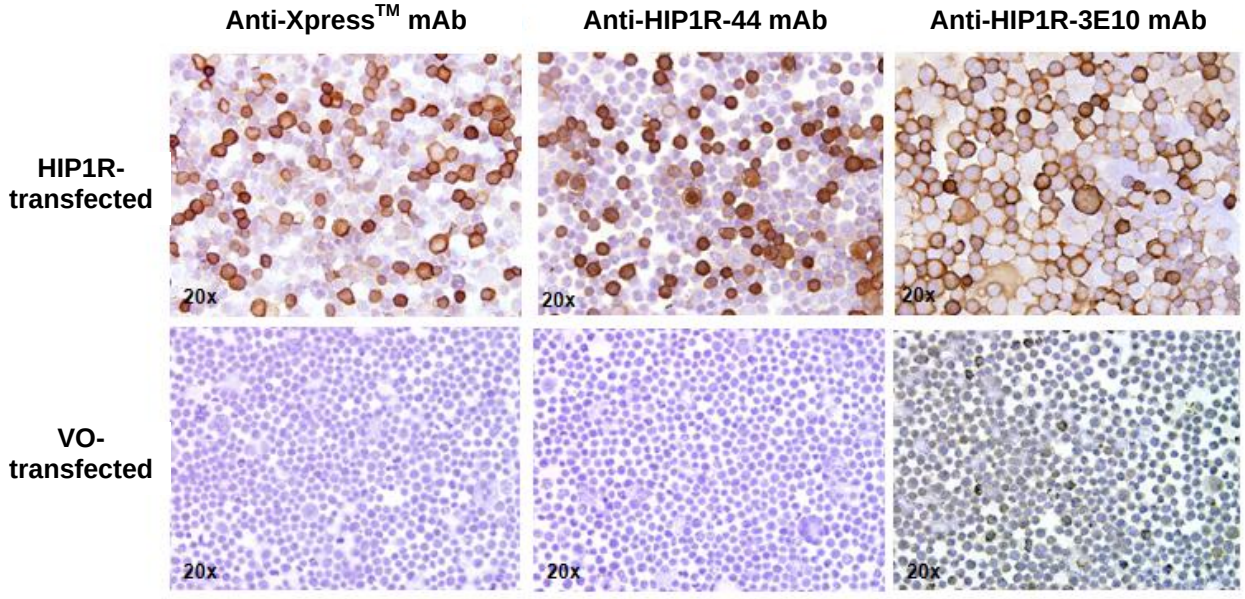

Fig 3.5 Validation of anti-HIP1R monoclonal antibodies

Immunolabelling with the anti-Xpress™ (Invitrogen) tag antibody confirmed expression of the recombinant HIP1R protein. Anti-HIP1R-44 and HIP1R-3E10 mAbs successfully immunolabelled HIP1R-transfected 293T cells. No labelling was observed in the VO-transfected cells by using anti-Xpress™ antibodies and anti-HIP1R-44 mAb. Some background staining was noted using anti-HIP1R-3E10 mAb in both HIP1R- and VO-

transfected cells. Key: HIP1R-transfected: Full-length HIP1R-transfected cells; VO-transfected: Vector only-transfected cells.

The anti-HIP1R-44 mAb was also reactive with formalin-fixed paraffin-embedded (FFPE) HIP1R transfectants, confirming that it was able to recognise a formalin-resistant epitope in the human protein (Fig 3.6). The anti-HIP1R-3E10 mAb was also tested on FFPE HIP1R transfectants but yielded high non-specific background staining, thus only the anti-HIP1R-44 mAb was used for further experimental work.

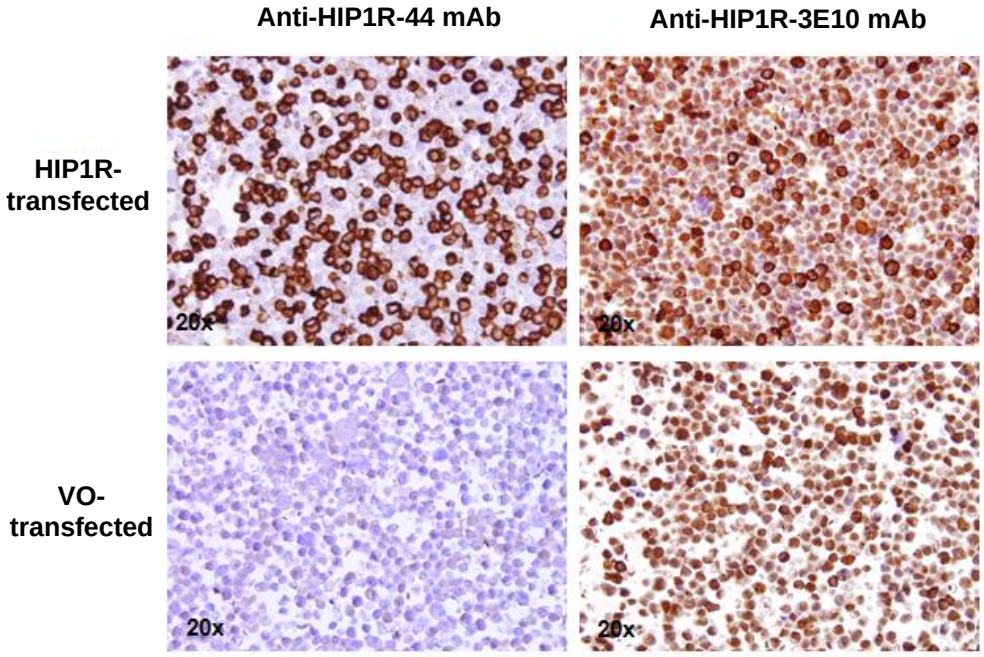

Fig 3.6 Recognition of formalin-resistant epitope by HIP1R monoclonal antibodies
Immunoperoxidase labelling of HIP1R transfectants with the anti-HIP1R-3E10 mAb clone yielded much higher background staining of untransfected cells, in contrast with specific immunolabelling using the anti-HIP1R-44 mAb.

HIP1R and its only known mammalian relative, HIP1 share high sequence homology (49%, Fig 3.7). Thus, we decided to test the possible cross-reactivity of the HIP1R-44 mAb against the HIP1 protein (as we also needed to make HIP1 transfection construct for other studies shown in the next chapter), even though this was fairly unlikely as the immunogen was not from a highly conserved region.

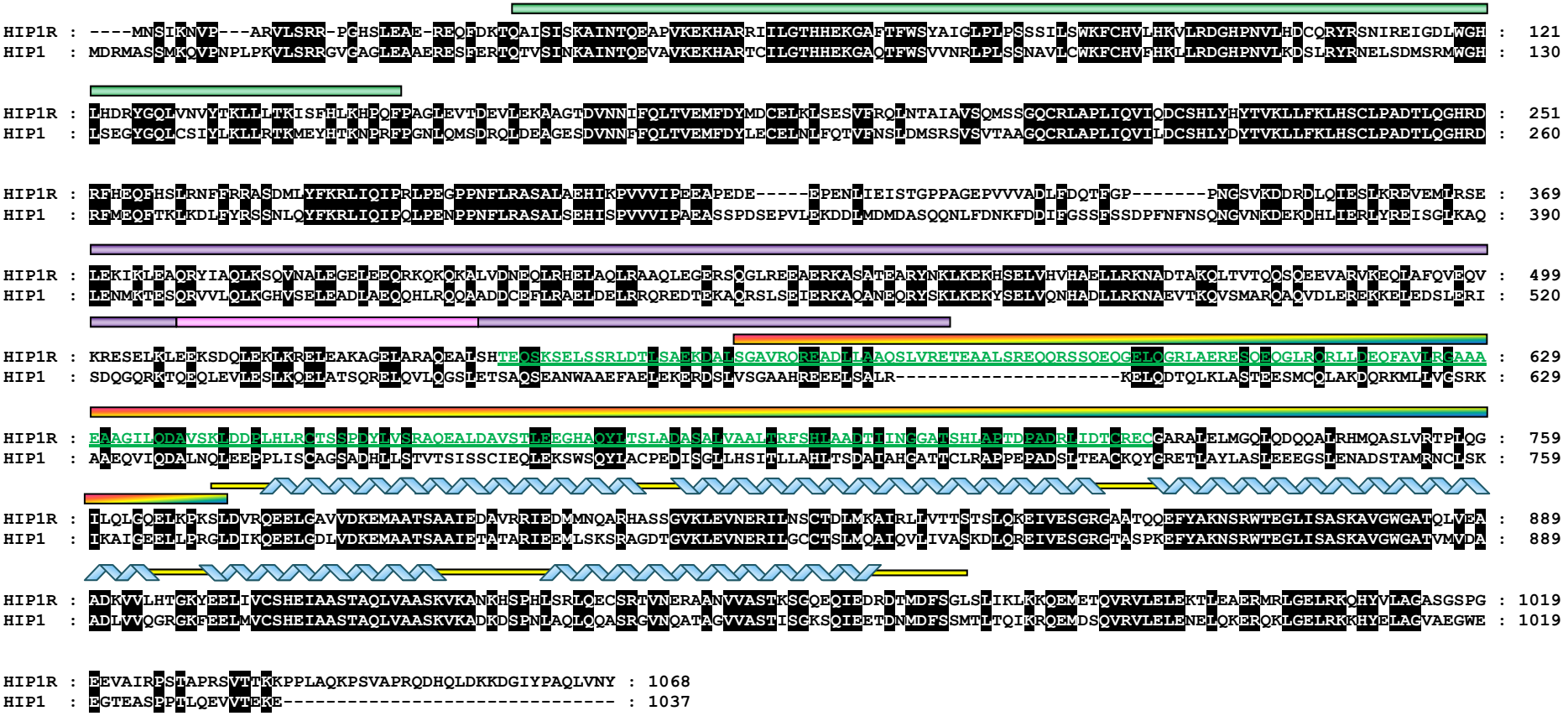

Fig 3.7 Alignment of amino acid sequences of HIP1R and HIP1

The rainbow box above the alignment represents the immunogen sequence of BD Transduction Laboratories anti-HIP1R-44 mAb that shares little homology with corresponding HIP1 sequence. The green, underlined sequence is the HIP1R protein region used on protein array experiments and it does not share more than 3 consecutive amino acid residues with HIP1.The green, purple and pink boxes represent ANTH, leucine zipper and coiled-coil domain of HIP1R, respectively. The crystal structure of HIP1R THATCH core has been resolved (Brett et al., 2006) and it consists of 5 alpha-helices (blue) joined by connecting loops (yellow) shown in corresponding shapes.

A full-length *HIP1* plasmid construct was obtained from Origene (SC108827) and used to generate transfected cells to test for cross reactivity with the HIP1R antibody. A well characterised anti-HIP1 mAb (anti-HIP1-4B10, from Abcam) confirmed expression of the recombinant HIP1 protein in 293T cells (vector-only transfected cells were unstained). The anti-HIP1R-44 mAb did not show cross-reactivity with the related HIP1 protein (Fig 3.8), confirming that it was HIP1R-specific.

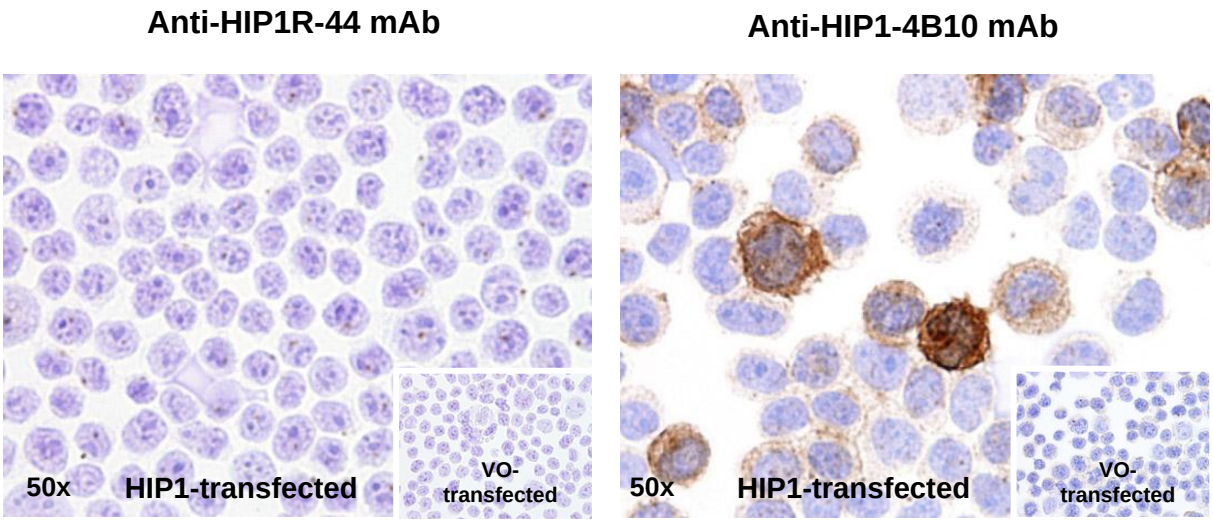

Fig 3.8 Validation of anti-HIP1R-44 mAb specificity for HIP1R protein

293T cells were transfected with full-length HIP1 cDNA or vector-only (VO) as control and stained with HIP1R or HIP1 mAb. The anti-HIP1R-44 mAb did not stain 293T cells expressing the related HIP1 protein, confirming specificity of the antibody against HIP1R.

3.3 VALIDATION OF IMMUNOREACTIVITY AGAINST THE HIP1R ANTIGEN BY WESTERN BLOTTING

The portion of HIP1R on the protein array from Dublin shares very little sequence identity with the HIP1 protein (Fig 3.7), suggesting that the humoural immune response detected is HIP1R-specific. The serologic immunoreactivity against both the HIP1R and HIP1 antigens was further investigated in the same set of patients' sera by Western blotting.

Full-length *HIP1R* and *HIP1* constructs were transfected into 293T cells to obtain lysates containing the protein for screening with patients' sera by Western blotting, along with the vector-only transfected 293T cells. It is of note that the proteins used in the protein array screening were expressed in a bacterial system, and the proteins used for Western blotting analysis were expressed in mammalian 293T cells. Fig 3.9 shows a representative GC-DLBCL patient's serological-reactivity against the HIP1R protein but not HIP1.

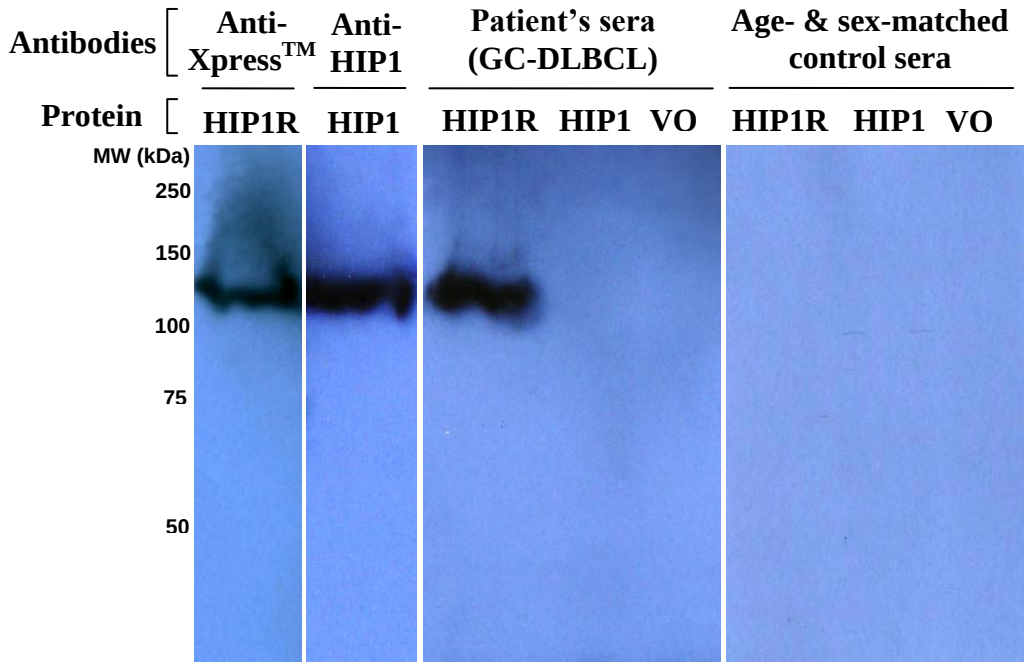

Fig 3.9 Presence of HIP1R autoantibodies in a representative GC-DLBCL patient's sera measured by Western blotting

Recombinant proteins were obtained from the full-length HIP1R- or HIP1-transfected 293T cells and their expression was validated with anti-Xpress™ tag antibody or anti-HIP1-4B10 mAb, respectively. HIP1R recombinant protein was also validated by immunoblotting with anti-HIP1R-44 mAb shown in the next chapter. VO: Proteins from vector-only transfected 293T cells.

Table 3.3 summarises the immunological reaction against the HIP1R antigen screened by protein arrays in comparison with Western blotting screening results. There was a correlation between the frequency of HIP1R autoantibodies in the patients' sera screened by both techniques, indicating the reproducibility of HIP1R results obtained from protein array screening. In addition, none of the lymphoma patients had HIP1 autoantibodies by Western blotting, confirming that the immunological recognition of the full-length mammalian expressed protein was HIP1R-specific. The recombinant proteins obtained from Dublin were not used for validation of serological-reactivity by Western blotting because of the difficulties with the poly-His tagged proteins elaborated in section 3.1.7. Furthermore, there was no HIP1 protein from Dublin for comparison to determine specificity of the antibody response.

Table 3.3 Frequency of autoantibodies against HIP1R antigen

Lymphoma Subtypes	**Frequency**		
	Protein arrays	**Western blots**	
		Full-length HIP1R	**Full-length HIP1**
FL	4/6	5/5	0/5
GC-DLBCL	3/5	1/4	0/4
Transformed DLBCL	2/4	1/3	0/3
NGC-DLBCL	1/5	2/5	0/5
MCL	1/5	1/5	0/5
Age- & Sex-Matched Control	1/5	1/5	0/5
TOTAL	12/30	11/27	0/27

NB: 5 sera from the protein array screening were unavailable for further study, hence the total number of patients' sera used in immunoblotting analysis (n = 30) was smaller than that used for array screening (n = 35)

DISCUSSION

Prior to this study, protein arrays derived from a human foetal brain library were used to identify candidate lymphoma autoantigens that were detected by antibodies in the sera from patients with different lymphoma subtypes. Of the cDNA clones from the human foetal brain library used to construct the protein array, 64% are predicted to encode full-length proteins (Lueking *et al*., 2003). Furthermore, this library has been normalised to obtain a non-redundant, unique cDNA set (Uniclone Set) using oligonucleotide fingerprinting (Herwig *et al*. 2000). Many of the clones on the array have been sequenced and experimentally confirmed to express the correct protein product in-frame with the His-tag. However, this is not the case for all the clones and interestingly there are rare cases where an immune response has recognised a protein that is not expressed in-frame with the His-tag. Thus, further experimental work is required to validate the array data that has been generated.

The protein array screening identified 11 antigens that elicit relatively high frequency immune responses across all B-NHL subtypes studied. Interestingly, the protein array screening also identified a set of six antigens in sera from lymphomas with a common cell-of-origin (FL, transformed-DLBCL and/or GC-DLBCL). Further validation with a larger number of serum samples would be of future interest to specifically test, with a statistically relevant sample size, whether lymphomas with common cellular origin share an autoantibody profile.

Approximately 15% of FL patients undergo spontaneous disease regression without treatment (Longo, 2006), however these patients cannot yet be distinguished from other FL patients by conventional diagnostic methodologies. The protein array data identified FL as the lymphoma subgroup eliciting the highest frequency recognition of the shortlisted tumour

antigens. It is tempting to speculate that the FL patients who undergo regression without treatment might be those with a more frequent immune response to tumour antigens. It would be interesting to investigate whether the number of antigens and titre of humoural immune response could in the future help to distinguish these FL patients. A striking observation, although in a very small sample size, was the low autoimmune response observed in NGC-DLBCL. It would also be of interest to investigate whether the overall poor prognosis of these patients may, in part, reflect loss of cancer immune surveillance which could contribute to tumour aggressiveness (Kim *et al.*, 2007). Clinical relevance of the humoural immune response in lymphoma is highlighted by our laboratory's recent finding that a high titre autoantibody response to the ALK oncoantigen correlates inversely with tumour dissemination and risk of relapse in paediatric ALK^+ ALCL (Ait-Tahar *et al*., 2010).

The antigens recognised by antibodies present in DLBCL sera that were identified by protein array screening did not overlap with those identified by SEREX methodology in our laboratory (Liggins *et al*., 2004). This might be due to the cDNA expression libraries being derived from different tissues, human foetal brain (RZPD, Germany) in this study, while Liggins *et al*. used a testis cDNA expression library (Stratagene, USA). Also, serum from only one DLBCL patient was used to screen the testis cDNA expression library by SEREX, in contrast with 14 DLBCL patients screened by protein arrays, in addition to different procedures and parameters (e.g. dilution factor of sera for screening purpose) used.

The ELISA validation of the antigens obtained from the protein array screening was not successful. However, this was not a direct comparison of the same samples using different techniques, as the proteins present on the array were not purified while the ELISA screening utilised proteins purified by a His-tag affinity column. The anti-His

immunoblotting showed the presence of many additional proteins, some of higher molecular weight than the target antigens, suggesting that these were poly-His containing *E. coli* proteins. Therefore, we decided to pursue a focussed study of the HIP1R and JMJD3 antigens and their role in lymphoma biology, rather than attempt further generic validation of the array data.

We initially expressed HIP1R in mammalian cells to enable us to validate commercially available antibodies to this molecule and confirm its immunological recognition by patients' sera. The use of bacterially expressed proteins to measure serological-reactivity is limited in scope for measuring autoreactive epitopes because they lack post-translational modification such as glycosylation or phosphorylation (Gunawardana and Diamandis, 2007). Therefore, we decided to validate the protein array findings by using full-length mammalian expressed recombinant antigens to measure autoreactivity by immunoblotting. The frequency of immunological recognition of HIP1R detected by both approaches was comparable, 12/30 (40%) and 11/27 (44%) of the lymphoma patients' sera showed immunological recognition of HIP1R using protein arrays and immunoblotting methodologies, respectively.

A previous study reported the presence of anti-HIP1 antibodies in sera from NHL patients by Western blotting of a bacterially expressed HIP1 recombinant protein spanning a C-terminal region of the protein (Bradley *et al*., 2007b). Bradley *et al*. then also functionally demonstrated that HIP1 expression was oncogenic in B cells. The functional relationship between HIP1 and HIP1R was a significant factor in our decision to study the role of HIP1R in lymphoma. However, our findings contrast with the results from the Bradley *et al*. study as we identified an immune response to HIP1R and not to the HIP1 antigen. The C-terminal

region of the HIP1 protein used in the Bradley *et al.* serological-reactivity experiments shared a very high sequence homology with C-terminus of HIP1R (Fig 3.10). Thus, it is not possible to conclusively distinguish autoantibodies recognising HIP1 from those recognising HIP1R using this recombinant protein. A lack of reactivity with the comparable region of HIP1R would be necessary to conclusively demonstrate HIP1 specificity.

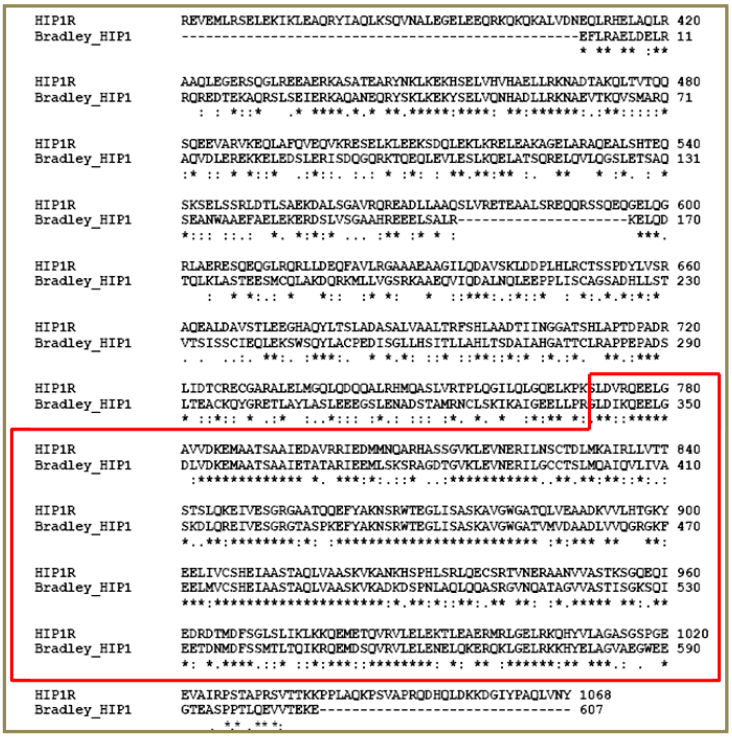

Fig 3.10 Alignment of full-length HIP1R with recombinant HIP1 protein from Bradley *et al.* (2007b) studies

The C-terminus of the HIP1 recombinant protein used by Bradley et al. B-NHL patients' sera screening showed a high cross-reactivity with the HIP1R protein as highlighted by the red box.

On this basis, we would have expected to have autoantibodies to this common C-terminal region in our patients' sera and thus to observe immunological recognition of both the HIP1 and HIP1R proteins. However, we only observed an immune response to the HIP1R protein, suggesting perhaps that these common C-terminal epitopes were not recognised. A possible explanation for this is that our autoantibody recognition was investigated by Western

blotting using full-length proteins expressed in mammalian cells, rather than against the bacterially expressed C-terminal protein fragment used by Bradley *et al*. These technical differences may explain the lack of HIP1 immunological recognition; in particular, post-translational modifications would not have been present in the bacterially expressed protein.

Our findings raise the possibility that HIP1R, rather than HIP1, might be the more frequently recognised of the two auto-antigens in lymphoma patients. This is consistent with the higher levels and frequency of HIP1R expression detected in B-NHL cell lines (compared to HIP1) that is demonstrated in the following chapter.

CHAPTER 4
EXPRESSION STUDIES OF HIP1R IN NORMAL AND MALIGNANT B CELLS

INTRODUCTION

4.1 TRANSCRIPTIONAL CHANGES IN NORMAL B CELLS

In order to investigate whether the expression pattern of HIP1R in B-cell malignancies is abnormal, HIP1R expression patterns in normal B-cell populations needed to be addressed. The developmental stages of B cells in the germinal centre (GC) have been described in Chapter 1. The transcriptional programme and the upregulation or downregulation of key transcription factors during the development of B cells in the GC are further described here.

After a naïve B-cell is activated via the interaction of the BCR with antigen, it initially progresses into a centroblast that retains the high levels of the transcriptional repressor PAX5, which is essential for guarding mature B-cell identity in naïve, GC and memory B cells (Cobaleda *et al*., 2007) and the BCL6 transcriptional repressor, which is required for GC formation (Dent *et al*., 1997). Differentiation of centroblasts into centrocytes through stimulation of CD40 by GC T cells results in downregulation of BCL6 expression via the upregulation of its repressor IRF4, which is activated by NF-κB (Falini *et al*., 2000). Inactivation of PAX5, via an unknown stimulus, as well as upregulation of IRF4 trigger the plasmacytic differentiation programme and the progression of centrocyte into pre-plasmablasts characterised by upregulation of XBP1, a bZip transcriptional activator required for the secretory phenotype of plasma cells (Shaffer *et al*., 2004). This is followed by the upregulation of BLIMP1, which further represses *BCL6* and *PAX5* transcription (Lin *et al*.,

2002) and is required for plasma-cell differentiation (Shapiro-Shelef *et al*., 2003). This drives the pre-plasmablast machinery into the formation of plasmablasts and terminally differentiated plasma cells (Fig 4.1).

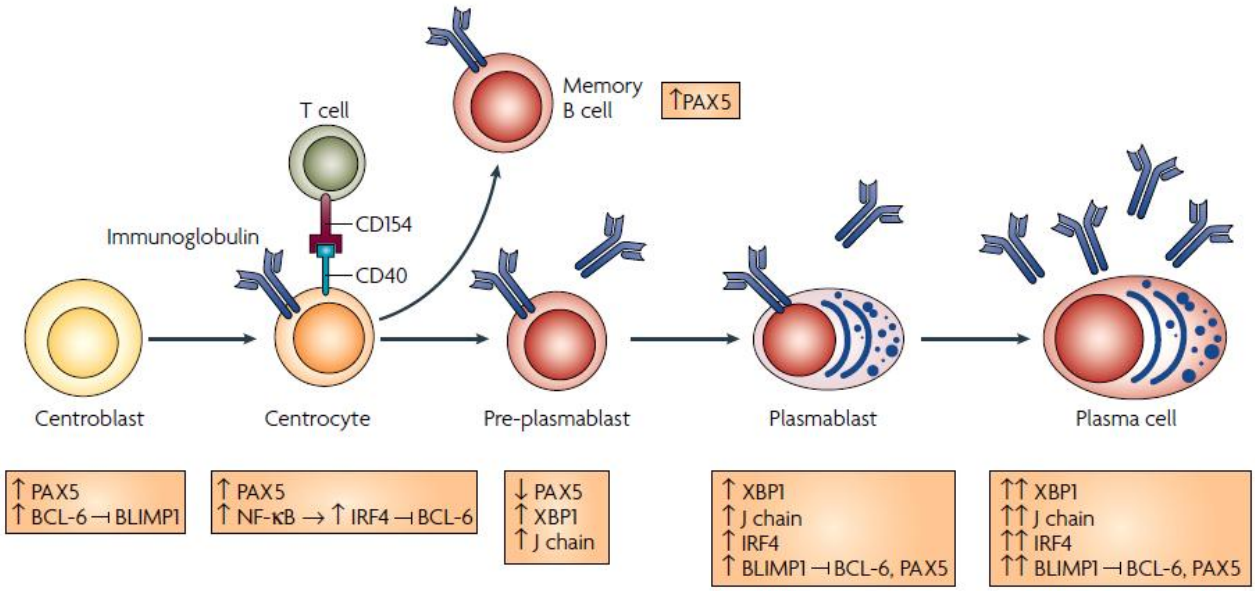

Fig 4.1 Changes in transcription factors expression from the maturation of centroblast into memory B-cell or plasma cell

The key transcription factor changes in the progression stages include downregulation of PAX5 and BCL6, and upregulation of IRF4, XBP1 and BLIMP1. The development of centroblast into a terminally-differentiated memory B-cell retains the expression of PAX5. Diagram adapted from Klein and Dalla-Favera (2008).

RESULTS

4.2 HIP1R AND HIP1 LEVELS IN NORMAL AND B-CELL MALIGNANCIES

4.2.1 *HIP1R* mRNA expression in a panel of normal tissues and lymphocyte populations

qRT-PCR analysis of a normal tissue-derived MTC^{TM} cDNA panel (Clontech, Takara BioEurope, France) pooled from a range of one to 550 individuals (Supplementary Table 2), depending on the cell- or tissue-type, showed widespread *HIP1R* expression in various normal tissues including tissues of the immune system (Fig 4.2). This widespread distribution of *HIP1R* expression in various tissues is consistent with the findings that HIP1R was ubiquitously expressed in a wide range of normal tissues at both the mRNA (e.g. brain, kidney, brain, spleen, thymus, liver, heart) (Seki *et al*., 1998) and protein levels (e.g. brain, kidney, pancreas, colon, spleen, tonsil, prostate) (Hyun *et al*., 2004a).

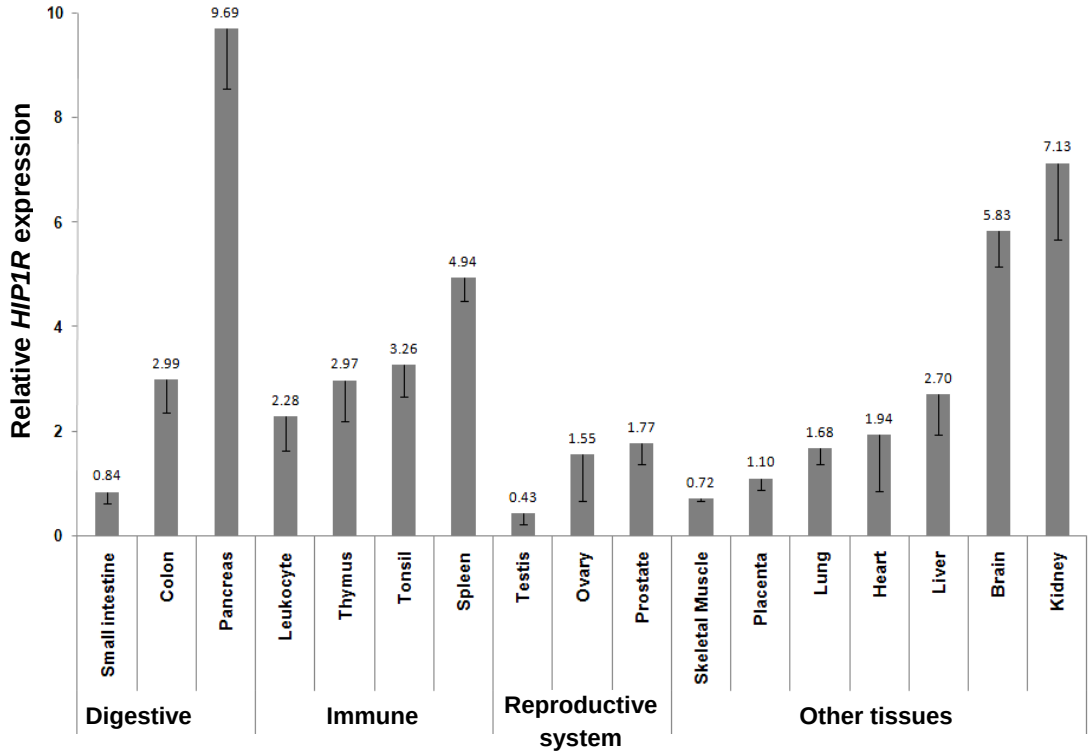

Fig 4.2 qRT-PCR analysis of *HIP1R* mRNA expression levels in normal human tissues (Clontech, Takara BioEurope)

HIP1R was ubiquitously expressed in a wide range of normal tissues including tissues of the immune system. qRT-PCR amplification was performed in triplicate using TaqMan pre-

verified probes to amplify HIP1R [TaqMan probe: Hs00391321_m1 (Applied Biosystems)], and relative gene expression was normalised according to expression of TATA-box binding protein [TBP, TaqMan probe: 4326322E (Applied Biosystems)] and compared to 293T levels using the formula $2^{-\Delta\Delta Ct}$.

HIP1R expression levels were further examined in normal B-cell and T-cell populations because of our specific interest in its expression in their malignant counterparts. qRT-PCR analysis on B- and T-cell populations purified from the peripheral blood and/or lymphoid tissues of healthy donors [kindly provided by Dr Charles Lawrie; Lawrie *et al.* (2007)] showed significantly higher *HIP1R* expression in B-cell subsets, compared to T-cell subsets ($p < 0.0001$) (Fig 4.3). *HIP1R* was most highly expressed in the $CD19^+$ (pan B-cell marker) and $CD27^+$ (marker of memory B cells) populations, suggesting that *HIP1R* levels are maintained from the transition of mature naïve B-cell stage into memory B cells. *HIP1R* was moderately expressed in GC B cells ($CD19^+/IgD^-/CD39^-$) purified from normal tonsils.

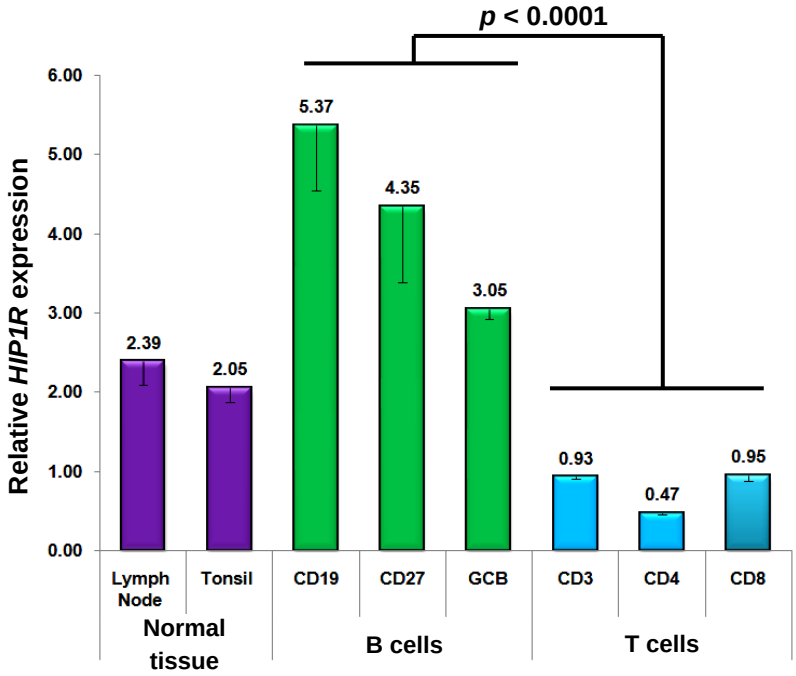

Fig 4.3 *HIP1R* expression in B and T cells

HIP1R levels were examined in cDNA from normal lymph node and tonsil (Ambion) and purified lymphocyte populations from peripheral blood by qRT-PCR. HIP1R mRNA levels

were significantly higher in B-cell than T-cell populations ($p < 0.0001$). qRT-PCR amplification was performed in triplicate using TaqMan probes to amplify HIP1R (TaqMan probe: Hs00391321_m1), and gene expression was normalised according to expression of TBP (TaqMan probe: 4326322E) and expressed relative to levels in 293T levels using the formula $2^{-\Delta\Delta Ct}$.

High levels of *HIP1R* expression in B cells is further supported by microarray data from the HaemAtlas (Watkins *et al*., 2009), which demonstrated higher *HIP1R* B-cell expression values in comparison with six other blood cell subsets (Fig 4.4A and 4.4B) including T-helper, T-cytotoxic lymphocytes, NK cells, granulocytes, megakaryocytes and monocytes ($p < 0.001$ for two independent *HIP1R* probesets). *HIP1*, in contrast, was highly expressed in the granulocyte population (Fig 4.4C).

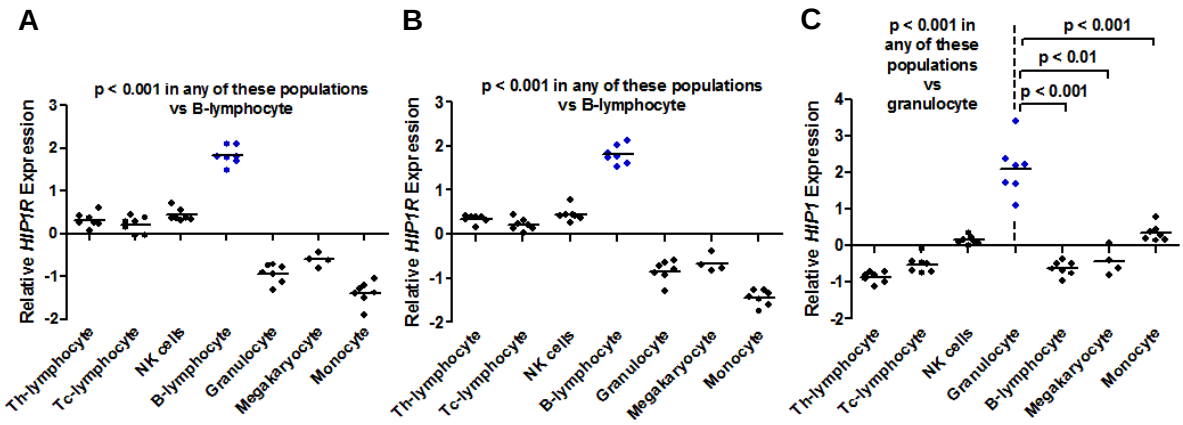

Fig 4.4 *HIP1R* (A and B) and *HIP1* (C) values in blood populations re-analysed from Haematology Expression Atlas (HaemAtlas) microarray data (Watkins *et al*., 2009)

HIP1R was significantly more highly expressed in B-cell than other lymphocyte subsets ($p < 0.01$). HIP1R probe ID: ILMN_1711699 (A) and ILMN_1812721 (B); HIP1 probe ID: ILMN_1697787 (C). All microarray values were log_2-transformed, median-centred and normalised to standard deviation.

4.2.2 Elucidation of HIP1R protein expression in normal B cells

High levels of *HIP1R* mRNA in B cells in comparison with other lymphocyte populations was followed by the investigation of HIP1R and HIP1 protein levels by

immunolabelling formalin-fixed paraffin-embedded (FFPE) reactive tonsil with the anti-HIP1R-44 mAb and the anti-HIP1-4B10 mAb. HIP1R was expressed in primary lymphoid follicles and scattered cells in the interfollicular areas of the tonsil (Fig 4.5A). In contrast, HIP1 was expressed in endothelium and only occasional expression was observed in tonsillar lymphocytes. In the secondary lymphoid follicles (i.e. follicles containing germinal centres), HIP1R was expressed in both the mantle zone and GC, with more frequent and higher intensity expression in the mantle zone than GC (Fig 4.5B).

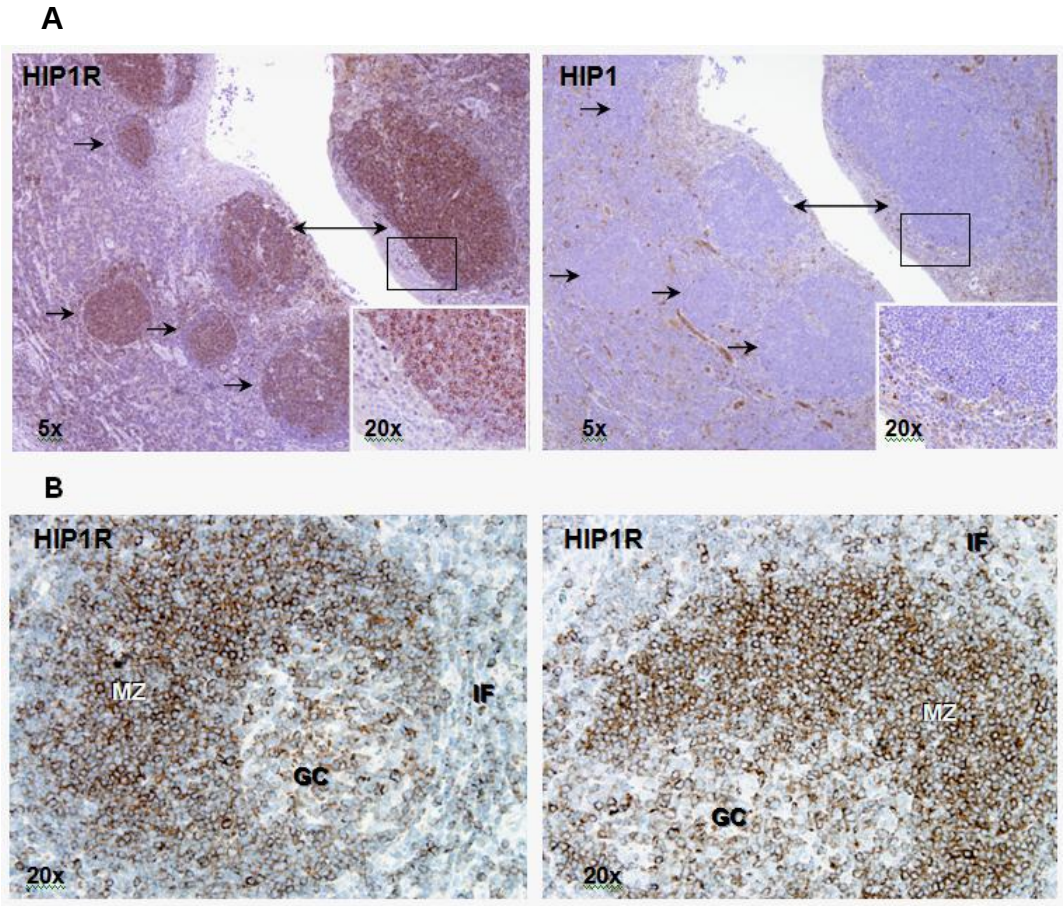

Fig 4.5 HIP1R and HIP1 expression patterns in FFPE reactive tonsil

A: The arrows denote primary lymphoid follicles. The 20x magnification inset picture represents the area of a B-cell follicle demonstrated by a designated box in the 5x magnification picture; B: HIP1R expression patterns in secondary lymphoid follicles showing tonsillar cells in the mantle zone with stronger HIP1R expression compared to the cells in the germinal centre. IF: Interfollicular region; GC: Germinal centre; MZ: Mantle zone.

HIP1R and HIP1 expression in B cells were further studied by double immunoenzymatic labelling for co-expression with PAX5, a transcription factor that is expressed from the pro-B-cell stage through all subsequent B-cell stages except plasma cells (Torlakovic *et al*., 2002). Immunolabelling of two independent FFPE reactive tonsils was performed with anti-HIP1R-44 or anti-HIP1-4B10 mAbs and detected using a brown substrate, followed by anti-PAX5 (clone 24, BD) labelling and detection using a blue substrate. HIP1R expression was present in the majority of $PAX5^+$ tonsillar B cells, particularly in the mantle zone. In contrast, HIP1 expression was absent in most tonsillar cells, and present only in very occasional $PAX5^+$ cells (Fig 4.6).

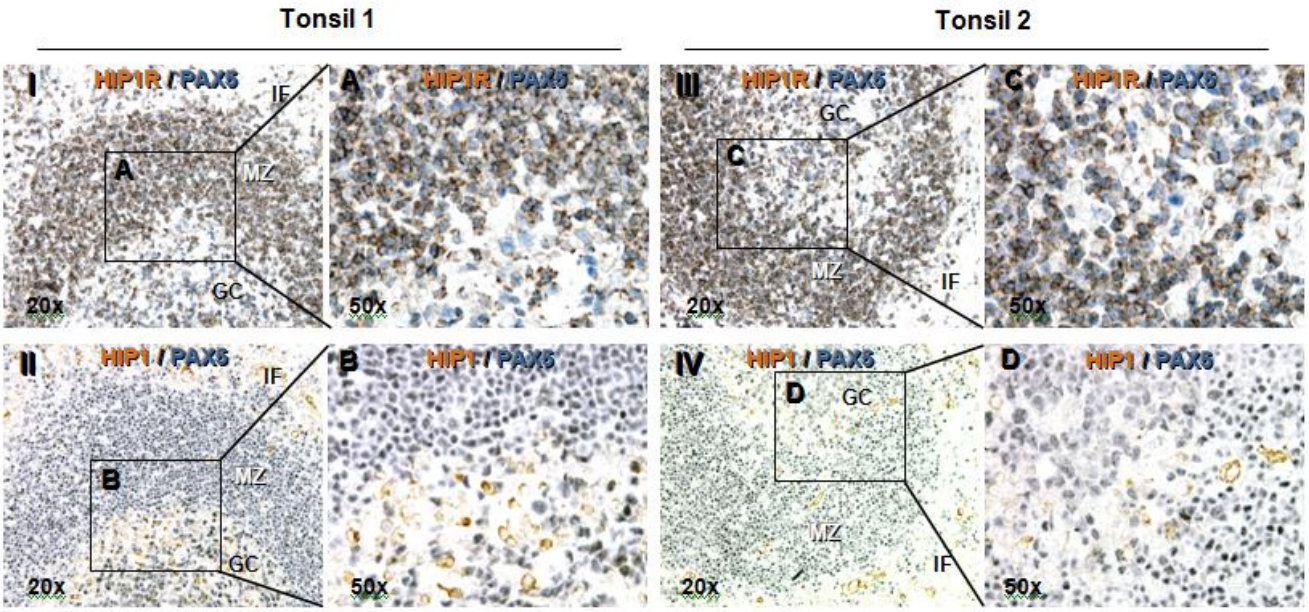

Fig 4.6 Double immunoenzymatic labelling of HIP1R or HIP1 with PAX5 in two independent FFPE reactive tonsils

Co-expression of HIP1R and PAX5 was observed in virtually all cells of the mantle zone around the germinal centre, and other regions of the tonsil. HIP1 was rarely expressed in $PAX5^+$ cells. Both HIP1R and HIP1 expression was present in the cytoplasm and PAX5 in the nucleus. The 50x magnification pictures (panel A to D) correspond to the designated box in its 20x counterpart (panel I to IV). IF: Interfollicular region; GC: Germinal centre; MZ: Mantle zone.

To confirm that HIP1R is more highly expressed in tonsillar B cells than in T cells at the protein level, immunofluorescent double-labelling on FFPE reactive tonsil of HIP1R with CD3 (polyclonal, Dako) labelling T cells or CD20 (clone L26, "in house") labelling B cells was performed. Isotype-specific antibodies labelled with fluorescein isothiocyanate (FITC) (green) or Texas Red (red) fluorochromes were used as secondary antibodies while cell nuclei were labelled with DAPI (blue). HIP1R was co-expressed with CD20 but little or undetectable co-expression was observed with CD3, indicating that in tonsil, HIP1R is preferentially expressed in B cells rather than the T-cell populations (Fig 4.7).

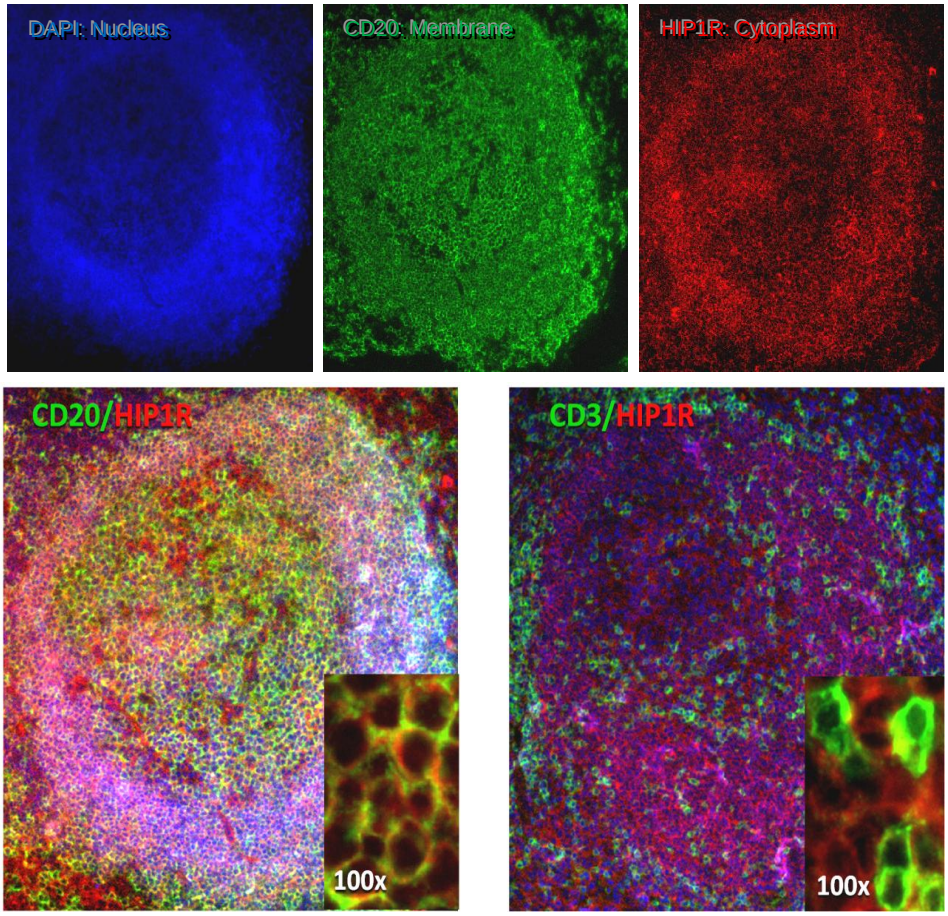

Fig 4.7 Immunofluorescent double-labelling of FFPE reactive tonsil sections with CD20 or CD3 and HIP1R

DAPI fluorescent stain was used to label the nuclei, FITC to label CD20 or CD3 in the membrane, and HIP1R in the cytoplasm was labelled with Texas Red. HIP1R was expressed in $CD20^+$ B cells and not in $CD3^+$ T cells.

4.2.3 Characterisation of HIP1R protein expression in B-cell subsets

HIP1R protein expression in activated B cells and plasma cells was examined by double immunoenzymatic labelling. CD30, a member of the tumour necrosis factor receptor (TNFR) superfamily, is a marker of both activated B and T cells (Stein *et al*., 2000). HIP1R expression in activated cells was first examined by double immunoenzymatic with a CD30 mAb (clone BerH2, "in house") in two independent FFPE reactive tonsils. A total of only 10 $CD30^+$ cells were observed from both tonsils combined (Fig 4.8) and only 1 of the $CD30^+$ cells had weak HIP1R expression (Fig 4.8I).

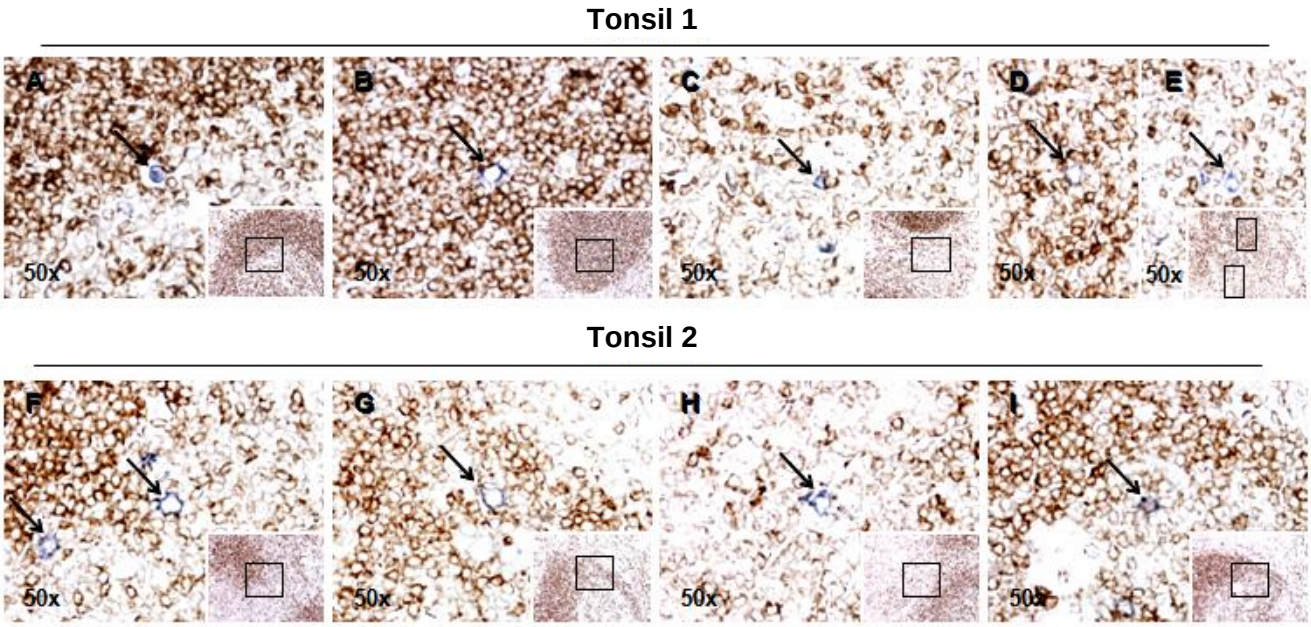

Fig 4.8 Double immunoenzymatic labelling of HIP1R with CD30 in two FFPE tonsils

HIP1R expression (in brown) was not present in $CD30^+$ cells (panel A-H) except one $CD30^+$ cell (in blue) with weak HIP1R expression (panel I) denoted by arrows. HIP1R expression is present in the cytoplasm and CD30 on the membrane. The 50x magnification pictures correspond to the designated box in the inset pictures.

Due to the scarcity of $CD30^+$ cells in the reactive tonsils studied, other activated B-cell markers were needed to further confirm the findings that HIP1R is rarely expressed in this subset. IRF4/MUM1 is a transcription factor directly involved in plasma cell differentiation that is expressed in a subset of GC or activated B cells (Klein and Dalla-Favera, 2008), activated T cells, and is highly expressed in plasmablast and plasma cells (Falini *et al*., 2000).

HIP1R expression in these subsets was examined by double immunoenzymatic labelling with two commercial anti-IRF4/MUM1 mAbs from Dako and Santa Cruz (California, USA) in two independent FFPE reactive tonsils (Fig 4.9). The vast majority of $IRF4/MUM1^+$ cells lying in the germinal centres and interfollicular areas were HIP1R-negative. There were occasional $IRF4/MUM1^+$ cells within the GC with weak HIP1R co-expression, indicating that HIP1R is weakly expressed in a subset of activated tonsillar B or T cells, plasmablasts and plasma cells.

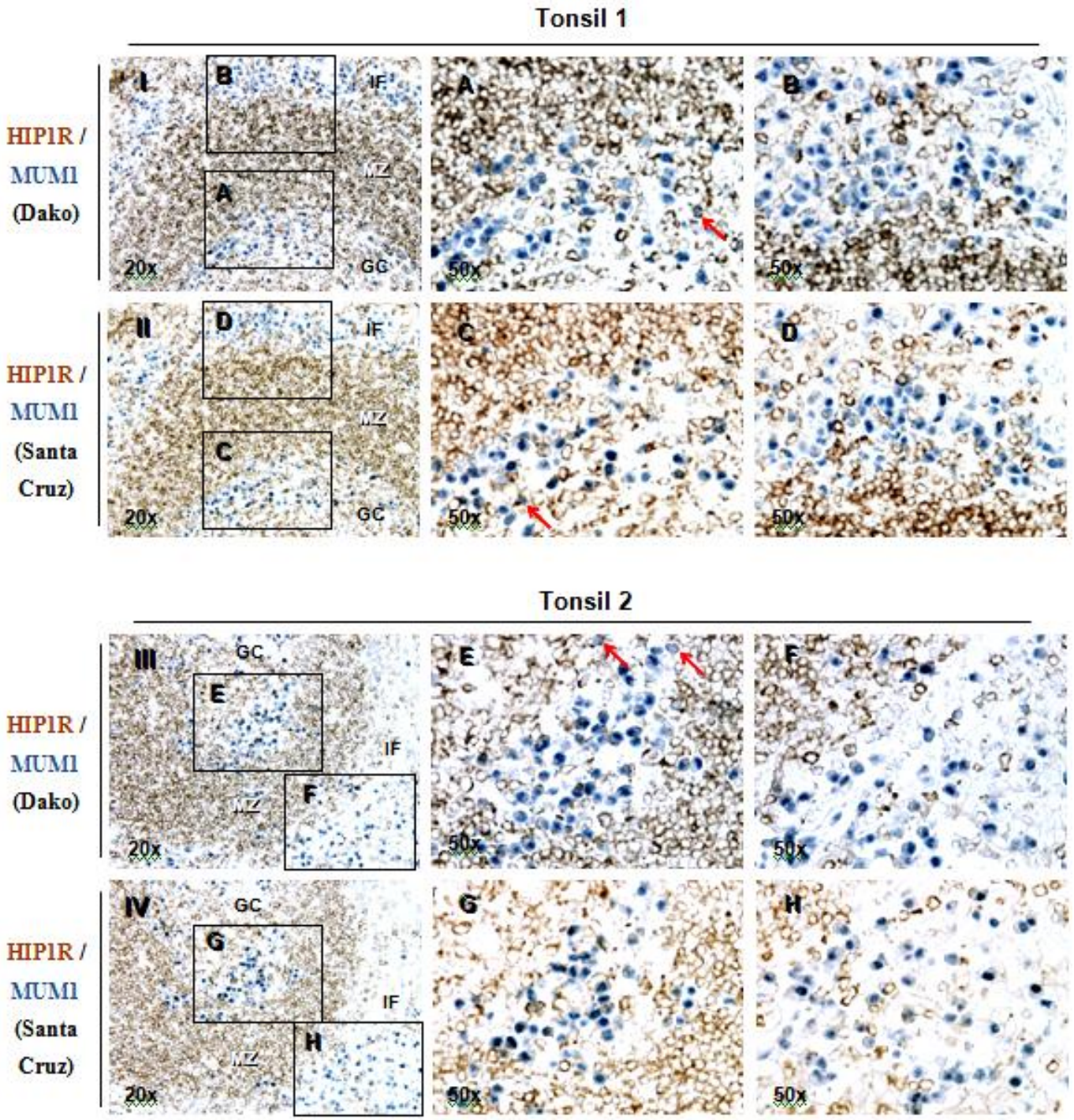

Fig 4.9 Double immunoenzymatic labelling of HIP1R with MUM1 in two independent FFPE reactive tonsils

Co-expression of HIP1R and MUM1 was absent in the vast majority of tonsillar cells except some occasional cells in the GC with weak expression denoted by the arrows. HIP1R is localised in the cytoplasm and MUM1 in the nucleus. The 50x magnification pictures (panel A to H) correspond to the designated box in its 20x counterpart (panel I to IV).

IF: Interfollicular region; GC: Germinal centre; MZ: Mantle zone.

The observation that HIP1R was not expressed in IRF4/MUM1$^+$ tonsillar cells in the interfollicular areas while occasional expression was observed in IRF4/MUM1$^+$ GC cells suggests that HIP1R expression changes with B-cell differentiation. It is decreased in plasma cells as they leave the germinal centres, residing in interfollicular areas. This was further investigated by double immunoenzymatic labelling of HIP1R-positive cells with an anti-CD38 mAb (Vector Laboratories, Peterborough) labelling GC B cells and plasma cells, an anti-CD138 mAb (Dako) and an anti-XBP1 mAb (a kind gift from Dr Giovanna Roncador, CNIO, Madrid) both of which label plasma cells, and an anti-BCL6 mAb (Dako) that labels GC B cells in FFPE reactive tonsils.

HIP1R was expressed in the majority of BCL6$^+$ cells in the GC. It was also expressed in some CD38$^+$ and XBP1$^+$ GC B cells but not in CD38$^+$, XBP1$^+$ or CD138$^+$ interfollicular B cells (Fig 4.10), consistent with the absence of HIP1R co-expression in MUM1$^+$ interfollicular B cells. This indicates that HIP1R expression is lost during terminal differentiation to plasma cells.

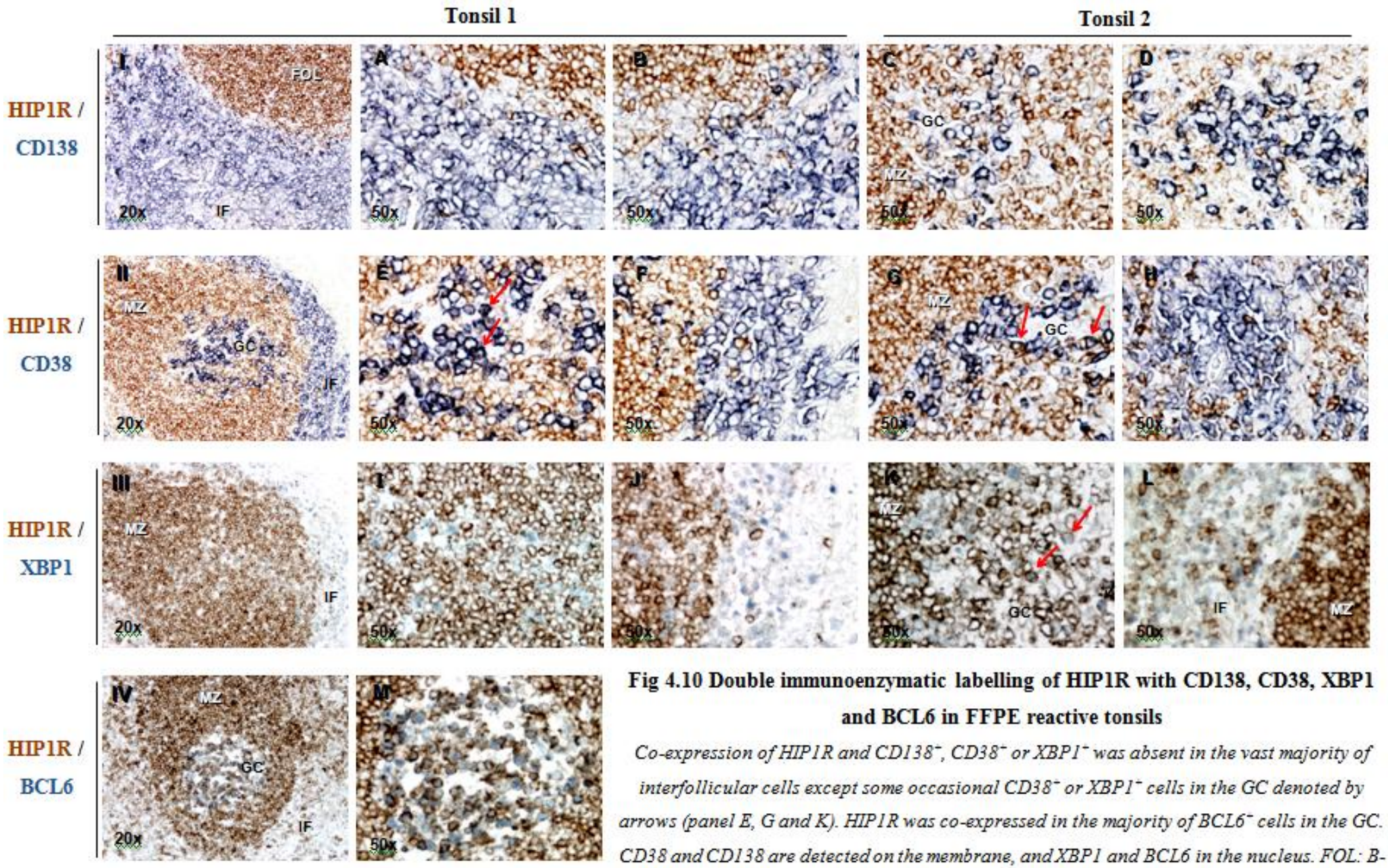

Fig 4.10 Double immunoenzymatic labelling of HIP1R with CD138, CD38, XBP1 and BCL6 in FFPE reactive tonsils

Co-expression of HIP1R and CD138$^+$, CD38$^+$ or XBP1$^+$ was absent in the vast majority of interfollicular cells except some occasional CD38$^+$ or XBP1$^+$ cells in the GC denoted by arrows (panel E, G and K). HIP1R was co-expressed in the majority of BCL6$^+$ cells in the GC. CD38 and CD138 are detected on the membrane, and XBP1 and BCL6 in the nucleus. FOL: B-cell follicle; IF: Interfollicular region; GC: Germinal centre; MZ: Mantle zone.

4.2.4 HIP1R and HIP1 mRNA and protein expression in a panel of cell lines derived from haematological malignancies

To investigate the relevance of HIP1R expression in haematological malignancies, its expression was initially studied in a panel of cell lines and compared to that of HIP1. Fig 4.11 shows *HIP1R* mRNA levels by qRT-PCR in a panel of cell lines derived from haematological malignancies (n = 25) and purified B- and T-cell populations, after normalising to an internal *TBP* control and expressing values relative to the 293T cell line that was used as a reference. *HIP1R* was most highly expressed in GC-DLBCL and in cell lines corresponding to another GC-derived lymphoma, Burkitt's lymphoma (BL), and in normal B-cell populations but not T-cell populations.

However, lower *HIP1R* levels was observed in B-NHL except BL and certain GC-DLBCL cell lines in comparison with purified B-cell populations ($CD19^+$ and GC B cells). Two GC-DLBCL cell lines (SUDHL4 and SUDHL6) showed higher *HIP1R* levels than normal GC B-cell populations, suggesting a subset of GC-derived lymphomas (i.e. GC-DLBCL, BL), which share a common COO, might show overexpression of HIP1R. The ABC-DLBCL cell lines had significantly lower *HIP1R* levels in comparison with those of GC-DLBCL ($p < 0.05$), suggesting that *HIP1R* might be a marker for distinguishing GC- versus ABC-DLBCL. Immunoblotting experiments showed the presence of HIP1R protein in lymphoma cell lines with relatively abundant *HIP1R* mRNA expression levels.

Comparing *HIP1R* with *HIP1* expression levels in a similar panel of haematological cell lines (n = 27, Fig 4.12), *HIP1R* was more widely and highly expressed than *HIP1* in the cell line panel and in purified B-cell populations. *HIP1* was only highly expressed in HLY-1, NCI-H929, KMH-2 and Granta-519, all originating from different subtypes of lymphomas. The majority of the cell lines (n = 17) did not express *HIP1* and others had low *HIP1* expression (n = 6). Immunoblotting experiments showed the expression of HIP1 protein correlated with *HIP1* mRNA expression levels. An interesting observation is that the two (of five) ABC-DLBCL cell lines (HLY-1 and RIVA) and one (of three) HL cell line (KM-H2) that expressed HIP1R were also positive for HIP1 expression.

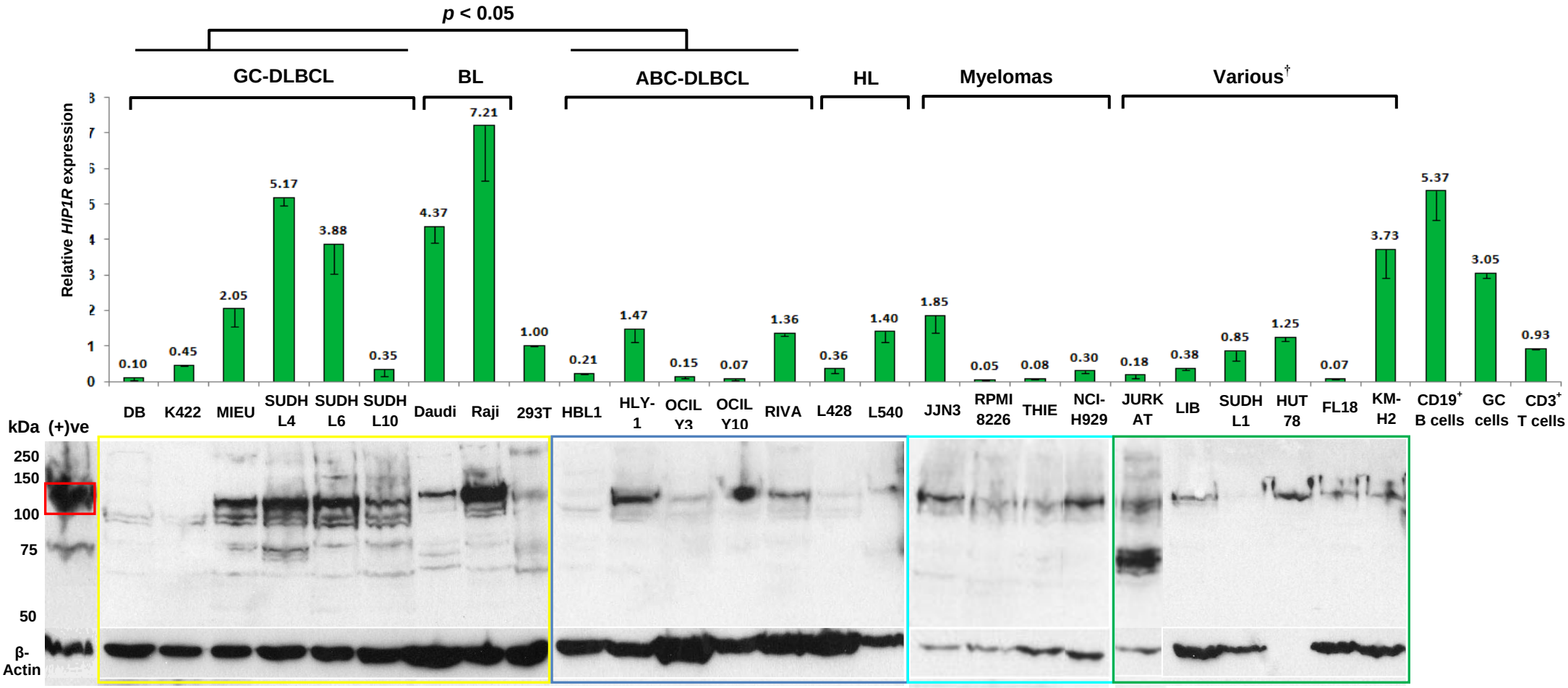

Fig 4.11 HIP1R mRNA and protein expression levels in a panel of cell lines

HIP1R mRNA levels in each cell line are graphically presented and their corresponding protein levels are illustrated on Western blots below. Proteins derived from HIP1R-transfected 293T cells were used as positive control for Western blotting. ***β****-actin as a loading control is shown in the botton Western blot panels. Each panel of Western blot investigated on separate SDS-PAGE gels is highlighted in box with alternating colours. HIP1R mRNA levels were significantly different in GC-DLBCL versus ABC-DLBCL ($p < 0.05$), and ABC-DLBCL showed significantly lower levels of HIP1R than normal B cells ($p < 0.01$). † Jurkat: T-cell leukaemia; LIB: Unclassified DLBCL; SUDHL1: ALCL; HUT78: CTCL; FL18: FL; KM-H2: HL.*

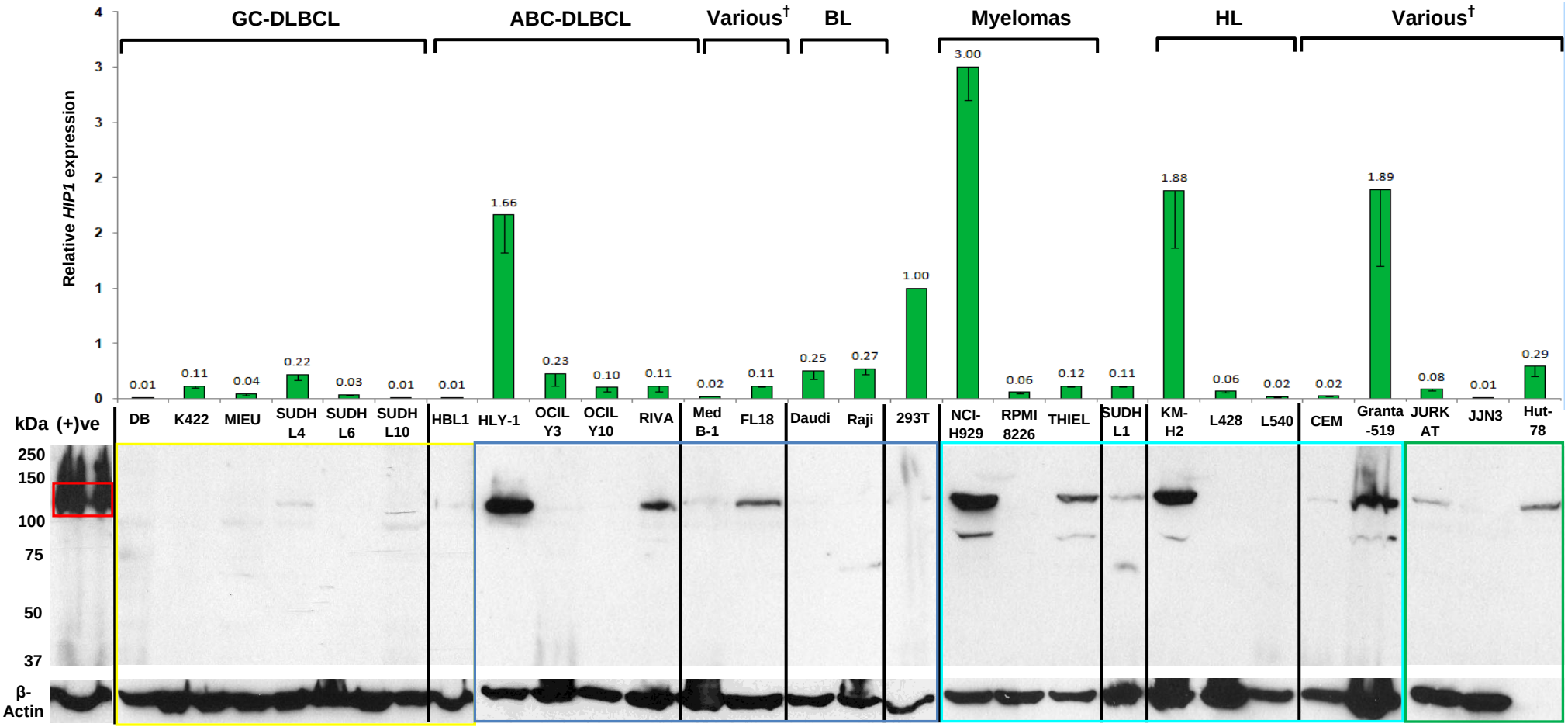

Fig 4.12 HIP1 mRNA and protein expression levels in a panel of cell lines

*HIP1 mRNA levels of each cell line were presented on a graph and their corresponding protein levels on Western blots. Proteins derived from HIP1-transfected 293T cells were used as a positive control and **β**-actin as loading control shown on the bottom Western blot panels. Each panel of Western blot investigated on separate SDS-PAGE gels is highlighted in box with alternating colours.*

† MedB-1: PM-DLBCL; FL18: FL; SUDHL1: ALCL; CEM: T-cell leukaemia; Granta-519: MCL; Jurkat, JJN3: Myeloma; HUT78: CTCL.

4.3 ASSOCIATION OF HIP1R WITH B-CELL MOLECULES

4.3.1 Inference of molecules associated with HIP1R by ARACNe

Our study so far has identified interesting expression patterns of HIP1R in both FFPE tonsils and cell lines, with HIP1R high-level expression in normal B cells and its apparent downregulation in certain subtypes of B-NHL. Although the interactomes involving HIP1R have been partially characterised, such as the proven ability of HIP1R to bind clathrin and actin proteins (Brett *et al*., 2006; Wilbur *et al*., 2008), insights into the association of HIP1R with other molecules by means of GEP clustering has not been documented.

To allow the prediction of molecules associated with HIP1R expression at a genome-wide level, the ARACNe algorithm was adopted to investigate these associations in a microarray dataset containing 100 samples of normal and malignant B cells by using the software geWorkbench (genomics Workbench) version 2.0.1. This allows the analysis and visualisation of data from a wide range of genomics domains such as gene expression, protein structure and systems biology (Floratos *et al*., 2010) (http://wiki.c2b2.columbia.edu/workbench/index.php/Home).

The *HIP1R* sub-network was generated by using the default criteria of "mutual information" score of 0.3 (preset by the software), and this uncovered a potential *HIP1R* association with 12 molecules: *BCL7A*, *CD79A*, *CR1*, *DENND3*, *LRRFIP1*, *MLXIP*, *OSBPL8*, *PIM2*, *TNFRSF10B*, *PTPRE*, *INPP5F*, and *GANAB* at the transcript level. This further links HIP1R with known molecules frequently documented as being involved in B-NHL pathogenesis: BCL7A, PIM2 and CD79A (Zani *et al*., 1996; Hoefnagel *et al*., 2005; Davis *et al*., 2010).

Further probing into the *HIP1R* subnetwork with a less stringent criteria of 0.1 mutual information score generated a further 264 molecules associated with *HIP1R* (Fig 4.13). Due to the complexity of the much larger network generated, molecules known to be associated with lymphocyte function from the literature were included together with the initial 12 molecules (probed with a more stringent criterion). This resulted in the identification of 32 molecules to be further tested by Pearson correlation coefficient analysis to investigate: 1) The positive or inverse association with *HIP1R*, as the network does not provide this information; 2) Whether the associations are significant tested by an independent statistical analysis i.e. validating the associations generated by ARACNe algorithm.

The final correlation analysis uncovered that *HIP1R* is inversely-associated with the oncogene *PIM2* kinase, *LEF1* (Lu *et al*., 2004), and *CD6* glycoprotein present on the surface of T cells (Gimferrer *et al*., 2003) (Table 4.1 and Fig 4.14). *HIP1R* is positively-associated with *CD22* which is a negative regulator of BCR signalling (Monroe, 2006) and certain surface proteins (CD83, IgJ). Interestingly, *HIP1R* is positively-associated with known GC-DLBCL markers *BCL7A* and *HIF1A* (Blenk *et al*., 2007), in line with higher *HIP1R* levels in GC-DLBCL compared to ABC-DLBCL ($p < 0.05$) observed earlier in qRT-PCR studies on the panel of lymphoma cell lines.

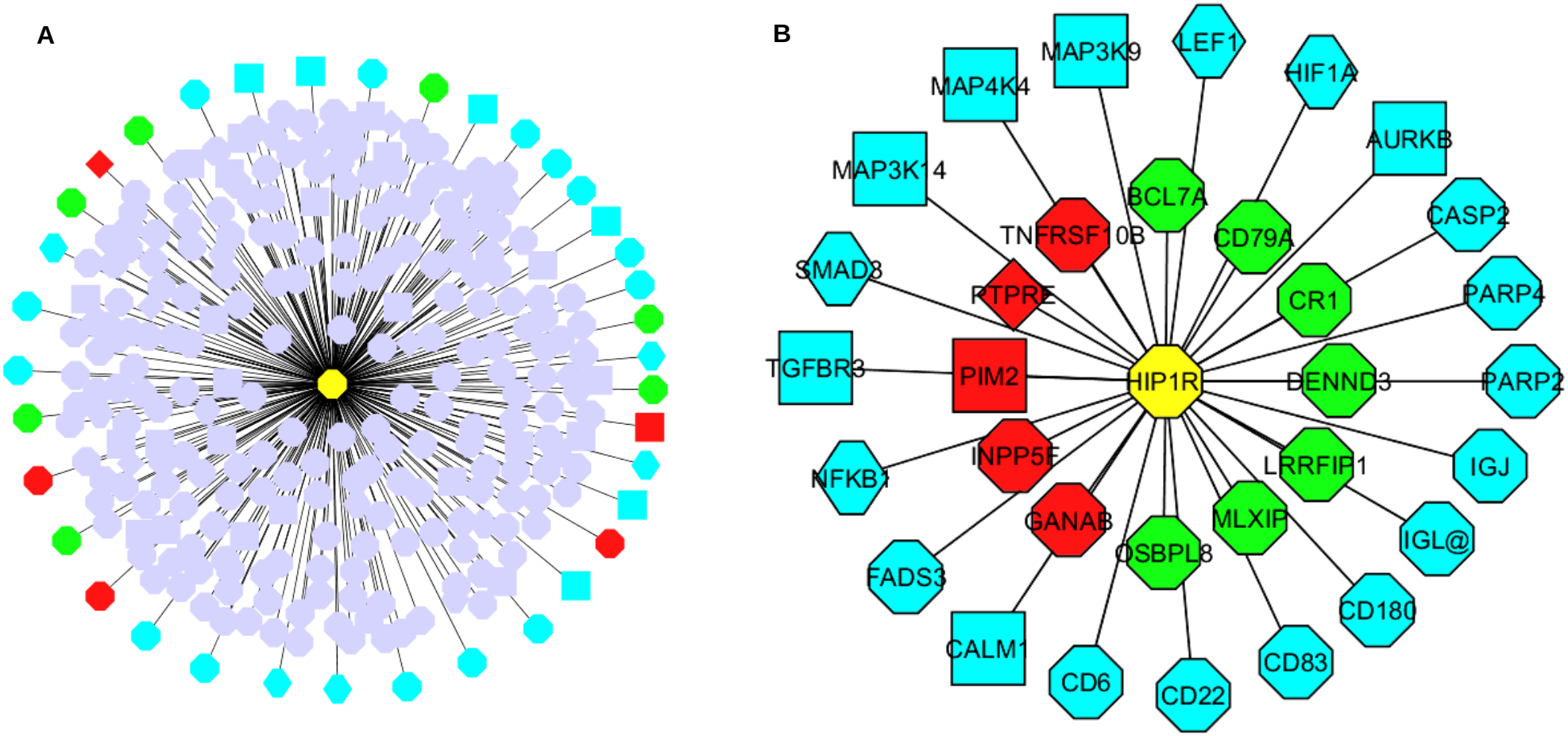

Fig 4.13 *HIP1R* subnetwork generated by ARACNe algorithm

A: The HIP1R subnetwork generated with a less stringent criteria; B: Molecules associated with HIP1R generated with a more stringent criteria are in green and red nodes, and the selected molecules from panel A are in aqua nodes.

Genes	Pearson correlation coefficient	*p*-value
MLXIP	0.648147	<0.000001
CR1	0.628916	<0.000001
DENND3	0.582722	<0.000001
HIF1A	0.544889	<0.000001
BCL7A	0.527275	<0.000001
MAP4K4	0.498135	<0.000001
IGJ	0.452287	0.000002
OSBPL8	0.450515	0.000003
CD22	0.447151	0.000003
SMAD3	0.442348	0.000004
LRRFIP1	0.40855	0.000025
FADS3	0.405447	0.000029
CD83	0.337269	0.000602
CASP2	0.310419	0.001672
AURKB	0.303145	0.002174
PARP4	-0.5558	<0.000001
LEF1	-0.4949	<0.000001
TGFBR3	-0.4644	0.000001
PIM2	-0.40582	0.000029
INPP5F	-0.40143	0.000036
PTPRE	-0.38783	0.00007
MAP3K9	-0.37392	0.000132
CD6	-0.28974	0.003544

Table 4.1 Correlation significance of ARACNe-inferred genes with *HIP1R*

Genes without significant correlation were excluded

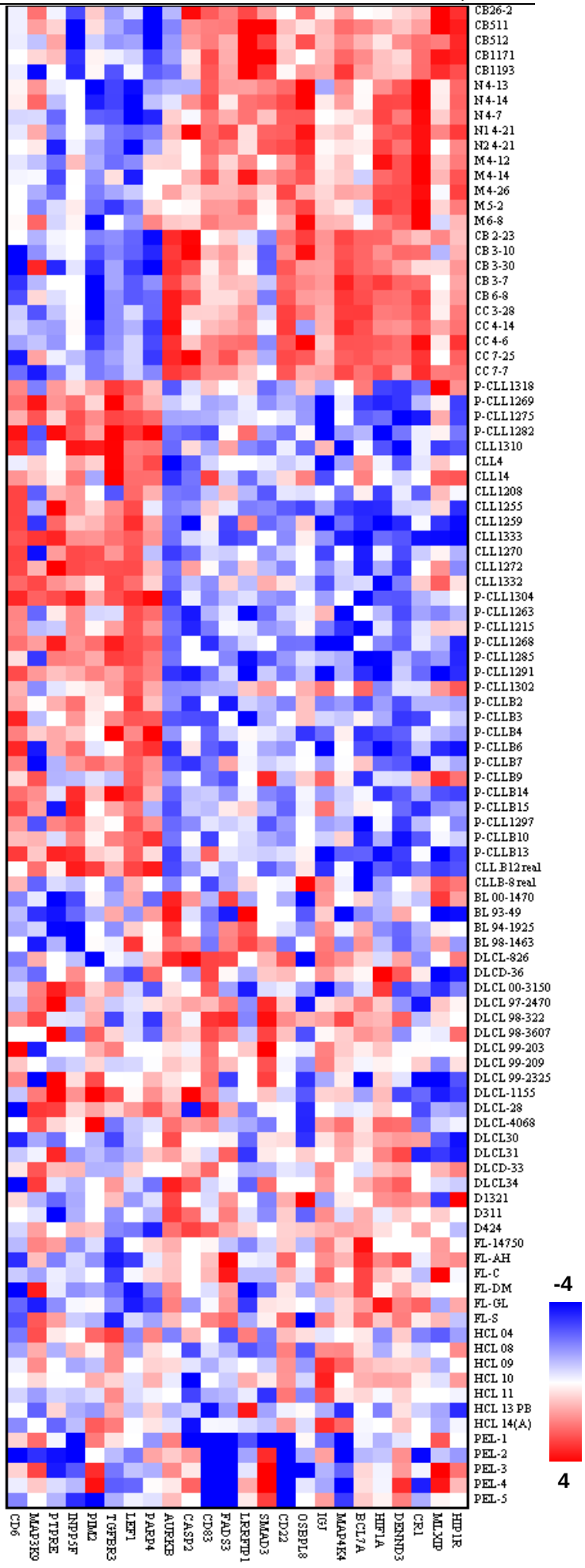

Fig 4.14 HeatMap visualisation of genes significantly correlated with *HIP1R*

Total number of samples and genes are 100 and 24, respectively.

4.3.2 Putative association of HIP1R with MYC and AKAP12

qRT-PCR studies on a panel of cell lines indicated that *HIP1R* levels in Raji and Daudi (BL lines) were similar to those of normal B-cell populations. Microarray gene expression profiling data presented in the following chapter also identified relatively high levels of *HIP1R* in BL, compared to other B-cell lymphomas. We therefore considered reasons why BL might retain *HIP1R* expression and one such possibility is an association with the transcription factor MYC. This proto-oncogene is constitutively activated by chromosome translocations targeting the immunoglobulin heavy chain or light chain loci and is associated with 100% of BL (Klein and Dalla-Favera, 2008). HIP1R is one of 662 putative MYC protein modulators, identified by MINDy algorithm, whose expression levels correlates with the transcript levels of a subset of MYC target genes (Wang *et al*., 2009b). Thus, MINDy analysis is used here to identify the putative MYC target genes whose expression level might be affected by the co-expression of *HIP1R* with *MYC*.

MINDy analysis was run on the same set of samples as used earlier in the ARACNe algorithm by using geWorkbench software. As in ARACNe analysis, the values of the samples were initially filtered, $\log_2$-transformed, normalised to median value of the microarray dataset before scaling down the range of the values to +4 (maximum) and -4 (minimum). This culminated in a long list of 43 genes whose expression might be negatively affected by an association between *HIP1R* and *MYC* (Fig 4.15).

To determine whether any of these genes are known MYC target genes, the presence of the 43 genes was examined on the 340 literature-validated targets on the MYC database (Zeller *et al*., 2003; http://www.myccancergene.org/index.asp). This analysis resulted in a list of 5 MYC target genes, *NOLC1, PRDX4, S100A2, GM2A* and *AKAP12,* whose expression

was affected by the presence of *HIP1R*. Further visualisation of the HeatMaps generated by MINDy demonstrated a pattern of *AKAP12* downregulation in the presence of both *MYC* and *HIP1R*. This pattern did not occur in the absence of *HIP1R* expression (Fig 4.15C).

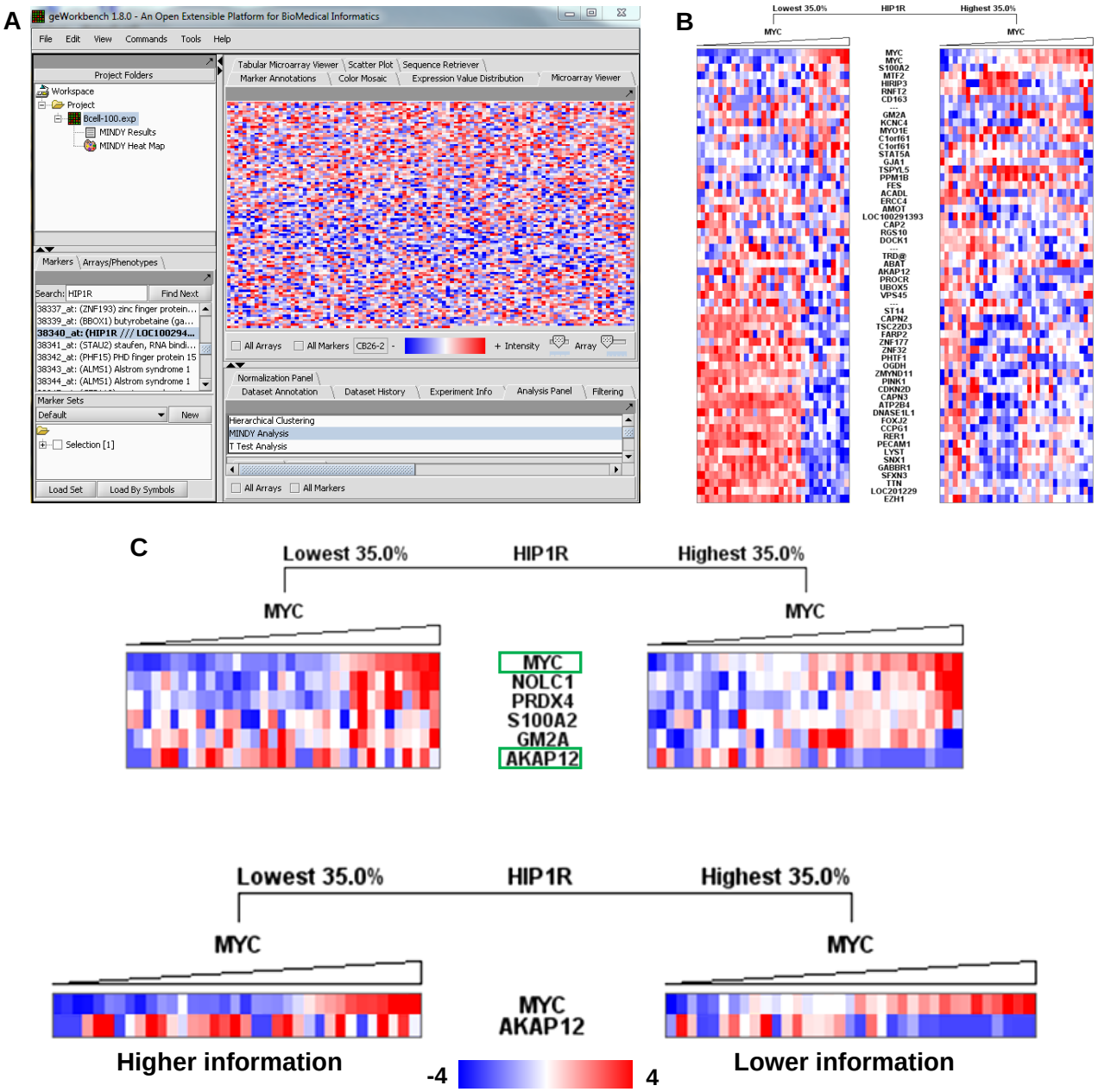

Fig 4.15 MINDy algorithm prediction of genes that might be affected by HIP1R modulation of MYC activity

A: geWorkbench interface; B: Long list of genes affected by HIP1R modulation of MYC; C: Shortlisted MYC target genes identified by MYC targets database with focus on AKAP12. NB: AKAP12 levels decreased in the presence of high HIP1R and MYC levels.

To validate these associations, primers were designed for SYBRGreen qRT-PCR analysis for expression of *NOLC1*, *PRDX4* and *AKAP12*, in siRNA-mediated downregulation of HIP1R expression (or si*HIP1R*) in Raji cells; a cell line derived from BL patient with *MYC* locus translocation and constitutively overexpressing MYC. Three different siRNA duplexes assigned as "si1", "si2" and "si3" targeting different *HIP1R* regions together with a scramble siRNA control were successfully used to electroporate the cells by using the Amaxa Nucleofector system (Lonza). Knockdown of HIP1R expression was achieved after 48 and 72 hours with the re-emergence of HIP1R expression after 96 hours, and depletion of HIP1R expression by si3 was inferior to si1 and si2 (Fig 4.16).

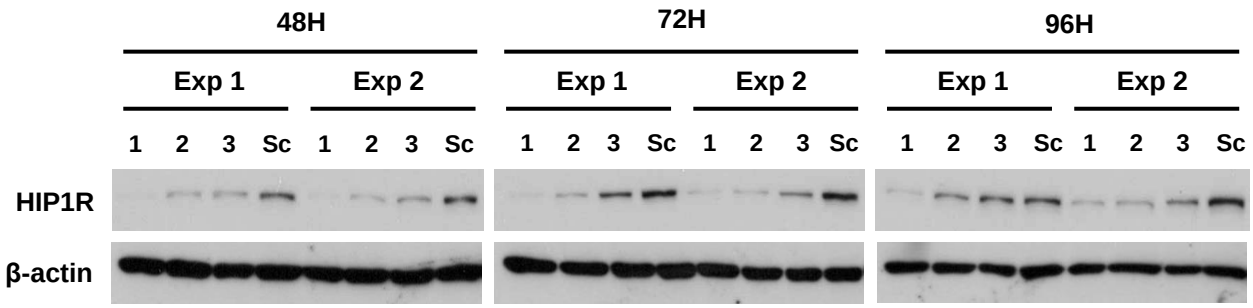

Fig 4.16 Validation of siRNA-mediated knockdown of HIP1R by immunoblotting

HIP1R silencing was effective after 48 and 72 but not 96 hours of HIP1R knockdown. si3 (assigned as 3) yielded less HIP1R depletion compared to si1 and si2 (assigned as 1 and 2, respectively). Sc: Cells treated with a scramble siRNA.

Thus, the samples treated with si1 and si2 for 72 hours were used to investigate the expression levels of *NOLC1*, *PRDX4* and *AKAP12*. The mRNA levels of *NOLC1* and *PRDX4* did not change significantly but *AKAP12* expression increased upon HIP1R depletion by both si1 and si2 significantly in two independent experiments ($p < 0.05$) (Fig 4.17), in parallel with MINDy predictions.

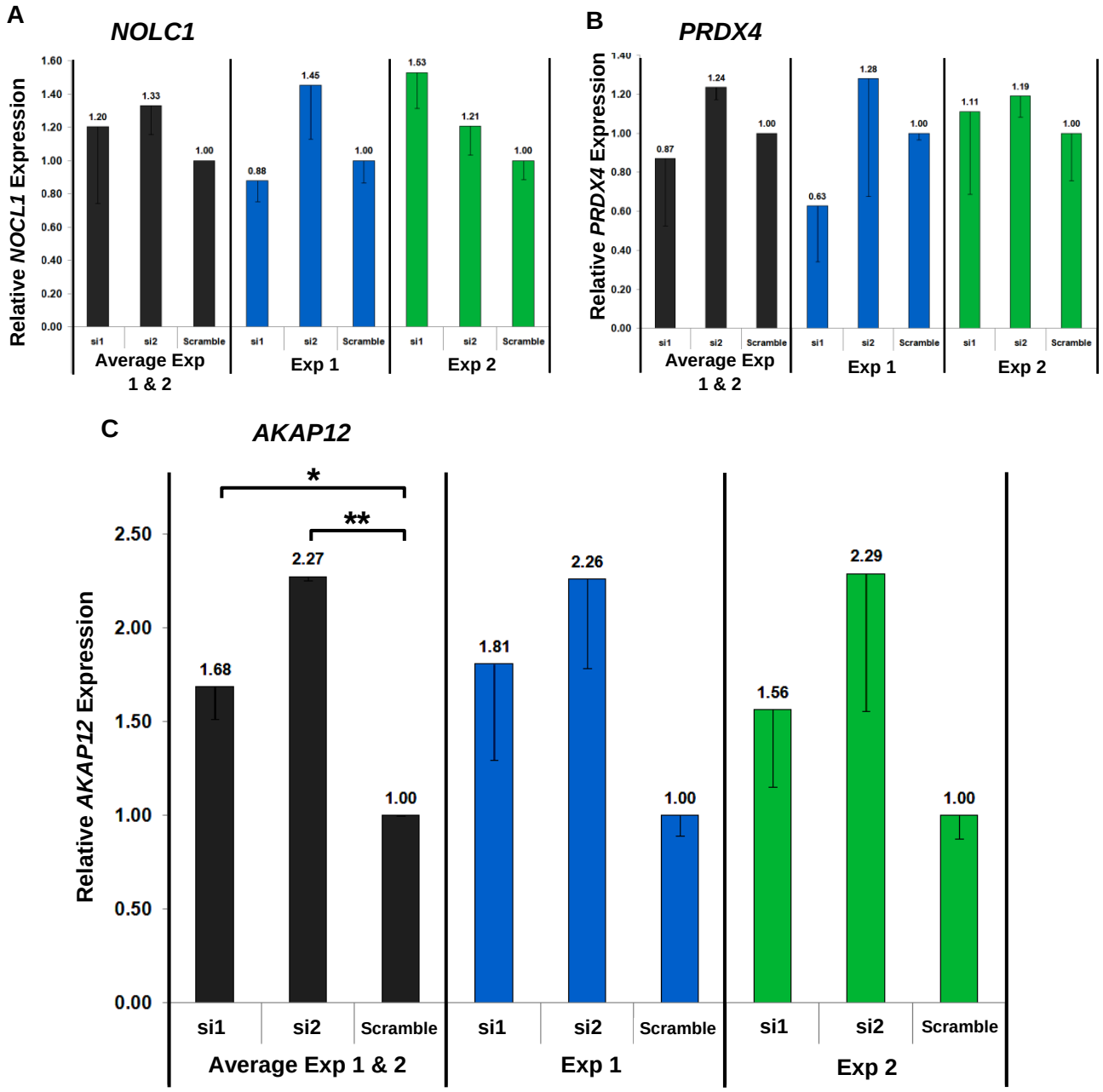

Fig 4.17 qRT-PCR analysis of *NOLC1, PRDX4* and *AKAP12* levels in si*HIP1R* Raji cells

Inconsistent changes in NOLC1 (A) and PRDX4 levels (B) were observed, but AKAP12 expression increased significantly (C) upon HIP1R depletion by both si1 and si2 in two independent experiments. Key: ** *: $p < 0.01$;* * *: $p < 0.05$.*

This study suggests that HIP1R might be capable of affecting the transcriptional activity of MYC at the post-translational level on at least one of its targets, *AKAP12* in the context of Raji cells, via an unknown mechanism. One possibility is that HIP1R may alter upstream signalling that may modulate MYC or its co-factors or regulators.

DISCUSSION

HIP1R is expressed in most normal tissues and at high levels in normal B cells. This was confirmed by double labelling studies on reactive tonsils with antibodies to PAX5, CD3, CD20, CD30, IRF4/MUM1, CD138, CD38, XBP1 and BCL6. These studies have indicated that HIP1R is widely expressed in naïve B cells, and its expression is lost on terminal differentiation into plasma cells. This raises the possibility that the NF-κB signalling pathway or other putative regulators implicated in B-cell activation or maturation (e.g. FOXP1, IRF4/MUM1) may affect HIP1R levels. This hypothesis is explored in the next chapter.

HIP1R is still maintained at high levels in $CD27^+$ memory B cells compared to $CD19^+$ B cells. One possible explanation is via its regulation by STAT5 since siRNA-mediated silencing of STAT5 in a type of prostate cancer cell line showed downregulation of *HIP1R* levels (Gu *et al*., 2010), and phosphorylated STAT5 is proposed to mediate differentiation of memory B cells versus plasma cells by regulating BCL6 expression (Scheeren *et al*., 2005). Fig 4.18 shows the proposed HIP1R expression patterns in normal B-cell subsets.

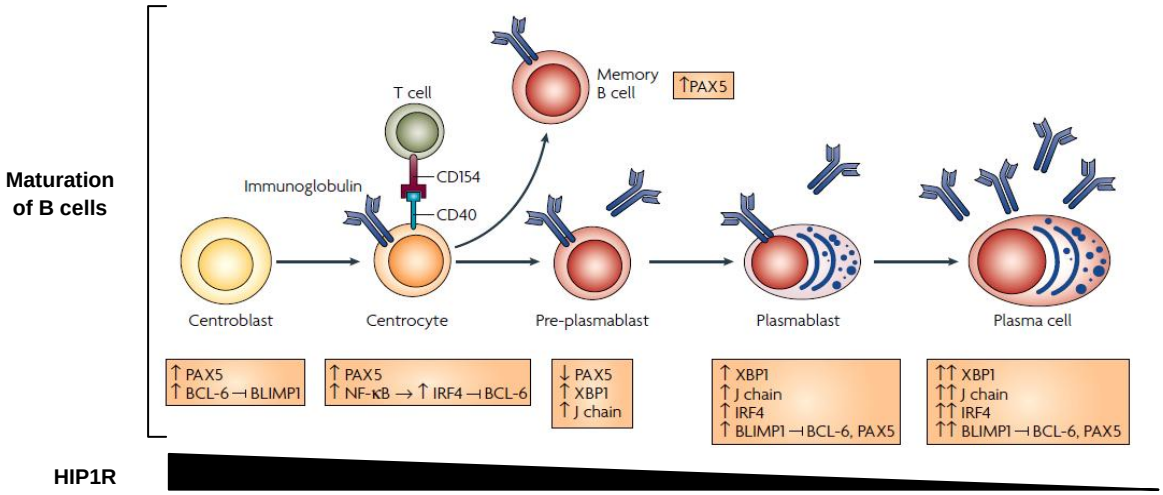

Fig 4.18 Proposed HIP1R expression levels in different subsets of normal B cells

HIP1R expression decreases as the B-cell matures from centroblast into terminally-differentiated plasma cell. Diagram adapted from Klein and Dalla-Favera (2008) with modifications.

The high-level expression of HIP1R in GC-derived lymphoma cell lines and in normal B-cell populations, but not in T-cell populations, is consistent with the high frequency of autoantibodies against the HIP1R antigen in the sera from patients with GC-derived lymphomas and B-cell NHL (shown in Chapter 3). However, the expression level of *HIP1R* in lymphoma cell lines was commonly lower than levels in normal B cells, particularly in the case of ABC-DLBCL ($p < 0.01$, ABC-DLBCL cell lines versus $CD19^+$, $CD27^+$ and GC B cell subsets), suggesting that HIP1R expression might be downregulated in certain B-cell NHL subtypes.

Comparison of tonsillar GC B cells with GC-derived lymphomas, which share a common cellular origin, also raises the possibility that these lymphomas do not show a reduction in *HIP1R* expression and may sometimes show increased expression. Thus we cannot rule out the possibility that HIP1R overexpression in some GC-derived lymphoma patients may explain their immunological recognition of this antigen.

HIP1R was more widely and highly expressed than HIP1 in both lymphoma cell lines and normal lymphocytes. Bradley *et al*. (2007b) reported that HIP1 was overexpressed in 68% of NHL and 64% in B-cell lymphomas, consistent with the presence of HIP1 autoantibodies in lymphoma patients' sera in that study. However, this 2007 report contradicts previous findings from the same group, Rao *et al*. (2002), describing HIP1 expression as being absent in 80% of primary lymphomas with the remaining 20% having low levels of HIP1 expression. Both of these studies, and our own, used the same anti-HIP1-4B10 mAb for IHC staining of the lymphoma samples. The findings by Rao *et al*. (2002) correlate with our observations that HIP1 is not commonly expressed in B-cell lymphomas and this is likely to explain the lack of immunological recognition of the HIP1 antigen shown

in the previous chapter by immunoblotting of HIP1-transfected cell lysates. This further supports our data that serological-reactivity in B-cell NHL patients is predominantly against the HIP1R autoantigen rather than HIP1.

The inference of molecules associated with *HIP1R* by ARACNe algorithm has identified positive associations with the known GC-DLBCL markers, *BCL7A* and *HIF1A* (Blenk *et al*., 2007). This suggests that *HIP1R* expression might be able to distinguish the GC- from ABC-DLBCL subtype. A positive association was identified between *HIP1R* and *HIF1A*, an independent good-prognostic indicator of R-CHOP-treated DLBCL patients (Evens *et al*., 2010). In contrast, *HIP1R* expression was inversely correlated with that of the *PIM2* kinase, which is overexpressed in CLL and B-cell NHL (Cohen *et al*., 2004), and with the poor prognostic indicator of B-cell CLL *LEF1* (Erdfelder *et al*., 2010). Together with the expression data in lymphoma cell lines, these correlations support the hypothesis that HIP1R expression might be indicative of prognosis in DLBCL patients. This is explored further in the next chapter.

The apparent frequent association of *HIP1R* with *MYC* because of their co-expression in BL was further explored as a potentially functional relationship using the MINDy algorithm. This identified *AKAP12* as a MYC target gene whose expression was affected by the co-expression of *HIP1R*. This prediction was experimentally investigated and showed *AKAP12* (A-kinase anchor protein 12) upregulation upon knockdown of HIP1R expression by two independent siRNAs in two independent experiments in Raji cells with constitutive expression of MYC.

AKAP12 is a member of the structurally diverse AKAP proteins that share a common function of binding protein kinase A (PKA), a cell growth related protein (Choi *et al*., 2004) that plays an important role in the completion of cytokinesis (Choi *et al*., 2008), and it is a confirmed MYC target (O'Connell *et al*., 2003). Although the association of AKAP12 with lymphomas is not known, there was an inverse correlation between *AKAP12* expression and the overall survival of acute leukaemia patients (Yildirim *et al*., 2007) and its overexpression is noted in individuals with aggressive unmutated CLL (Dighiero and Hamblin, 2008).

In normal B cells, *AKAP12* expression is reduced as the pre-B cells from bone marrow enter the mature B-cell repertoire whereby its expression is further markedly decreased (Suryani *et al*., 2010). This contrasts with high expression of HIP1R in mature naïve B-cell populations present in the mantle zone surrounding the germinal centres in follicles of reactive tonsils. In addition, data mining of deposited microarray datasets from Oncomine (https://www.oncomine.org) indicates that *AKAP12* is overexpressed in DLBCL ($p < 0.0001$) and FL ($p = 0.022$). The inverse expression patterns between *HIP1R* and *AKAP12* suggest that HIP1R might co-operate with MYC to downregulate *AKAP12* expression, and that HIP1R is capable of affecting the transcriptional activity of MYC via an unknown mechanism of post-translational modulation. Further investigation of these findings could provide a future avenue for HIP1R research. Firstly, it will be important to extend these studies to include additional BL cell lines. Then the dependence of this observation on co-expression of MYC will need to be confirmed, e.g. by investigating *AKAP12* levels after siRNA for HIP1R in cell lines without constitutive MYC expression.

In this chapter, the expression patterns of HIP1R and HIP1 in normal and malignant B cells, and the possible functional association of HIP1R with the MYC target *AKAP12* in a BL cell line have been explored. HIP1R expression patterns in DLBCL cell lines and its positive correlation with other GC-DLBCL markers in microarray datasets suggest that HIP1R expression is downregulated in ABC-DLBCL. As DLBCL subtyping is of significant interest in our laboratory, the expression, roles and putative regulators of HIP1R in DLBCL were investigated and the data are presented in the next chapter.

CHAPTER 5
HIP1R AS A DLBCL SUBTYPING MARKER AND THE PUTATIVE REGULATORS AND ROLES OF HIP1R

INTRODUCTION

5.1 BCR SIGNALLING IN DLBCL

BCR signalling in normal B cells has been explored in Chapter 1 (Introduction). The abnormal BCR signalling identified specifically in ABC-DLBCL which has been described as "chronic active" BCR signalling that contrasts with that of tonic signalling, is further introduced here.

GC-DLBCL have a gene expression profile that is characteristic of normal GC B cells, and this DLBCL subtype also has a higher rate of immunoglobulin class switch recombination (CSR) events, the mechanism that modifies immunoglobulin isotype IgM and IgD to IgG, IgA or IgE (Lenz *et al.*, 2007b). In contrast, ABC-DLBCL have a gene expression profile similar to that of activated normal B cells and rely on constitutive NF-κB signalling for survival (Lam *et al.*, 2005). In the NF-κB pathway, formation of a multiprotein subunit to ubiquitinate TRAF6 requires activation of the CARD11 protein kinase that forms a multiprotein complex with BCL10 and MALT1 (CBM complex) which is required for downstream signalling events (Lenz and Staudt, 2010).

Recent studies have shed light on the genetic lesions in DLBCL, particularly ABC-DLBCL, and their consequences for BCR signalling and/or NF-κB activation, both of which have a key role in disease pathogenesis (Davis *et al.*, 2010). Approximately 10% of ABC-DLBCL patients acquire CARD11 mutations, found within the coiled-coil domain, that activate NF-κB signalling independently of ligand-induced BCR activation (Lenz *et al.*,

2008b). However, the majority of ABC-DLBCL retain wild-type CARD11 and are dependent on BCR signalling for activation of the NF-κB pathway that is required for their survival. Approximately 20% of ABC-DLBCL have mutated proximal BCR subunits, CD79b (18%) or CD79a (2%), one function of which is to maintain the cell surface BCR in the presence of chronic active BCR signalling (Davis *et al.*, 2010). The third genetic lesion involves the biallelic loss of the negative NF-κB regulator, A20, and this occurs in approximately 8% of DLBCL patients (Kato *et al.*, 2009). Fig 5.1 summarises the consequences of these genetic lesions on the BCR signalling pathways in ABC-DLBCL.

A recent unpublished observation (Klein and Pasqualucci, 2010) pointed that genetic lesions involving CARD11, CD79b and A20 are mutually exclusive and account for about 50% of ABC-DLBCL. Notwithstanding the genetic lesions that occur in ABC-DLBCL, the vast majority (or approximately 90% after exclusion of cases with CARD11 mutations) still require ligand-induced BCR signalling, and mechanisms that increase or stabilise the surface BCR would promote BCR signalling pathways. Thus, the regulation of surface BCR levels is instrumental to prevent the alteration of BCR signalling homeostasis. Regulation of surface BCR involves mechanisms rendered by clathrin (Stoddart *et al.*, 2002) and the actin cytoskeleton (Onabajo *et al.*, 2008; Sharma *et al.*, 2009), which might involve HIP1R because of its ability to link clathrin with the actin cytoskeleton (Poupon *et al.*, 2008).

In this chapter, the expression patterns of HIP1R in DLBCL were first explored by GEP data-mining. This was followed by qRT-PCR on a series of DLBCL patients' cDNA samples and immunolabelling of a larger series of DLBCL TMAs, followed by investigations of putative regulators of HIP1R in DLBCL. The final sections explored the putative roles of HIP1R in DLBCL by si*HIP1R* and lenti-HIP1R system in DLBCL cell lines.

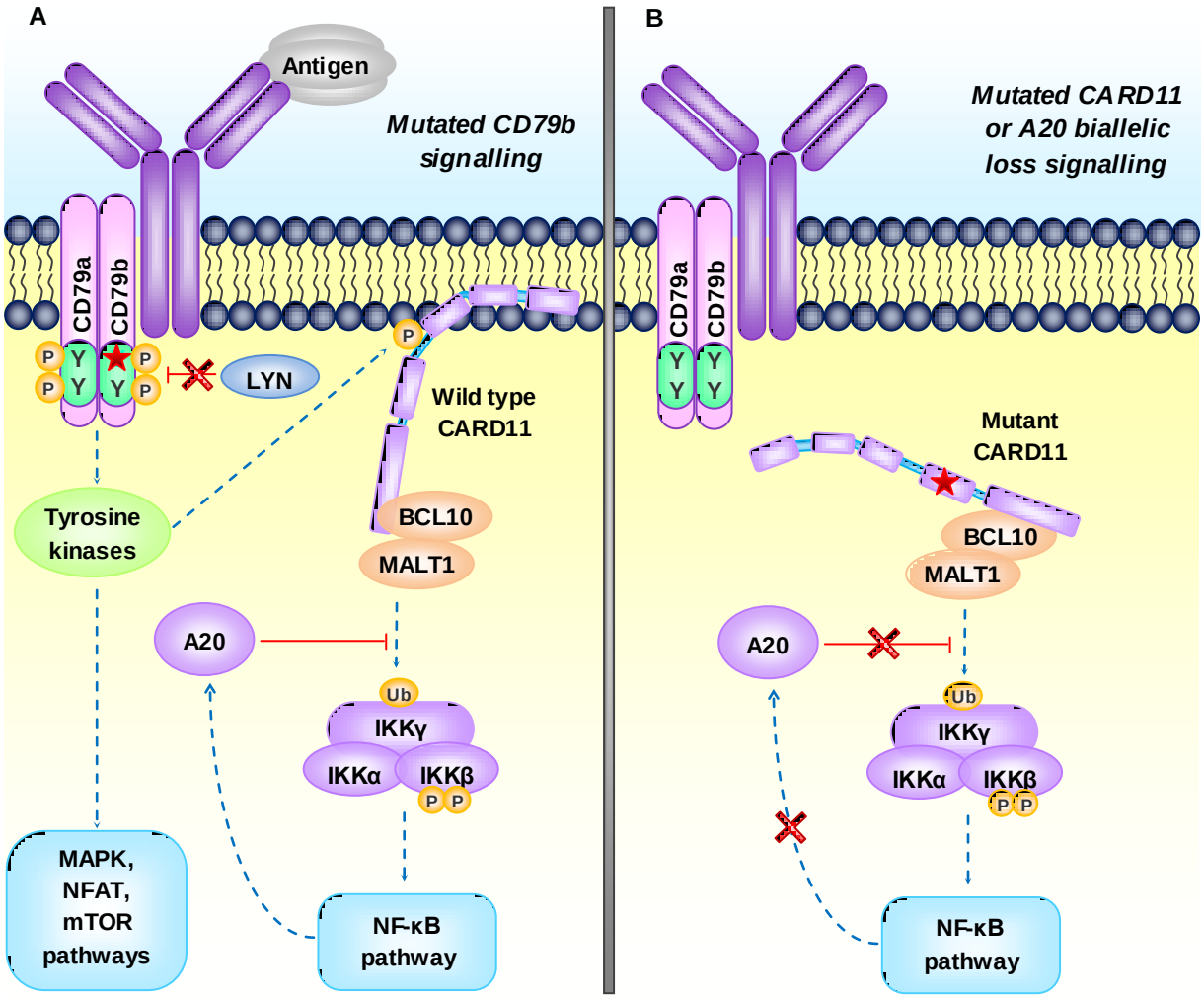

Fig 5.1 Genetic lesions in ABC-DLBCL and the activation of BCR signalling pathways

A: "Chronic active" BCR signalling in ABC-DLBCL with wild type CARD11 can acquire mutation in the BCR proximal subunits of CD79a or CD79b (CD79b shown in this example) that inhibits the activities of LYN, increasing downstream signalling of four important pathways for cell proliferation and survival;

B: Mutation in a coiled-coil domain of CARD11 confers its independence on ligand-induced signalling via activities of tyrosine kinases to activate the NF-κB pathway. The biallelic loss of A20 with its diminished inhibitory activities downstream of CBM protein complex also contributes to increased NF-κB signalling pathway.

Key: ⟶ *Direct positive regulation;* - - -→ *Indirect positive regulation;* ⟙ *Direct inhibition;* - - -⟙ *Indirect inhibition;* ✖ *Inhibited regulation;* ★ *Mutation*

RESULTS

5.2 HIP1R EXPRESSION IN DLBCL PATIENTS' SAMPLES

5.2.1 *HIP1R* mRNA expression levels in B-NHL patient samples

To investigate whether expression patterns of *HIP1R* across the panel of B-cell lymphoma cell lines studied correlate with patient samples from different lymphoma subgroups, mining of microarray data from the Oncomine database (http://www.oncomine.org) was conducted for differential *HIP1R* expression in normal B cells versus B-cell lymphomas. Two independent microarray datasets from Alizadeh *et al.* (2000) (Fig 5.2) and Basso *et al.* (2005) (Fig 5.3) showed downregulation of *HIP1R* levels in DLBCL compared to normal B cells (NBC) purified from peripheral blood or cord blood ($p < 0.0001$). *HIP1R* was also significantly downregulated in other B-cell lymphomas in the Basso *et al.* dataset. *HIP1R* levels were consistently able to distinguish between GC-DLBCL and ABC-DLBCL in 3 independent datasets from Alizadeh *et al.* ($p = 0.019$), Dave *et al.* (2006) ($p < 0.0001$) (Fig 5.4) and Hummel *et al.* (2006) ($p < 0.0001$) (Fig 5.5).

HIP1R levels were also significantly higher in BL versus DLBCL in both the Dave *et al.* ($p < 0.0001$) and Hummel *et al.* ($p < 0.0007$) datasets in which both microarray studies attempted to distinguish the diagnosis of BL versus DLBCL by means of differential gene expression. *HIP1R* was chosen as one of 217 gene-expression based predictor of BL in Dave *et al.* studies, discriminating BL from DLBCL. These observations are consistent with qRT-PCR analysis on cell lines in Chapter 4 whereby BL cell lines showed higher levels of *HIP1R* than DLBCL cell lines ($p < 0.001$).

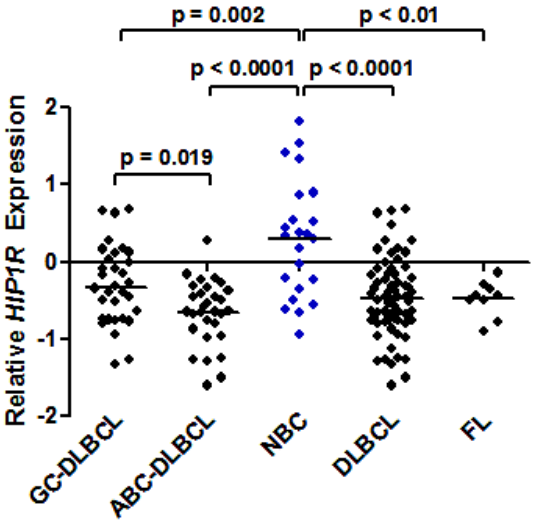

Fig 5.2 Comparison of *HIP1R* levels in normal B cells with DLBCL and FL re-analysed from Alizadeh *et al*. (2000)

NBC: Normal B cells (n = 23); DLBCL (n = 67); FL (n = 9); GC-DLBCL (n = 34); ABC-DLBCL (n = 30). HIP1R probe ID: IMAGE 1334485

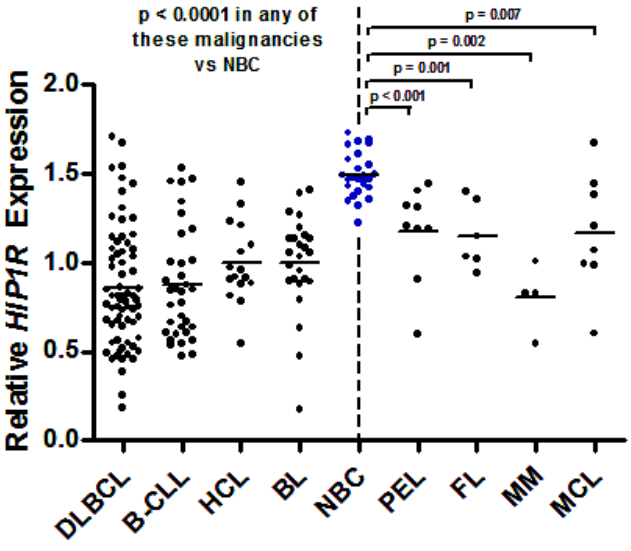

Fig 5.3 Comparison of *HIP1R* levels in normal B cells with B-cell lymphomas re-analysed from Basso *et al*. (2005)

NBC: Normal B cells (n = 25); DLBCL (n = 69); B-CLL (n = 34); HCL (n = 16); BL (n = 25); PEL (n = 9); FL (n = 6); MM (n = 4); MCL (n = 8). HIP1R probe ID: 38340_at

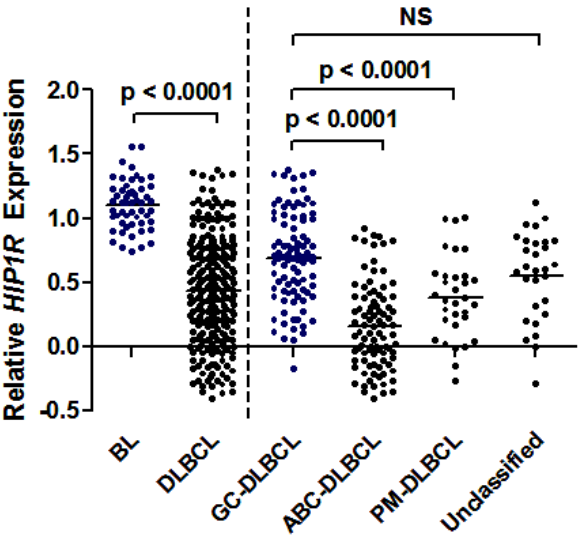

Fig 5.4 Comparison of *HIP1R* levels in DLBCL subtypes and BL re-analysed from Dave *et al*. (2006)

BL (n = 54); DLBCL (n = 249); GC-DLBCL (n = 95); ABC-DLBCL (n = 91); PM-DLBCL (n = 33); Unclassified DLBCL (n = 30). Comparison of BL with GC-DLBCL: p < 0.0001. HIP1R probe ID: 38340_at

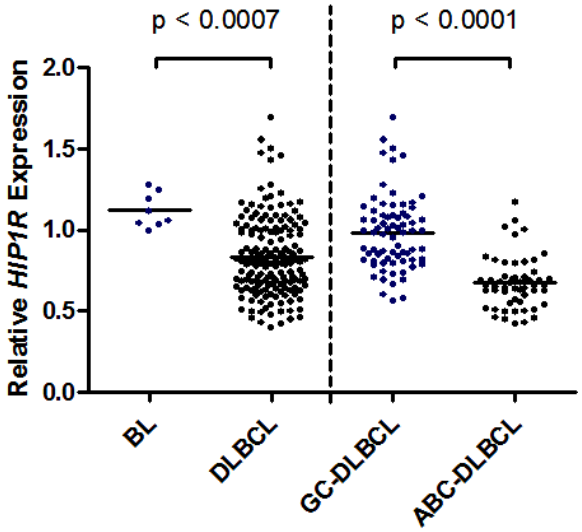

Fig 5.5 Comparison of *HIP1R* levels in DLBCL subtypes and BL re-analysed from Hummel *et al*. (2006)

BL (n = 8); DLBCL (n = 166); GC-DLBCL (n = 74); ABC-DLBCL (n = 55). HIP1R probe ID: 38340_at

qRT-PCR analysis of *HIP1R* mRNA levels in a validated series of DLBCL (n = 28) (kindly provided by Dr. Charles Lawrie) showed that *HIP1R* levels could discriminate GC-DLBCL from ABC-DLBCL by utilising both Hans *et al.* (2004) ($p < 0.05$) and Choi *et al.* (2009) ($p < 0.01$) algorithms (Fig 5.6), with the latter algorithm stratifying the cases more effectively in terms of their *HIP1R* levels. This observation is consistent with the microarray data that indicate differential *HIP1R* expression in GC- versus ABC-DLBCL.

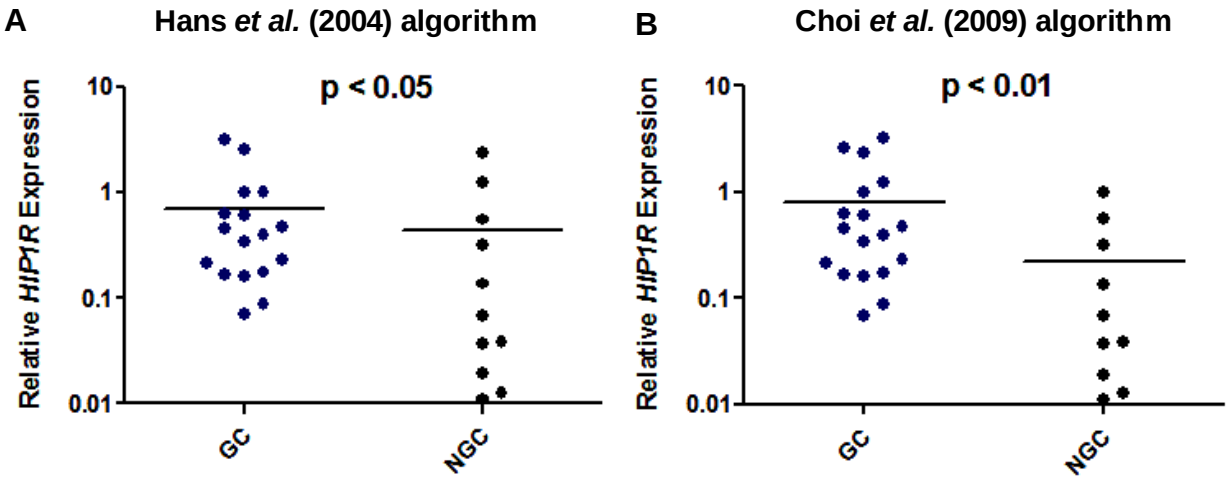

Fig 5.6 Stratification of DLBCL cases based on *HIP1R* mRNA levels by qRT-PCR

A: Stratification of cases based on Hans et al. algorithm. GC: GC-DLBCL (n = 17); NGC: NGC-DLBCL (n = 11); B: Stratification of cases based on Choi et al. algorithm. GC: GC-DLBCL (n = 18); NGC: NGC-DLBCL (n = 10). HIP1R expression was normalised against GAPDH and expressed relative to normal tonsil using the formula $2^{-\Delta\Delta Ct}$*. The scatter plots were drawn on a* $\log_{10}$ *scale and a bar represents the mean.*

Consistent with the clinical relevance of COO based DLBCL subtyping, downregulation of *HIP1R* levels indicate a trend towards inferior survival in CHOP-treated DLBCL patients as shown in Fig 5.7, microarray data re-analysed from Alizadeh *et al.* (2000) dataset (LLMPP website: http://llmpp.nih.gov/lymphoma/). This suggests that downregulation of *HIP1R* levels alone might be indicative of poor prognosis independently of DLBCL subtyping algorithms.

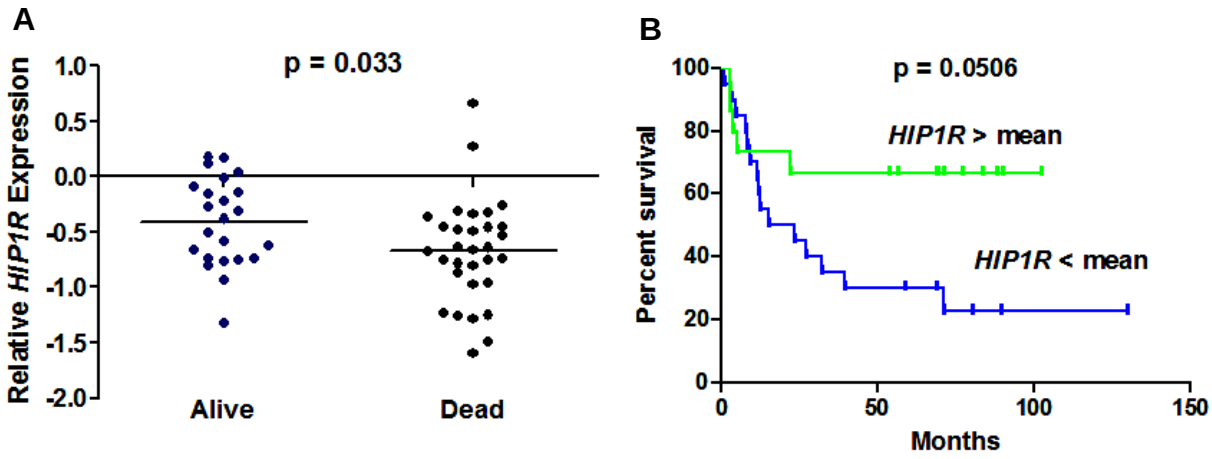

Fig 5.7 Survival trends of CHOP-treated DLBCL patients based on *HIP1R* levels

A: HIP1R expression levels in patients classified as "Alive" (n = 23), or "Dead" (n = 31); B: Kaplan-Meier curves illustrating survival according to HIP1R expression levels. HIP1R < mean (n = 20) indicates HIP1R levels less than the mean value of all 35 cases analysed; HIP1R > mean (n = 15) indicates HIP1R levels more than the mean value of the 35 cases. Data re-analysed from Alizadeh et al. (2000).

5.2.2 HIP1R protein expression in DLBCL patient samples

As protein expression is usually detected for routine diagnostic purposes, we investigated whether HIP1R protein levels are predictive of clinical outcome in CHOP- and/or R-CHOP-treated DLBCL. A collaboration was established with Dr Randy Gascoyne (BC Cancer Agency, Canada) who kindly provided 4 series of DLBCL tissue microarrays (TMA) from patients treated with CHOP or R-CHOP chemotherapy regimen with 5-year survival data, and each series was assigned as follows: 1) "Rituximab NBF" (n = 157); 2) "LLMPP" (n = 50); 3) "Roche 1" (n = 20); 4) "Roche 2" (n = 46). The combined number of DLBCL biopsies investigated was 273. Each individual patient's biopsies were arrayed in duplicate cores and within each series of TMA, normal reactive tonsils were included in duplicates as controls.

Immunolabelling of the four TMA series was performed with the validated anti-HIP1R-44 mAb and scoring of the cases was conducted by myself, Dr Alison Banham, Dr Karen Pulford and independently by a qualified pathologist Dr Elizabeth Soilleux (NDCLS, Oxford).

Scoring of each case includes a qualitative (or intensity) score, by comparing the staining intensity of the malignant cells to normal B cells in the mantle zone of germinal centres of the internal tonsil controls (Fig 5.8 and Fig 5.9), quantitative (or frequency) score with a cut-off value of 50% positive cells, and 3 other categories generated from qualitative/quantitative scoring: "Qualitative dichotomised", "Quantitative dichotomised" and "Qualitative + Quantitative". Dichotomised categories set a cut-off value to determine a "negative" (score "1" in this case) or "positive" (score "2") case based on qualitative or quantitative assessment only, whereas "Qualitative + Quantitative" allows diagnosis of a case not biased to either qualitative or quantitative assessment (Table 5.1).

Table 5.1 Scoring criteria for HIP1R immunolabelling studies in DLBCL TMA series

Qualitative		Qualitative dichotomised		Quantitative		Quantitative dichotomised		Qualitative (L) + Quantitative (N)	
Score	**Definition**	**Score**	**Definition**	**Score**	**Definition**	**Score**	**Definition**	**Score**	**L + N**
0	Negative			0	Negative			0	0 + 0
1	Intensity less than normal B cells	1	Qualitative score of 0 or 1	1	< 50% positive cells	1	Quantitative score of 0 or 1	2	1 + 1
2	Intensity similar to normal B cells	2	Qualitative score of 2 or 3	2	≥ 50% positive cells	2	Quantitative score of 2	3	2 + 1 or 1 + 2
3	Intensity more than normal B cells							4	2 + 2 or 3 + 1
								5	3 + 2

NB: In the "Qualitative (L) + Quantitative (N)" category, there is not a combined score of 1 e.g. if a case with "Qualitative" and "Quantitative" score of 1 and 1, respectively, it has a score of 2 in the "L + N"category.

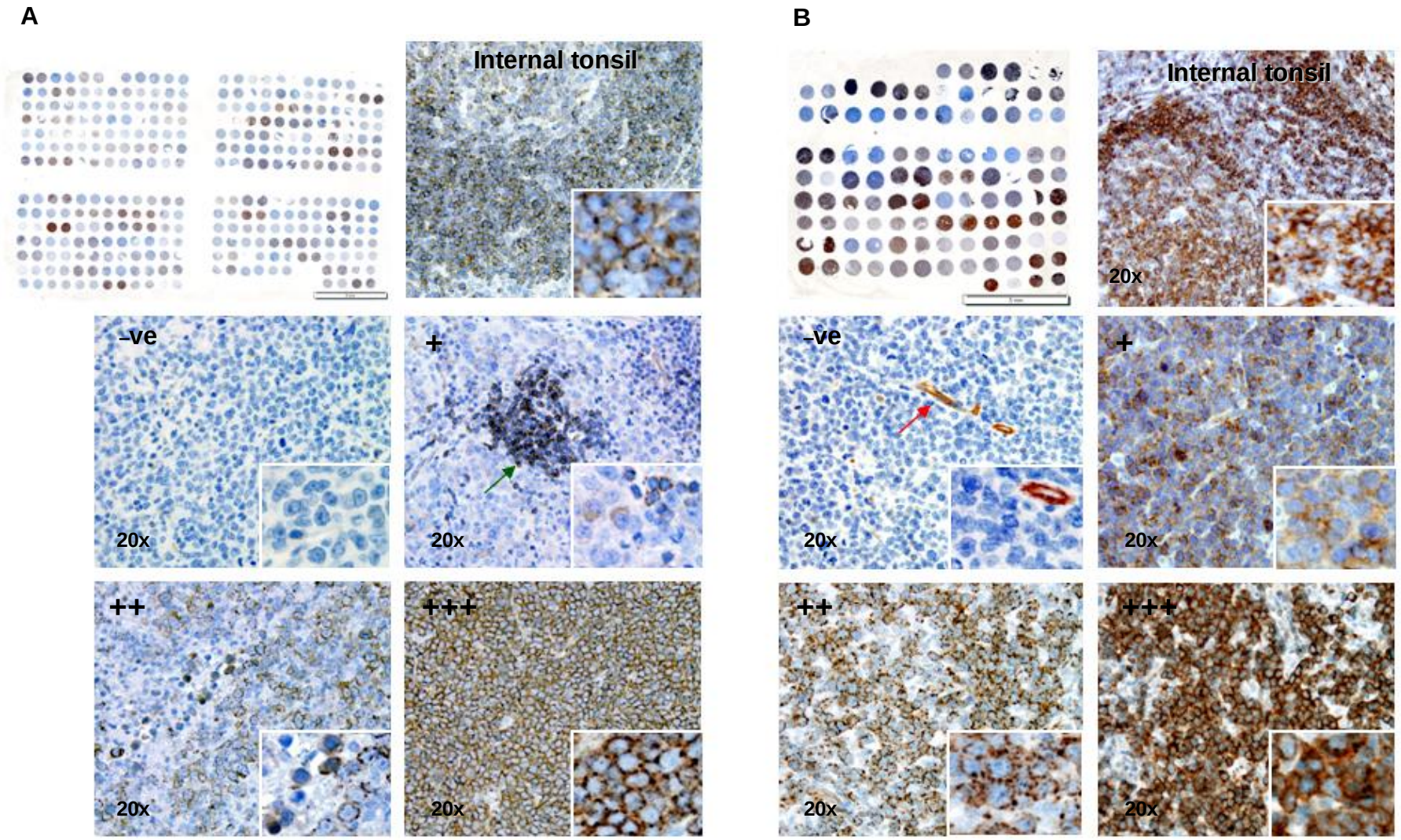

Fig 5.8 Immunolabelling of HIP1R in "Rituximab NBF" series (panel A, n = 157) and "LLMPP" series (panel B, n = 50)

-ve, +, ++, +++ correspond to qualitative score of 0, 1, 2, 3 respectively. Some of the cases had residual normal B cells expressing HIP1R (green arrow on panel A) or stained endothelium (red arrow on panel B).

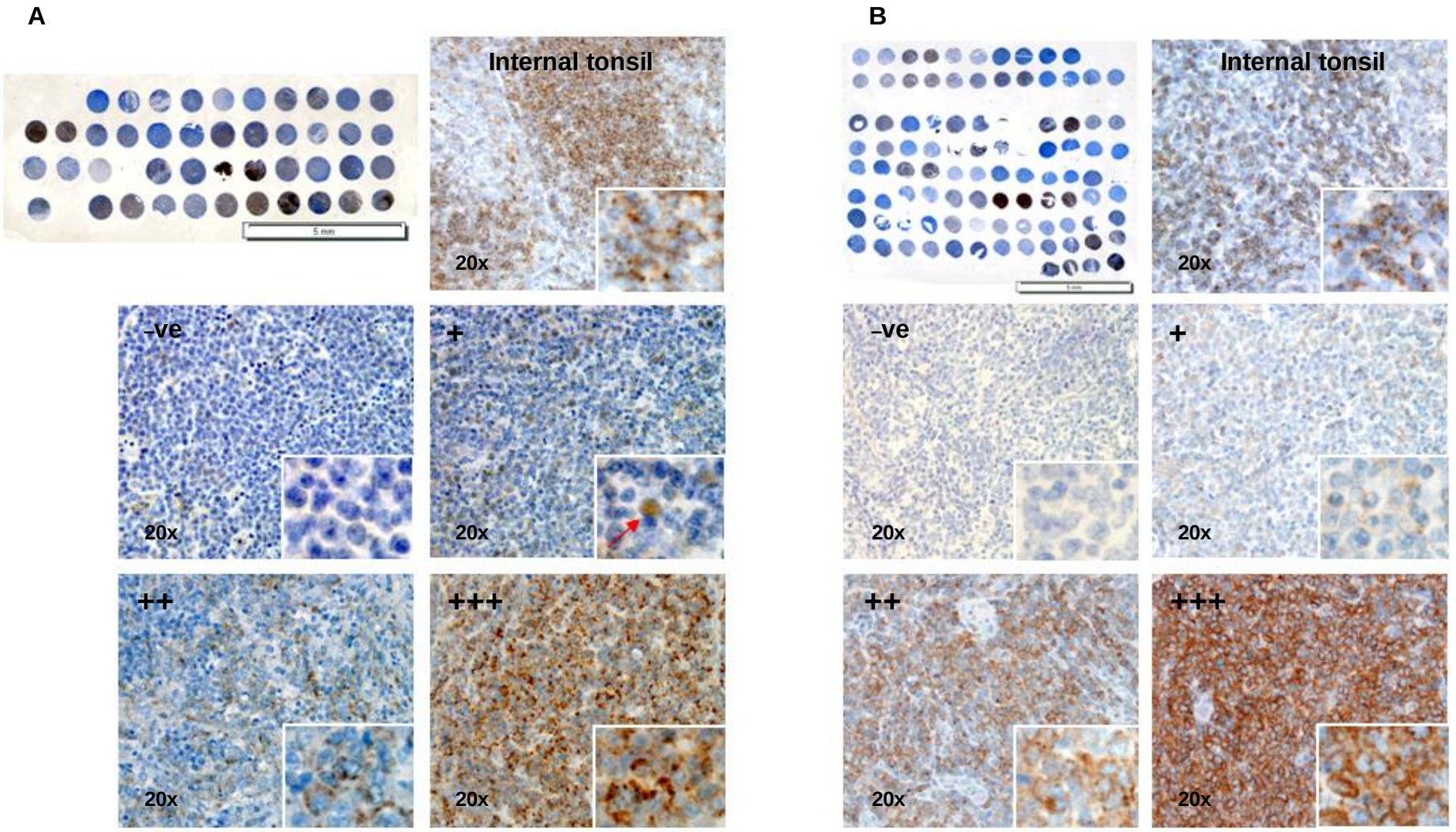

Fig 5.9 Immunolabelling of HIP1R in "Roche 1" series (panel A, n = 20) and "Roche 2" series (panel B, n = 46)

-ve, +, ++, +++ correspond to qualitative score of 0, 1, 2, 3 respectively. Some of the cases in the Roche series had HIP1R nuclear labelling (red arrow on panel A).

Nearly all cases with demonstrable HIP1R staining showed that expression was localised in the cytoplasm of the tumour cells. Exceptions were two (10%) cases in the "Roche 1" series and 11 (23.9%) in the "Roche 2" series where HIP1R staining was detected in the nucleus. As this nuclear protein was identified in a small number of cells in a very minor group of patients, only the clinical relevance of cytoplasmic HIP1R expression was analysed.

Higher HIP1R protein expression was significantly associated with GC-DLBCL in comparison with NGC-DLBCL in the combined "LLMPP" and "Roche 1" series (n = 70) [in both series' DLBCL subtyping was based on the Hans *et al.* (2004) algorithm] in both quantitative and qualitative categories (Table 5.2). This confirms that HIP1R is a DLBCL subtyping marker whose expression is highly associated with GC-DLBCL. These data are consistent with the subtyping capabilities of *HIP1R* previously demonstrated at the mRNA level.

Interestingly, four GC-DLBCL biopsies displayed higher expression of HIP1R than seen in mantle zone B cells of internal tonsil controls (the "Qualitative" category of Table 5.2). This supports the possibility that some GC-DLBCL cases may overexpress HIP1R and that this might contribute to the immunological recognition of this antigen by GC-DLBCL patients.

Table 5.2 Association of HIP1R protein levels with GC- or NGC-DLBCL

Category	Score	GC-DLBCL (n)	NGC-DLBCL (n)	*p* value
Qualitative	0	1	9	0.0620
	1	17	22	
	2	10	7	
	3	4	0	
Quantitative	0	1	9	**0.0012**
	1	2	10	
	2	29	19	
Qualitative dichotomised	1	18	31	**0.0212**
	2	14	7	
Quantitative dichotomised	1	3	19	**0.0003**
	2	29	19	
Qualitative + Quantitative	0	1	9	**0.0346**
	2	2	9	
	3	15	14	
	4	10	6	
	5	4	0	

Number of cases: GC-DLBCL (n = 32); NGC-DLBCL (n = 38). NB: In the "Qualitative + Quantitative" category, there is not a combined score of 1.

5.2.3 HIP1R protein expression and clinical outcome

The relationship between HIP1R protein expression and clinical outcome of DLBCL patients was also examined. After exclusion of PM-DLBCL and those cases where staining was not assessable (i.e. necrotic tissue or no lymphoma was present), a total of 256 cases receiving CHOP or R-CHOP chemotherapy regimen with clinical outcome were investigated.

In this combined series of DLBCL patients (n = 256) that contains both CHOP and R-CHOP treated patients, the intensity of HIP1R protein expression was not predictive of overall survival. However, a higher frequency of HIP1R expression showed a non-significant trend toward better overall survival (p = 0.072) (Fig 5.10). Within the CHOP treated cohort of DLBCL patients, HIP1R protein expression was not predictive of overall survival stratified according to the intensity of expression, but higher frequency of HIP1R expression again showed a non-significant trend toward improved overall survival (p = 0.060).

In the R-CHOP cohort of patients, stratification of cases based on the intensity or frequency of HIP1R protein expression was not predictive of survival. This might indicate that addition of Rituximab into the CHOP chemotherapy regimen erases any relationship between HIP1R protein expression levels and response to this B-cell targeted immuno-chemotherapy.

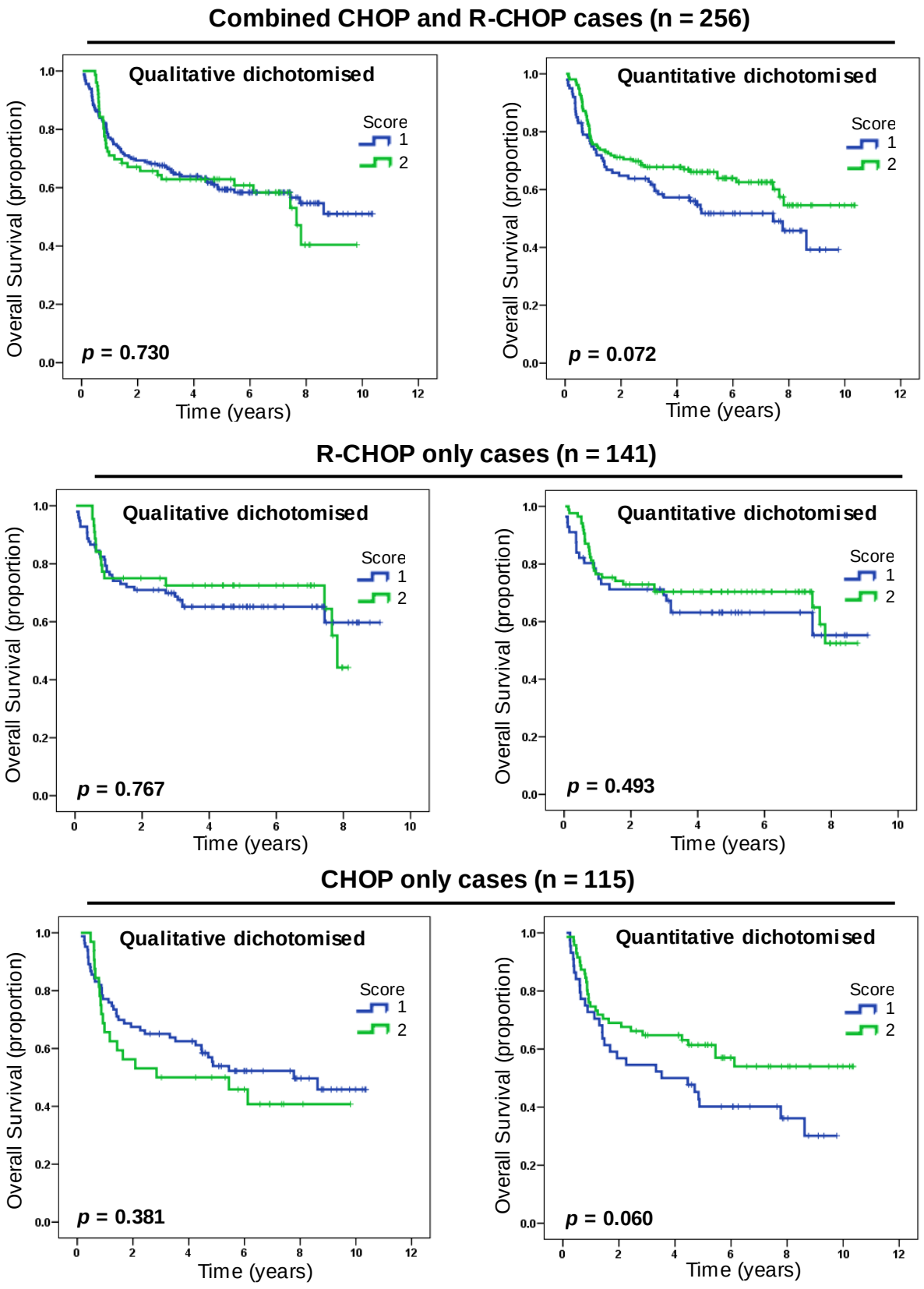

Fig 5.10 Overall survival for DLBCL patients according to HIP1R protein expression

Intensity of HIP1R protein expression was not predictive of survival in DLBCL patients treated with CHOP or R-CHOP regimen. Higher frequency of HIP1R expression showed a trend toward better survival in patients treated with CHOP only regimen (p = 0.060).

5.3 POTENTIAL REGULATORS OF HIP1R

5.3.1 HIP1R levels in response to activation of non-malignant B cells

ABC-DLCBL is characterised by a gene expression profile similar to that of non-malignant activated B cells (Alizadeh *et al.*, 2000; Shaffer *et al.*, 2002). To elucidate whether downregulation of HIP1R in ABC-DLBCL is a disease-related process rather than response to normal B-cell activation, the level of HIP1R expression was investigated in B cells, purified from peripheral blood buffy coat preparations using negative immunomagnetic selection methods (Naïve B Cell Isolation Kit, Miltenyi Biotech Ltd), both before and after activation with anti-IgM or IL-2 and SAC. IHC using a cocktail of B-cell antibodies (anti-CD19, anti-CD20 and anti-CD22) confirmed successful B-cell purification (Fig 5.11). Based on microscopic observation, more than 95% of the cells showed positive staining by the cocktail of B-cell antibodies.

Many of the RNA polymerase II transcribed genes that are usually used as qRT-PCR normalisation controls were affected by B-cell activation (Dr Philip Brown, personal communication). Therefore, in the B-cell activation experiments the *18S rRNA* gene was used as a normalising gene whose expression remained stable in response to activation stimuli. *HIP1R* mRNA expression was upregulated in response to non-malignant B-cell activation, $p < 0.05$ from 2 independent experiments (Fig 5.12A). Western blotting of lysates prepared from the same experiments also demonstrated that the HIP1R protein was upregulated in the activated B cells (Fig 5.12B). Immunoblotting of the same set of samples with anti-IRF4 mAb (clone M-17) confirmed successful B-cell activation via IRF4 induction. GC-DLBCL (SUDHL4) and ABC-DLBCL (HBL1) cell lines were also run in parallel with the activated B cells in the Western blotting analysis and showed that HIP1R had an inverse expression pattern with IRF4 in DLBCL cells but not in the activated B cells. These data

suggest that downregulation of HIP1R in ABC-DLBCL might be a disease-related process in DLBCL that does not reflect the induction of HIP1R seen on normal B-cell activation.

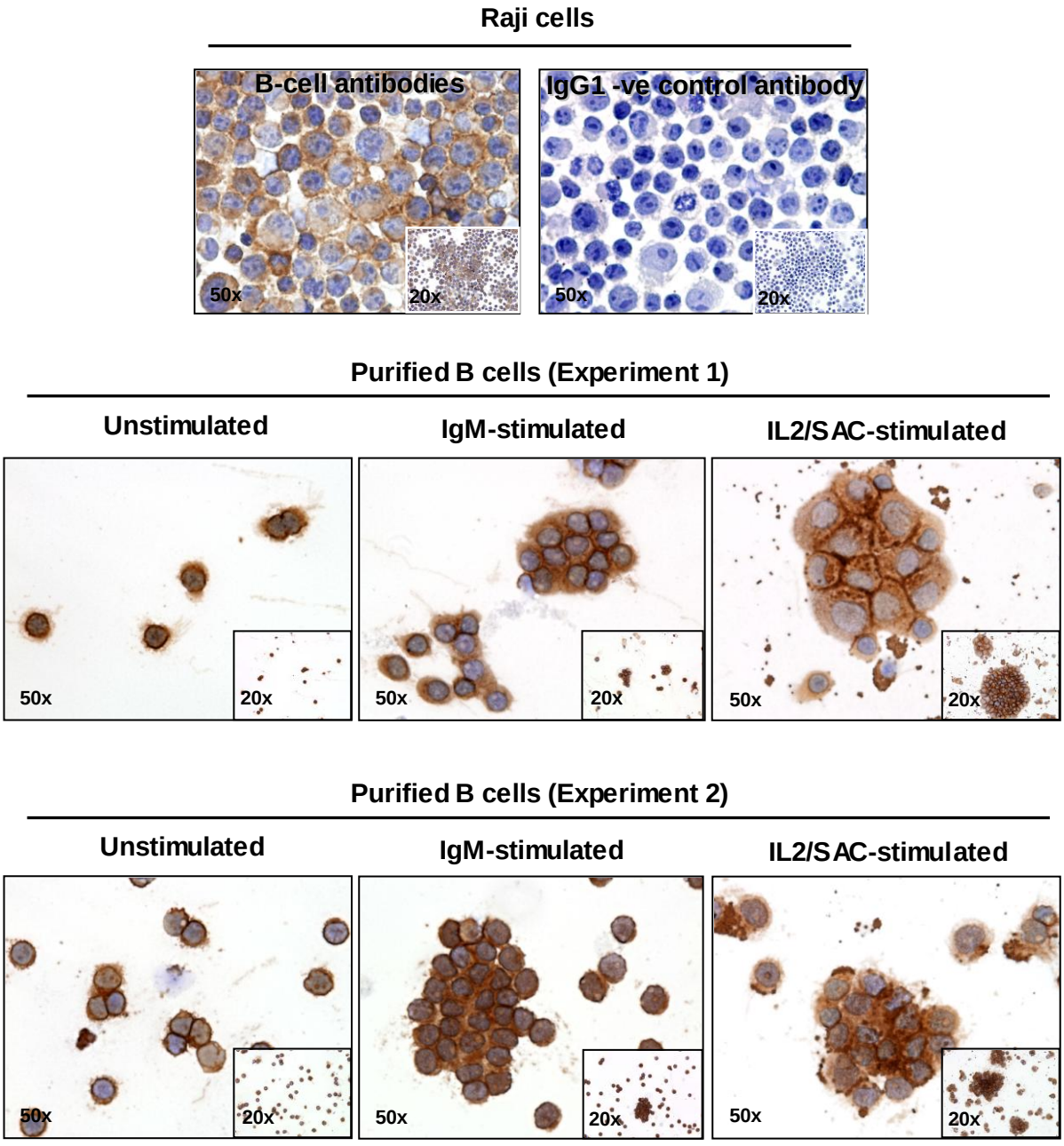

Fig 5.11 Validation of purified non-malignant B cells from peripheral blood in two independent experiments

Immunoperoxidase labelling of purified non-malignant B cells without stimulation or after stimulation with anti-IgM or IL2 and SAC (IL2/SAC) using a cocktail of monoclonal antibodies against B-cell markers: anti-CD19 (clone HD37), anti-CD20 (clone L26) and anti-CD22 (clone 4KB128). Raji cells were used as positive controls for labelling using this cocktail of antibodies.

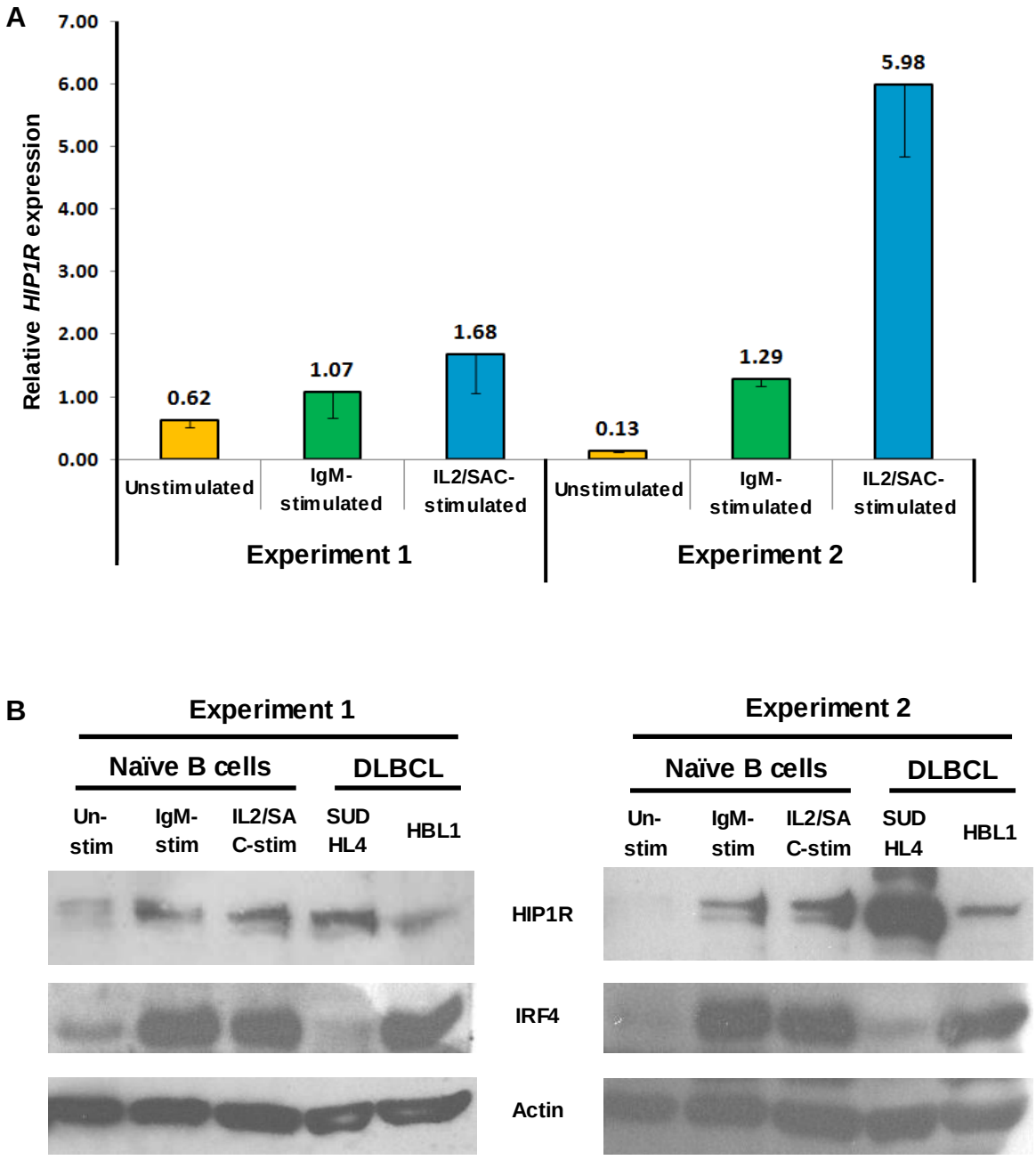

Fig 5.12 Upregulation of HIP1R protein and mRNA levels in stimulated non-malignant B cells purified from peripheral blood

A: HIP1R mRNA levels in unstimulated and stimulated (for 44 hours) non-malignant B cells purified from human peripheral blood by negative immunomagnetic selection (Miltenyi Biotech Ltd). qRT-PCR amplification was performed in triplicate using TaqMan pre-verified probes to amplify HIP1R (TaqMan probe: Hs00391321_m1), and relative gene expression was normalised according to expression of 18S rRNA control gene (TaqMan probe: 4319413E). This individual value was compared with the mean of the normalised values using the formula $2^{-\Delta\Delta Ct}$*; B: HIP1R protein levels in the same set of samples detected using*

anti-HIP1R-44 mAb. Successful activation was demonstrated by upregulated IRF4 levels. Protein lysates from GC-DLBCL (SUDHL4) and ABC-DLBCL (HBL1) derived cell lines were also run in parallel. Key: Unstim: unstimulated; IgM-stim: stimulated by anti-IgM antibodies; IL2/SAC-stim: stimulated by IL2 and SAC.

5.3.2 Regulation of gene transcription

HIP1R is markedly downregulated in ABC-DLBCL, yet not by normal B-cell activation, thus a question arises as to the mechanism(s) potentially responsible for HIP1R downregulation. As *HIP1R* transcript levels correlate well with protein expression, mechanisms that regulate *HIP1R* at the level of transcription and/or mRNA stability are most likely to regulate its expression.

Regulation of gene transcription could be achieved via different mechanisms. One of the mechanisms involves chromosomal abnormalities such as pre-existing mutation of either *CDKN2A* or *TP53* in transformed-FL (Fitzgibbon *et al.*, 2007), and the mutation of *CARD11* (Ngo *et al.*, 2006) or *CD79b* (Davis *et al.*, 2010) in DLBCL. Overexpression of HIP1R (maps on chromosome 12, at 12q24.31) has been observed in trisomy 12 (+12) CLL (Porpaczy *et al.*, 2009), indicating that *HIP1R* locus is amplified in +12 CLL. However, there are no reports that the *HIP1R* locus is deleted in DLBCL or publications reporting its mutation in tumours.

Another mode of gene regulation is via epigenetic regulatory mechanisms which include methylation, acetylation, phosphorylation, ubiquitinylation and sumoylation (Lachner *et al.*, 2003). The best-known epigenetic modification is DNA methylation involving the genomic regions CpG islands (Esteller, 2008). Genomic methylation has recently been implicated in DLBCL (Pike *et al.*, 2008) and FL (O'Riain *et al.*, 2009), resulting in the

reduction of gene expression particularly that of tumour suppressor genes. Search for CpG islands 10 kb upstream of *HIP1R* transcription start site (TSS) by using EMBOSS CpGPlot (http://www.ebi.ac.uk/Tools/emboss/cpgplot/) showed that *HIP1R* contained a promoter CpG island from -384 to +4 relative to TSS, suggesting that *HIP1R* promoter could be methylated to silence its transcriptional activation.

MiRNAs direct their post-transcriptional repression of protein translation by binding to complementary sequences in the 3' untranslated regions (3' UTRs) of the mRNA of protein-coding genes (Bartel, 2009). As we do not see a post-transcriptional block in HIP1R expression then any potential miRNA regulation is most likely to be via degradation of the transcript. This is a less common mechanism in animals, compared to plants, that occurs when there is high homology between the microRNA and its target (Ambros, 2004). MiRNAs have been frequently implicated in lymphomas, including elevation of *miR-21* in serum from DLBCL (Lawrie *et al.*, 2008). Higher expression of *miR-637* or *miR-302* has been associated with inferior survival in DLBCL patients (Lawrie *et al.*, 2009), and mice conditionally overexpressing *miR-21* developed pre-B-cell lymphoma that regressed on inactivation of the miR (Medina *et al.*, 2010). *mir-24* was the only microRNA predicted to target *HIP1R* using TargetScan (http://www.targetscan.org) and this binding site was conserved in six other species out of 22. In addition, miRanda (http://www.microrna.org) also predicted more than 10 other miRNAs potentially targeting *HIP1R* including *mir-20a* and *mir-93* which were found to be upregulated in DLBCL, and *mir-132* that was upregulated in NGC-DLBCL (Lawrie *et al.*, 2009). As none showed particularly high homology to the *HIP1R* transcript, they were not pursued as potential regulators of HIP1R expression.

A well-documented mechanism of regulating gene transcription is via direct binding of a transcription factor to the promoter of its target genes. Key transcription factors, such as IRF4 and FOXP1, respond to B-cell activation stimuli and are associated with COO subtypes in DLBCL. Our laboratory has a long-standing interest in studying lymphoma-associated transcription factors and reagents available for their characterisation. As both IRF4 and FOXP1 binding sites were identified upstream of the transcriptional start site for *HIP1R*, the possible role of these transcription factors in downregulating HIP1R expression was further investigated.

5.3.3 IRF4 and FOXP1 binding sites in *HIP1R* promoter region

Two putative transcriptional regulators were chosen on the basis that binding sites for both are present in the *HIP1R* promoter and both are significantly overexpressed in ABC-DLBCL as follows:

IRF4: Interferon-regulatory factor 4 is a well-documented IRF family of transcription factor overexpressed in ABC-DLBCL (Alizadeh *et al.*, 2000), and it represses *BCL6*, a known GC-DLBCL marker, expression by binding its promoter region (Saito *et al.*, 2007). The double-labelling studies in the previous chapter showed rare co-expression of HIP1R with IRF4 in reactive tonsils, suggesting a potential negative regulatory role for IRF4.

FOXP1: Forkhead Box P1 is a member of the FOX family of transcription factors and is a marker of ABC-DLBCL strongly associated with inferior survival in this DLBCL subtype (Banham *et al.*, 2005; Choi *et al.*, 2009). Targets of FOXP1 have been elucidated in certain tissues such as T1α in lung cells (Shu *et al.*, 2007), however its targets in ABC-DLBCL are unknown. FOXP1 short isoforms ($FOXP1_S$) of around 60-65 kDa are highly-expressed in

ABC-DLBCL in comparison with the full length protein ($FOXP1_{FL}$) of about 75 kDa (Brown *et al.*, 2008) that is the predominant isoform in tonsil tissue. Brown *et al.* showed that $FOXP1_S$ expression is upregulated upon activation of B cells purified from peripheral blood which represents an additional mechanism for upregulating FOXP1 expression in DLBCL. Alternative splicing of *FOXP1* occurs in ABC-DLBCL and it is being explored as a mechanism generating the smaller *FOXP1* isoforms. We believe that these FOXP1 isoforms probably reflect truncation of the N-terminus of the full length FOXP1 protein. Our laboratory is further investigating the hypothesis that smaller potentially oncogenic FOXP1 proteins are functionally distinct from the full length protein and that they play a role in ABC-DLBCL pathogenesis.

The possible IRF4 and FOXP1 binding sites upstream of *HIP1R* TSS were initially examined. Investigation of *HIP1R* promoter sites uncovered a *Forkhead* consensus binding site within 1kb upstream of *HIP1R* TSS (-969 until -950 upstream of TSS) and this region shares a highly significant Foxp1 consensus binding site determined by Wang *et al.* (2003) (Fig 5.13). Wang *et al.* also showed the presence of a Foxp1 binding site within the promoter of *SV40* and *NFAT* (wild type) and confirmed the Foxp1 binding by EMSA. The putative FOXP1 binding site in *HIP1R* is more highly-conserved than those of *SV40* and *NFAT*, further strengthening the potential of FOXP1 to regulate HIP1R expression.

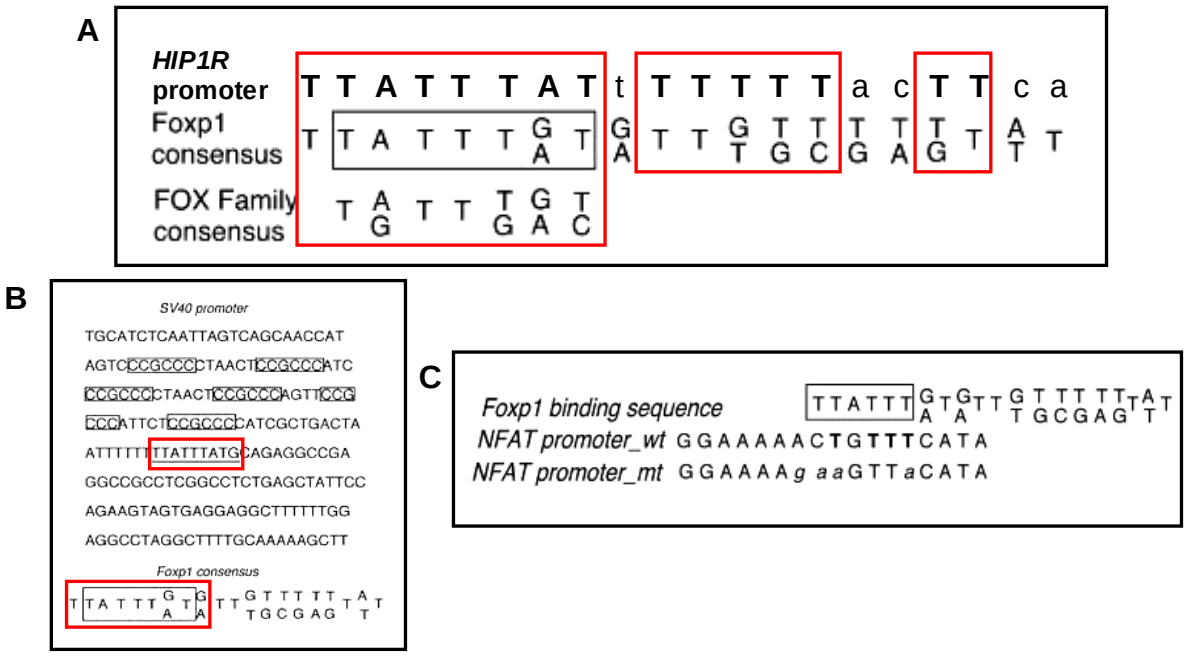

Fig 5.13 Presence of FOXP1 binding site in *HIP1R* promoter region

FOXP1 binding site in HIP1R promoter region (A, red box) is more conserved than those of SV40 (B, red box) and NFAT (wild type) (C, in bold). Diagrams adapted from Wang et al. (2003) with modifications.

A DNA oligonucleotide containing an IRF4 binding site identical to that seen in the *CD38* gene (5'-AAGTGAAAC-3') was used to crystallise the DNA binding domain of IRF4 (Escalante *et al.*, 2002), and IRF4 has a characteristic consensus DNA binding sequence (5'-AANNGAAAC-3') (Allan *et al.*, 2010). Thus, the presence of consensus sequence of 5'-AANNGAAAC-3' within 5kb upstream of *HIP1R* TSS was investigated. Interestingly, *HIP1R* has two IRF4 regulatory consensus sites: 5'-AAGGAAAC-3' within 1.5 kb upstream of TSS, and 5'-AAAAGAAAC-3' within 5 kb upstream of TSS (Fig 5.14).

Fig 5.14 Presence of IRF4 binding site in *HIP1R* promoter region

A: The IRF4 binding consensus site (highlighted in turquoise and yellow) within 1.5 kb upstream of HIP1R TSS (in red fonts); B: IRF4 binding consensus site (highlighted in turquoise and yellow) within 5 kb upstream of HIP1R TSS.

The presence of both IRF4 and FOXP1 binding sites within 5 kb upstream of *HIP1R* TSS suggests that *HIP1R* might be regulated by one or both transcription factors. Investigations correlating *HIP1R* mRNA expression with those of *IRF4* and *FOXP1* were performed by qRT-PCR in a panel of more than 20 haematological cell lines, lymphoma or leukaemia, and normal tissues. The results were compared by plotting line graphs of *HIP1R* versus a transcription factor and the expression patterns across the panel of cell lines were examined (Fig 5.15). This demonstrated that *HIP1R* showed an inverse relationship with both *IRF4* and *FOXP1* in the DLBCL subsets as anticipated. Interestingly, a positive relationship of *HIP1R* with *IRF4* was observed in the myeloma cell lines NCI-H929, RPMI8226 and Thiel, a pattern that was not observed with *FOXP1* in RPMI8226 and Thiel, suggesting that putative regulatory of IRF4 on *HIP1R* might be restricted to ABC-DLBCL or not as widespread as FOXP1.

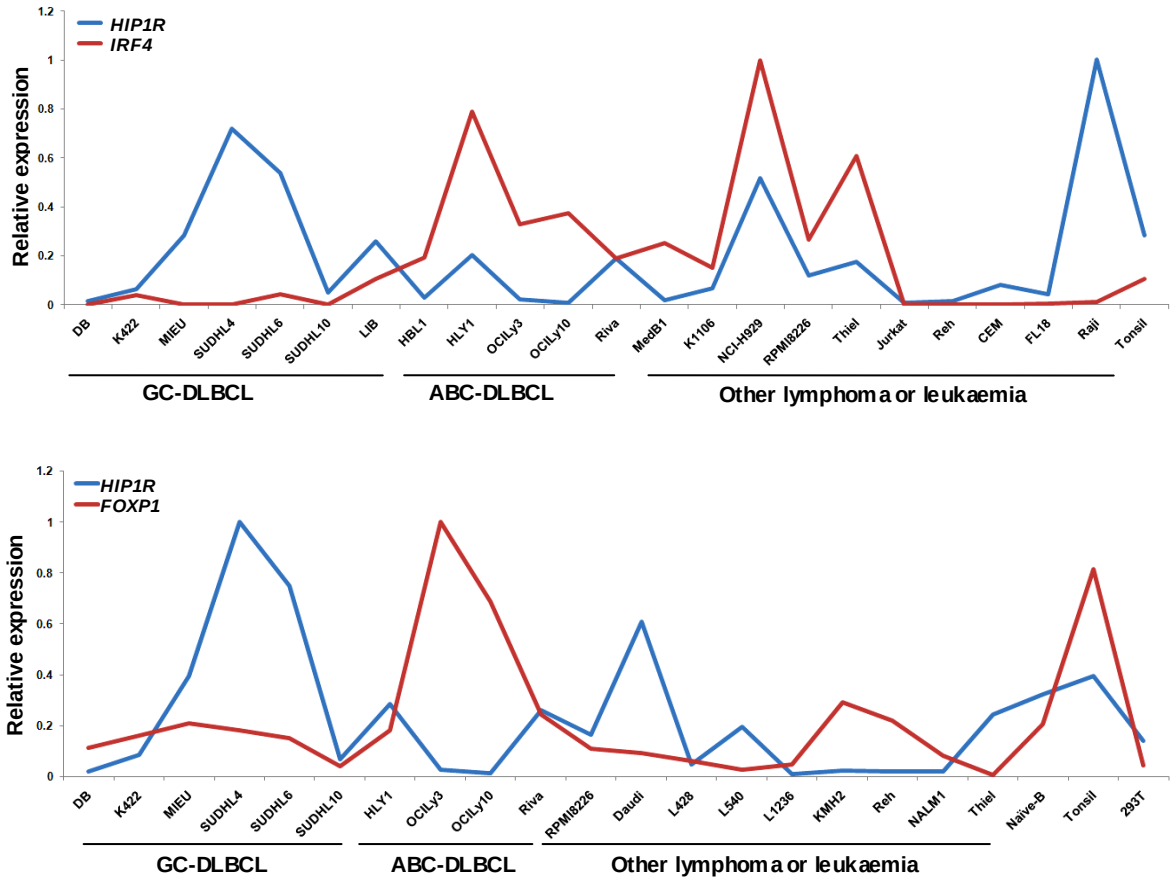

Fig 5.15 Correlation of *HIP1R* with *IRF4* and *FOXP1* mRNA levels

The relative gene expression values were normalised according to expression values of TBP (TaqMan probe: 4326322E) and compared to 293T levels using the formula $2^{-\Delta\Delta Ct}$. All values were then scaled down between the ranges of 0 to 1 to allow comparison not biased by extreme values. qRT-PCR data of FOXP1 mRNA levels were kindly provided by Dr Philip Brown. HIP1R TaqMan probe: Hs00391321_m1; IRF4 TaqMan Probe: Hs00180031_m1; FOXP1 TaqMan Probe: Hs00212860_m1.

Since FOXP1 is predominantly a transcriptional repressor (Koon *et al.*, 2007), in contrast with IRF4 which is predominantly a transcriptional activator (Shaffer *et al.*, 2009), it is likely that *HIP1R* expression might be repressed by FOXP1. Furthermore, as our laboratory has a long-standing interest in the role of FOXP1 in DLBCL, the putative role of FOXP1 repressing *HIP1R* transcription in DLBCL was pursued further.

5.3.4 *HIP1R* mRNA levels in FOXP1-depleted cell lines

An ongoing project in the laboratory is to use unbiased methods to identify FOXP1 targets by gene expression profiling and to compare their regulation by short versus long FOXP1 proteins. Knockdown of FOXP1 by two independent siRNAs designated "si5" and "si6" in OCI-LY3 (predominantly expressing $FOXP1_S$) and DB (expressing $FOXP1_{FL}$ only) cells for 48 hours, and validation by Western blotting was performed by Dr Philip Brown (Fig 5.16).

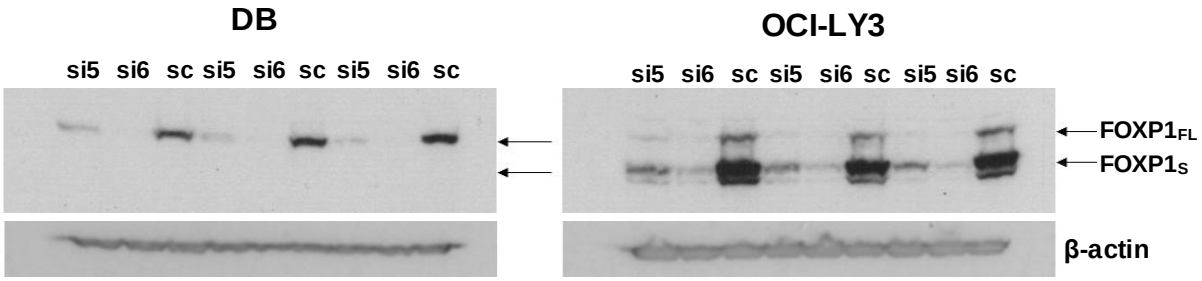

Fig 5.16 Validation of FOXP1 knockdown by two independent *FOXP1* siRNAs
Immunoblotting of two siFOXP1-treated (si5 and si6) and scramble siRNA-treated (sc) DB and OCI-Ly3 cell lines (48 h) with anti-FOXP1 mAb (JC12, "in house" antibody). $FOXP1_S$ was only present in OCI-LY3 cells. This experiment was performed by Dr Philip Brown. Silencing was also confirmed at the transcript level (data not shown).

The samples were then used for gene expression profiling on Whole Human Gene Expression Microarray (Agilent Technologies, USA) containing 16,268 transcripts performed by Oxford Gene Technology (Oxford, UK). All intensity values of si*FOXP1*-treated samples generated from the microarray were normalised against those of scramble-treated, log-transformed to obtain the up- or down-regulated genes in fold-change, and *p* values corrected with false discovery rate were generated by Oxford Gene Technology

In OCI-LY3 cells, *HIP1R* was ranked in the top 1.5% (top 245 out of 16,268) of genes significantly upregulated after depletion of FOXP1 in triplicate experiments ($p < 0.05$). In contrast, the change of *HIP1R* levels in DB was not significant (Fig 5.17A). qRT-PCR analysis of *HIP1R* levels in the same set of FOXP1-depleted cells was used to validate the gene expression profiling observations. The qRT-PCR analysis confirmed that *HIP1R* was significantly upregulated in si*FOXP1*-treated OCI-LY3 ($p < 0.05$) but not DB cells (Fig 5.17B). Interestingly, this experiment suggests that HIP1R might be downregulated by $FOXP1_S$ in ABC-DLBCL and that it may not be regulated by the $FOXP1_{FL}$ protein that is expressed in tonsil and a subgroup of GC-DLCBL.

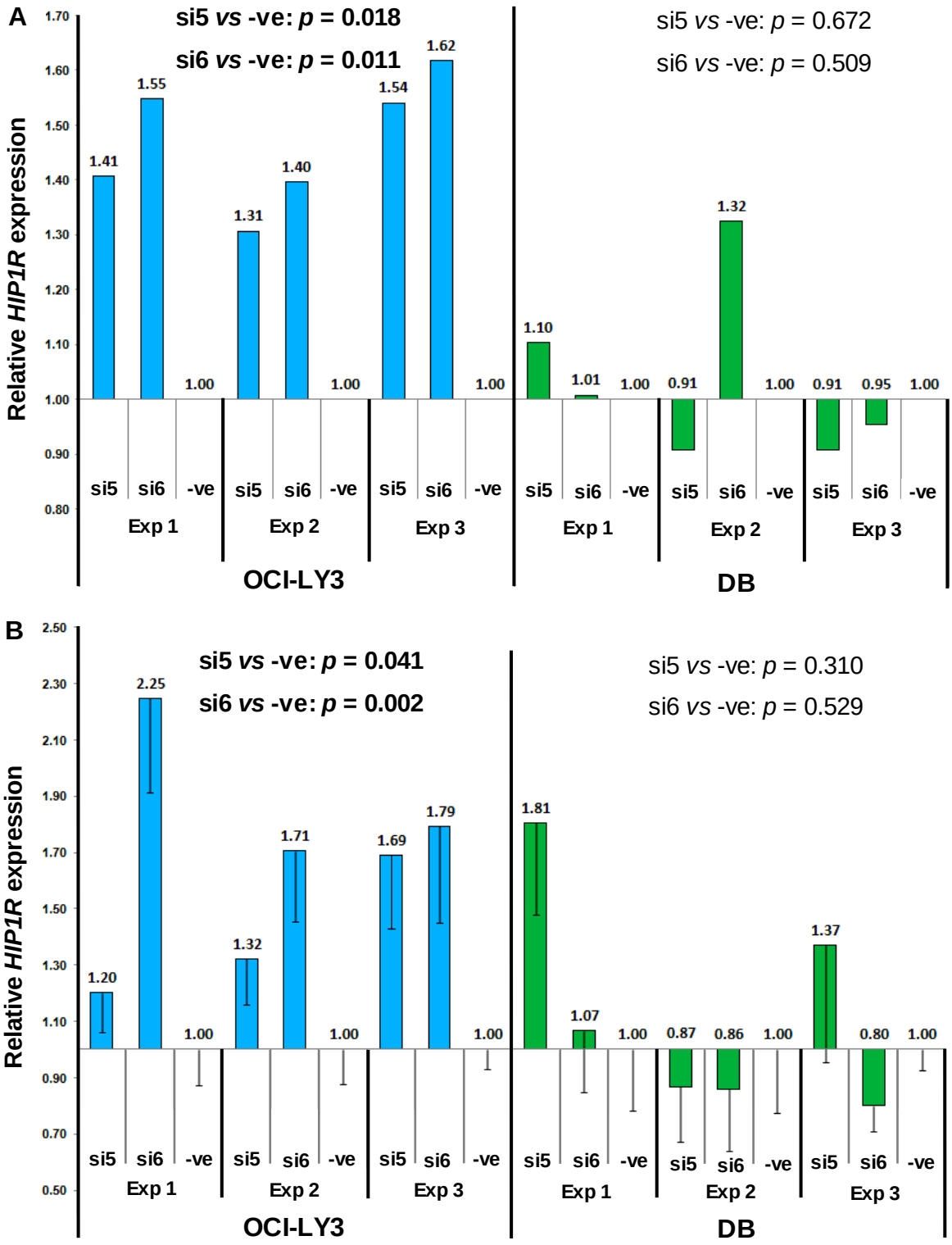

Fig 5.17 *HIP1R* levels in si*FOXP1*-treated OCI-LY3 and DB cell lines for 48 hours

HIP1R levels increased significantly in siFOXP1-treated OCI-LY3 cells but not DB cells examined by both microarray (A) and qRT-PCR (B) experiments. Error bars in qRT-PCR experiment were generated from triplicate values using TaqMan probes to amplify HIP1R (TaqMan probe: Hs00391321_m1) and gene expression was normalised according to expression of 18S ribosomal RNA (TaqMan probe: 4319413E) and expressed relative to the scrambled control. Key: si5 or si6: FOXP1 siRNA; -ve: scramble siRNA.

I analysed the si*FOXP1* microarray dataset of OCI-LY3 by using Ingenuity Pathways Analysis or IPA (Ingenuity Systems, http://www.ingenuity.com) for Dr Banham's LLR site visit. It was noted that HIP1R appeared in one of the canonical networks stored by IPA. This analysis identified networks of FOXP1 target genes and, as one of the networks has an association with *HIP1R,* it is further described here.

IPA analyses RNA expression data in the context of literature-defined biological pathways and responses, as well as canonical information stored in the Ingenuity Pathways Knowledge Base. IPA functional analysis could identify biological functions that are most significantly represented by a group of genes and present the pathways in the form of biological networks. All relationships are supported by at least one published reference or from canonical pathways stored by IPA (Kash *et al.*, 2006).

Genes from the data set that met the 1.5-fold change cut-off were considered for analysis, and this showed that *HIP1R* might have an association with MAP kinases and NFAT molecules (Fig 5.18), both of which have been implicated in B-cell receptor signalling (as introduced in the Introduction chapter). In addition, HIP1R was shown to bind Rho guanine nucleotide exchange factor 1 (ARHGEF1) from the IPA analysis. ARHGEF1 is an intracellular protein expressed by all hematopoietic cells that regulates signalling via G protein-coupled receptors (GPCRs), and is required for B-cell migration and immune responses (Girkontaite *et al.*, 2001; Francis *et al.*, 2006). Finally, the IPA analysis could assist further in the understanding of HIP1R interactome in malignant or normal B cells.

A

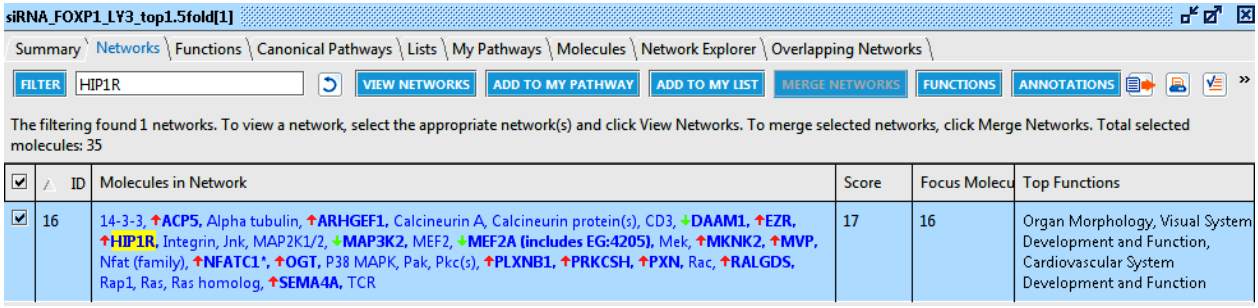

B

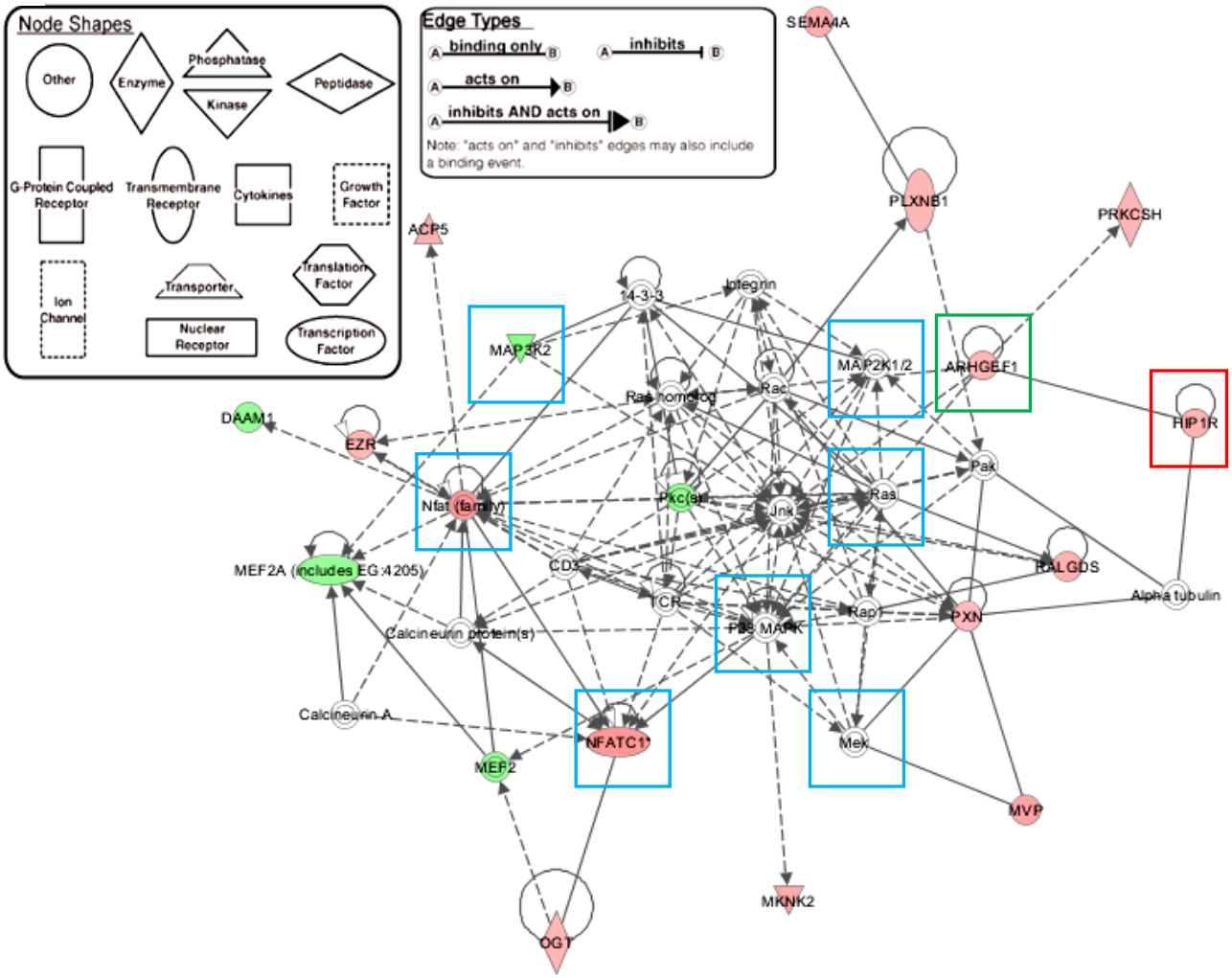

Fig 5.18 *HIP1R* might associate with MAP kinases and NFAT from IPA analysis

A: Cluster of genes (in bold) affected by siFOXP1; B: Genes are represented as nodes, red and green nodes represent upregulated and downregulated genes, respectively, affected by siFOXP1; the direct/indirect biological relationship between two nodes is represented as an edge (line). HIP1R (red box) might associate with MAPKs and NFATs (blue boxes) in the network and binds with ARHGEF1 (green box).

5.4 PHENOTYPICAL CHANGES IN si*HIP1R* AND LENTI-HIP1R CELLS

Since HIP1R is markedly downregulated in the ABC-DLBCL subtype, re-introduction of HIP1R expression in ABC-DBLCL cell line would be the most logical experiment to be carried out to investigate the functional significance of this observation. However, this experiment was delayed by the process of obtaining the safety permission to perform lentiviral laboratory work that was only approved in February this year. Thus, while waiting for the safety permission approval, investigations on the phenotypical changes of si*HIP1R* in DLBCL and Raji (BL) cell lines were carried out first.

5.4.1 Cell proliferation and viability of si*HIP1R* cells

To investigate the potential role of HIP1R in B-cell NHL, siRNA-mediated knockdown of HIP1R was performed in six different cell lines with high levels of HIP1R: four GC-DLBCL (MIEU, SUDHL4, SUDHL6, SUDHL10), one ABC-DLBCL (Riva) and one BL (Raji) cell lines.

si1, si2 (targeting *HIP1R*) or scramble (control) siRNAs were electroporated into the B-cell lines and silencing was confirmed by qRT-PCR analysis of *HIP1R* transcripts after 48 hours (Fig 5.19). A significant reduction in *HIP1R* mRNA levels in si1- and si2-treated versus the scramble-treated cells was observed in five of the six cell lines, the exception being SUDHL6. The cell proliferation rate was investigated by conducting an MTS assay every 24 hours for four days. However, there were no significant changes in the proliferation rate in both si1- and si2-treated cells versus those of scrambled-treated cells at any time points under normal culture conditions in the transient knockdown system (Fig 5.19).

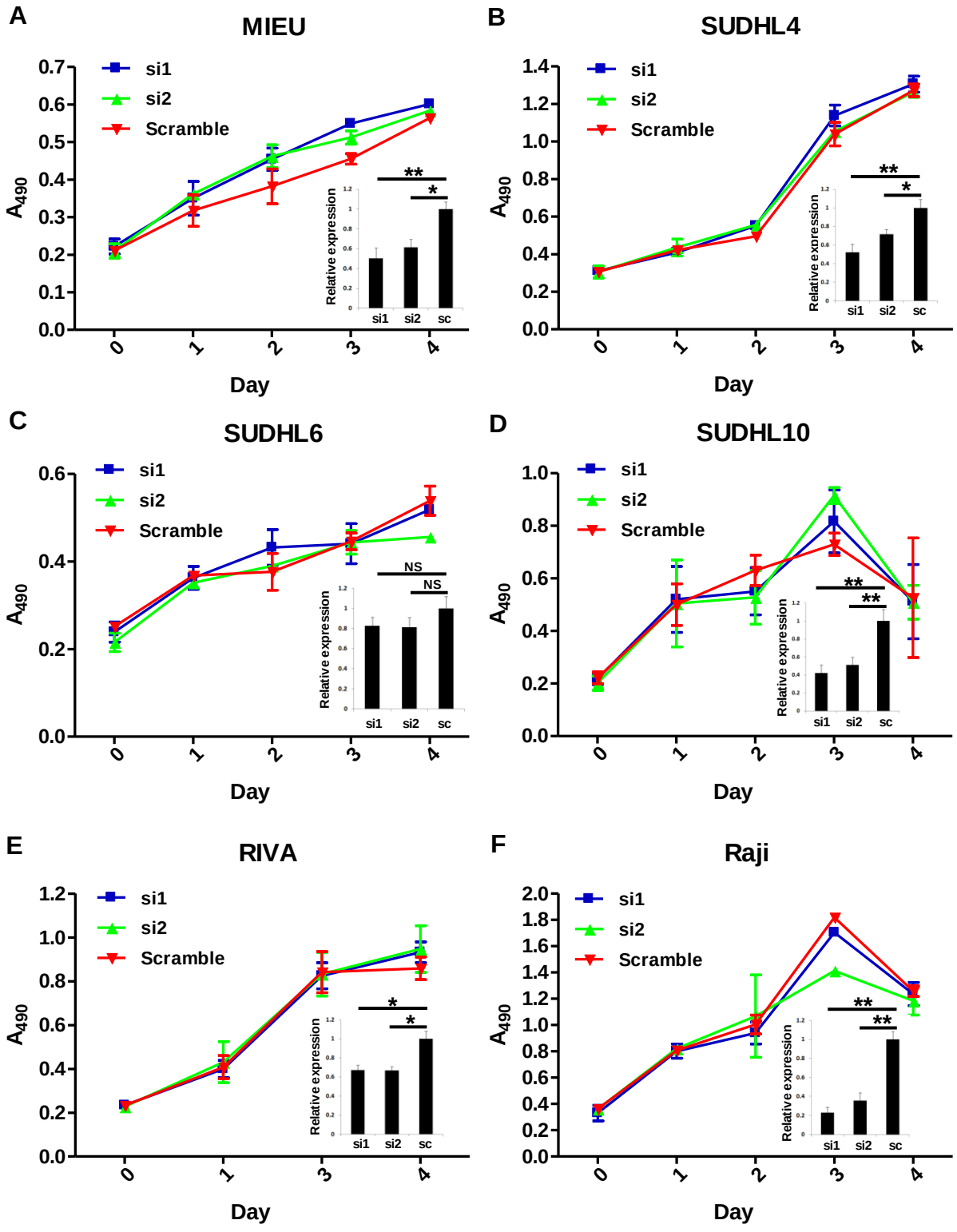

Fig 5.19 Proliferation of si*HIP1R*-treated cells in GC-DLBCL (A-D), ABC-DLBCL (E) and BL (F) cell lines measured by MTS assay

*Data represent single experiment (A-C) and from two independent experiments (D-F). Each data point represents mean ± standard deviation of triplicate absorbance values. Knockdown of HIP1R validated by qRT-PCR of 48-hour post-treatment samples are shown in the graphs. Key: **: $p < 0.01$; *: $p < 0.05$; NS: Not significant.*

The si*HIP1R* cells that showed no changes in survival and proliferation capabilities suggest that the presence or absence of HIP1R expression in GC-DLBCL does not affect the viability of the GC-DLBCL subtype.

5.4.2 Levels of BCR subunits in si*HIP1R* cells

HIP1R has a role in linking clathrin to the actin cytoskeleton (Poupon *et al.*, 2008) and internalisation of the BCR requires both clathrin (Stoddart *et al.*, 2002) and the actin cytoskeleton (Onabajo *et al.*, 2008; Sharma *et al.*, 2009). HIP1R is significantly downregulated in ABC-DLBCL, a subtype requiring chronic active BCR signalling for survival (Davis *et al.*, 2010). Thus, we generated the hypothesis that HIP1R might be downregulated in ABC-DLBCL because this could potentially promote increased BCR levels on the cell surface. A similar mechanism that contributes to upregulated BCR signalling has already been proposed for mutations of CD79b (Davis *et al.*, 2010).

siRNA-mediated knockdown of HIP1R expression in SUDHL10 (GC-DLBCL), Riva (ABC-DLBCL) and Raji (BL) was performed. Knockdown of HIP1R expression was validated by Western blotting (Fig 5.20).

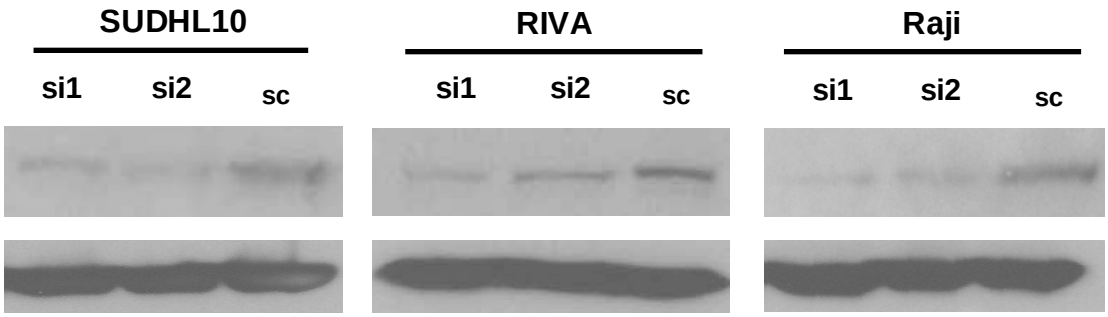

Fig 5.20 Validation of HIP1R knockdown by two independent *HIP1R* siRNAs

Immunoblotting of two siHIP1R-treated (si1 and si2) and scramble siRNA-treated (sc) SUDHL10, Riva and Raji cell lines (72 h) with anti-HIP1R-44 mAb. Silencing was also confirmed at the transcript level (Fig 5.19).

This was followed by investigations on the levels of surface BCR subunits by flow cytometry stained with PE-conjugated anti-IgM mAb, PE-conjugated anti-CD79b mAb or an isotype matched (IgG1) negative control antibody to test for the specificity of the FACS staining. Increased levels of surface IgM was observed in Riva utilising two independent HIP1R siRNAs, si1 and si2 compared to scramble siRNA control. Increased surface IgM was also observed, but less consistently, in Raji (si1 only) and SUDHL10 (si2 only) (Fig 5.21).

Ratio of the mean fluorescent intensity (MFI) of si1 and si2 versus scramble siRNAs after deducting MFI of isotype control showed that increase of surface IgM in Riva was 1.7- and 2-fold in si1 and si2, respectively, consistent with the shift in flow cytometry graphs. SUDHL10 and Raji populations showed a similar increase in MFI of HIP1R siRNAs versus those of scramble but yielded higher error bars. Comparison of the scrambled siRNA-treated cells stained with anti-IgM or isotype (IgG1) control antibody showed that Riva had moderate levels of surface IgM but that there were very low or undetectable levels of surface IgM in SUDHL10 and Raji cells.

There was a 2-fold increase in CD79b levels in SUDHL10 cells treated with the same set of siRNAs in two independent experiments and the fold-change increased with time, from 48 hours to 72 hours post-treatment (Fig 5.22). Both si1- and si2-treated SUDHL10 cells consistently showed an increase in CD79b levels, and no changes in CD79b levels were observed in Riva and Raji (data not shown), suggesting that regulation of BCR proximal units (IgM or CD79b) might be distinct from one another. Comparison of the scrambled siRNA-treated cells stained with anti-CD79b or isotype (IgG1) control antibody showed that SUDHL10 had high levels of surface CD79b protein.

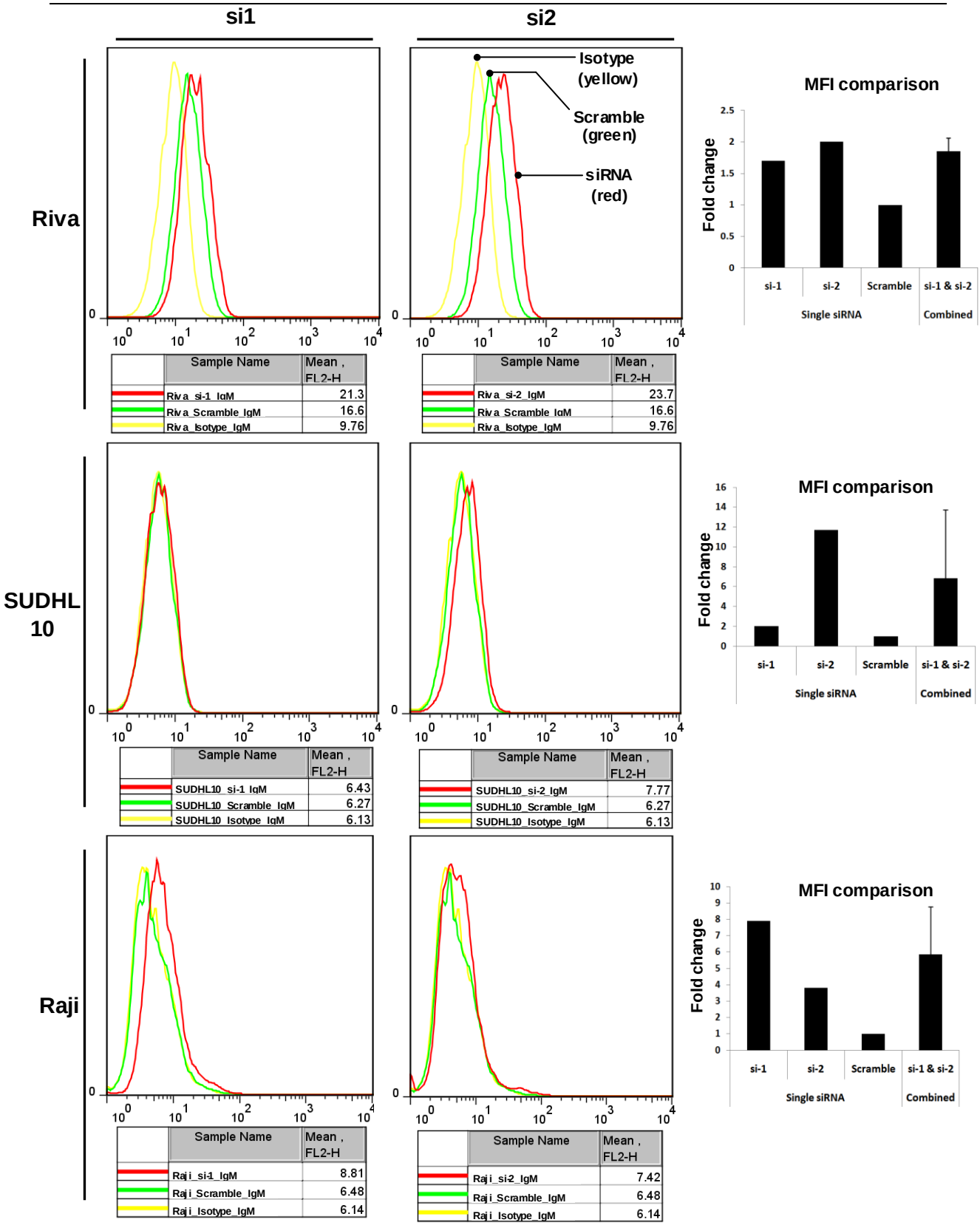

Fig 5.21 Surface IgM levels in si*HIP1R*- or scramble siRNA-treated cell lines

Cells were tested after 72 hours of knockdown representing 2 independent experiments. The graphs were plotted in a log-scale on the x-axis, and the y-axis denotes relative number of cells. Ratio of MFI in si1 and si2 cells compared with scramble-treated cells shown in corresponding graph.

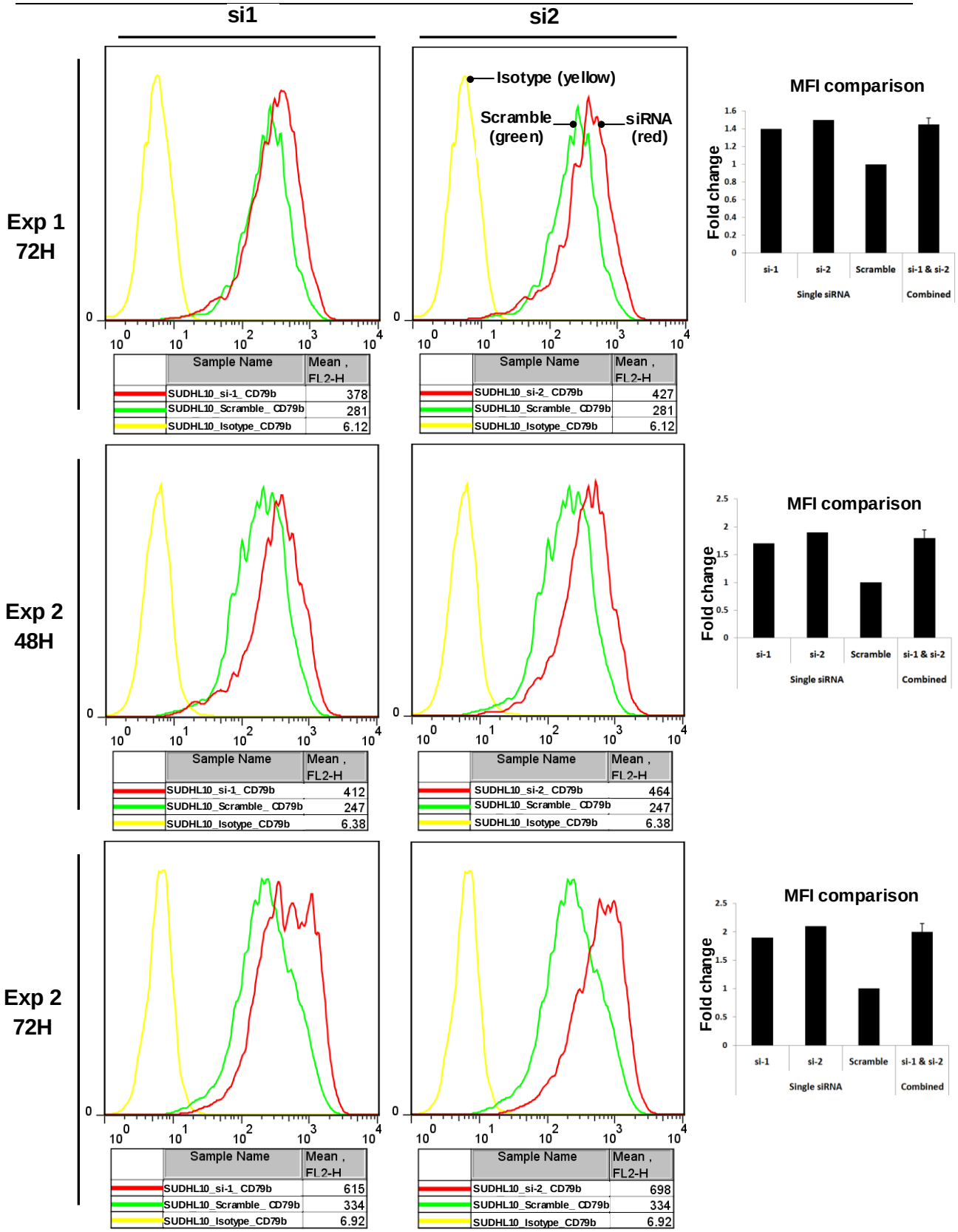

Fig 5.22 Surface CD79b levels in si*HIP1R*- or scramble siRNA-treated SUDHL10

Cells were tested in 2 independent experiments (Exp 1 and Exp 2), and a time-course of 48 hours and 72 hours was conducted in the second experiment. The MFI graphs are consistent with the increased CD79b levels in the si1- and si2-treated cell populations.

The increase of BCR subunit's levels in si*HIP1R* cells showed that HIP1R has the potential to regulate the levels of cell surface expression of BCR components, and this provides future avenues for investigating BCR levels upon overexpression of HIP1R in appropriate ABC-DLBCL cell lines.

5.4.3 Cell proliferation and viability in lenti-HIP1R cells

From the experience of our laboratory working on lymphoma cell lines, use of standard plasmid-based and lipid-mediated transfection agents such as Fugene (Roche) and Lipofectamine (Invitrogen) to transfect lymphoma cell lines yielded very low transfection efficiency, usually less than 20%. Such low transfection efficiency limits the conclusions that can be made on the phenotypic changes due to the overexpression of a gene. This could be resolved by antibiotic selection of stable transfectants expressing a gene of interest via the antibiotic resistant gene to obtain the pure population of cells. However, high transfection efficiency in lymphoma cell lines is generally also required for successful antibiotic selection of the stable transfectants (Dr Paola Bignone personal communication). Adoption of viral-mediated delivery of the gene of interest (*HIP1R*) represents an alternative approach to enable high frequency of transduced lymphoma cells and to generate stable clones expressing the transgene.

Once the safety permission to perform lentiviral laboratory work was obtained, the full-length *HIP1R* cDNA construct, that had been generated for antibody and immune response validations, was utilised by subcloning the full-length *HIP1R* insert into an intermediate vector (pENTR^{TM}/D-TOPO, Invitrogen). This was followed by the final subcloning of the insert to a lentiviral vector (pLenti6.3/TO/V5-DEST^{TM}, Invitrogen) that was successfully generated and confirmed by sequencing (Fig 5.23). Primarily, this lentiviral

experiment was a test for the ability to perform lentiviral delivery, the best cell lines to be used in terms of transduction efficiency, and to determine which time point to apply antibiotic selection for generating cells stably expressing HIP1R before performing downstream experiments.

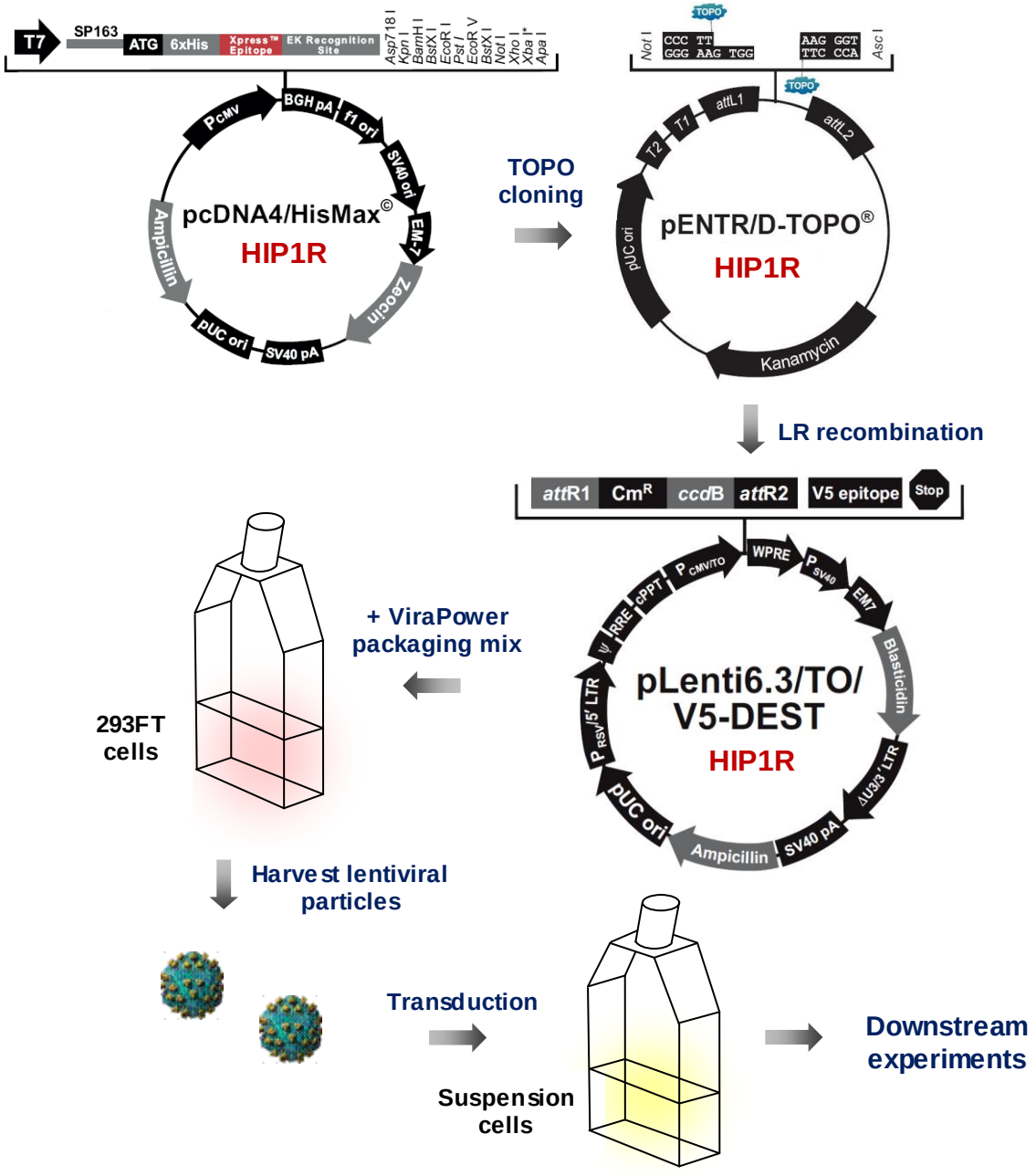

Fig 5.23 Generation of HIP1R lentiviral particles and transduction procedures

Sequencing was conducted after cloning into each construct to confirm full-length HIP1R cDNA was present. Downstream experiments primarily included immunostaining of transduced suspension cells.

Lentiviral-mediated HIP1R or GFP (lenti-HIP1R or lenti-GFP) ectopic expression was undertaken in six DLBCL cell lines with low or absent levels of HIP1R: four ABC-DLBCL (HBL1, OCI-LY3, OCI-LY10 and U2932) and two GC-DLBCL (DB and K422) cell lines. Three cell lines were successfully transduced with lenti-HIP1R or lenti-GFP (DB, OCI-LY3, OCI-LY10), this was confirmed by immunostaining of HIP1R and fluorescent imaging of GFP at 24 h, 48 h and 96 h time points (Fig 5.24).

Surprisingly, both of the ABC-DLBCL cell lines (OCI-LY3 and OCI-LY10) that were successfully transduced with lenti-HIP1R demonstrated a significant reduction in cell size and disrupted morphology at all 3 time points (24, 48, 96 h post-transduction, detected by immunostaining of PFA-fixed cells) compared to those that were not infected by lenti-HIP1R. However, the transduction efficiency of the lenti-GFP construct (< 5% at all 3 time points) was much lower than that of the lenti-HIP1R construct (> 20% at 24 h time point and decreased gradually over time), preventing comparison with a suitable control for the lenti-HIP1R cells with disrupted morphology, and only a few selected GFP-positive cells were shown in Fig 5.24.

Similar effects were observed in lenti-HIP1R transduced DB cells but the morphology and cell size changes were not as dramatic as those observed with OCI-LY3 and OCI-LY10 cells at 24 h post-transduction. Thus, more detailed focus on lenti-HIP1R transduced OCI-LY3 and OCI-LY10 cells are presented in Fig 5.25.

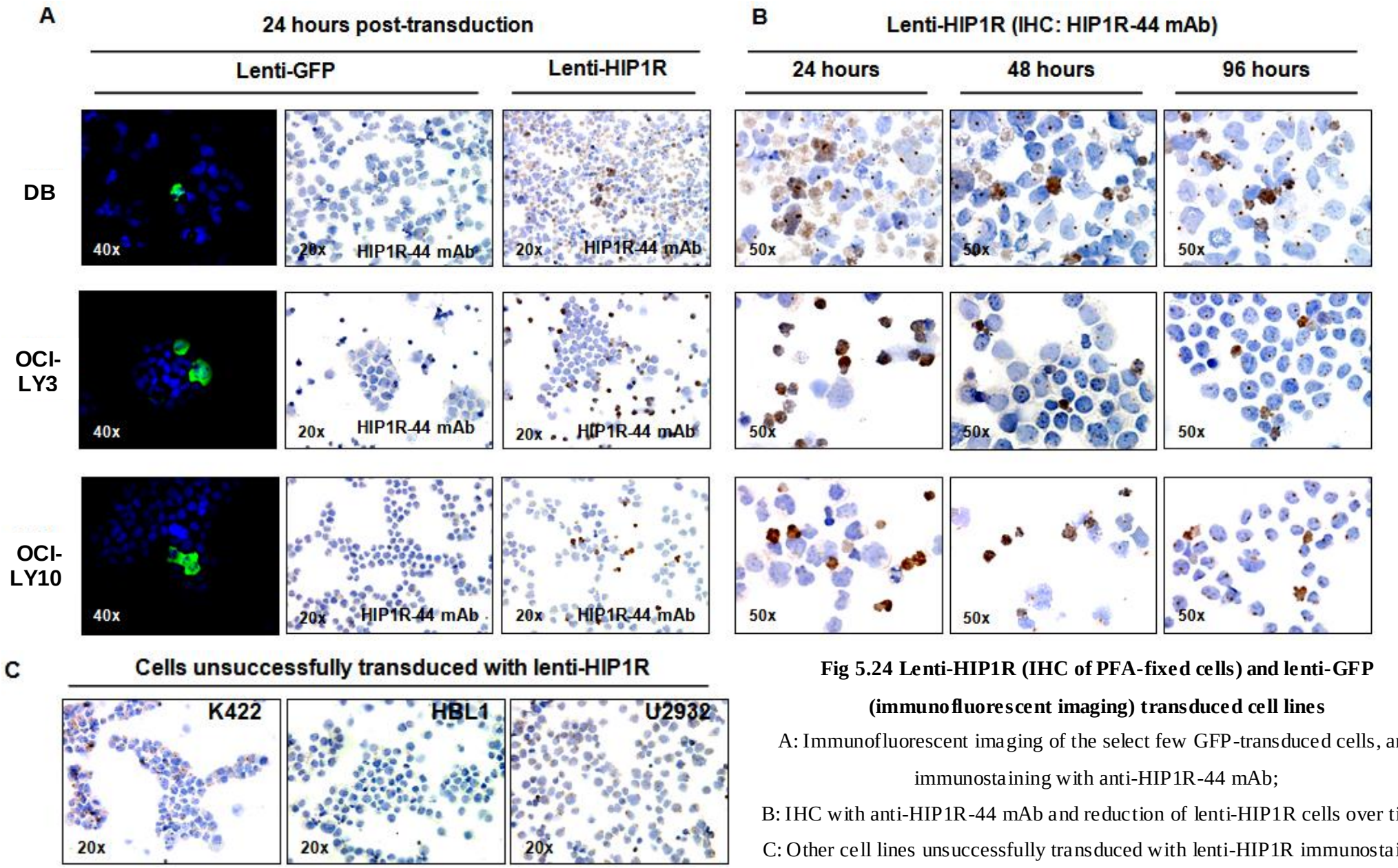

Fig 5.24 Lenti-HIP1R (IHC of PFA-fixed cells) and lenti-GFP (immunofluorescent imaging) transduced cell lines

A: Immunofluorescent imaging of the select few GFP-transduced cells, and immunostaining with anti-HIP1R-44 mAb;

B: IHC with anti-HIP1R-44 mAb and reduction of lenti-HIP1R cells over time;

C: Other cell lines unsuccessfully transduced with lenti-HIP1R immunostained with anti-HIP1R-44 mAb.

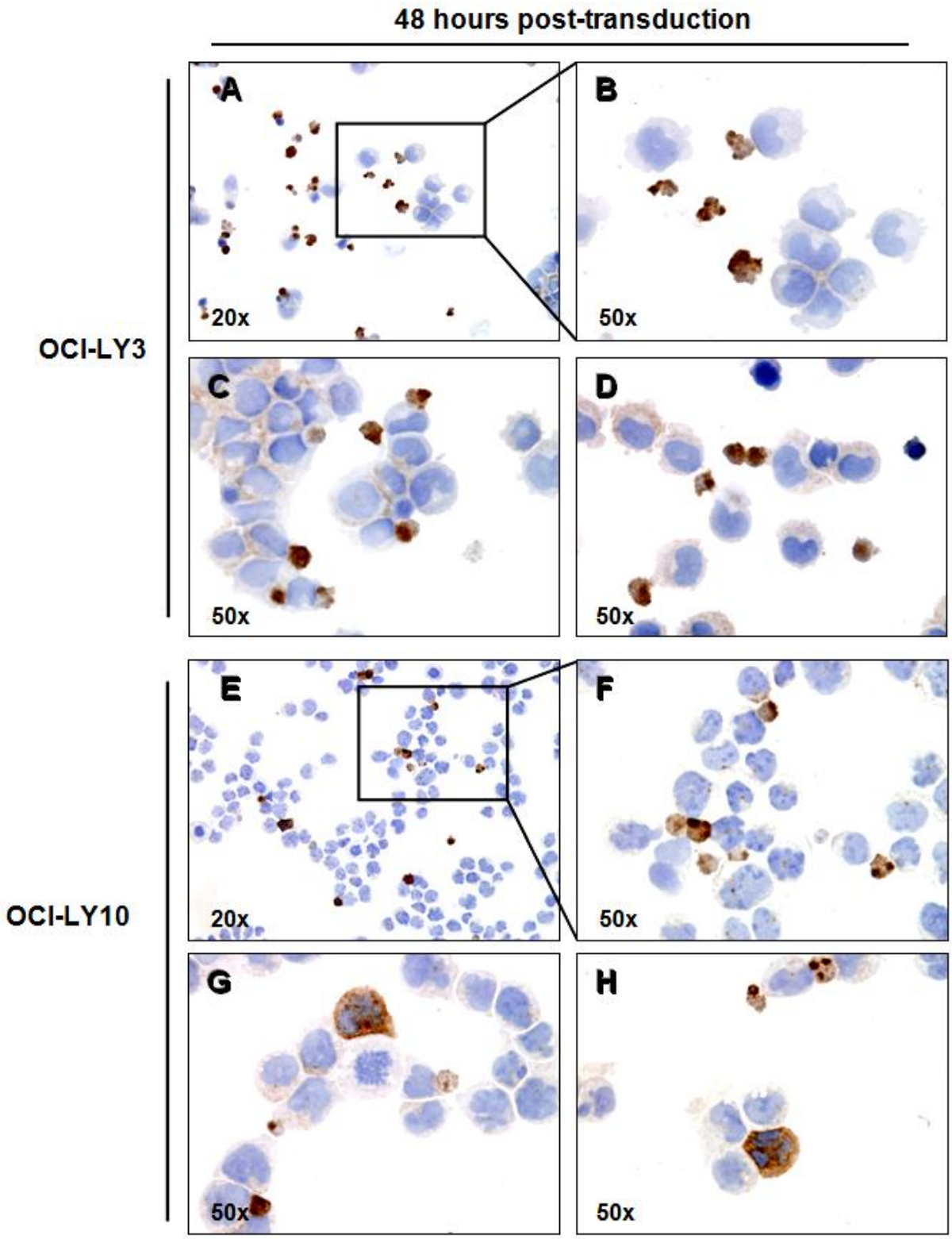

Fig 5.25 Morphology changes of lenti-HIP1R-transduced ABC-DLBCL cell lines

Size reduction and morphology disruption were frequently observed in ABC-DLBCL cells transduced with lenti-HIP1R (A-H). Cells were immunolabelled with anti-HIP1R-44 mAb.

Due to laboratory safety restrictions, cells transduced with lentiviral vector must undergo appropriate fixation (2% PFA) before performing downstream experiments outside of the tissue culture hood. Thus, the MTS assay that requires unfixed or viable cells could not be utilised. An alternative was used whereby cells showing overexpression of HIP1R (detected by immunoperoxidase labelling), and cells not overexpressing HIP1R were counted using a 10 mm graticule. The ratio of HIP1R-positive versus HIP1R-negative cells in percentages were calculated and presented on a stacked column (Fig 5.26). The lenti-HIP1R-transduced cells reduced in number over-time compared to those that did not overexpress HIP1R significantly ($p < 0.01$, 24-hour versus 96-hour post-transduction in all three cell lines). Transduction experiments were performed in triplicates with similar observations. However, this data lack lenti-GFP cells as controls, thereby it could only suggest a reduction in lenti-HIP1R cells that might be attributable to HIP1R overexpression.

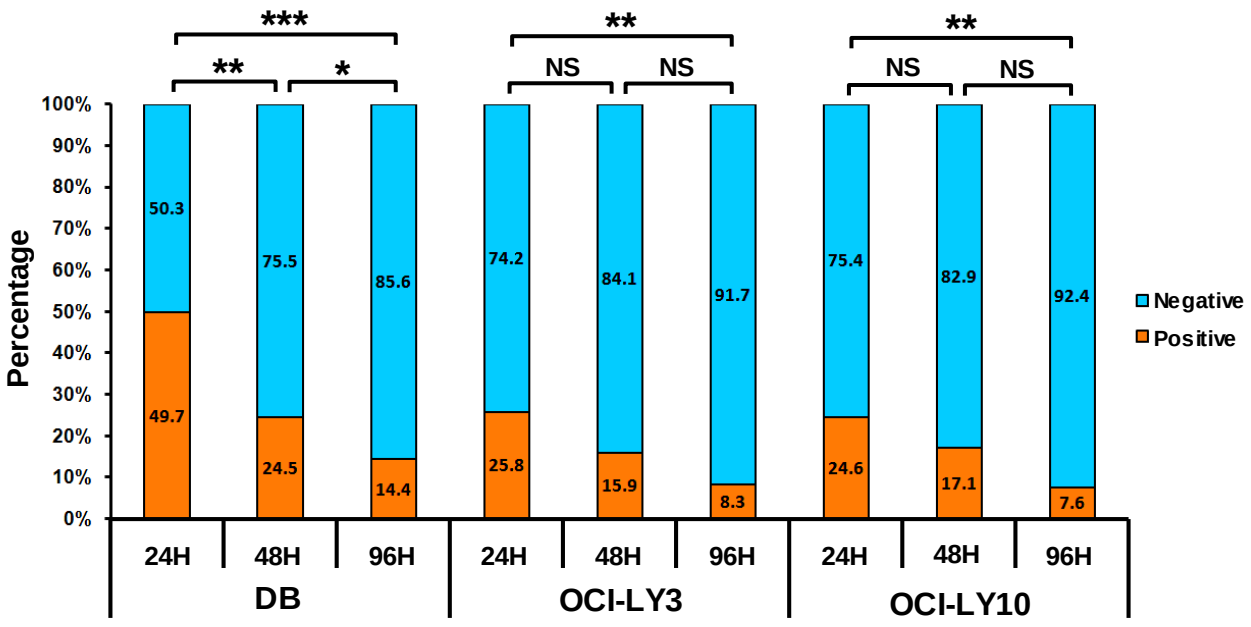

Fig 5.26 Reduction of HIP1R-positive cells over-time of lenti-HIP1R transduced cells

*The reduction of HIP1R-positive cells was significant in all three cell lines ($p < 0.01$, 24-hour versus 96-hour post-transduction). p values were calculated based on the comparison of cells proportion (in percentage). Key: NS: not significant; *****: $p < 0.05$; ******: $p < 0.01$; *******: $p < 0.001$*

DB, OCI-LY3 and OCI-LY10 transduced cells were subsequently treated with blasticidin for 10 days. Both lenti-HIP1R and lenti-GFP transduced OCI-LY3 and OCI-LY10 cells were killed by the treatment, most probably due to low transduction efficiency. However, both lenti-HIP1R and lenti-GFP transduced DB cells survived the blasticidin treatments. Immunoperoxidase labelling showed that the proportion of cells expressing HIP1R in DB cells was observed to be less than those expressing GFP (Fig 5.27). This suggests that repression of both *GFP* and *HIP1R* transgene while maintaining the expression of blasticidin-resistant gene might occur. The proportion of HIP1R-positive cells was significantly less than those of GFP-positive cells ($p < 0.05$), suggesting that the frequency of repression on the *HIP1R* transgene (via an unknown mechanism) was significantly higher. The occurrence of silenced transgene expression in lentiviral vector via DNA methylation has been documented (Zhang *et al.*, 2010).

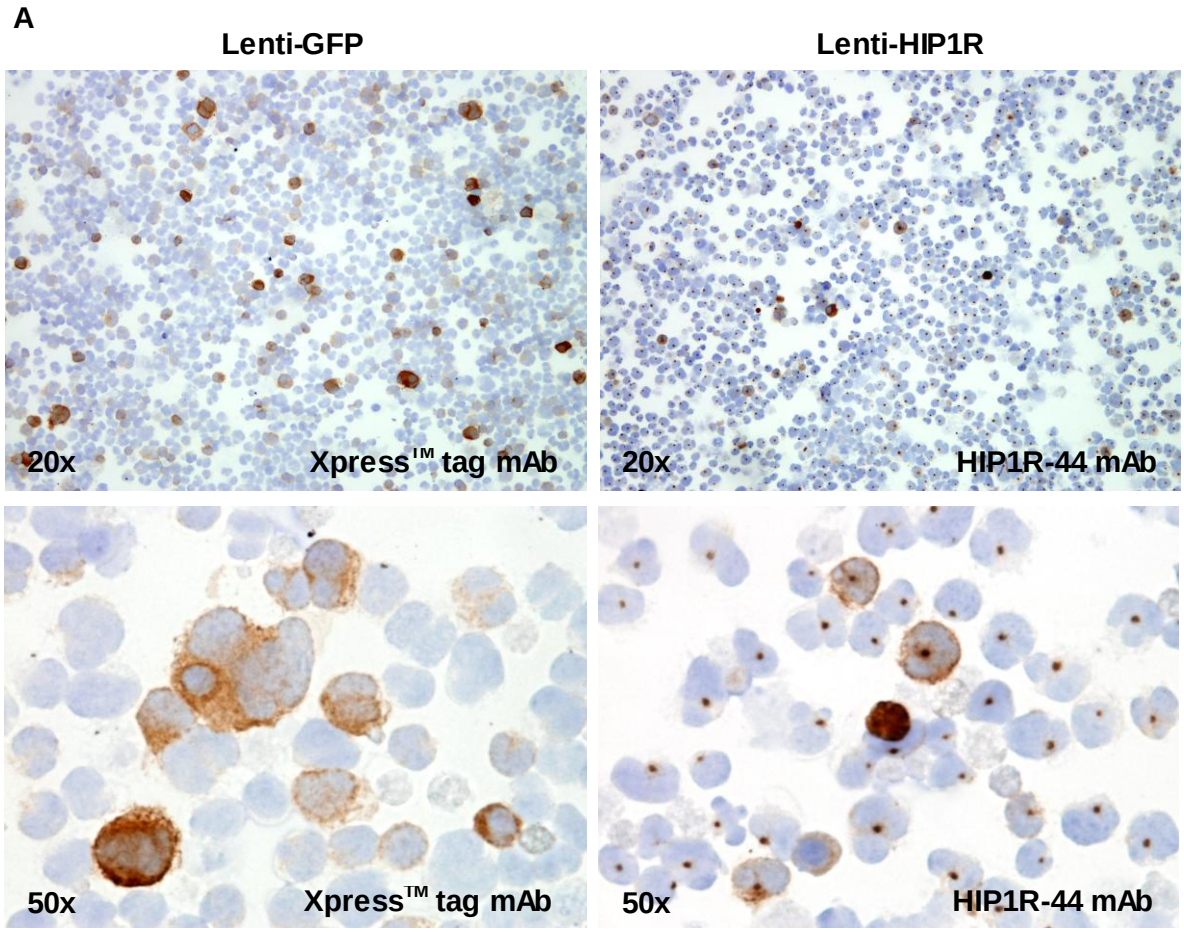

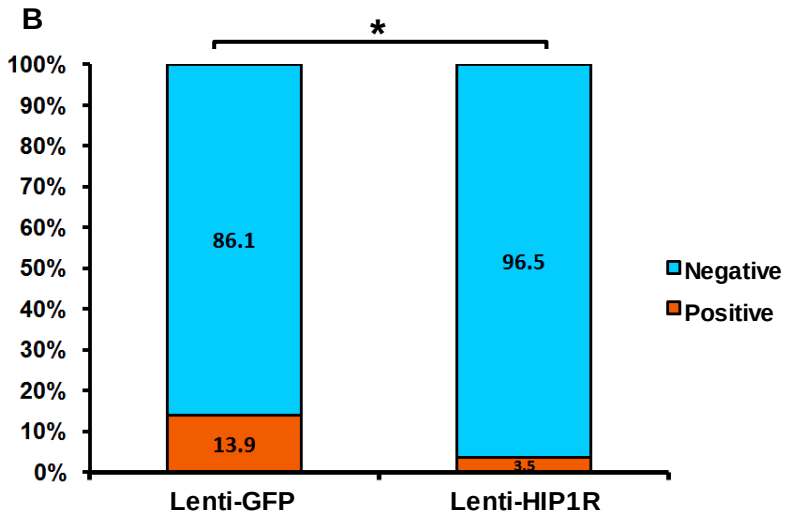

Fig 5.27 Comparison of lenti-HIP1R and lenti-GFP transduced DB cells after blasticidin treatment

*A: The cells were treated with blasticidin for 10 days, the media was then replaced without blasticidin and let grown for 48 hours before imunolabelling was performed. B: The proportion of HIP1R-positive cells was less than those of GFP-positive cells ($p < 0.05$). NB: In Panel A of lenti-HIP1R cells (magnification 50x) had labelling of low, endogenous HIP1R protein, most probably localised in the Golgi that was also observed in other cell lines (293T and other B-NHL). Key: *****: $p < 0.05$*

We initially planned to generate ABC-DLBCL cells stably overexpressing HIP1R for downstream experiments, e.g. to analyse the changes in the levels of BCR subunits. However, the possible lethality of HIP1R overexpression impeded further downstream experiments. Employing an inducible overexpression system could be an alternative approach to achieving a pure population of stable transfectants expressing HIP1R.

DISCUSSION

Microarray data, qRT-PCR analysis and immunolabelling studies on a series of DLBCL samples confirmed a highly significant downregulation of HIP1R at both mRNA and protein levels in ABC-DLBCL compared to GC-DLBCL and normal B cells. HIP1R as a discriminator of GC- versus ABC-DLBCL subgroup is also supported by a recent study

(Davis *et al.*, 2010) that selected *HIP1R* as one of 96 gene-based discriminator of GC- versus ABC-DLBCL derived cell lines. The 96 genes also including validated GC-DLBCL markers (e.g. *BCL6*, *LMO2*), and the genes were chosen based on differential expression in GC-DLBCL versus ABC-DLBCL in primary biopsy samples ($p < 0.0001$). The lack of inclusion of *HIP1R* in earlier gene lists (Alizadeh *et al.*, 2000) may reflect the comparison of DLBCL subtyping genes with their expression levels in DLBCL versus their potential non-malignant COO. The high-level expression of *HIP1R* in activated peripheral blood B cells that we identified is not consistent with the low level expression in ABC-DLBCL.

Stratification of DLBCL based on *HIP1R* mRNA levels was more effectively recapitulated by the Choi *et al.* (2009) algorithm than the Hans *et al.* (2004) algorithm. Further studies could address whether inclusion of HIP1R, with its commercially available antibody that has been well-validated in this study (anti-HIP1R-44 mAb), into the Choi *et al.* algorithm might improve concordance with GEP further. We are also interested in investigating whether a reciprocal relationship between FOXP1 and HIP1R could represent a method for identifying DLBCL patients with high-level expression of smaller FOXP1 isoforms. This is important because the current JC12 monoclonal antibody cannot distinguish FOXP1 isoforms by IHC and target genes that do so may be useful for improving the utility of FOXP1 as a DLBCL biomarker.

Higher frequency of HIP1R protein expression in DLBCL patients treated with CHOP chemotherapy regimen identified their trend toward better overall survival ($p = 0.060$). The intensity or frequency of HIP1R protein expression was not predictive of survival in this series of R-CHOP cohort of DLBCL patients. However, COO subtyping in one of the 3 series of R-CHOP-treated patients (the “Rituximab NBF” series) showed a non-significant trend

toward inferior outcome (p = 0.07) (Shustik *et al.*, 2010). Thus, it would be of interest to investigate the association of HIP1R expression with survival in other series where COO subtyping is prognostic in R-CHOP-treated patients.

To address the issue whether downregulation of HIP1R is a disease-related process or whether it purely reflects the activation status of normal B cells, HIP1R levels were examined in non-malignant B cells purified from peripheral blood with or without BCR stimulation. Both mRNA and protein levels of HIP1R were upregulated upon stimulation with anti-IgM or IL2 and SAC in two independent experiments. Furthermore, there was an inverse expression pattern with IRF4 in DLBCL and in tonsillar lymphocytes, but not in non-malignant activated B cells from peripheral blood. In contrast, the reverse is observed for FOXP1, which correlates with IRF4 in DLBCL and in activated peripheral blood B cells, but not in tonsillar B cells (Alison Banham, personal communication). Thus, HIP1R might be downregulated in ACB-DLBCL through a disease-related process other than normal B-cell activation.

The putative regulator of HIP1R was investigated. FOXP1 may downregulate *HIP1R* expression by binding to its promoter region. This is supported by the presence of a highly conserved FOXP1 binding sequence in *HIP1R* promoter within 1kb of TSS. Furthermore, *HIP1R* levels were consistently upregulated in FOXP1-depleted OCI-LY3 cells investigated by qRT-PCR and microarray approach. Short isoform $FOXP1_S$ (60-65 kDa) is a more likely candidate than the full-length $FOXP1_{FL}$ protein (75 kDa) since the upregulated *HIP1R* levels were markedly observed in FOXP1-depleted OCI-LY3 cells but not in DB cells, and $FOXP1_S$ is highly expressed in ABC-DLBCL (Brown *et al.*, 2008).

The exact role of FOXP1 in regulating HIP1R expression needs to be addressed by examining the protein levels of HIP1R in si*FOXP1*-treated samples and final confirmation of *HIP1R* as a direct target *in vivo* requires chromatin immunoprecipitation (ChIP) experiments. In addition, the si*FOXP1* analysis on *HIP1R* levels does not rule out the possibility that IRF4 is another putative regulator of HIP1R expression in DLBCL (or that IRF4 and FOXP1 may have a functional relationship), and this is another future avenue of studies.

In addition, the IPA analysis of FOXP1 targets from the microarray experiments suggests an association of HIP1R with ARHGEF1, and this might provide further insights into the interactome of HIP1R in B cells.

The hypothesis that HIP1R has the potential to regulate surface BCR levels is supported by well-documented literature that HIP1R links clathrin to the actin cytoskeleton. Surface IgM levels increased after knockdown of HIP1R particularly in Riva cells (ABC-DLBCL subtype) that has higher levels of surface IgM than Raji and SUDHL10 cells. ABC-DLBCL subtype relies on chronic active BCR signalling (Davis *et al.*, 2010) and the increase in surface BCR levels after knockdown of HIP1R might provide the selective pressure for HIP1R downregulation in ABC-DLCBL. Furthermore, surface CD79b was markedly increased in SUDHL10 cells after depletion of HIP1R. This indicates that HIP1R does indeed have the potential ability to regulate surface BCR levels in DLBCL.

si*HIP1R* cells did not appear to have significant changes in cell viability and proliferation rate compared with its scramble-treated counterparts. However, stable knockdown or overexpression is superior to transient system for the cells to present phenotypical or morphological changes (Ngo *et al.*, 2006; Davis *et al.*, 2010). Overexpression

of HIP1R mediated by a lentiviral vector showed that lenti-HIP1R transduced OCI-LY3, OCI-LY10 (ABC-DLBCL subtype) and DB (GC-subtype) cells had disrupted morphologies with significant reduction in cell size and number over-time ($p < 0.01$). This suggests that overexpression of HIP1R might induce apoptosis in both ABC- and GC-DLBCL cells lacking HIP1R expression. This phenotype, that was also observed in OCI-LY3 (a cell line with mutated CARD11 with constitutive NF-κB signalling independently of BCR signalling), suggests that overexpression of HIP1R might be toxic to ABC-DLBCL via a mechanism other than regulating surface BCR levels. A possible alternative mechanism is that HIP1R induces caspase-mediated cell death, a mechanism that has been shown by Kim *et al.* (2009), in the ABC-DLBCL. The morphology changes were more quickly observable in the ABC-DLBCL subtype cells (post 24-hour of transduction) indicating that overexpression of HIP1R has a larger effect on ABC-DLBCL. This is consistent with HIP1R downregulation in ABC-DLBCL subtype.

In the lenti-HIP1R and lenti-GFP transduced DB cells that underwent blasticidin selection for 10 days, the proportion of HIP1R-transduced cells was much less than GFP-transduced cells ($p < 0.05$). This suggests that transgene expression of HIP1R, and to a much lesser extent GFP, declined over time while expression of the blasticidin resistant gene remained. Silenced transgene expression in lentiviral vector could occur via DNA methylation (Zhang *et al.*, 2010). HIP1R might be detrimental to the viability of DB cells and this might provide a selective pressure to repress *HIP1R* transgene than *GFP* transgene expression.

The possible involvement of HIP1R in the apoptosis of B-cell NHL, particularly DLBCL, is a future avenue of investigation.

CHAPTER 6
JMJD3 AS A PUTATIVE LYMPHOMA AUTOANTIGEN

INTRODUCTION

6.1 JMJD3 ANTIGEN

JMJD3 was one of the 'short' listed 35 antigens identified using the protein arrays. It was recognised by a humoural immune response in three out of five GC-DLBCL patients (or 60% of this subtype) and one out of four transformed DLBCL patients (25%). In total, the JMJD3 autoantigen was recognised by four out of 25 (16%) of B-NHL patients' sera screened by protein arrays.

To recapitulate the reasons why we were interested in this molecule for further validation from the 'short' list of B-NHL antigens, JMJD3 was highly topical and had the potential to play a role in lymphoma through epigenetic regulation of gene expression (Agger *et al.*, 2007; De Santa *et al.*, 2007). Epigenetic changes have been shown to be important in regulating gene expression in B-NHL particularly FL (Rahmatpanah *et al.*, 2006; O'Riain *et al.*, 2009) and DLBCL (Shi *et al.*, 2007; Pike *et al.*, 2008). Moreover, JMJD3 has been positively associated with blood cell activation whereby murine Jmjd3 is upregulated by NF-κB in macrophages during inflammatory responses (De Santa *et al.*, 2007), suggesting that JMJD3 might be associated with activation of B cells, and possibly with B-NHL particularly ABC-DLBCL.

In this chapter, validation of commercial JMJD3 antibodies was first explored followed by the attempts to validate JMJD3 as a lymphoma autoantigen. Finally, *JMJD3* mRNA expression patterns in a panel of haematological malignancies cell lines were investigated.

RESULTS

6.2 VALIDATION OF JMJD3 ANTIBODIES

Several JMJD3 antibodies were available commercially but as little data were available concerning their characterisation, this was further investigated. The full-length *JMJD3* cDNA plasmid construct containing a Myc tag was kindly provided by Prof Charlie Degui Chan (Shanghai Institutes for Biological Sciences, China). Cytospin preparations of COS-1 cells transfected with the full-length *JMJD3* construct were used to validate five commercially-available JMJD3 rabbit anti-human polyclonal antibodies (pAb) from Abcam (ab38113), Cell Signaling (3457) and Abgent ("N-term", "C-term", and "Center").

Immunolabelling with an anti-Myc mAb (Santa Cruz) confirmed nuclear and some cytoplasmic recombinant JMJD3 expression (Fig 6.1). Three commercial JMJD3 antibodies [Abcam (ab38113), Cell Signaling (3457) and Abgent "N-term"] yielded similar staining intensity or frequency with anti-Myc antibody specifically on transfected cells. Two exhibited non-specific labelling of both transfected and untransfected COS-1 cells (Fig 6.1E and F) and were excluded from further studies.

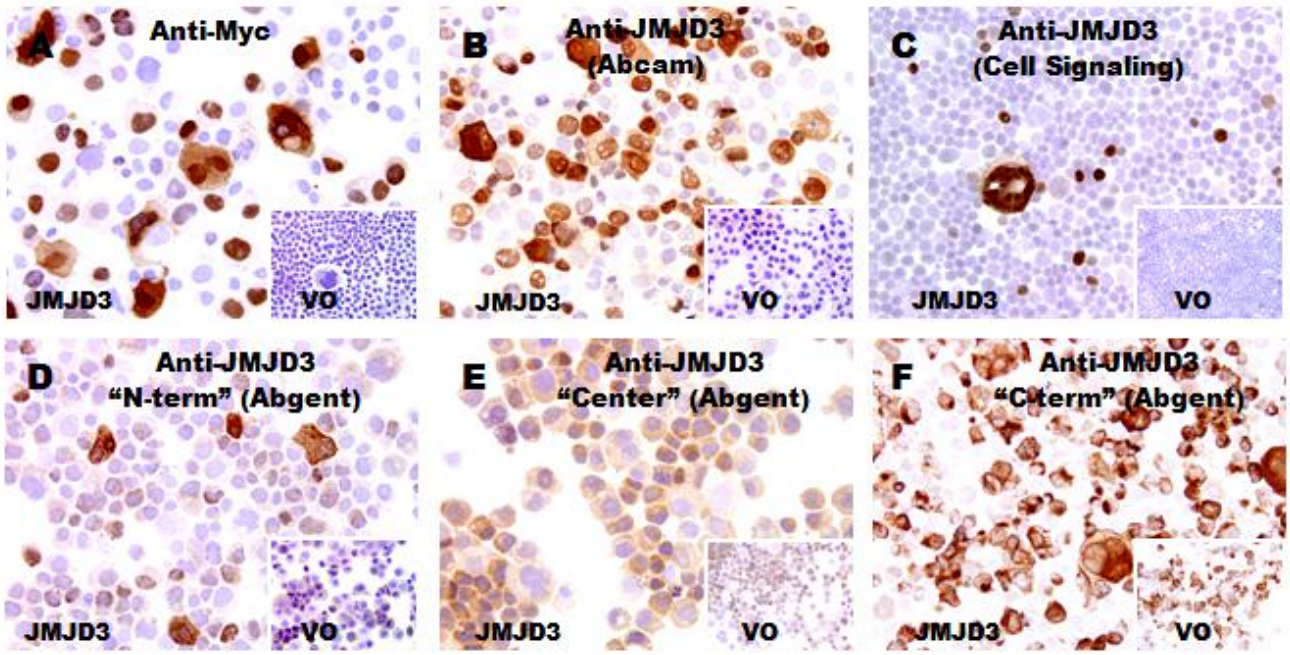

Fig 6.1 Validation of a panel of anti-JMJD3 polyclonal antibodies

JMJD3 transfectants were immunolabelled with anti-Myc to detect the epitope tag (A) and five JMJD3 pAbs (B-F). Three antibodies (from Abcam, Cell Signaling and Abgent "N-term") yielded comparable staining patterns to immunolabelling with the anti-Myc mAb and little background. NB: All transfectants were derived from COS-1 cells except for panel (C) derived from 293T cells. Key: JMJD3: JMJD3-transfected cells; VO: vector-only transfected cells.

Immunostaining of JMJD3-transfected COS-1 cells on FFPE sections also showed that the three JMJD3 pAbs were able to recognise a formalin-resistant epitope (Fig 6.2). Fewer transfected cells were labelled using the Abgent N-terminal antibody, suggesting that this reagent might not be as sensitive as the other antibodies for JMJD3 detection.

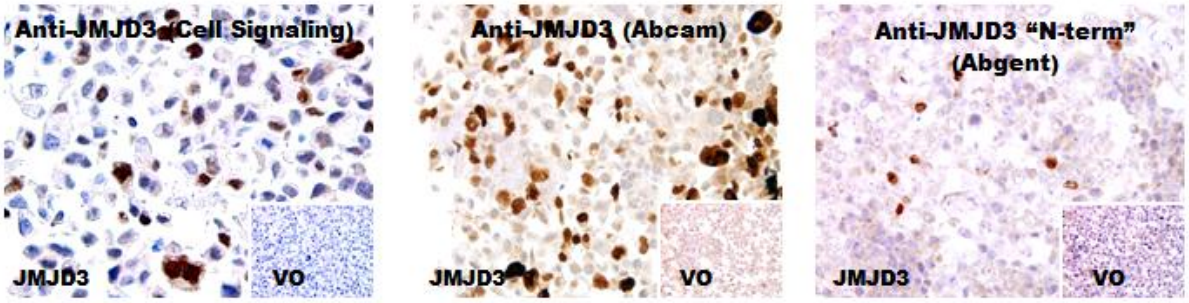

Fig 6.2 Recognition of formalin-resistant epitope by JMJD3 polyclonal antibodies

Immunoperoxidase labelling of JMJD3 COS-1 transfectants with three JMJD3 rabbit pAbs confirmed the ability of these antibodies to recognise a formalin-resistant epitope. Key: JMJD3: JMJD3-transfected cells; VO: vector-only transfected cells.

The full immunogen sequences for all the JMJD3 pAbs tested in this study have not been released and there is only one JMJD3 antibody (that is not commercially available) with a fully described immunogen (798-1095 aa of JMJD3) (Fig 6.3) generated by Agger *et al.* (2009). JMJD3 shares 32% and 31% sequence homology with UTX and UTY (members in the same JmjC family), respectively. Neither the full-length *UTX* and *UTY* cDNAs were available as IMAGE clones.

The validated JMJD3 pAb "N-term" (Abgent), which recognised the N-terminus of JMJD3 protein, is unlikely to detect UTX or UTY proteins based on the lack of homology between JMJD3 with UTX and UTY amino acid sequence over the N-terminal regions (Fig 6.3). Importantly, the protein fragment used on the protein array for patients' serum screening also shares very little homology with UTX and UTY. It was therefore likely that the serum immunoreactivity against JMJD3 on the protein array was specific. The Western blotting data illustrated in the following sections ruled out investigation of serum reactivity against the full length JMJD3 protein and raised concerns regarding the antibody specificity necessary for studies of endogenous protein expression. Thus, no cross-reactivity studies were pursued to test cross-reactivity with either patients' sera or commercial antibodies with UTX or UTY.

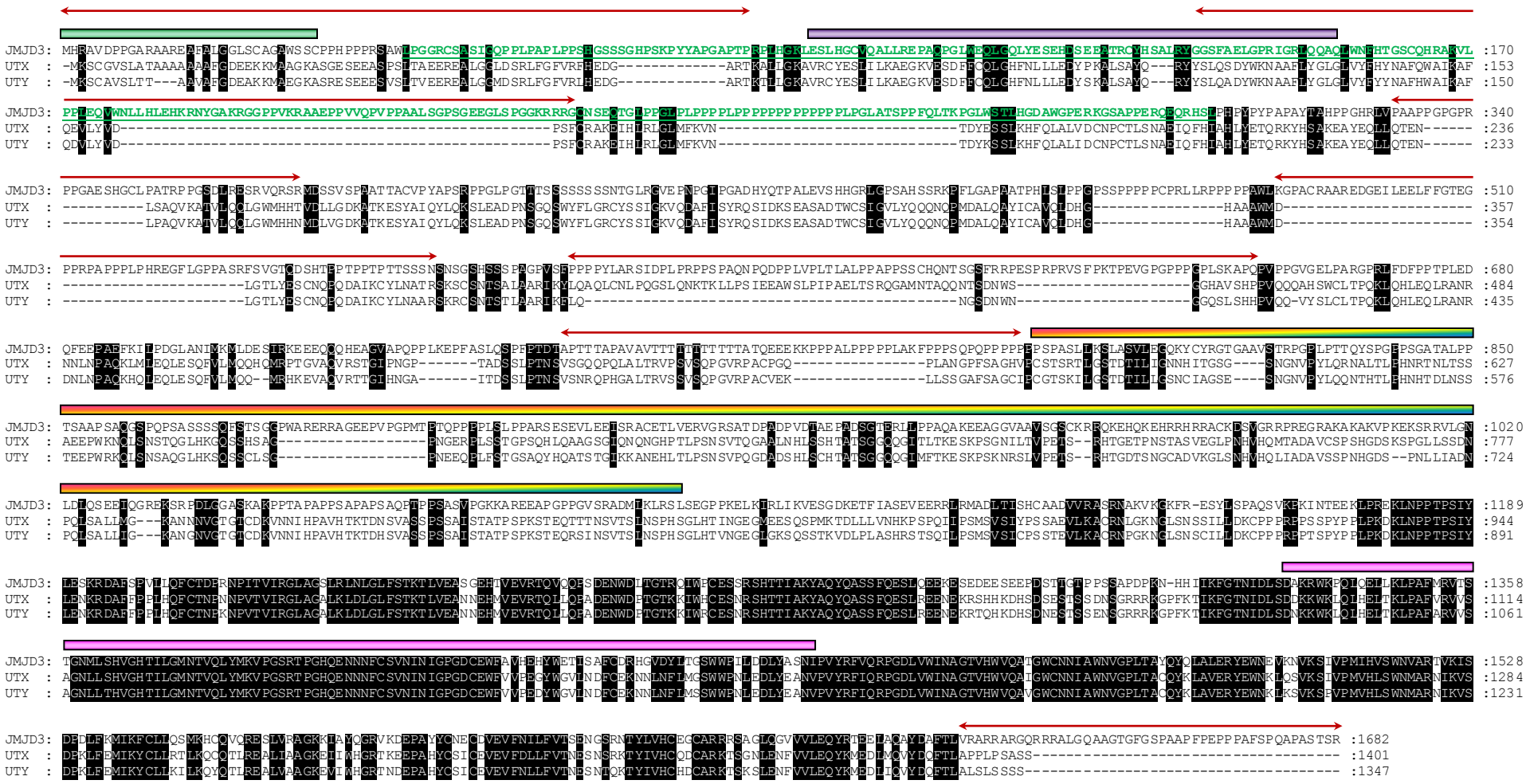

Fig 6.3 Alignment of amino acid sequences of JMJD3, UTX and UTY

The green, underlined sequence is the JMJD3 protein region used on protein array experiments that shares little homology with UTX and UTY. The rainbow box above the alignment represents the mAb generated by Agger et al. (2009). The red arrows denote ideal JMJD3 regions for antibody recognition to avoid cross-reactivity with UTX or UTY. JMJD3 has a JmjC domain at the C-terminus (represented by pink box), sharing a high consensus with the JmjC domain of both UTX and UTY. The green and purple boxes represent Prokar lipoprotein and tetratricopeptide-like helical domain, respectively. Domain predictions carried out using InterPro (http://www.ebi.ac.uk/interpro/)

6.3 ATTEMPTS TO VALIDATE JMJD3 AS A LYMPHOMA AUTOANTIGEN

Problems with the stability of the JMJD3 protein were encountered when analysing antibody reactivity by Western blotting. Anti-JMJD3 pAb "N-term" (Abgent) was initially able to weakly detect the full-length JMJD3 protein (predicted molecular weight: 180kDa) by Western blotting, but its expression in subsequent experiments from frozen, stored lysates could not be detected by using the same pAb (Fig 6.4). Blotting of JMJD3-transfected 293T cell lysates with another anti-JMJD3 pAb (Abcam) also failed to detect the JMJD3 protein. Although there is a strong band specifically in the transfected cells (at just under 150kDa) with this second antibody, this was not detected with the Myc antibody and thus is unlikely to represent recombinant JMJD3. Furthermore, a repeat transfection also failed to generate detectable JMJD3 protein (data not shown).

The detection of multiple bands in the initial blotting experiment with the Myc tag antibody and the failure of this antibody to detect proteins in subsequent blotting of the same samples suggest that the JMJD3 protein may well be unstable. The additional bands observed in untransfected COS-1 cells might represent detection of endogenous JMJD3 proteins. However, no immunolabelling of untransfected COS-1 cells was observed with these antibodies. Thus, a more likely alternative is that the antibodies are not sufficiently specific for JMJD3 and that they also detect other proteins in this application.

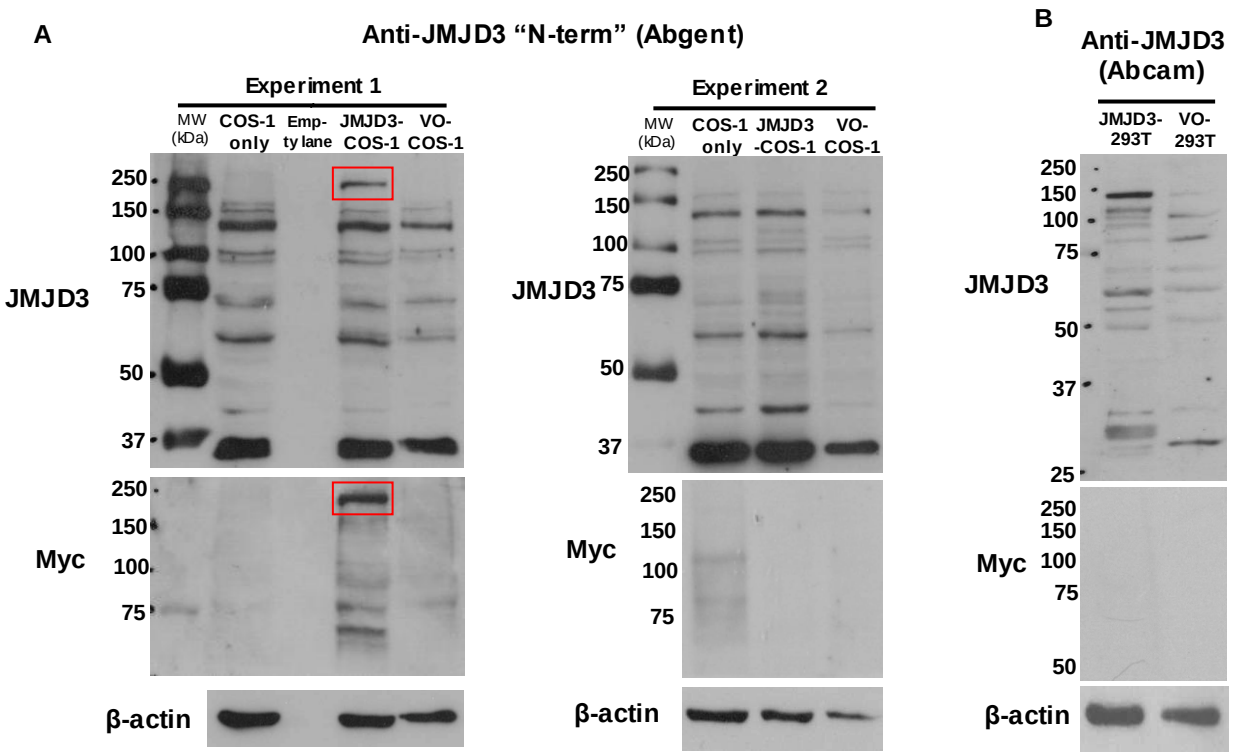

Fig 6.4 Immunoblotting of JMJD3 transfectants by two JMJD3 polyclonal antibodies

(A) The same JMJD3-transfected COS-1 cells were used for immunoblotting in Experiment 1 and Experiment 2. No JMJD3 protein was detected in Experiment 2 using either the anti-JMJD3 "N-term" (Abgent) or the anti-Myc tag antibody. The red box denotes the detected JMJD3 full-length protein.

(B) Blotting of JMJD3 or vector-only transfected 293T cells with another pAb, anti-JMJD3 (Abcam), also failed to detect the JMJD3 protein, and lack of JMJD3 expression was confirmed using the anti-Myc tag antibody.

Key: JMJD3-COS-1: JMJD3-transfected COS-1 cells; VO-COS-1: Vector-only-trasnfected COS-1 cells; JMJD3-293T: JMJD3-transfected 293T cells; VO-293T: Vector-only-transfected 293T cells

The group in Dublin also encountered stability issues with this antigen while trying to obtain purified protein. As the commercial JMJD3 and Myc antibodies were barely able to detect the recombinant JMJD3 protein, it seemed unlikely that detection using patients' sera would be successful. In our experience, blotting with patients' sera is rarely as effective as

that with a specific antibody (lower antibody titres and higher background signals from other antibodies in the sera can cause significant technical difficulties) even when high-level stable expression of the target antigen is achievable. Based on these data, no further attempt was made to use JMJD3 transfectants to evaluate the potential immune response to this antigen in patients' sera.

6.4 *JMJD3* mRNA EXPRESSION STUDIES

JMJD3 mRNA expression studies were performed to elucidate whether this antigen could be pursued further. qRT-PCR studies on a panel of lymphoma cell lines (n = 16), myeloma cell lines (n = 2), normal subset of cells (n = 7) and "non-cancer" tissues (n = 4) showed that *JMJD3* had lower levels in ABC-DLBCL compared to IgM-activated normal peripheral B cells population. *JMJD3* levels showed a trend towards higher expression in GC-DLBCL than ABC-DLBCL cell lines (p = 0.08), and its expression in GC-DLBCL did not show difference from $CD19^+$-purified peripheral B cells or the GC subset of normal B cells (GCB) (Fig 6.5).

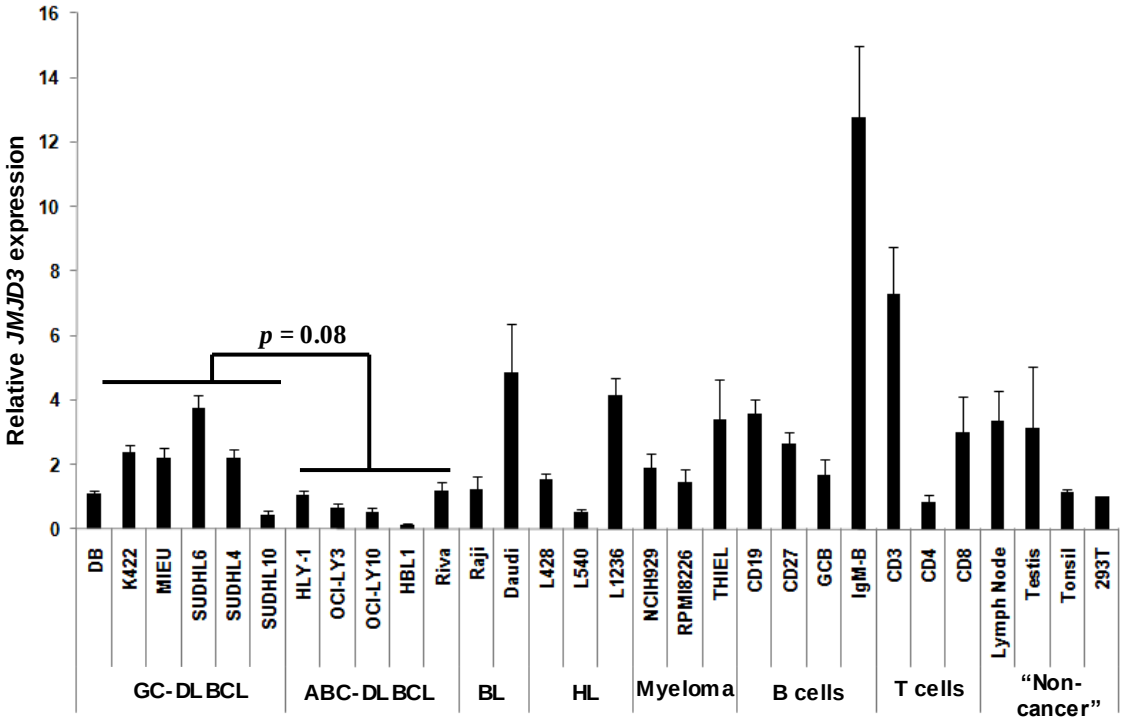

Fig 6.5 *JMJD3* mRNA expression levels in a panel of cell lines

JMJD3 transcript levels were determined in cell lines derived from haematological malignancies, normal lymphocyte subpopulations and normal tissues. CD19, CD27, GCB, and IgM-B denote CD19$^+$, CD27$^+$, germinal centre, and IgM-stimulated B cells, respectively, derived from peripheral blood by MACS magnetic separation (Miltenyi Biotech). qRT-PCR amplification was performed in triplicate using TaqMan pre-verified probes to amplify JMJD3 (TaqMan probe: Hs00389738_m1). Gene expression was normalised according to expression of TBP (TaqMan probe: 4326322E) and expressed relative to levels in 293T using the formula $2^{-\Delta\Delta Ct}$.

High *JMJD3* expression in IgM-stimulated normal B-cell subsets is of interest in view of the GEP data by Basso *et al.* (2005) of stimulated Ramos (BL cell line) cells. In this experiment, Ramos cells transduced with a retroviral expression vector (PINCO) carrying cDNA encoding enhanced green fluorescence protein (EGFP) were co-cultivated with NIH3T3 [stably expressing CD40L or "CD40(+)ve"] or NIH3T3 [empty vector or "CD40(-)ve"], before stimulation with antibodies were performed. Mining of *JMJD3* expression

values from Oncomine in that particular dataset showed *JMJD3* upregulation upon stimulation of Ramos cells alone with anti-CD40 antibodies, upregulated in "CD40(+)ve" versus "CD40(-)ve", and also upregulation upon stimulation of "CD40(+)ve" cells with anti-IgM antibodies (Basso *et al.*, 2005) (Fig 6.6).

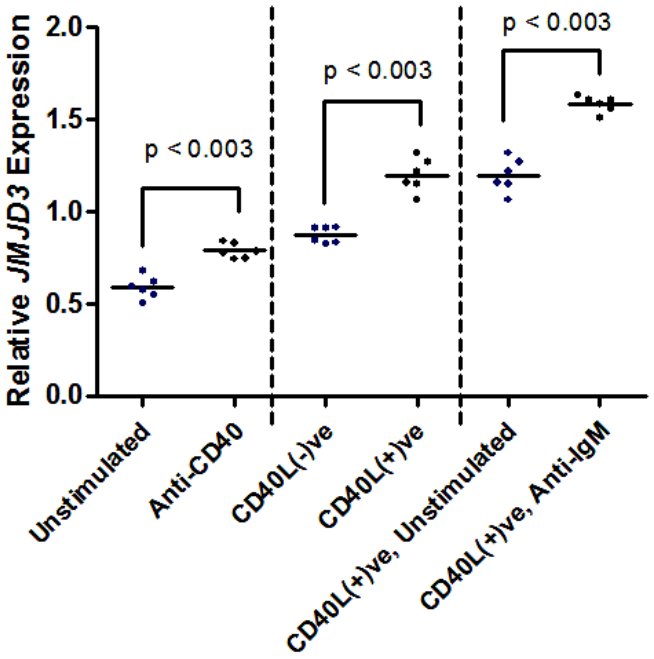

Fig 6.6 *JMJD3* upregulation in Ramos-stimulated cells

Upregulation of JMJD3 expression was observed upon stimulation with anti-CD40 or anti-IgM antibodies, which might be of interest with regard to the high JMJD3 levels in our IgM-stimulated peripheral B cells.

DISCUSSION

COS-1 or 293T cells transfected with a full-length *JMJD3* plasmid construct were used to successfully validate the ability of three commercial JMJD3 antibodies to detect this protein by IHC. These antibodies recognised a formalin-resistant epitope, technically enabling future immunolabelling studies. However, this requires further validation of their JMJD3 specificity and ability to detect the endogenous protein.

Western blotting data demonstrated, in one experiment, the recognition of multiple Myc-tagged JMJD3 species in transfected COS-1 cells. However, difficulties with JMJD3 protein expression and/or stability were encountered in subsequent experiments. Immunoblotting with frozen, stored lysates of JMJD3-transfected cells with two JMJD3 antibodies and the Myc-tag antibody failed to detect the JMJD3 protein, suggesting that the protein might be unstable or degraded after freeze-thaw cycles. Furthermore, the strong bands observed in untransfected COS-1 cells (which were unlabelled by immunohistochemistry with the same antibodies) suggested that the JMJD3 antibodies might not be sufficiently specific to detect the endogenous JMJD3 protein. Because of these technical difficulties with reagents, neither the immune response to JMJD3 nor its patterns of endogenous protein expression were pursued further.

qRT-PCR analysis was performed to investigate the expression of *JMJD3* in lymphoma cell lines and normal lymphocytes to ascertain whether this molecule should be further pursued, despite the technical difficulties with existing reagents. This demonstrated that *JMJD3* was expressed in GC-DLBCL, which is consistent with the high frequency of sera from GC-derived DLBCL that contained antibodies to this protein.

The high level of *JMJD3* expression in normal activated B cells is an interesting contrast to the low levels observed in ABC-DLBCL cell lines, raising the possibility that JMJD3 expression in ABC-DLBCL may be regulated by a disease-related process rather than common COO. This observation is consistent with the findings of Agger *et al.* (2009) who reported that JMJD3 is upregulated by the MAPK signalling pathway. This pathway can be activated via BCR signalling triggered by the stimulation of exogenous antigens. Agger *et al.* also suggested that JMJD3 might be under-expressed in lymphomas in comparison with

normal B cells, and that downregulation of JMJD3 is sufficient to immortalise primary mouse embryonic fibroblasts, suggesting that *JMJD3* could act as a tumour suppressor gene. In addition, constitutive activation of NF-κB has been shown in a few subtypes of lymphoma, particularly in ABC-DLBCL (Chng *et al.*, 2009), and *Jmjd3* is directly upregulated by NF-κB in mouse (De Santa *et al.*, 2007).

The future avenues for studies on JMJD3, as well as HIP1R, are laid out in the next, final chapter.

CHAPTER 7
CONCLUSIONS AND FUTURE DIRECTIONS

7.1 CONCLUSIONS

7.1.1 Lymphoma-associated antigens

The initial aim of my project was to independently validate the humoural immune response to selected lymphoma antigens identified by the group in Dublin, and to prioritise a smaller number of antigens for further validation and characterisation. Our group were particularly interested in identifying novel lymphoma biomarkers that had the potential to play a functional role in disease pathogenesis.

Attempts to validate the 'short' list of 35 antigens (from protein array screening) by ELISA were unsuccessful. We believe this largely reflects the differences between the proteins present in *E. coli* lysates that were used to construct protein arrays and the recombinant proteins purified by His-tag column used for the ELISA screening. Thus, further development of protein microchips for non-invasive diagnosis could not be implemented at this stage due to the antigen validation necessary to support this. An alternative validation approach to take this further would perhaps be the generation of a focussed protein array for the 35 antigens. Screening with much larger number of serum samples, which is essential to validate both the frequency and disease specificity of recognition by the sera from both lymphoma patients and normal individuals, could then be pursued.

Nonetheless, HIP1R was successfully validated by Western blotting as a B-NHL autoantigen. We conclude that the recognition of a full-length mammalian expressed recombinant protein by the B-NHL patients' sera was specific to HIP1R, and not HIP1. This

contrasts with the findings by Bradley *et al.* (2007) who reported HIP1 as a lymphoma autoantigen using a bacterially expressed HIP1 protein sharing significant sequence identity with HIP1R. The antigen recognition frequency is consistent with our observation that HIP1R was more widely and highly expressed than HIP1 in B-NHL cell lines, and with a report by Rao *et al.* (2002) that showed lack of HIP1 expression in lymphomas. Validation of JMJD3 was impeded by the apparent instability of recombinant JMJD3 protein which could potentially be circumvented in the future by using fresh cell lysates transfected with *JMJD3* plasmid without undergoing any freeze-thaw for immunoblotting with patients' sera.

7.1.2 HIP1R as a DLBCL subtyping marker

The international prognostic index (IPI) proposed nearly two decades ago remains the clinical measure used to predict outcome for DLBCL patients (Flowers *et al.*, 2010). However, more than 25% of low-risk patients defined by IPI have less than 5-year OS (Westin and Fayad, 2009). The revised IPI (R-IPI) proposed as a better prognostic index for R-CHOP-treated patients (Sehn *et al.*, 2007) was contradicted by other studies that showed improved outcomes in all IPI categories in R-CHOP-treated patients (Feugier *et al.*, 2005; Pfreundschuh *et al.*, 2006). COO subtyping of DLBCL patients represents an alternative approach to identify clinically-relevant subgroups using biological rather than purely clinical data. Identification of prognostic markers related to the biologic mechanisms of disease progression could also enable the design of novel therapies.

In this study, HIP1R expression distinguished GC- from ABC-DLBCL at both mRNA and protein levels. This might explain the higher frequency of HIP1R antigen recognition by GC-DLBCL patients' immune response screened by protein arrays, as their tumours generally expressed higher levels of the HIP1R antigen. Data from immunolabelling DLBCL

biopsies also raises the possibility that some GC-DLBCL (at least 4 patients) but no NGC-DLBCL, may actually have elevated levels of qualitative HIP1R protein expression compared to normal mantle zone B cells. A report identifying statistically significant (p = 0.003) amplification of the 12q24 region including the *HIP1R* locus in GC-DLBCL (Lenz *et al.*, 2008c) is particularly relevant to this finding. Copy numbers changes and/or mutations of the *HIP1R* locus in DLBCL should be further investigated due to their potential causal association with disease pathogenesis.

There is insufficient data concerning the role of HIP1R in B cells to understand the biological basis for its potential upregulation versus downregulation in different DLBCL subtypes. The identification of slightly different molecular weight of HIP1R proteins in B-NHL cell lines, which may or may not correlate with differentially phosphorylated HIP1R proteins that have been reported (Repass *et al.*, 2007; Brady *et al.*, 2010), could be significant. Interestingly, phosphorylated Hip1r in *Dictyostelium* cells localises to puncta on the plasma membrane and this is dependent on the presence of another clathrin-associated protein, epsin (Repass *et al.*, 2007). Furthermore, this epsin-dependent membrane recruitment and phosphorylation of Hip1r is also required for normal actin and clathrin dynamics at the plasma membrane. Antibodies that distinguish the phosphorylated form of HIP1R would be helpful to enable further characterisation of the importance of this post-translational modification in lymphoma.

Another distinct possibility reflects the multiple roles of HIP1R. In addition to its role in regulating cell surface components, HIP1R has also been implicated as a BCL2 family interacting protein that is involved in the intrinsic cell death pathway (Kim *et al.*, 2009). Thus HIP1R might have distinctly different roles in DLBCL subtypes.

Whether HIP1R will be used in distinguishing GC- versus ABC-DLBCL in routine pathological diagnosis is difficult to assess based on the propensity of other well-documented subtyping or prognostic markers utilised in the Hans *et al.* (2004) or the increased accuracy of Choi *et al.* (2009) algorithm, which has achieved 93% concurrence with GEP. However, the commercially available anti-HIP1R-44 mAb used in this study was validated for IHC on FFPE sections with little background immunostaining, and without cross-reactivity with the highly homologous HIP1 protein. This suggests that HIP1R could be another candidate subtyping marker for improving the concordance with GEP should the need arise in the future. Another possibility is that HIP1R may represent a marker of altered expression levels and/or stability of BCR components. As discussed in later sections this becomes particularly relevant when considering markers of likely response to DLBCL therapies that target the BCR.

The smaller isoforms of the FOXP1 transcription factor are putative regulators of *HIP1R* transcriptional repression in ABC-DLBCL. Similarly to HIP1R, $FOXP1_S$ is also induced upon activation of peripheral blood B cells with anti-IgM or IL2/SAC (Brown *et al.*, 2008). This suggests that the regulation of HIP1R expression by $FOXP1_S$ might be a disease-associated event in ABC-DLBCL (as HIP1R levels are high in activated peripheral blood B cells and low in ABC-DLBCL, while $FOXP1_S$ isoforms are abundant in both), an avenue of research discussed in the "Future Directions" section. If FOXP1 isoforms have different activities in normal and malignant activated B cells then investigating their regulation of *HIP1R* transcription might shed some light on the mechanism. Furthermore, reciprocal expression of HIP1R and FOXP1 might be useful for identifying this functional relationship in clinical samples.

7.1.3 Functional roles of HIP1R in normal and malignant B cells

The ability of endogenous HIP1R expression to downregulate surface BCR levels, particularly CD79b in DLBCL cells, identified in this thesis provides a rational explanation for HIP1R downregulation in B-cell lymphoma. The majority of normal and malignant B cells remain dependent on antigenic stimulation for both survival and proliferation (Küppers, 2005). Thus it is possible that a reduction in HIP1R expression could provide B cells with a selective advantage that might contribute to clonal B-cell expansion.

There are several examples in the literature that illustrate the importance of the BCR and in particular CD79b. In murine B cells, mutations in the CD79b ITAM tyrosine residues lead to exaggerated BCR signalling that was achieved by increased surface BCR levels derived from inhibiting receptor internalisation (Gazumyan *et al.*, 2006). *CD79b* mutations are also implicated in increasing surface BCR levels in ABC-DLBCL cells to maintain the chronic active BCR signalling that is essential for their survival (Davis *et al.*, 2010). However, mutation of *CD79b* occurs in HBL1 and TMD8 but not in OCI-LY3, and yet all three DLBCL cell lines have low levels of *HIP1R* [(TMD8 was shown to have low *HIP1R* mRNA levels by Davis *et al.* (2010)].

The presence of downregulated HIP1R in the presence of *CD79b* mutation suggests that these could make different contributions to the malignant phenotype by conferring distinct selective advantages. One such possibility, which is supported by the existing literature (Engqvist-Goldstein *et al.*, 2001; Hyun *et al.*, 2004b), is that the BCR is not the only cell surface receptor that is affected by HIP1R. Another possible explanation is that ABC-DLBCL with mutated *CD79b* still requires low levels of HIP1R expression to minimise BCR internalisation. Since downregulation of HIP1R expression in ABC-DLBCL is

widespread including ABC-DLBCL with mutated *CD79b*, we speculate that pre-malignant clones with decreased HIP1R expression might be selected early in the genesis of ABC-DLBCL through increased BCR signalling.

Another important consideration is the biological significance of the upregulation of HIP1R expression that occurs on normal B-cell activation. Because of the relatively low numbers of human B cells available for study, experiments were limited and were performed only at the later time points (44 h) used for previous studies. However, in the future it will be key to study earlier time points (e.g. < 1 h) to determine both the kinetics and magnitude of altered levels of HIP1R expression in response to BCR stimulation. It would be interesting to compare B-cell activation in Hip1r deficient B cells from *Hip1r* knockout mice to those in normal B cells to help determine the role of HIP1R in B-cell activation.

In normal B-cell subsets, HIP1R is highly expressed in mature B cells ($PAX5^+$ or $CD20^+$ B cells), GC B cells ($BCL6^+$), but rarely expressed in plasma cells ($MUM1^+$, $XBP1^+$, $CD38^+$ or $CD138^+$). The function(s) of HIP1R in normal B cells, and reasons for the absence of HIP1R expression in plasma cells were beyond the scope of this DPhil project. It is possible that the phenotypical changes observed in B-NHL cells upon knockdown of HIP1R might represent the generic function of HIP1R in normal B cell homeostasis i.e. maintenance of surface BCR levels.

In plasma cells, XBP1 induces the expression of target genes involved in trafficking of immunoglobulin molecules from the Golgi network to the plasma membrane (Shaffer *et al.*, 2004), leading to immunoglobulin secretion (Tirosh *et al.*, 2005; Shapiro-Shelef and Calame, 2005). HIP1R has been implicated in the biogenesis of lysosomes from trans-Golgi

network (TGN) (Carreno *et al.*, 2004) and there are strong similarities between the clathrin-mediated endocytic machinery at both the plasma membrane and TGN (reviewed by McNiven and Thompson, 2006). Whether HIP1R might negatively regulate the secretion of immunoglobulin from TGN to the plasma membrane by targeting the transport of immunoglobulin to lysosomes, providing an explanation for HIP1R downregulation in plasma cells, remains to be defined.

7.1.4 Potential associations of HIP1R with DLBCL therapies

Long-term survival still eludes many DLBCL patients who relapse early following first-line R-CHOP regimen. These patients often respond poorly to second-line rituximab-containing regimens (e.g. R-ICE or R-DHAP) even when bolstered with high-dose therapy and autologous stem cell transplantation (Gisselbrecht *et al.*, 2010). More effective novel therapies are required to treat these patients (Flowers *et al.*, 2010). Recent reports have shown that targeting BCR components or signalling molecules is a novel therapeutic approach.

There are several lines of evidence implicating BCR components/signalling as an attractive therapeutic target: 1) Inhibition of BCR expression disrupts the proliferation and survival of B-NHL cells (Gururajan *et al.*, 2006; Davis *et al.*, 2010); 2) Inhibition of Syk, the tyrosine kinase that binds phosphorylated-CD79a/b to trigger downstream signalling, kills B-NHL cell lines (Young *et al.*, 2009) and has pro-survival effects in DLBCL and CLL patients (Friedberg *et al.*, 2010); 3) Targeting BCR components could enhance the release of drug from antibody-drug conjugates (ADC) because CD79a/b is trafficked to lysosomes for antigen presentation (Drake *et al.*, 1999). In addition, targeting other receptors of B cells is utilised for treatments of autoimmune diseases, such as anti-CD22 epratuzumab in Sjögren's syndrome and systemic lupus erythematosus (reviewed by Goldenberg, 2006).

Development of ADC targeting the clonal surface IgM on tumour cells is challenging as the recognition of unique epitopes that do not cross-react with circulating IgM are close to the cell surface and may be inaccessible to large antibody molecules (Mallikaratchy *et al.*, 2010). CD79b represents an attractive target as it is not released for circulation in peripheral blood, and it is expressed in almost all types of B-NHL (Cabezudo *et al.*, 1999; Olejniczak *et al.*, 2006). Also, ADC targeting CD79b have been well-tolerated, showing limited toxicity in the treatment of B-NHL patients (Zheng *et al.*, 2009). Indeed, ADCs targeting CD79b killed B-NHL cell lines *in vitro* and low doses in xenograft models resulted in regression of FL, MCL and BL *in vivo*: anti-CD79b ADCs being more effective than anti-CD79a ADCs (Polson *et al.*, 2007). Anti-CD79b ADCs were internalised in GC-DLBCL cells to lysosome-like compartment, enhancing the release of active metabolites from ADC.

It is likely that HIP1R might make some contribution to the ADC internalisation observed by Polson *et al.*, since it is commonly expressed in GC-DLBCL and our studies showed that HIP1R expression affects surface CD79b levels. If restoration of HIP1R expression in ABC-DLBCL cells leads to cell death, reduction of BCR signalling via reduced surface CD79b levels could be a mechanism attributing to the detrimental effects.

In addition, it is possible that restoration of HIP1R expression in B-NHL could increase the occurrence of surface CD79b internalisation to lysosomes, enhancing the effectiveness of drug release in lymphoma cells. This is consistent with the findings that HIP1R has an essential role in enabling the production of lysosomes important in degrading ligand-activated receptors (Carreno *et al.*, 2004). This evidence suggests avenues of further research into the likelihood of enhancing drug release by altering the expression of HIP1R.

7.2 FUTURE DIRECTIONS

7.2.1 Restoration of HIP1R expression in ABC-DLBCL cells

In this study, overexpression of HIP1R in ABC-DLBCL could not be achieved using the current lentiviral-mediated expression system. Retroviral-mediated transduction has been successfully used to infect several B-NHL cell lines and this could eventually be adopted as an alternative strategy (Basso *et al.*, 2004; Ngo *et al.*, 2006; Davis *et al.*, 2010). However, the next step would be utilisation of inducible lentiviral expression systems such as a tetracycline-repressor (TETR) system. This could be an ideal approach to introducing genes with detrimental effects on cancer cell growth because it is challenging to establish stable transformants expressing such genes (Kitamura *et al.*, 2003). Inducible expression systems allow the control of gene expression activation by culturing the infected cells in the presence or absence of appropriate antibiotics. Thus, the stable cell line is generated without any contribution of the transgene to the cell phenotype.

Inducible lentiviral expression can be achieved by co-transfecting the DLBCL cell lines with another virus containing the plasmid conferring tetracycline regulation. This is preferable to the published retroviral system, which would require obtaining ABC-DLBCL cell lines already expressing the ecotropic retroviral receptor from other research groups or to generate these cells within our laboratory when necessary. These cells expressing the retroviral receptor are required for the infection with an ecotropic retrovirus expressing TETR. After infection of B-NHL cells and selection of clones expressing TETR, induction of HIP1R expression is achieved by addition of certain antibiotics such as doxycycline. Downstream experiments on inducing HIP1R expression primarily include cell viability by MTS assay, or staining with Annexin V to investigate the occurrence of apoptosis. These cells would also be used to examine changes in surface BCR levels.

7.2.2 Mechanism of regulation of HIP1R expression

Significant increase of *HIP1R* levels in FOXP1-depleted ABC-DLBCL cells warrants the elucidation of putative direct binding capabilities of $FOXP1_S$ (rather than $FOXP1_{FL}$ protein) to the *HIP1R* promoter, *in vivo*, in ABC- and GC-DLBCL cell lines using chromatin immunoprecipitation. Luciferase reporter and/or EMSA assays would then confirm that mutation of the forkhead site abrogated FOXP1 binding. Another ongoing project in the laboratory is the silencing of IRF4 expression by siRNA transient system. HIP1R levels could also be examined in si*IRF4*-treated ABC-DLBCL cells to elucidate whether IRF4 also has the potential to regulate *HIP1R* expression. FOXP1 silencing did not restore *HIP1R* levels to those in mature B cells and thus, there is scope for more than one regulator.

7.2.3 Mechanism of HIP1R regulating BCR

The ability of HIP1R to regulate surface BCR levels could be further consolidated by studying putative mechanisms rendered by HIP1R in promoting BCR internalisation. To recapitulate, there are several lines of evidence indicating that HIP1R might be involved in the endocytic machinery controlling surface BCR: 1) Regulation of surface BCR levels involves mechanisms rendered by clathrin (Stoddart *et al.*, 2002) and the actin cytoskeleton (Onabajo *et al.*, 2008; Sharma *et al.*, 2009); 2) HIP1R is able to link the interaction of clathrin with the actin cytoskeleton (Engqvist-Goldstein *et al.*, 1999; Poupon *et al.*, 2008); 3) HIP1R binds to cortactin to control actin filament elongation for proper formation of clathrin coat surrounding receptors (Le Clainche *et al.*, 2007); 4) Cortactin is expressed in normal B cells from tonsil (Muzio *et al.*, 2007), while its expression is absent in T cells (Gomez *et al.*, 2006), correlating the expression patterns of HIP1R in normal B and T lymphocytes.

We propose that formation of actin filaments, which provides mechanical force for internalisation of BCR components, requires association of clathrin coat to the actin cytoskeleton by HIP1R. Also, binding of HIP1R with cortactin controls the formation of actin filaments surrounding the clathrin coat (Fig 7.1). This would first be investigated by immunofluorescent labelling of clathrin or actin in si*HIP1R* cells to observe whether mislocalisation of these proteins could be caused by depletion of HIP1R. This could suggest whether the association of clathrin coat to actin cytoskeleton is disrupted by the absence of HIP1R. This is further explored by co-immunoprecipitation of HIP1R with clathrin, actin or cortactin to indicate its capability of binding these proteins in B cells. This could suggest the mechanism of BCR internalisation involving HIP1R-clathrin-actin-cortactin complexes.

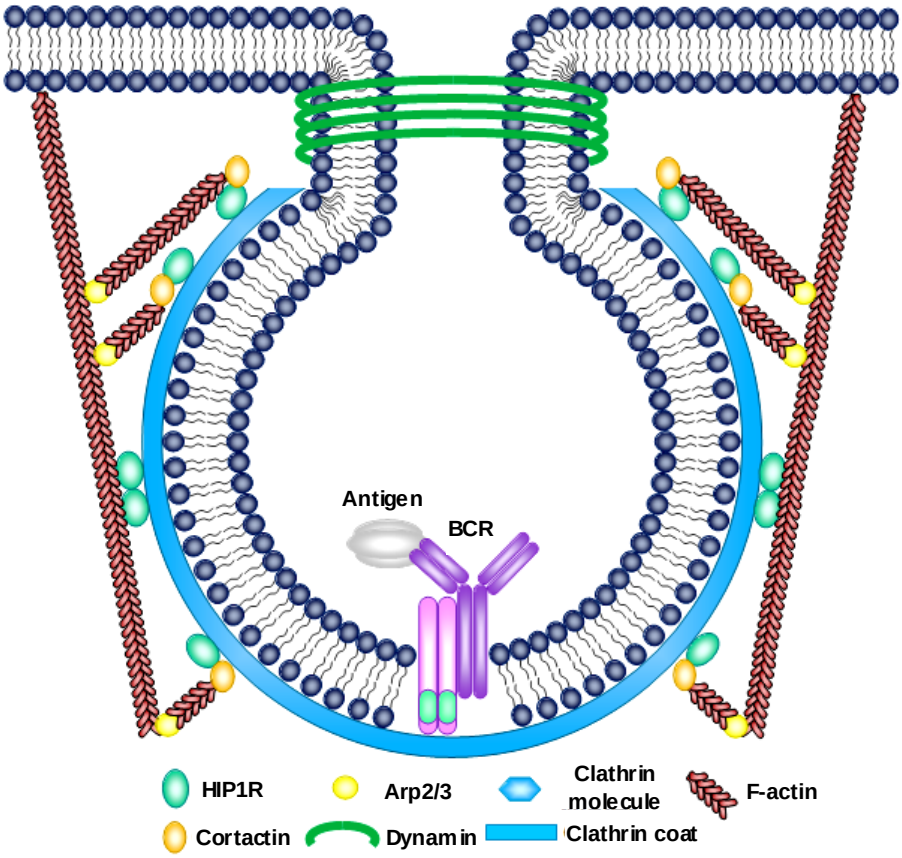

Fig 7.1 Proposed mechanisms of HIP1R regulating surface BCR internalisation

HIP1R might regulate the internalisation of BCR by facilitating the proper formation of clathrin coat surrounding BCR by linking clathrin to actin cytoskeleton, providing the mechanical force for internalisation before final pinching off by dynamin molecule.

HIP1R-cortactin complex might control the formation (or elongation) of F-actin surrounding the clathrin coat, presumably to provide optimal mechanical force for BCR internalisation. Arp2/3 facilitates the polymerisation of actin filaments (Suetsugu et al., 2002).

To the best of our knowledge, this is the first study directly implicating HIP1R in the context of cancer and association with its putative functions. This is because numerous other studies focus on the fundamental role of HIP1R and its involvement in the complex endocytic machinery (reviewed by Gottfried *et al.*, 2010). The ability of HIP1R to regulate the levels of other receptors such as EGFR and transferrin (Engqvist-Goldstein *et al.*, 2001; Hyun *et al.*, 2004b) provide further avenues of research on HIP1R in other cancer types that depend on signalling rendered by these receptors. In addition, as HIP1R is expressed in numerous different human tissues, the likelihood of HIP1R expression alteration in the genesis of common malignancies has the potential to be widespread.

This thesis has identified prospects for HIP1R in assessing the subtyping of DLBCL patients. If its role in regulating surface BCR receptor levels is substantiated and/or HIP1R has a role in regulating DLBCL survival, then HIP1R has the potential to generate and/or assist novel therapeutic avenues targeting BCR components in DLBCL. In terms of identifying a molecule with a potentially causal role in disease pathogenesis, this project has been successful. Future work is now essential to fully determine the significance of HIP1R in the pathogenesis of B-NHL.

REFERENCES

Abolhassani N, Iyama T, Tsuchimoto D, *et al.* NUDT16 and ITPA play a dual protective role in maintaining chromosome stability and cell growth by eliminating dIDP/IDP and dITP/ITP from nucleotide pools in mammals. *Nucleic Acids Res* 2010;1-13

Agger K, Closs PAC, Christensen J, *et al.* UTX and JMJD3 are histone H3K27 demethylases involved in HOX gene regulation and development. *Nature* 2007;449:731-734

Agger K, Cloos PAC, Rudkjær L, *et al.* The H3K27me3 demethylase JMJD3 contributes to the activation of the *INK4A-ARF* locus in response to oncogene- and stress-induced senescence. *Gene Dev* 2009;23:1171-1176

Ait-Tahar K, Damm-Welk C, Burkhardt B, *et al.* Correlation of the autoantibody response to the ALK oncoantigen in pediatric anaplastic lymphoma kinase-positive anaplastic large cell lymphoma with tumor dissemination and relapse risk. *Blood* 2010;115:3314-3319

Al-Tourah AJ, Gill KK, Chhanabhai M, *et al.* Population-based analysis of incidence and outcome of transformed non-Hodgkin's lymphoma. *J Clin Oncol* 2008;26:5165-5169

Alberts B, Bray D, Lewis J, *et al.* Molecular biology of the cell. (4th Ed) 2002.

Alizadeh AA, Eisen MB, Davis RE, *et al.* Distinct types of diffuse large B-cell lymphoma identified by gene expression profiling. *Nature* 2000;403:503-511.

Alizadeh AA, Gentles AJ, Lossos IS, Levy R. Molecular outcome prediction in diffuse large-B-cell lymphoma. *New Engl J Med* 2009;360:2794-2795

Allan JM, Sunter NJ, Bailey JR, *et al.* Variant IRF4/MUM1 associates with CD38 status and treatment-free survival in chronic lymphocytic leukaemia. *Leukemia* 2010;24:877-881

Ambros V. The functions of animal microRNAs. *Nature* 2004;431:350-355

Amin ND, Zheng YL, Kesavapany S, *et al.* Cyclin-dependent kinase 5 phosphorylation of human septin SEPT5 (hCDCrel-1) modulates exocytosis. *J Neurosci* 2008;28:3631-3643

Andersen K, Smith-Sørensen B, Pedersen KB, *et al.* Interferon-gamma suppresses S100A4 transcription independently of apoptosis or cell cycle arrest. *Br J Cancer* 2003;88:1995-2001

Anderson KS, Ramachandran N, Wong J, *et al.* Application of protein microarrays for multiplexed detection of antibodies to tumor antigens in breast cancer. *J Proteome Res* 2008;7:1490-1499

Angers S, Thorpe CJ, Biechele TL, *et al.* The KLHL12-Cullin-3 ubiquitin ligase negatively regulates the Wnt-β-catenin pathway by targeting Dishevelled for degradation. *Nat Cell Biol* 2006;8:348-357

Armitage JO, Weisenburger DD. New approach to classifying non-Hodgkin's lymphomas: clinical features of the major histologic subtypes. Non-Hodgkin's Lymphoma Classification Project. *J Clin Oncol* 1998;16:2780-2795

Atanackovic D, Arfsten J, Cao Y, *et al*. Cancer-testis antigens are commonly expressed in multiple myeloma and induce systemic immunity following allogeneic stem cell transplantation. *Blood* 2007;109;1103-1112

Baldwin RW. Tumour-specific immunity against spontaneous rat tumours. *Int J Cancer* 1966;1:257-264.

Ballester B, Ramuz O, Gisselbrecht C, *et al*. Gene expression profiling identifies molecular subgroups among nodal peripheral T-cell lymphomas. *Oncogene* 2006;25;1560-1570

Banham AH, Connors JM, Brown PJ, *et al*. Expression of the FOXP1 transcription factor is strongly associated with inferior survival in patients with diffuse large B-cell lymphoma. *Clin Cancer Res* 2005;11:1065-1072

Bannister AJ, Schneider R, Kouzarides T. Histone methylation: dynamic or static? *Cell* 2002;109:801-806

Barna M, Pusic A, Zollo O, *et al*. Suppression of Myc oncogenic activity by ribosomal protein haploinsufficiency. *Nature* 2008;456:971-977

Baron BW, Nucifora G, McCabe N, *et al*. Identification of the gene associated with the recurring chromosomal translocations t(3;14)(q27;q32) and t(3;22)(q27;q11) in B-cell lymphomas. *Proc Natl Acad Sci U S A* 1993;90:5262–5266

Barradas M, Anderton E, Acosta JC, *et al*. Histone demethylase JMJD3 contributes to epigenetic control of INK4a/ARF by oncogenic RAS. *Genes Dev* 2009;23:1177-1182

Bartel DP. MicroRNAs: target recognition and regulatory functions. *Cell* 2009;136:215-233

Basso K, Margolin AA, Stolovitzky G, *et al*. Reverse engineering of regulatory networks in human B cells. *Nat Genet* 2005;37:382-390

Bea S, Zettl A, Wright G, *et al*. Diffuse large B-cell lymphoma subgroups have distinct genetic profiles that influence tumor biology and improve gene-expression-based survival prediction. *Blood* 2005;106:3183-3190.

Beites CL, Xie H, Bowser R, Trimble WS. The septin CDCrel-1 binds syntaxin and inhibits exocytosis. *Nat Neurosci* 1999;2:434-439

Bell R, Petticrew M, Sheldon T. The performance of screening tests for ovarian cancer: results of a systematic review. *Br J Obstet Gynaecol* 1998;105:1136-1147

Bende RJ, Smit LA, van Noesel CJ. Molecular pathways in follicular lymphoma. *Leukemia* 2007;21:18-29

Bernstein SH, Burack WR. The incidence, natural history, biology, and treatment of transformed lymphomas. *Hematology Am Soc Hematol Educ Program*. 2009:532-541

Bi Q, Tan T, Xiang X, *et al*. Detection of breast cancer-related antigens through cDNA phage-displayed protein microarray. *Biol Chem* 2010;391:831-835

Bibb JA, Yan Z, Svenningsson P, *et al.* Severe deficiencies in dopamine signaling in presymptomatic Huntington's disease mice. *Proc Natl Acad Sci U S A* 2000;97;6809-6814

Bitoun M, Maugenre S, Jeannet PY, *et al.* Mutations in dynamin 2 cause dominant centronuclear myopathy. *Nat Genet* 2004;37:1207-1209

Bitoun M, Durieux AC, Prudhon B, *et al.* Dynamin 2 mutations associated with human diseases impair clathrin-mediated receptor endocytosis. *Hum Mutat* 2009;30:1419-1427

Blenk S, Engelmann J, Weniger M, *et al.* Germinal Center B Cell-Like (GCB) and Activated B Cell-Like (ABC) Type of Diffuse Large B Cell Lymphoma (DLBCL): Analysis of Molecular Predictors, Signatures, Cell Cycle State and Patient Survival. *Cancer Inform* 2007;3:399-420

Blobel GA. CBP and p300: versatile coregulators with important roles in hematopoietic gene expression. *J Leukoc Biol* 2002;71:545-556

Bonifacino JS, Lippincott-Schwartz J. Coat proteins: shaping membrane transport. *Nat Rev Mol Cell Biol* 2003;4:409-414

Boyer LA, Plath K, Zeitlinger J, *et al.* Polycomb complexes repress developmental regulators in murine embryonic stem cells. *Nature* 2006;441:349-353

Bracken AP, Pasini D, Capra M, *et al.* EZH2 is downstream of the pRB-E2F pathway, essential for proliferation and amplified in cancer. *EMBO J* 2003;22:5323-5335

Bradley SV, Holland EC, Liu GY, *et al.* Huntingtin interacting protein 1 is a novel brain tumor marker that associates with epidermal growth factor receptor. *Cancer Res* 2007a;67:3609-3615

Bradley SV, Smith MR, Hyun TS, *et al.* Aberrant Huntingtin interacting protein 1 in lymphoid malignancies. *Cancer Res* 2007b;67:8923-8931

Brady RJ, Damer CK, Heuser JE, O'Halloran TJ. Regulation of Hip1r by epsin controls the temporal and spatial coupling of actin filaments to clathrin-coated pits. *J Cell Sci* 2010;123:3652-3661

Brett TJ, Legendre-Guillemin V, McPherson PS, *et al.* Structural definition of the F-actin-binding THATCH domain from HIP1R. *Nat Struct Mol Biol* 2006;13;121-130

Brown PJ, Ashe SL, Leich E, *et al.* Potentially oncogenic B-cell activation-induced smaller isoforms of FOXP1 are highly expressed in the activated B cell-like subtype of DLBCL. *Blood* 2008;111:2816-2824.

Buajeeb W, Zhang X, Ohyama H, *et al.* Interaction of the CDK2-associated protein-1, $p12^{DOC-1/CDK2AP1}$, with its homolog, $p14^{DOC-1R}$. *Biochem Bioph Res Co* 2004;315; 998-1003

Bunting PS. Screening for prostate cancer with prostate-specific antigen: beware the biases. *Clin Chim Acta* 2002;315:71-97

Busse M, Feta A, Presto J, *et al.* Contribution of EXT1, EXT2, and EXTL3 to heparan sulfate chain elongation. *J Biol Chem* 2007;282;32802-32810

Büssow K, Cahill D, Nietfeld W, *et al.* A method for global protein expression and antibody screening on high-density filters of an arrayed cDNA library. *Nucleic Acids Res* 1998;26:5007-5008

Byers RJ, Sakhinia E, Joseph P, *et al.* Clinical quantitation of immune signature in follicular lymphoma by RT-PCR-based gene expression profiling. *Blood* 2008;111:4764-4770

Cabezudo E, Carrara P, Morilla R, Matutes E. Quantitative analysis of CD79b, CD5 and CD19 in mature B-cell lymphoproliferative disorders. *Haematologica* 1999;84:413-418

Calderwood MA, Venkatesan K, Xing L, *et al.* Epstein-Barr virus and virus human protein interaction maps. *Proc Natl Acad Sci U S A* 2007;104;7606-7611

Camós M, Esteve J, Jares P, *et al.* Gene expression profiling of acute myeloid leukemia with translocation t(8;16)(p11;p13) and *MYST3-CREBBP* rearrangement reveals a distinctive signature with a specific pattern of *HOX* gene expression. *Cancer Res* 2006;66:6947-6954

Campbell AJ, Lyne L, Brown PJ, *et al.* Aberrant expression of the neuronal transcription factor FOXP2 in neoplastic plasma cells. *Br J Haematol* 2010;149:221-230

Cao R, Wang L, Wang H, *et al.* Role of histone H3 lysine 27 methylation in Polycomb-group silencing. *Science* 2002;298:1039-1043

Carlotti E, Wrench D, Matthews J, *et al.* Transformation of follicular lymphoma to diffuse large B-cell lymphoma may occur by divergent evolution from a common progenitor cell or by direct evolution from the follicular lymphoma clone. *Blood* 2009;113:3553-3557

Carreno S, Engqvist-Goldstein AE, Zhang CX, *et al.* Actin dynamics coupled to clathrin-coated vesicle formation at the trans-Golgi network. *J Cell Biol* 2004;165:781-788

Carreras J, Lopez-Guillermo A, Fox BC, *et al.* High numbers of tumor-infiltrating FOXP3-positive regulatory T cells are associated with improved overall survival in follicular lymphoma. *Blood* 2006;108:2957-2964

Casciola-Rosen L, Nagaraju K, Plotz P, *et al.*. Enhanced autoantigen expression in regenerating muscle cells in idiopathic inflammatory myopathy. *J Exp Med* 2005;201:581-601

Castella A, Joshi S, Raaschou T, Mason N. Pattern of malignant lymphoma in the United Arab Emirates - a histopathologic and immunologic study in 208 native patients. *Acta Oncol* 2001;40:660-664

Cengiz B, Gunduz E, Gunduz M, *et al.* Tumor-specific mutation and downregulation of *ING5* detected in oral squamous cell carcinoma. *Int J Cancer* 2010;127:2088-2094

Cha SC, Kwak LW, Ruffini PA, *et al.* Cloning of B cell lymphoma-associated antigens using modified phage-displayed expression cDNA library and immunized patient sera. *J Immunol Methods* 2006;312:79-93

Chang EJ, Ha J, Oerlemans F, *et al.* Brain-type creatine kinase has a crucial role in osteoclast-mediated bone resorption. *Nat Med* 2008;14;966-972

Chen CY, Brodsky FM. Huntingtin-interacting protein 1 (Hip1) and Hip1-related protein (Hip1R) bind the conserved sequence of clathrin light chains and thereby influence clathrin assembly in vitro and actin distribution in vivo. *J Biol Chem* 2005;280:6109-6117

Chen L, Juszczynski P, Takeyama K, *et al.* Protein tyrosine phosphatase receptor-type O truncated (PTPROt) regulates SYK phosphorylation, proximal B-cell receptor signaling and cellular proliferation. *Blood* 2006;108:3428-3433

Chen L, Monti S, Juszczynski P, *et al.* SYK-dependent tonic B-cell receptor signaling is a rational treatment target in diffuse large B-cell lymphoma. *Blood* 2008;15:2230-2237

Chen CS, Sullivan S, Anderson T, *et al.* Identification of novel serological biomarkers for inflammatory bowel disease using *Escherichia coli* proteome chip. *Mol Cell Proteomics* 2009;8:1765-1776

Cheung KJ, Johnson NA, Affleck JG, *et al.* Acquired *TNFRSF14* mutations in follicular lymphoma are associated with worse prognosis. *Cancer Res* 2010 Nov 2 (E-publication ahead of print)

Chng WJ, Remstein ED, Fonseca R, *et al.* Gene expression profiling of pulmonary mucosa-associated lymphoid tissue lymphoma identifies new biologic insights with potential diagnostic and therapeutic applications. *Blood* 2009;113:635-645

Cho-Vega JH, Troncoso P, Do KA, *et al.* Combined laser capture microdissection and serial analysis of gene expression from human tissue samples. *Modern Pathol* 2005;18:577-584

Choi MC, Jong HS, Kim TY, *et al.* AKAP12/Gravin is inactivated by epigenetic mechanism in human gastric carcinoma and shows growth suppressor activity. *Oncogene* 2004;23:7095-7103

Choi MC, Lee YU, Kim SH, *et al.* A-kinase anchoring protein 12 regulates the completion of cytokinesis. *Biochem Biophys Res Commun* 2008;373:85-89

Choi WW, Weisenburger DD, Greiner TC, *et al.* A new immunostain algorithm classifies diffuse large B-cell lymphoma into molecular subtypes with high accuracy. *Clin Cancer Res* 2009;15:5494-5502

Cobaleda C, Schebesta A, Delogu A, Busslinger M. Pax5: the guardian of B cell identity and function. *Nat Immunol* 2007;8:463-470

Cohen AM, Grinblat B, Bessler H, *et al.* Increased expression of the hPim-2 gene in human chronic lymphocytic leukemia and non-Hodgkin lymphoma. *Leuk Lymphoma* 2004;45:951-955

Coiffier B, Lepage E, Briere J, *et al.* CHOP chemotherapy plus rituximab compared with CHOP alone in elderly patients with diffuse large-B-cell lymphoma. *New Engl J Med* 2002;346:235-242

Cooper CD, Liggins AP, Ait-Tahar K, *et al.* PASD1, a DLBCL-associated cancer testis antigen and candidate for lymphoma immunotherapy. *Leukemia* 2006;20:2172-2174

Copie-Bergman C, Gaulard P, Leroy K, *et al.* Immuno-fluorescence in situ hybridization index predicts survival in patients with diffuse large B-cell lymphoma treated with R-CHOP: a GELA study. *J Clin Oncol* 2009;27:5573-5579

Crabtree GR, Olson EN. NFAT signaling: choreographing the social lives of cells. *Cell* 2002;109:S67-79

Dave M, Wright G, Tan B, *et al.* Prediction of survival in follicular lymphoma based on molecular features of tumor-infiltrating immune cells. *New Engl J Med* 2004;351:2159-2169

Dave SS, Fu K, Wright GW, *et al.* Molecular diagnosis of Burkitt's lymphoma. *New Engl J Med* 2006;354:2431-2442

David G, Alland L, Hong SH, *et al.* Histone deacetylase associated with mSin3A mediates repression by the acute promyelocytic leukemia-associated PLZF protein. *Oncogene* 1998;16:2549-2556

Davidsson J, Andersson A, Paulsson K, *et al.* Tiling resolution array comparative genomic hybridization, expression and methylation analyses of dup(1q) in Burkitt lymphomas and pediatric high hyperdiploid acute lymphoblastic leukemias reveal clustered near-centromeric breakpoints and overexpression of genes in 1q22-32.3. *Hum Mol Genet* 2007;16;2215-2225

Davies AJ, Rosenwald A, Wright G, *et al.* Transformation of follicular lymphoma to diffuse large B-cell lymphoma proceeds by distinct oncogenic mechanisms. *Br J Haematol* 2007;136:286-293

Davis RE, Brown KD, Siebenlist U, Staudt LM. Constitutive nuclear factor κB activity is required for survival of activated B cell-like diffuse large B cell lymphoma cells. *J Exp Med* 2001;194:1861-1874

Davis RE, Ngo VN, Lenz G, *et al.* Chronic active B-cell-receptor signalling in diffuse large B-cell lymphoma. *Nature* 2010;463:88-94

de Graaf K, Hekerman P, Spelten O, *et al.* Characterization of cyclin L2, a novel cyclin with an arginine/serine-rich domain: phosphorylation by DYRK1A and colocalization with splicing factors. *J Biol Chem* 2004;279:4612-4614

De Santa F, Totaro MG, Prosperini E, *et al.* The histone H3 lysine-27 demethylase Jmjd3 links inflammation to inhibition of polycomb-mediated gene silencing. *Cell* 2007;130:1083-1094

De Santa F, Narang V, Yap ZH, *et al.* Jmjd3 contributes to the control of gene expression in LPS-activated macrophages. *EMBO J* 2009;28:3341-3352

Debrincat, MA, Zhang JG, Willson TA, *et al.* Ankyrin repeat and suppressors of cytokine signaling box protein Asb-9 targets creatine kinase B for degradation. *J Biol Chem* 2007;282;4728-4737

Dent AL, Shaffer AL, Yu X, *et al.* Control of inflammation, cytokine expression, and germinal center formation by BCL-6. *Science* 1997;276:589-592

Diesinger I, Bauer C, Brass N, *et al.* Toward a more complete recognition of immunoreactive antigens in squamous cell lung carcinoma. *Int J Cancer* 2002;102:372-378

Dietrich N, Bracken AP, Trinh E, *et al.* Bypass of senescence by the polycomb group protein CBX8 through direct binding to the INK4A-ARF locus. *EMBO J* 2007;26:1637-1648

Dighiero G, Hamblin TJ. Chronic lymphocytic leukaemia. *Lancet* 2008;371:1017-1029

Disis ML, Calenoff E, McLaughlin G, *et al.* Existent T-cell and antibody immunity to HER-2/neu protein in patients with breast cancer. *Cancer Res* 1994;54:16-20

Doherty GJ, McMahon HT. Mechanisms of endocytosis. *Annu Rev Biochem* 2009;78:857-902

Dohner H, Stilgenbauer S, Benner A, *et al.* Genomic aberrations and survival in chronic lymphocytic leukemia. *N Engl J Med* 2000;343:1910-1916

Doyon Y, Cayrou C, Ullah M, *et al.* ING tumor suppressor proteins are critical regulators of chromatin acetylation required for genome expression and perpetuation. *Mol Cell* 2006;21:51-64

Drake JR, Lewis TA, Condon KB, *et al.* Involvement of MIIC-like late endosomes in B cell receptor-mediated antigen processing in murine B cells. *J Immunol* 1999;162:1150-1155

Duffy MJ. Role of tumor markers in patients with solid cancers: A critical review. *Eur J Intern Med* 2007;18:175-184

Dunleavy K, Pittaluga S, Czuczman MS, *et al.* Differential efficacy of bortezomib plus chemotherapy within molecular subtypes of diffuse large B-cell lymphoma. *Blood* 2009;113:6069-6076

Dutton A, O'Neil JD, Milner AE, *et al.* Expression of the cellular FLICE-inhibitory protein (c-FLIP) protects Hodgkin's lymphoma cells from autonomous Fas-mediated death. *Proc Natl Acad Sci U S A* 2004;101;6611-6616

Edamatsu H, Kaziro Y, Itoh H. LUCA15, a putative tumour suppressor gene encoding an RNA-binding nuclear protein, is down-regulated in ras-transformed Rat-1 cells. *Genes Cells* 2000;5:849-58

Eichmüller S, Usener D, Dummer R, *et al.* Serological detection of cutaneous T-cell lymphoma-associated antigens. *Proc Natl Acad Sci U S A* 2001;98:629-634

Ekström K, Vajdic CM, Falster M, *et al.* Autoimmune disorders and risk of non-Hodgkin lymphoma subtypes: a pooled analysis within the InterLymph Consortium. *Blood* 2008;111:4029-4038

Engelhorn ME, Guevara-Patino JA, Noffz G, *et al.* Autoimmunity and tumor immunity induced by immune responses to mutations in self. *Nat Med* 2006;12:198-206.

Engqvist-Goldstein AE, Kessels MM, Chopra VS, *et al.* An actin-binding protein of the Sla2/Huntingtin interacting protein 1 family is a novel component of clathrin-coated pits and vesicles. *J Cell Biol* 1999;147:1503-1518

Engqvist-Goldstein AE, Warren RA, Kessels MM, *et al.* The actin-binding protein Hip1R associates with clathrin during early stages of endocytosis and promotes clathrin assembly in vitro. *J Cell Biol* 2001;154:1209-1223

Engqvist-Goldstein AE, Zhang CX, Carreno S, *et al.* RNAi-mediated Hip1R silencing results in stable association between the endocytic machinery and the actin assembly machinery. *Mol Biol Cell* 2004;15:1666-1679

Erdfelder F, Hertweck M, Filipovich A, *et al.* High lymphoid enhancer binding factor-1 expression is associated with disease progression and poor prognosis in chronic lymphocytic leukemia. *Hematol Rev* 2010;2:e3

Escalante CR, Brass AL, Pongubala JM, *et al.* Crystal structure of PU.1/IRF-4/DNA ternary complex. *Mol Cell* 2002;10:1097-1105

Esteller M. Epigenetics in cancer. *N Engl J Med* 2008;358:1148-1159

Evens AM, Sehn LH, Farinha P, *et al.* Hypoxia-inducible factor-1α expression predicts superior survival in patients with diffuse large B-cell lymphoma treated with R-CHOP. *J Clin Oncol* 2010;28:1017-1024.

Falini B, Fizzotti M, Pucciarini A, *et al.* A monoclonal antibody (MUM1p) detects expression of the MUM1/IRF4 protein in a subset of germinal center B cells, plasma cells, and activated T cells. *Blood* 2000;95:2084-2092

Fang JY, Richardson BC. The MAPK signalling pathways and colorectal cancer. *Lancet Oncol* 2005;6:322-327

Farinha P, Masoudi H, Skinnider BF, *et al.* Analysis of multiple biomarkers shows that lymphoma-associated macrophage (LAM) content is an independent predictor of survival in follicular lymphoma (FL). *Blood* 2005;106:2169-2174

Federico M, Bellei M, Marcheselli L, *et al.* Follicular lymphoma international prognostic index 2: a new prognostic index for follicular lymphoma developed by the international follicular lymphoma prognostic factor project. *J Clin Oncol* 2009;27:4555-4562

Feuerhake F, Kutok JL, Monti S, *et al.* NFκB activity, function, and target-gene signatures in primary mediastinal large B-cell lymphoma and diffuse large B-cell lymphoma subtypes. *Blood* 2005;106:1392-1399

Feugier P, Van Hoof A, Sebban C, *et al.* Long-term results of the R-CHOP study in the treatment of elderly patients with diffuse large B-cell lymphoma: a study by the Groupe d'Etude des Lymphomes de l'Adulte. *J Clin Oncol* 2005;23:4117-4126

Fernández-Madrid F, Tang N, Alansari H, *et al.* Autoantibodies to annexin XI-A and other autoantigens in the diagnosis of breast cancer. *Cancer Res* 2004;64:5089-5096

Fitzgibbon J, Iqbal S, Davies A, *et al.* Genome-wide detection of recurring sites of uniparental disomy in follicular and transformed follicular lymphoma. *Leukemia* 2007;21:1514-1520

Floratos A, Smith K, Ji Z, *et al.* geWorkbench: an open source platform for integrative genomics. *Bioinformatics* 2010;26:1779-1780

Flowers CR, Sinha R, Vose JM. Improving outcomes for patients with diffuse large B-cell lymphoma. *CA Cancer J Clin* 2010 Oct 28 (E-publication ahead of print)

Fo CS, Coleman CS, Wallick CJ, *et al.* Genomic organization, expression profile, and characterization of the new protein PRA1 domain family, member 2 (PRAF2). *Gene* 2006;371:154-165

Ford ME, Havstad SL, Demers R, Johnson CC. Effect of false-positive prostate cancer screening results on subsequent positive cancer screening behavior. *Cancer Epidemiol Biomarkers Prev* 2005;14:190-194

Fox SB, Brown P, Han C, *et al.* Expression of the forkhead transcription factor FOXP1 is associated with estrogen receptor-α and improved survival in primary human breast carcinomas. *Clin Cancer Res* 2004;10:3521-3527.

Francannet C, Cohen-Tanugi A, Le Merrer M, *et al.* Genotype-phenotype correlation in hereditary multiple exostoses. *J Med Genet* 2001;38:430-434

Francis SA, Shen X, Young JB, *et al.* Rho GEF Lsc is required for normal polarization, migration, and adhesion of formyl-peptide-stimulated neutrophils. *Blood* 2006;107:1627-1635

Friedberg JW, Taylor MD, Cerhan JR, *et al.* Follicular lymphoma in the United States: first report of the national LymphoCare study. *J Clin Oncol* 2009;27:1202-1208

Friedberg JW, Sharman J, Sweetenham J, *et al.* Inhibition of Syk with fostamatinib disodium has significant clinical activity in non-Hodgkin lymphoma and chronic lymphocytic leukemia. *Blood* 2010;115:2578-2585

Fu K, Weisenburger DD, Choi WWL, *et al.* Addition of rituximab to standard chemotherapy improves the survival of both the germinal center B-cell-like and non-germinal center B-cell-like subtypes of diffuse large B-cell lymphoma. *J Clin Oncol* 2008;26:4587-4594.

Fujii K, Kondo T, Yokoo H, *et al.* Protein expression pattern distinguishes different lymphoid neoplasms. *Proteomics* 2005;5:4274-4286.

Fujita T, Igarashi J, Okawa ER, *et al.* CHD5, a tumor suppressor gene deleted from 1p36.31 in neuroblastomas. *J Natl Cancer Inst* 2008;100:940-949

Fushimi K, Ray P, Kar A, *et al.* Up-regulation of the proapoptotic caspase 2 splicing isoform by a candidate tumor suppressor, RBM5. *Proc Natl Acad Sci U S A* 2008;105:15708-15713

Fuss J, Linn S. Human DNA polymerase ε colocalizes with proliferating cell nuclear antigen and DNA replication late, but not early, in S phase. *J Biol Chem* 2001;277;8658-8666

Gaglio A, Saredi D, Compton A. NuMA is required for the organization of microtubules into aster-like mitotic arrays. *J Cell Biol* 1995;131:693-708

Gao WM, Kuick R, Orchekowski RP, *et al.* Distinctive serum protein profiles involving abundant proteins in lung cancer patients based upon antibody microarray analysis. *BMC Cancer* 2005;5:110

Gatter K, Pezzella F. Diffuse large B-cell lymphoma. *Diagn Histopathology* 2009;16:69-81

Gazumyan A, Reichlin A, Nussenzweig MC. Igβ tyrosine residues contribute to the control of B cell receptor signaling by regulating receptor internalization. *J Exp Med* 2006;203:1785-1794

Ghetie V, Ward ES. Multiple roles for the major histocompatibility complex class I- related receptor FcRn. *Annu Rev Immunol* 2000;18:739-766

Gil J, Bernard D, Martínez D, Beach D. Polycomb CBX7 has a unifying role in cellular lifespan. *Nat Cell Biol* 2004;6:67-72

Gilmore TD. Introduction to NF-κB: players, pathways, perspectives. *Oncogene* 2006;25:6680-6684

Gimferrer I, Farnós M, Calvo M, *et al.* The accessory molecules CD5 and CD6 associate on the membrane of lymphoid T cells. *J Biol Chem* 2003;278:8564-8571

Girkontaite I, Missy K, Sakk V, *et al.* Lsc is required for marginal zone B cells, regulation of lymphocyte motility and immune responses. *Nat Immunol* 2001;2:855-862

Gisselbrecht C, Glass B, Mounier N, *et al.* Salvage regimens with autologous transplantation for relapsed large B-cell lymphoma in the rituximab era. *J Clin Oncol* 2010 Jul 26 (E-publication ahead of print)

GO Consortium. The Gene Ontology (GO) database and informatics resource. *Nucleic Acids Res* 2004;32;D258-D261

Goldenberg DM. Epratuzumab in the therapy of oncological and immunological diseases. *Expert Rev Anticancer Ther* 2006;6:1341-1353

Gomez TS, McCarney SD, Carrizosa E, *et al.* HS1 functions as an essential actin-regulatory adaptor protein at the immune synapse. *Immunity* 2006;24:741-752

Gottfried I, Ehrlich M, Ashery U. The Sla2p/HIP1/HIP1R family: similar structure, similar function in endocytosis? *Biochem Soc Trans* 2010;38:187-191

Greiner TC, Dasgupta C, Ho VV, *et al*. Mutation and genomic deletion status of *ataxia telangiectasia mutated* (*ATM*) and *p53* confer specific gene expression profiles in mantle cell lymphoma. *Proc Natl Acad Sci U S A* 2006;103:2352-2357

Gu L, Dagvadorj A, Lutz J, *et al*. Transcription factor Stat3 stimulates metastatic behavior of human prostate cancer cells in vivo, whereas Stat5b has a preferential role in the promotion of prostate cancer cell viability and tumor growth. *Am J Pathol* 2010;176:1959-1972

Gunawardana CG, Diamandis EP. High throughput proteomic strategies for identifying tumour-associated antigens. *Cancer Lett* 2007;249:110-119

Gurney KA, Cartwright RA. Increasing incidence and descriptive epidemiology of extranodal non-Hodgkin lymphoma in parts of England and Wales. *Hematology J* 2002;3:95-104.

Gururajan M, Jennings CD, Bondada S. Cutting edge: constitutive B cell receptor signaling is critical for basal growth of B lymphoma. *J Immunol* 2006;176:5715-5719

Halliday T, Baxter T. Lymphoma: pictorial review. *Eur Radiol*. 2003;13:1154-1164

Han W, Han MR, Kang JJ, *et al*. Genomic alterations identified by array comparative genomic hybridization as prognostic markers in tamoxifen-treated estrogen receptor-positive breast cancer. *BMC Cancer* 2006;6:92

Hanash S. Disease proteomics. *Nature* 2003;422:226-232

Hans CP, Weisenburger DD, Greiner TC, *et al*. Confirmation of the molecular classification of diffuse large B-cell lymphoma by immunohistochemistry using a tissue microarray. *Blood* 2004;103:275-282

Hardie DL, Johnson GD, Khan M, MacLennan IC. Quantitative analysis of molecules which distinguish functional compartments within germinal centers. *Eur J Immunol* 1993;23:997-1004

Harris NL, Jaffe ES, Diebold J, *et al*. World Health Organization classification of neoplastic diseases of the hematopoietic and lymphoid tissues: report of the Clinical Advisory Committee meeting-Airlie House, Virginia, November 1997. *J Clin Oncol* 1999;17:3835-3849

Hastings ML, Allemand E, Duelli DM, *et al*. Control of pre-mRNA splicing by the general splicing factors PUF60 and U2AF^{65}. *PLoS ONE* 2007;2:e538

Hayden MS, Ghosh S. Shared principles in NF-κB signaling. *Cell* 2008;132:344-362

Hayes S, Chawla A, Corvera S. TGFβ receptor internalization into EEA1-enriched early endosomes: role in signaling to Smad2. *J Cell Biol* 2002;158:1239-1249

Herwig R, Schmitt AO, Steinfath M, *et al.* Information theoretical probe selection for hybridisation experiments. *Bioinformatics* 2000;16:890-898

Hinrichsen L, Meyerholz A, Groos S, Ungewickell EJ. Bending a membrane: How clathrin affects budding. *Proc Natl Acad Sci U S A* 2006;103:8715-8720

Hoefnagel JJ, Dijkman R, Basso K, *et al.* Distinct types of primary cutaneous large B-cell lymphoma identified by gene expression profiling. *Blood* 2005;105:3671-3678

Holleman A, Cheok MH, den Boer ML, *et al.* Gene-expression patterns in drug-resistant acute lymphoblastic leukemia cells and response to treatment. *New Engl J Med* 2004;351:533-542

Hong S, Cho YW, Yu LR, *et al.* Identification of JmjC domain-containing UTX and JMJD3 as histone H3 lysine 27 demethylases. *Proc Natl Acad Sci U S A* 2007;104:18439-18444

Horn S, Lueking A, Murphy D, *et al.* Profiling humoral autoimmune repertoire of dilated cardiomyopathy (DCM) patients and development of a disease-associated protein chip. *Proteomics* 2006;6:605-613

Horsman DE, Gascoyne RD, Coupland RW, *et al.* Comparison of cytogenetic analysis, southern analysis, and polymerase chain reaction for the detection of t(14; 18) in follicular lymphoma. *Am J Clin Pathol* 1995;103:472-478

Huang Y, Tan M, Gosink M, *et al.* Histone deacetylase 5 is not a p53 target gene, but its overexpression inhibits tumor cell growth and induces apoptosis. *Cancer Res* 2002;62;2913-2922

Huang S, Shen Q, MaoWG, *et al.* JWA, a novel signaling molecule, involved in the induction of differentiation of human myeloid leukemia cells. *Biochem Biophys Res Commun* 2006a;341:440-450

Huang S, Shen Q, MaoWG, *et al.* JWA, a novel signaling molecule, involved in all-trans retinoic acid induced differentiation of HL-60 cells. *J Biomed Sci* 2006b;13:357-371

Hudson ME, Pozdnyakova I, Haines K, *et al.* Identification of differentially expressed proteins in ovarian cancer using high-density protein microarrays. *Proc Natl Acad Sci U S A* 2007;104:17494-17499

Hunt KE, Reichard KK. Diffuse large B-cell lymphoma. *Arch Pathol Lab Med* 2008;132:118-124

Hübscher U, Maga G, Spadari S. Eukaryotic DNA polymerases. *Annu Rev Biochem* 2002;71:133-163

Hyun TS, Li L, Oravecz-Wilson KI, *et al.* Hip1-related mutant mice grow and develop normally but have accelerated spinal abnormalities and dwarfism in the absence of HIP1. *Mol Cell Biol* 2004a;24:4329-4340

Hyun TS, Rao DS, Saint-Dic D, *et al.* HIP1 and HIP1r stabilize receptor tyrosine kinases and bind 3-phosphoinositides via epsin N-terminal homology domains. *J Biol Chem* 2004b;14:14294-14306

Inagaki H, Matsushima Y, Nakamura K, *et al.* A large DNA-binding nuclear protein with RNA recognition motif and serine/arginine-rich domain. *J Biol Chem* 1996;271:12525-12531

Ishii M, Wen H, Corsa CA, *et al.* Epigenetic regulation of the alternatively activated macrophage phenotype. *Blood* 2009;114:3244-3254

Ishikawa J, Taniguchi T, Takeshita A, Maekawa M. Increased creatine kinase BB activity and *CKB* mRNA expression in patients with hematologic disorders: Relation to methylation status of the *CKB* promoter. *Clin Chim Acta* 2005;361;135-140

Itoh T, Koshiba S, Kigawa T, *et al.* Role of the ENTH domain in phosphatidylinositol-4,5-bisphosphate binding and endocytosis. *Science* 2001;291:1047-1051

Ivkovic S, Blau S, Polanskaya O, *et al.* ARPP-21: murine gene structure and promoter identification of a neuronal phosphoprotein enriched in the limbic striatum. *Brain Res* 1996;709;10-16

Iyer NG, Özdag H, Caldas C. p300/CBP and cancer. *Oncogene* 2004;23:4225-4231

Jacobs IJ, Skates SJ, MacDonald N, *et al.* Screening for ovarian cancer: a pilot randomised controlled trial. *Lancet* 1999;353:1207-1210

Jain RN, Al-Menhali AA, Keeley TM, *et al.* Hip1r is expressed in gastric parietal cells and is required for tubulovesicle formation and cell survival in mice. *J Clin Invest* 2008;118:2459-2470

Jantzen HM, Admon A, Bell SP, Tjian R. Nucleolar transcription factor hUBF contains a DNA-binding motif with homology to HMG proteins. *Nature* 1990;344:830-836

Jensen LR, Bartenschlager H, Rujirabanjerd S, *et al.* A distinctive gene expression fingerprint in mentally retarded male patients reflects disease-causing defects in the histone demethylase KDM5C. *PathoGenetics* 2010;3:2

Jenuwein T, Allis CD. Translating the histone code. *Science* 2001;293:1074-1080

Jiang S, Seng S, Avraham HK, *et al.* Process elongation of oligodendrocytes is promoted by the Kelch-related protein MRP2/KLHL1. *J Biol Chem* 2007;282:12319-12329

Joseph-Pietras D, Gao Y, Zojer N, *et al.* DNA vaccines to target the cancer testis antigen PASD1 in human multiple myeloma. *Leukemia* 2010;24:1951-1959

Kajikawa S, Nakayama H, Suzuki M, *et al.* Increased expression of rat ribosomal protein L4 mRNA in 5-azacytidine-treated PC12 cells prior to apoptosis. *Biochem Biophys Res Commun* 1998;252;220-224

Kash JC, Tumpey TM, Proll SC, *et al.* Genomic analysis of increased host immune and cell death responses induced by 1918 influenza virus. *Nature* 2006;443:578-581

Kato M, Sanada M, Kato I, *et al.* Frequent inactivation of A20 in B-cell lymphomas. *Nature* 2009;459:712-717

Katus HA, Remppis A, Looser S**,** *et al.* Enzyme linked immuno assay of cardiac troponin T for the detection of acute myocardial infarction in patients. *J Mol Cell Cardiol* 1989;21:1349-1353

Kerr JR, Kaushik N, Fear D, *et al.* Single-nucleotide polymorphisms associated with symptomatic infection and differential human gene expression in healthy seropositive persons each implicate the cytoskeleton, integrin signaling, and oncosuppression in the pathogenesis of human parvovirus B19 infection. *J Infect Dis* 2005;192:276-286

Kijanka G, Murphy D. Protein arrays as tools for serum autoantibody marker discovery in cancer. *J Proteomics* 2009;72:936-944

Kijanka G, Hector S, Kay EW, *et al.* Human IgG antibody profiles differentiate between symptomatic patients with and without colorectal cancer. *Gut* 2010;59:69-78

Kim R, Emi M, Tanabe K. Cancer immunoediting from immune surveillance to immune escape. *Immunology* 2007;121:1-14

Kim JH, Yoon S, Won M, *et al.* HIP1R interacts with a member of Bcl-2 family, BCL2L10, and induces BAK-dependent cell death. *Cell Physiol Biochem* 2009;23:43-52

Kitamura T, Koshino Y, Shibata F, *et al.* Retrovirus-mediated gene transfer and expression cloning: powerful tools in functional genomics. *Exp Hematol* 2003;31:1007-1014

Klein U, Dalla-Favera R. Germinal centres: role in B−cell physiology and malignancy. *Nat Rev Immunol* 2008;8:22-33

Klein U, Pasqualucci L. B-cell receptor signaling derailed in lymphomas. *Immunol Cell Biol* 2010;88:346-347

Klose RJ, Kallin EM, Zhang Y. JmjC-domain-containing proteins and histone demethylation. *Nat Rev Genet* 2006;7:715-727

Koomoa DLT, Go RCV, Wester K, Bachmann AS. Expression profile of PRAF2 in the human brain and enrichment in synaptic vesicles. *Neurosci Lett* 2008;436:171-176

Koon HB, Ippolito GC, Banham AH, Tucker PW. FOXP1: a potential therapeutic target in cancer. *Expert Opin Ther Targets* 2007;11:955-965

Koroleva EP, Lagar'kova MA, Khlgatian SV, *et al.* Serological study of a repertoire of human cancer antigens and autoantigens. *Mol Biol (Mosk)* 2004;38:233-238

Krackhardt AM, Witzens M, Harig S, *et al.* Identification of tumor-associated antigens in chronic lymphocytic leukemia by SEREX. *Blood* 2002;100:2123-2131

Kraus M, Alimzhanov MB, Rajewsky N, Rajewsky K. Survival of resting mature B lymphocytes depends on BCR signaling via the Igα/β heterodimer. *Cell* 2004;117:787-800.

Kung AL, Rebel VI, Bronson RT, *et al.* Gene dose-dependent control of hematopoiesis and hematologic tumor suppression by CBP. *Gene Dev* 2000;14:272-277

Küppers R, Klein U, Hansmann ML, Rajewsky K. Cellular origin of human B-cell lymphomas. *New Engl J Med* 1999;341:1520-1529

Küppers R. Mechanisms of B-cell lymphoma pathogenesis. *Nat Rev Cancer* 2005;5:251-262

Küppers, R. The biology of Hodgkin's lymphoma. *Nat Rev Cancer* 2009;9:15-27

L'Espérance S, Bachvarova M, Tetu B, *et al.* Global gene expression analysis of early response to chemotherapy treatment in ovarian cancer spheroids. *BMC Genomics* 2008;9:99

Lachner M, O'Sullivan RJ, Jenuwein T. An epigenetic road map for histone lysine methylation. *J Cell Sci* 2003;116:2117-2124

Lajmanovich A, Irisarri M, Molens JP, *et al.* Impairment of death-inducing signalling complex formation in CD95-resistant human primary lymphoma B cells. *Brit J Haematol* 2004;124;746-753

Lam KP, Kuhn R, Rajewsky K. In vivo ablation of surface immunoglobulin on mature B cells by inducible gene targeting results in rapid cell death. *Cell* 1997;90:1073-1083.

Lam LT, Davis RE, Pierce J, *et al.* Small molecule inhibitors of IκB kinase are selectively toxic for subgroups of diffuse large B-cell lymphoma defined by gene expression profiling. *Clin Cancer Res* 2005;11:28-40

Latres E, Malumbres M, Sotillo R, *et al.* Limited overlapping roles of $P15^{INK4b}$ and $P18^{INK4c}$ cell cycle inhibitors in proliferation and tumorigenesis. *EMBO J* 2000;19;3496-3506

Lavoie JN, L'Allemain G, Brunet A, *et al.* Cyclin D1 expression is regulated positively by the p42/p44MAPK and negatively by the p38/HOGMAPK pathway. *J Biol Chem* 1996;271:20608-20616

Lawrie CH, Soneji S, Marafioti T, *et al.* MicroRNA expression distinguishes between germinal center B cell-like and activated B cell-like subtypes of diffuse large B cell lymphoma. *Int J Cancer* 2007;121:1156-1161

Lawrie CH, Gal S, Dunlop HM, *et al.* Detection of elevated levels of tumour-associated microRNAs in serum of patients with diffuse large B-cell lymphoma. *Br J Haematol* 2008;141:672-675

Lawrie CH, Chi J, Taylor S, *et al.* Expression of microRNAs in diffuse large B cell lymphoma is associated with immunophenotype, survival and transformation from follicular lymphoma. *J Cell Mol Med* 2009;13:1248-1260

Le Clainche C, Pauly BS, Zhang CX, *et al.* A Hip1R-cortactin complex negatively regulates actin assembly associated with endocytosis. *EMBO J* 2007;26:1199-1210

Le Roy C, Wrana JL. Clathrin- and non-clathrin-mediated endocytic regulation of cell signalling. *Nat Rev Mol Cell Biol* 2005 6:112-126

Lee SJ, Lee JR, Hahn HS, *et al.* PIAS1 interacts with the KRAB zinc finger protein, ZNF133, via zinc finger motifs and regulates its transcriptional activity. *Exp Mol Med* 2007;39:450-457

Legendre-Guillemin V, Metzler M, Charbonneau M, *et al.* HIP1 and HIP12 display differential binding to F-actin, AP2, and clathrin. Identification of a novel interaction with clathrin light chain. *J Biol Chem* 2002;277:19897-19904.

Lemercier C, Verdel A, Galloo B, *et al.* mHDA1/HDAC5 histone deacetylase interacts with and represses MEF2A transcriptional activity. *J Biol Chem* 2000;275;15594-15599

Lenz G, Wright G, Dave S, *et al.* Gene expression signatures predict overall survival in diffuse large B cell lymphoma treated with rituximab and CHOP-like chemotherapy. *Blood* 2007a;110:Abstract 348

Lenz G, Nagel I, Siebert R, *et al.* Aberrant immunoglobulin class switch recombination and switch translocations in activated B cell-like diffuse large B cell lymphoma. *J Exp Med* 2007b;204:633-643

Lenz G, Wright G, Dave SS, *et al.* Stromal gene signatures in large-B-cell lymphomas. *New Engl J Med* 2008a;359:2313-2323

Lenz G, Davis RE, Ngo VN, *et al.* Oncogenic CARD11 mutations in human diffuse large B cell lymphoma. *Science* 2008b;319:1676-1679

Lenz G, Wright GW, Emre NC, *et al.* Molecular subtypes of diffuse large B-cell lymphoma arise by distinct genetic pathways. *Proc Natl Acad Sci U S A*. 2008c;105:13520-13525

Lenz G, Staudt LM. Aggressive lymphomas. *New Engl J Med* 2010;362:1417-1429

Leone PE, Walker BA, Jenner MW, *et al.* Deletions of *CDKN2C* in multiple myeloma: Biological and clinical implications. *Clin Cancer Res* 2008;14;6033-6041

Li H, Jie S, Zou P, Zou G. CDNA microarray analysis of chronic myeloid leukemia. *Int J Hematol* 2002;75:388-393

Li JF, Liu LD, Ma SH, *et al.* HTRP-an immediate-early gene product induced by HSV1 infection in human embryo fibroblasts, is involved in cellular co-repressors. *J Biochem* 2004;136:169-176

Li J, Okamoto H, Yin C, *et al.* Proteomic characterization of primary diffuse large B-cell lymphomas in the central nervous system. *J Neurosurg* 2008;109;536-546

Li Z, Zhang W, Wu M, *et al.* Gene expression-based classification and regulatory networks of pediatric acute lymphoblastic leukemia. *Blood* 2009;114:4486-4493

Li X, Nishida T, Noguchi A, *et al.* Decreased nuclear expression and increased cytoplasmic expression of ING5 may be linked to tumorigenesis and progression in human head and neck squamous cell carcinoma. *J Cancer Res Clin Oncol* 2010;136:1573-1583

Lichtman MA, Beutler E, Seligsohn U, *et al.* (eds.) Williams Hematology (7th Ed) 2007

Lin KI, Angelin-Duclos C, Kuo TC, Calame K. Blimp-1-dependent repression of Pax-5 is required for differentiation of B cells to immunoglobulin M-secreting plasma cells. *Mol Cell Biol* 2002;22:4771-4780

Ling K, Doughman RL, Firestone AJ, *et al.* Type Iγ phosphatidylinositol phosphate kinase targets and regulates focal adhesions. *Nature* 2002;420;89-93

Liggins AP, Guinn BA, Hatton CS, *et al.* Serologic detection of diffuse large B-cell lymphoma-associated antigens. *Int J Cancer* 2004a;110:563-569

Liggins AP, Brown PJ, Asker K, *et al.* A novel diffuse large B-cell lymphoma-associated cancer testis antigen encoding a PAS domain protein. *Br J Cancer* 2004b;91:141-149

Liggins AP, Guinn BA, Banham AH. Identification of lymphoma-associated antigens using SEREX. *Methods Mol Med* 2005;115:109-128

Lo YM, Chan LY, Lo KW, *et al.* Quantitative analysis of cell-free Epstein-Barr virus DNA in plasma of patients with nasopharyngeal carcinoma. *Cancer Res* 1999;59:1188-1191

Loeser S, Penninger JM. Regulation of peripheral T cell tolerance by the E3 ubiquitin ligase Cbl-b. *Semin Immunol* 2007;19:206-214

Loijens JC, Anderson RA. Type I phosphatidylinositol-4-phosphate 5-kinases are distinct members of this novel lipid kinase family. *J Biol Chem* 1996;271;32937-32943

Longo DL. Idiotype vaccination in follicular lymphoma: knocking on the doorway to cure. J *Natl Cancer Inst* 2006;98:1263-1265.

Lossos IS, Czerwinski DK, Alizadeh AA, *et al.* Prediction of survival in diffuse large-B-cell lymphoma based on the expression of six genes. *New Engl J Med* 2004;350:1828-1837

Lowe SW, Sherr CJ. Tumor suppression by Ink4a-Arf: progress and puzzles. *Curr Opin Genet Dev* 2003;13:77-83

Lu M, Nakamura RM, Dent ED, *et al.* Aberrant expression of fetal RNA-binding protein p62 in liver cancer and liver cirrhosis. *Am J Pathol* 2001;159:945-953

Lu D, Zhao Y, Tawatao R, *et al.* Activation of the Wnt signaling pathway in chronic lymphocytic leukemia. *Proc Natl Acad Sci U S A* 2004;101:3118-3123

Lueking A, Possling A, Huber O, *et al.* A nonredundant human protein chip for antibody screening and serum profiling. *Mol Cell Proteomics* 2003;2:1342-1349

Lueking A, Huber O, Wirths C, *et al.* Profiling of alopecia areata autoantigens based on protein microarray technology. *Mol Cell Proteomics* 2005;4:1382-1390

Ma Y, Visser L, Roelofsen H, *et al.* Proteomics analysis of Hodgkin lymphoma: identification of new players involved in the cross-talk between HRS cells and infiltrating lymphocytes. *Blood* 2008;11:2339-2346

Macian F. NFAT proteins: key regulators of T-cell development and function. *Nat Rev Immunol* 2005;5:472-484

Mallikaratchy PR, Ruggiero A, Gardner JR, *et al.* A multivalent DNA aptamer specific for the B-cell receptor on human lymphoma and leukemia. *Nucleic Acids Res* 2010 Oct 28 (E-publication ahead of print)

Margolin AA, Nemenman I, Basso K, *et al.* ARACNE: an algorithm for the reconstruction of gene regulatory networks in a mammalian cellular context. *BMC Bioinformatics* 2006;7:S7

Matolcsy A, Schattner EJ, Knowles DM, Casali P. Clonal evolution of B cells in transformation from low- to high-grade lymphoma. *Eur J Immunol* 1999;29:1253-1264

Matsushima Y, Matsumura K, Ishii S, *et al.* Chromosomal assignment of the chicken NP220 gene encoding a large DNA-binding nuclear protein and its targeted disruption in chicken DT40 *Cytotechnology* 2000;33:109-115

McCullagh P, Chaplin T, Meerabux J, *et al.* The cloning, mapping and expression of a novel gene, BRL, related to the AF10 leukaemia gene. *Oncogene* 1999;18:7442-7452

McNiven MA, Thompson HM. Vesicle formation at the plasma membrane and trans-Golgi network: the same but different. *Science* 2006;313:1591-1594

Medina PP, Nolde M, Slack FJ. OncomiR addiction in an in vivo model of microRNA-21-induced pre-B-cell lymphoma. *Nature* 2010;467:86-90

Megonigal MD, Rappaport EF, Jones DH, *et al.* t(11;22)(q23;q11.2) in acute myeloid leukemia of infant twins fuses MLL with hCDCrel1, a cell division cycle gene in the genomic region of deletion in DiGeorge and velocardiofacial syndromes. *Proc Natl Acad Sci U S A* 1998;95:6413-6418

Mestre-Escorihuela C, Rubio-Moscardo F, Richter JA, *et al.* Homozygous deletions localize novel tumor suppressor genes in B-cell lymphomas. *Blood* 2007;109;271-280

Metzler M, Helgason CD, Dragatsis I, *et al.* Huntingtin is required for normal hematopoiesis. *Hum Mol Genet* 2000;9:387-394

Metzler M, Legendre-Guillemin V, Gan L, *et al.* HIP1 functions in clathrin-mediated endocytosis through binding to clathrin and adaptor protein 2. *J Biol Chem* 2001;276:39721-39726

Metzler M, Gan L, Wong TP, *et al.* NMDA receptor function and NMDA receptor-dependent phosphorylation of huntingtin is altered by the endocytic protein HIP1. *J Neurosci* 2007;27:2298-2308

Meyer C, Kowarz E, Hofmann J, *et al.* New insights to the *MLL* recombinome of acute leukemias. *Leukemia* 2009;23:1490-1499

Miclet E, Stoven V, Michels PA, *et al.* NMR spectroscopic analysis of the first two steps of the pentose-phosphate pathway elucidates the role of 6-phosphogluconolactonase. *J Biol Chem* 2001;276:34840-34846

Mills IG, Gaughan L, Robson C, *et al.* Huntingtin interacting protein 1 modulates the transcriptional activity of nuclear hormone receptors. *J Cell Biol* 2005;170:191-200

Molteni CG, Cazzaniga G, Condorelli DF, *et al.* Successful application of OPLS-DA for the discrimination of wild-type and mutated cells in acute lymphoblastic leukemia. *QSAR Comb Sci* 2009;28:822-828

Monroe JG. Ligand-independent tonic signaling in B-cell receptor function. *Curr Opin Immunol* 2004;16:288-295

Monroe JG. ITAM-mediated tonic signalling through pre-BCR and BCR complexes. *Nat Rev Immunol* 2006;6:283-294

Montes-Moreno S, Roncador G, Maestre L, *et al.* Gcet1 (centerin), a highly restricted marker for a subset of germinal center-derived lymphomas. *Blood* 2008;111:351-358

Montoto S, Davies AJ, Matthews J, *et al.* Risk and clinical implications of transformation of follicular lymphoma to diffuse large B-cell lymphoma. *J Clin Oncol* 2007;25:2426-2433

Morin RD, Johnson NA, Severson TM, *et al.* Somatic mutations altering EZH2 (Tyr641) in follicular and diffuse large B-cell lymphomas of germinal-center origin. *Nat Genet* 2010;42:181-185

Mosesson Y, Mills GB, Yarden Y. Derailed endocytosis: an emerging feature of cancer. *Nat Rev Cancer* 2008;8:835-850

Mosolits S, Harmenberg U, Rudén U, *et al.* Autoantibodies against the tumour-associated antigen GA733-2 in patients with colorectal carcinoma. *Cancer Immunol Immunother* 1999;47:315-320

Mounier N, Briere J, Gisselbrecht C, *et al.* Rituximab plus CHOP (R-CHOP) overcomes bcl-2-associated resistance to chemotherapy in elderly patients with diffuse large B-cell lymphoma (DLBCL). *Blood* 2003;101:4279-4284

Mourtada-Maarabouni M, Keen J, Clark J, *et al.* Candidate tumor suppressor LUCA-15/RBM5/H37 modulates expression of apoptosis and cell cycle genes. *Exp Cell Res* 2006;312:1745-1752

Mukoyama M, Nakao K, Saito Y, *et al.* Increased human brain natriuretic peptide in congestive heart failure. *N Engl J Med* 1990;323:757-758

Mullighan CG, Phillips LA, Su X, *et al.* Genomic analysis of the clonal origins of relapsed acute lymphoblastic leukemia. *Science* 2008;322;1377-1380

Muto A, Hoshino H, Madisen L, *et al.* Identification of Bach2 as a B-cell-specific partner for small maf proteins that negatively regulate the immunoglobulin heavy chain gene 3' enhancer. *EMBO J* 1998;17;5734-5743

Muzio M, Scielzo C, Frenquelli M, *et al.* HS1 complexes with cytoskeleton adapters in normal and malignant chronic lymphocytic leukemia B cells. *Leukemia* 2007;21:2067-2070

Nairn AV, Kinoshita-Toyoda A, Toyoda H, *et al.* Glycomics of proteoglycan biosynthesis in murine embryonic stem cell differentiation. *J Proteome Res* 2007;6;4374-4387

Nam MJ, Madoz-Gurpide J, Wang H, *et al.* Molecular profiling of the immune response in colon cancer using protein microarrays: occurrence of autoantibodies to ubiquitin C-terminal hydrolase L3. *Proteomics* 2003;3:2108-2115

Neben K, Tews B, Wrobel G, *et al.* Gene expression patterns in acute myeloid leukemia correlate with centrosome aberrations and numerical chromosome changes. *Oncogene* 2004;23:2379-2384

Newton K, Harris AW, Strasser A. FADD/MORT1 regulates the pre-TCR checkpoint and can function as a tumour suppressor. *EMBO J* 2000;19:931-941

Ngo VN, Davis RE, Lamy L, *et al.* A loss-of-function RNA interference screen for molecular targets in cancer. *Nature* 2006;441:106-110

Nilsson LM, Keller UB, Yang C, *et al.* Ink4c is dispensable for tumor suppression in Myc-induced B-cell lymphomagenesis. *Oncogene* 2007;26:2833-2839

Nyman H, Adde M, Karjalainen-Lindsberg ML, *et al.* Prognostic impact of immunohistochemically defined germinal center phenotype in diffuse large B-cell lymphoma patients treated with immunochemotherapy. *Blood* 2007;109:4930-4935.

Nyman H, Jerkeman M, Karjalainen-Lindsberg ML, *et al.* Prognostic impact of activated B-cell focused classification in diffuse large B-cell lymphoma patients treated with R-CHOP. *Mod Pathol* 2009;22:1094-1101

O'Connell BC, Cheung AF, Simkevich CP, *et al.* A large scale genetic analysis of c-Myc-regulated gene expression patterns. *J Biol Chem* 2003;278:12563-12573

O'Riain C, O'Shea DM, Yang Y, *et al.* Array-based DNA methylation profiling in follicular lymphoma. *Leukemia* 2009;23:1858-1866

Oh JJ, Razfar A, Delgado I, *et al.* 3p21. 3 tumor suppressor gene *H37/Luca15/RBM5* inhibits growth of human lung cancer cells through cell cycle arrest and apoptosis. *Cancer Res* 2006;66:3419-3427

Olejniczak SH, Stewart CC, Donohue K, Czuczman MS. A quantitative exploration of surface antigen expression in common B-cell malignancies using flow cytometry. *Immunol Invest* 2006;35:93-114

Oliver ER, Saunders TL, Tarlé SA, Glaser T. Ribosomal protein L24 defect in Belly spot and tail (*Bst*), a mouse *Minute*. *Development* 2004;131:3907-3920

Onabajo OO, Seeley MK, Kale A, *et al*. Actin-binding protein 1 regulates B cell receptor-mediated antigen processing and presentation in response to B cell receptor activation. *J Immunol* 2008;180:6685-6695

Oravecz-Wilson KI, Kiel MJ, Li L, *et al*. Huntingtin Interacting Protein 1 mutations lead to abnormal hematopoiesis, spinal defects and cataracts. *Hum Mol Genet* 2004;13:851-867

Oyake T, Itoh K, Motohashi H, *et al*. Bach proteins belong to a novel family of BTB-basic leucine zipper transcription factors that interact with MafK and regulate transcription through the NF-E2 site. *Mol Cell Biol* 1996;16;6083-6095

Oyarzo MP, Medeiros LJ, Atwell C, *et al*. c-FLIP confers resistance to FAS-mediated apoptosis in anaplastic large-cell lymphoma. *Blood* 2006;107:2544-2547

Pasqualucci L, Neumeister P, Goossens T, *et al*. Hypermutation of multiple proto-oncogenes in B-cell diffuse large-cell lymphomas. *Nature* 2001;412:341-346

Peculis BA, Reynolds K, Cleland M. Metal determines efficiency and substrate specificity of the nuclear NUDIX decapping proteins X29 and H29K (Nudt16). *J Biol Chem* 2007;282;24792-24805.

Peh SC, Shaminie J, Jayasurya P, *et al*. Spectrum of malignant lymphoma in Queen Elizabeth Hospital, Sabah. *Med J Malaysia* 2003;58:546-555

Pelengaris S, Khan M, Evan G. c-MYC: more than just a matter of life and death. *Nat Rev Cancer* 2002;2:764-776

Pezzolo A, Cinti R, Negri F, *et al*. Chromosomal imbalances in pediatric Burkitt-like lymphoma and review of the literature in relation to other germinal center derived B-cell tumors. *Leuk Lymphoma* 2006;47:2359-2364

Pfreundschuh M, Trumper L, Osterborg A, *et al*. CHOP-like chemotherapy plus rituximab versus CHOP-like chemotherapy alone in young patients with good-prognosis diffuse large-B-cell lymphoma: a randomized controlled trial by the MabThera International Trial (MInT) Group. *Lancet Oncol* 2006;7:379-391

Pike BL, Greiner TC, Wang X, *et al*. DNA methylation profiles in diffuse large B-cell lymphoma and their relationship to gene expression status. *Leukemia* 2008;22:1035-1043

Pole JC, Carmichael P, Griffin JL. Identification of transcriptional biomarkers induced by SERMS in human endometrial cells using multivariate analysis of DNA microarrays. *Biomarkers* 2004;9:447-460

Polson AG, Yu SF, Elkins K, *et al.* Antibody-drug conjugates targeted to CD79 for the treatment of non-Hodgkin lymphoma. *Blood* 2007;110:616-623

Porpaczy E, Bilban M, Heinze G, *et al.* Gene expression signature of chronic lymphocytic leukaemia with Trisomy 12. *Eur J Clin Invest* 2009;39:568-575

Poupon V, Girard M, Legendre-Guillemin V, *et al.* Clathrin light chains function in mannose phosphate receptor trafficking via regulation of actin assembly. *Proc Natl Acad Sci U S A* 2008;105:168-173

Praefcke GJK, McMahon HT. The dynamin superfamily: universal membrane tubulation and fission molecules? *Nat Rev Mol Cell Bio* 2004;5:133-147

Prasad R, Leshkowitz D, Gu Y, *et al.* Leucine-zipper dimerization motif encoded by the *AF17* gene fused to *ALL-1* (*MLL*) in acute leukemia. *Proc Natl Acad Sci U S A* 1994;91:8107-8111

Preuss KD, Zwick C, Bormann C, *et al.* Analysis of the B-cell repertoire against antigens expressed by human neoplasms. *Immunol Rev* 2002;188:43-50

Pulford K, Falini B, Banham AH, *et al.* Immune response to the ALK oncogenic tyrosine kinase in patients with anaplastic large-cell lymphoma. *Blood* 2000;96:1605-1607.

Pulford K, Roberton H, Banham AH, *et al.* Immunochemical studies of antigenic lymphoma-associated proteins. *Br J Haematol* 2002;116:135-141.

Quijano S, Lopez A, Rasillo A, *et al.* Impact of trisomy 12, del(13q), del(17p), and del(11q) on the immunophenotype, DNA ploidy status, and proliferative rate of leukemic B-cells in chronic lymphocytic leukemia. *Cytometry B Clin Cytom* 2008;74:139-149.

Rajewsky, K. Clonal selection and learning in the antibody system. *Nature* 1996;381:751-758

Rahmatpanah FB, Carstens S, Guo J, *et al.* Differential DNA methylation patterns of small B-cell lymphoma subclasses with different clinical behavior. *Leukemia* 2006;20:1855-1862

Rakhilin SV, Olson PA, Nishi A, *et al.* A network of control mediated by regulator of calcium/calmodulin-dependent signaling. *Science* 2004;306;698-701

Ramachandran N, Raphael JV, Hainsworth E, *et al.* Next-generation high-density self-assembling functional protein arrays. *Nat Methods* 2008;5:535-538

Ramaswamy S, Ross KN, Lander ES, Golub TR. A molecular signature of metastasis in primary solid tumors. *Nat Genet* 2003;33:49-54.

Rao DS, Chang JC, Kumar PD, *et al.* Huntingtin interacting protein 1 Is a clathrin coat binding protein required for differentiation of late spermatogenic progenitors. *Mol Cell Biol* 2001;21:7796-7806

Rao DS, Hyun TS, Kumar PD, *et al.* Huntingtin-interacting protein 1 is overexpressed in prostate and colon cancer and is critical for cellular survival. *J Clin Invest* 2002;110:351-360

Raval A, Tanner SM, Byrd JC, *et al.* Downregulation of *Death-Associated Protein Kinase 1* (*DAPK1*) in chronic lymphocytic leukemia. *Cell* 2007;129;879-890

Regev A, Berho M, Jeffers LJ, *et al.* Sampling error and intraobserver variation in liver biopsy in patients with chronic HCV infection. *Am J Gastroenterol* 2002;97:2614-2618

Renthal W, Maze I, Krishnan V, *et al.* Histone deacetylase 5 epigenetically controls behavioral adaptations to chronic emotional stimuli. *Neuron* 2007;56;517-529

Repass SL, Brady RJ, O'Halloran TJ. Dictyostelium Hip1r contributes to spore shape and requires epsin for phosphorylation and localization. *J Cell Sci* 2007;120:3977-3988

Rhodes DR, Yu J, Shanker K, *et al.* ONCOMINE: a cancer microarray database and integrated data-mining platform. *Neoplasia* 2004;6:1-6

Ries LAG, Eisner MP, Kosary CL, *et al.* (eds.) SEER Cancer Statistics Review, 1973-2000. Bethesda, MD: National Cancer Institute, 2003

Rimsza LM, Roberts RA, Miller TP, *et al.* Loss of MHC class II gene and protein expression in diffuse large B-cell lymphoma is related to decreased tumor immunosurveillance and poor patient survival regardless of other prognostic factors: a follow-up study from the Leukemia and Lymphoma Molecular Profiling Project. *Blood* 2004;103:4251-4258

Robinson WH, Fontoura P, Lee BJ, *et al.* Protein microarrays guide tolerizing DNA vaccine treatment of autoimmune encephalomyelitis. *Nat Biotechnol* 2003;21:1033-1039

Rolli V, Gallwitz M, Wossning T, *et al.* Amplification of B cell antigen receptor signaling by a Syk/ITAM positive feedback loop. *Mol Cell* 2002;10:1057-1069

Ropero S, Setien F, Espada J, *et al.* Epigenetic loss of the familial tumor-suppressor gene exostosin-1 (EXT1) disrupts heparan sulfate synthesis in cancer cells. *Hum Mol Genet* 2004;13;2753-2765

Rosenwald A, Wright G, Chan WC, *et al.* The use of molecular profiling to predict survival after chemotherapy for diffuse large-B-cell lymphoma. *New Engl J Med* 2002;346:1937-1947

Rosenwald A, Staudt L. Gene expression profiling of diffuse large B-cell lymphoma. *Leuk Lymp* 2003;44:S41–47.

Ross ME, Zhou X, Song G, *et al.* Classification of pediatric acute lymphoblastic leukemia by gene expression profiling. *Blood* 2003;102:2951-2959

Roth J, Dittmer D, Rea D, *et al.* p53 as a target for cancer vaccines: recombinant canarypox virus vectors expressing p53 protect mice against lethal tumor cell challenge. *Proc Natl Acad Sci U S A* 1996;93:4781-4786.

Rowley JD. Chromosome studies in the non-Hodgkin's lymphomas: the role of the 14;18 translocation. *J Clin Oncol* 1988;6:919-925

Sabatini DM. mTOR and cancer: insights into a complex relationship. *Nat Rev Cancer* 2006;6:729-734

Sahin U, Türeci O, Schmitt H, *et al.* Human neoplasms elicit multiple specific immune responses in the autologous host. *Proc Natl Acad Sci U S A.* 1995;92:11810-11813

Saito M, Gao J, Basso K, *et al.* A signaling pathway mediating downregulation of BCL6 in germinal center B cells is blocked by BCL6 gene alterations in B cell lymphoma. *Cancer Cell* 2007;12:280-292

Sanij E, Poortinga G, Sharkey K, *et al.* UBF levels determine the number of active ribosomal RNA genes in mammals. *J Cell Biol* 2008;183:1259-1274

Santos-Rosa H, Schneider R, Bannister AJ, *et al.* Active genes are tri-methylated at K4 of histone H3. *Nature* 2002;419:407-411

Sarbassov DD, Ali SM, Sabatini DM. Growing roles for the mTOR pathway. *Curr Opin Cell Biol* 2005;17:596-603

Sato S, Fujita N, Tsuruo T. Involvement of 3-phosphoinositide-dependent protein kinase-1 in the MEK/MAPK signal transduction pathway. *J Biol Chem* 2004;279:33759-33767

Satoh T, Takeuchi O, Vandenbon A, *et al.* The Jmjd3-*Irf4* axis regulates M2 macrophage polarization and host responses against helminth infection. *Nat Immunol.* 2010;11:936-944

Scanlan MJ, Welt S, Gordon CM, *et al.* Cancer-related serological recognition of human colon cancer: Identification of potential diagnostic and immunotherapeutic targets. *Cancer Res* 2002;62:4041-4047

Scheeren FA, Naspetti M, Diehl S, *et al.* STAT5 regulates the self-renewal capacity and differentiation of human memory B cells and controls Bcl-6 expression. *Nat Immunol.* 2005;6:303-313

Schmidt S, Rainer J, Riml S, *et al.* Identification of glucocorticoid-response genes in children with acute lymphoblastic leukemia. *Blood* 2006;107;2061-2069

Schuettengruber B, Chourrout D, Vervoort M, *et al.* Genome regulation by polycomb and trithorax proteins. *Cell* 2007;128:735-745

Sehn LH, Berry B, Chhanabhai M, *et al.* The revised International Prognostic Index (R-IPI) is a better predictor of outcome than the standard IPI for patients with diffuse large B-cell lymphoma treated with R-CHOP. *Blood* 2007;109:1857-1861

Seki N, Muramatsu M, Sugano S, *et al.* Cloning, expression analysis, and chromosomal localization of HIP1R, an isolog of huntingtin interacting protein (HIP1). *J Hum Genet* 1998;43:268-271

Senetar MA, Foster SJ, McCann RO. Intrasteric inhibition mediates the interaction of the I/LWEQ module proteins Talin1, Talin2, Hip1, and Hip12 with actin. *Biochemistry* 2004;43:15418-15428

Shaffer AL, Rosenwald A, Staudt LM. Lymphoid malignancies: the dark side of B-cell differentiation. *Nat Rev Immunol*. 2002;2:920-932

Shaffer AL, Shapiro-Shelef M, Iwakoshi NN, *et al*. XBP1, downstream of Blimp-1, expands the secretory apparatus and other organelles, and increases protein synthesis in plasma cell differentiation. *Immunity* 2004;21:81-93

Shaffer AL, Emre NC, Lamy L, *et al*. IRF4 addiction in multiple myeloma. *Nature* 2008;454:226-231

Shaffer AL, Emre NCT, Romesser PB, Staudt M. IRF4: Immunity.Malignancy! Therapy? *Clin Cancer Res* 2009;15:2954-2961.

Shapiro-Shelef M, Lin KI, McHeyzer-Williams LJ, *et al*. Blimp-1 is required for the formation of immunoglobulin secreting plasma cells and pre-plasma memory B cells. *Immunity* 2003;19:607-620

Shapiro-Shelef M, Calame K. Regulation of plasma-cell development. *Nat Rev Immunol* 2005;5:230-242

Sharma S, Orlowski G, Song W. Btk regulates B cell receptor-mediated antigen processing and presentation by controlling actin cytoskeleton dynamics in B cells. *J Immunol* 2009;182:329-339

Shi Y, Lan F, Matson C, *et al*. Histone demethylation mediated by the nuclear amine oxidase homolog LSD1. *Cell* 2004;119:941-953

Shi H, Guo J, Duff DJ, *et al*. Discovery of novel epigenetic markers in non-Hodgkin's lymphoma. *Carcinogenesis* 2007;28:60-70

Shiseki M, Nagashima M, Pedeux RM, *et al*. p29ING4 and p28ING5 bind to p53 and p300, and enhance p53 activity. *Cancer Res* 2003;63:2373-2378

Shu W, Lu MM, Zhang Y, *et al*. Foxp2 and Foxp1 cooperatively regulate lung and esophagus development. *Dev* 2007;134:1991-2000

Shustik J, Han G, Farinha P, *et al*. Correlations between BCL6 rearrangement and outcome in patients with diffuse large B-cell lymphoma treated with CHOP or R-CHOP. *Haematologica* 2010;95:96-101

Skommer J, Wlodkowic D, Pelkonen J. Gene-expression profiling during curcumin-induced apoptosis reveals downregulation of CXCR4. *Exp Hematol* 2007;35:84-95

Solal-Celigny P, Roy P, Colombat P, *et al*. Follicular lymphoma international prognostic index. *Blood* 2004;104:1258-1265

Stein H, Foss HD, Dırkop H, *et al*. CD30-positive anaplastic large cell lymphoma: a review of its pathological, genetic and clinical features. *Blood* 2000;96:3681-3695.

Stockert E, Jäger E, Chen YT, *et al.* A survey of the humoral immune response of cancer patients to a panel of human tumor antigens. *J Exp Med* 1998;187:1349-1354

Stoddart A, Dykstra ML, Brown BK, *et al.* Lipid rafts unite signaling cascades with clathrin to regulate BCR internalization. *Immunity* 2002;17:451-462

Stoddart A, Jackson AP, Brodsky FM. Plasticity of B cell receptor internalization upon conditional depletion of clathrin. *Mol Biol Cell* 2005;16:2339-2348

Storey, JD and Tibshirani, R. Statistical significance for genome wide studies. *Proc Natl Acad Sci U S A* 2003;100;9440-9445

Strahl BD, Allis CD. The language of covalent histone modifications. *Nature* 2000;403:41-45

Sukpanichnant S. Analysis of 1983 cases of malignant lymphoma in Thailand according to the World Health Organization Classification. *Hum Pathol* 2004;35:224-230

Suryani S, Fulcher DA, Santner-Nanan B, *et al.* Differential expression of CD21 identifies developmentally and functionally distinct subsets of human transitional B cells. *Blood* 2010;115:519-529

Sutherland LC, Lerman M, Williams GT, Miller BA. LUCA-15 suppresses CD95-mediated apoptosis in Jurkat T cells. *Oncogene* 2001;20:2713-2719

Taylor KH, Kramer RS, Davis JW, *et al.* Ultradeep bisulfite sequencing analysis of DNA methylation patterns in multiple gene promoters by 454 sequencing. *Cancer Res* 2007;67:8511-8518

The Non-Hodgkin's Lymphoma Classification Project. A clinical evaluation of the International Lymphoma Study Group classification of non-Hodgkin's lymphoma. *Blood* 1997;89:3909-3918

Tirosh B, Iwakoshi NN, Glimcher LH, Ploegh HL. XBP-1 specifically promotes IgM synthesis and secretion, but is dispensable for degradation of glycoproteins in primary B cells. *J Exp Med* 2005;202:505-516

Tommerup N, Vissing H. Isolation and fine mapping of 16 novel human zinc finger-encoding cDNAs identify putative candidate genes for developmental and malignant disorders. *Genomics* 1995;27:259-264

Torlakovic E, Torlakovic G, Nguyen PL, *et al.* The value of anti-pax-5 immunostaining in routinely fixed and paraffin-embedded sections: a novel pan pre-B and B-cell marker. *Am J Surg Pathol* 2002;26:1343-1350

Torres-Montaner A, Bolívar J, Astola A, *et al.* Immunohistochemical detection of ribosomal transcription factor UBF and AgNOR staining identify apoptotic events in neoplastic cells of Hodgkin's disease and in other lymphoid cells. *J Histochem Cytochem* 2000;48:1521-1530

Tourneur L, Buzyn A, Chiocchia G. FADD adaptor in cancer. *Med Immunol* 2005;4;1

Tracey L, Pérez-Rosado A, Artiga MJ, *et al*. Expression of the NF-κB targets BCL2 and BIRC5/Survivin characterizes small B-cell and aggressive B-cell lymphomas, respectively. *J Pathol* 2005;206:123-134

Truffinet V, Pinaud E, Cogne´ N, *et al*. The 3' *IgH* locus control region is sufficient to deregulate a *c-myc* transgene and promote mature B cell malignancies with a predominant Burkitt-like phenotype. *J Immunol* 2007;179;6033-6042.

Tsang JC, Lo YM. Circulating nucleic acids in plasma/serum. *Pathology* 2007;39:197-207

Tsutsumi S, Taketani T, Nishimura K, *et al*. Two distinct gene expression signatures in pediatric acute lymphoblastic leukemia with MLL rearrangements. *Cancer Res* 2003;63:4882-4887

Türeci O, Mack U, Luxemburger U, *et al*. Humoral immune responses of lung cancer patients against tumor antigen NY-ESO-1. *Cancer Lett* 2006;236:64-71

van Haaften G, Dalgliesh GL, Davies H, *et al*. Somatic mutations of the histone H3K27 demethylase gene UTX in human cancer. *Nat Genet* 2009;41:521-523

van Riggelen, Yetil A, Felsher DW. MYC as a regulator of ribosome biogenesis and protein synthesis. *Nat Rev Cancer* 2010;10:301-309

Velichutina I, Melnick A. Regulation of Hox genes by Polycomb group protein EZH2 plays a critical role in diffuse large B-cell lymphoma cells. *Blood* 2007;110:Abstract 1562

Vieira AV, Lamaze C, Schmid SL. Control of EGF receptor signaling by clathrin-mediated endocytosis. *Science* 1996;274:2086-2089

Villuendas R, Sánchez-Beato M, Martínez JC, *et al*. Loss of p16/INK4A protein expression in non-Hodgkin's lymphomas is a frequent finding associated with tumor progression. *Am J Pathol* 1998;153:887-897

Viré E, Brenner C, Deplus R, *et al*. The Polycomb group protein EZH2 directly controls DNA methylation. *Nature* 2006;439:871-874

Vissing H, Meyer WK, Aagaard L, *et al*. Repression of transcriptional activity by heterologous KRAB domains present in zinc finger proteins. *FEBS Lett* 1995;369:153-157

Völkel P, Angrand PO. The control of histone lysine methylation in epigenetic regulation. *Biochimie* 2007;89:1-20

Wang Y, Pennock S, Chen X, Wang Z. Endosomal signaling of EGF receptor stimulates signal transduction pathways leading to cell survival. *Mol Cell Biol* 2002;22:7279-7290

Wang B, Lin D, Li C, Tucker P. Multiple domains define the expression and regulatory properties of Foxp1 forkhead transcriptional repressors. *J Biol Chem* 2003;278:24259-24268

Wang X, Wang Q, Hu W, Evers BM. Regulation of phorbol estermediated TRAF1 induction in human colon cancer cells through a PKC/RAF/ERK/NF-κB-dependent pathway. *Oncogene* 2004;23:1885-1895

Wang X, Yu J, Sreekumar A, *et al.* Autoantibody signatures in prostate cancer. *New Engl J Med* 2005;353:1224-1235

Wang Y, Lian L, Golden JA, *et al.* PIP5KIγ is required for cardiovascular and neuronal development. *Proc Natl Acad Sci U S A* 2007;104;11748-11753

Wang D, Long J, Dai F, *et al.* BCL6 Represses Smad signaling in transforming growth factor-β resistance. *Cancer Res* 2008;68;783-789

Wang K, Xu X, Nie Y, *et al.* Identification of tumor-associated antigens by using SEREX in hepatocellular carcinoma. *Cancer Lett* 2009a;281:144-150

Wang K, Saito M, Bisikirska BC, *et al.* Genome-wide identification of post-translational modulators of transcription factor activity in human B cells. *Nat Biotechnol* 2009b;27:829-839

Wanker EE, Rovira C, Scherzinger E, *et al.* HIP-I: a huntingtin interacting protein isolated by the yeast two-hybrid system. *Hum Mol Genet* 1997;6:487-495

Ward RL, Hawkins NJ, Coomber D, Disis ML. Antibody immunity to the HER-2/neu oncogenic protein in patients with colorectal cancer. *Hum Immunol* 1999;60:510-515

Ward ES, Zhou J, Ghetie V, Ober RJ. Evidence to support the cellular mechanism involved in serum IgG homeostasis in humans. *Int Immunol* 2003;15:187-195

Watkins NA, Gusnanto A, de Bono B, *et al.* AHaemAtlas: characterizing gene expression in differentiated human blood cells. *Blood* 2009;113;e1-e9

Wedemeyer N, Peoples R, Himmelbauer H, *et al.* Localization of the human HIP1 gene close to the elastin (ELN) locus on 7q11.23. *Genomics* 1997;46:313-315

Welling DB, Lasak JM, Akhmametyeva E, *et al.* cDNA microarray analysis of vestibular schwannomas. *Otol Neurotol* 2002;23:736-748

Wells RA, Catzavelos C, Kamel-Reid S. Fusion of retinoic acid receptor α to NuMA, the nuclear mitotic apparatus protein, by a variant translocation in acute promyelocytic leukaemia. *Nat Genet* 1997;17:109-113

Westin JR, Fayad LE. Beyond R-CHOP and the IPI in large-cell lymphoma: molecular markers as an opportunity for stratification. *Curr Hematol Malig Rep* 2009;4:218-224

Westlake, S. Report: Cancer incidence and mortality in the United Kingdom and constituent countries, 2003-05. 2008;91-97. Available on the Office for National Statistics website at: http://www.statistics.gov.uk/downloads/theme_health/HSQ40CancerUK2003-05.pdf

Wilbur JD, Chen CY, Manalo V, *et al.* Actin binding by Hip1 (huntingtin-interacting protein 1) and Hip1R (Hip1-related protein) is regulated by clathrin light chain. *J Biol Chem* 2008;283:32870-32879

Woods D, Parry D, Cherwinski H, *et al.* Raf-1 induced proliferation or cell cycle arrest is determined by the level of Raf activity with arrest mediated by p21Cip1. *Mol Cell Biol* 1997;17:5598-5611

Wouters BJ, Jorda` MA, Keeshan K, *et al.* Distinct gene expression profiles of acute myeloid/T-lymphoid leukemia with silenced *CEBPA* and mutations in *NOTCH1*. *Blood* 2007;110;3706-3714

Wrench D, Montoto S, Fitzgibbon J. Molecular signatures in the diagnosis and management of follicular lymphoma. *Curr Opin Hematol* 2010;17:333-340

Wright G, Tan B, Rosenwald A, *et al.* A gene expression-based method to diagnose clinically distinct subgroups of diffuse large B cell lymphoma. *Proc Natl Acad Sci U S A* 2003;100:9991-9996

Wu X, Molinaro C, Johnson N, Casiano CA. Secondary necrosis is a source of proteolytically modified forms of specific intracellular autoantigens: implications for systemic autoimmunity. *Arthritis Rheum* 2001;44:2642-2652

Yamamoto A, Shimizu E, Ogura T, Sone S. Detection of auto-antibodies against L-myc oncogene products in sera from lung cancer patients. *Int J Cancer* 1996;69:283-289

Yang CH, Snyder M. The nuclear-mitotic apparatus protein is important in the establishment and maintenance of the bipolar mitotic spindle apparatus. *Mol Biol Cell* 1992;3:1259-1267

Yang L, Li N, Wang C, *et al.* Cyclin L2, a novel RNA polymerase II-associated cyclin, is involved in pre-mRNA splicing and induces apoptosis of human hepatocellular carcinoma cells. *J Biol Chem* 2004;279:11639-11648

Yang J, Epling-Burnette PK, Painter JS, *et al.* Antigen activation and impaired Fas-induced death-inducing signaling complex formation in T-large-granular lymphocyte leukemia. *Blood* 2008;111:1610-1616

Ye BH, Rao PH, Chaganti RS, Dalla-Favera R. Cloning of bcl-6, the locus involved in chromosome translocations affecting band 3q27 in B-cell lymphoma. *Cancer Res* 1993;53:2732-2735

Ye X, Li Y, Huang Q, *et al.* The novel human gene MIP functions as a co-activator of hMafF. *Arch Biochem Biphys* 2006;449;87-93

Yeoh EJ, Ross ME, Shurtleff SA, *et al.* Classification, subtype discovery, and prediction of outcome in pediatric acute lymphoblastic leukemia by gene expression profiling. *Cancer Cell* 2002;1:133-143

Yildirim M, Paydas S, Tanriverdi K, *et al.* Gravin gene expression in acute leukaemias: clinical importance and review of the literature. *Leuk Lymphoma* 2007;48:1167-1172

Young RM, Hardy IR, Clarke RL, *et al.* Mouse models of non-Hodgkin lymphoma reveal Syk as an important therapeutic target. *Blood* 2009;113:2508-2516

Zani VJ, Asou N, Jadayel D, *et al.* Molecular cloning of complex chromosomal translocation t(8;14;12)(q24.1;q32.3;q24.1) in a Burkitt lymphoma cell line defines a new gene (BCL7A) with homology to caldesmon. *Blood* 1996;87:3124-3134

Zappa M, Ciatto S, Bonardi R, Mazzotta A. Overdiagnosis of prostate carcinoma by screening: an estimate based on the results of the Florence Screening Pilot Study. *Ann Oncol* 1998;9:1297-1300

Zeller KI, Jegga AG, Aronow BJ, *et al.* An integrated database of genes responsive to the Myc oncogenic transcription factor: identification of direct genomic targets. *Genome Biol* 2003;4:R69

Zhang D, Tai YC, Wong CHS, *et al.* Molecular response of leukemia HL-60 cells to genistein treatment, a proteomics study. *Leukemia Res* 2007;31;75-82

Zhang Y, Li H, Wang X, *et al.* Regulation of T cell development and activation by creatine kinase B. *PLoS ONE* 2009;4;1-13

Zhang F, Frost AR, Blundell MP, *et al.* A ubiquitous chromatin opening element (UCOE) confers resistance to DNA methylation-mediated silencing of lentiviral vectors. *Mol Ther* 2010;18:1640-1649

Zheng B, Fuji RN, Elkins K, *et al.* In vivo effects of targeting CD79b with antibodies and antibody-drug conjugates. *Mol Cancer Ther* 2009;8:2937-2946

Zhou FL, Zhang WG, Chen G, *et al.* Serological identification and bioinformatics analysis of immunogenic antigens in multiple myeloma. *Cancer Immunol Immunother* 2006;55:910-917

APPENDIX

Supplementary Table 1

Brief descriptions of the 'short' list of 35 lymphoma-associated antigens

Availability of commercial antibodies: "Y" denotes availability of antibodies; "N" denotes unavailability of antibodies. For simplicity, HIP1R and JMJD3 are ranked on top of the table, and subsequent rows are arranged by antigen's name in alphabetical order.

Antigen	Literature		Availability of antibody
	General function or association with other diseases	Association with haematological malignancies	
HIP1R	A cytoskeletal protein that facilitates clathrin-mediated endocytosis, (Mosesson *et al.*, 2008) and clathrin is associated with B-cell receptor internalisation, influencing B-cell signaling (Stoddart *et al.*, 2005). Autoantibodies against HIP1R antigens in colon cancer (Scanlan *et al.*, 2002). Stabilise pools of receptor tyrosine kinase (Hyun *et al.*, 2004b).	One of 217 gene-expression based predictor of BL, discriminating BL from DLBCL (Dave *et al.*, 2006). Related HIP1 protein shares biological functions and might be a lymphoma oncogene (Bradley *et al.*, 2007). Overexpressed in E2A-PBX1^{+} ALL (Yeoh *et al.*, 2002; Ross *et al.*, 2003; Li *et al.*, 2009). Strongly overexpressed in CLL with trisomy 12 and used as a surrogate marker by PCR (Porpaczy *et al.*, 2009)	Y
JMJD3	A demethylase catalysing the demethylation of H3K27me3 (Agger *et al.*, 2007), a function that is essential for cellular differentiation. Highly induced in activated macrophages (De Santa *et al.*, 2007)	JMJD3 is induced upon activation of the RAS–RAF pathway and contributes to the transcriptional activation of *p16INK4A* and suggested to be downregulated in NHLs (Agger *et al.*, 2009). Loss of p16INK4A expression in NHLs is frequently associated with tumour progression (Villuendas *et al.*, 1998)	Y
ARPP-21	A cyclic AMP-regulated phosphoprotein, highly enriched in striatum (Ivkovic *et al.*, 1996) and regulates calmodulin signaling (Rakhilin *et al.*, 2004). Downregulated in transgenic mouse model of Huntington's disease (Bibb *et al.*, 2000)	Copy number abnormalities in B-ALL (Mullighan *et al.*, 2008), one of 3 downregulated genes in glucocorticoid-induced ALL apoptosis (Schmidt *et al.*, 2006), one of 6 predictor genes that identified AML with silenced *CEBPA* (Wouters *et al.*, 2007)	N
CCNL2	A member of the cyclin family that promotes mRNA splicing and induces apoptosis (Yang *et al.*, 2004). Its activity may be regulated via phosphorylation by DYRK1A (de Graaf *et al.*, 2004)	Expressed in diffuse histiocytic lymphoma (U-937) and BL (Daudi and NAMALWA) cell lines, and other leukaemia lines (Yang *et al.*, 2004)	Y

CDK2AP2	A cell cycle inhibitor, interacts with CDK2AP1 that might render the inhibitory effects of CDK2AP1 on CDK2, and suppression of DNA replication (Buajeeb *et al.*, 2004)	Downregulated in BL (Truffinet *et al.*, 2007)	N
CKB	A creatine kinase vital in energy homeostasis (Debrincat *et al.*, 2007). Essential in bone-resorbing function of osteoclasts and *Ckb*$^{-/-}$ mice is more resistant to bone loss (Chang *et al.*, 2008). Modulates TCR-mediated signalling and regulates T-cell activation and thymocyte selection (Zhang *et al.*, 2009)	Upregulated in nodal PTCL (Ballester *et al.*, 2006). Increased in sera of MDS and CML patients (Ishikawa *et al.*, 2005). CKB locus gain in BL and high hyperdiploid ALL harbouring 1q gains (Davidsson *et al.*, 2007)	N
CDKN2C	An inhibitor of cyclin-D-dependent kinases (Nilsson *et al.*, 2007)	Its locus is frequently deleted in MCL (Mestre-Escorihuela *et al.*, 2007) and MM (Leone *et al.*, 2008), a small number of *Cdkn2c*$^{-/-}$ knockout mice developed B-cell lymphoma (Latres *et al.*, 2000) and it is dispensable for tumour suppression in *Eμ-Myc* transgenic mice (Nilsson *et al.*, 2007)	Y
CREBBP	A well-documented molecule, widely-expressed and interacts with a vast number of transcription factors including those involved in haematopoiesis (reviewed by Blobel, 2002) and functions as tumour suppressor in cancers (reviewed by (Iyer *et al.*, 2004)	CREBBP heterozygotes show defects in haematopoiesis and develop haematological malignancies (Kung *et al.*, 2000). Involved in MLL translocation in AML (Camós *et al.*, 2006)	Y
DNM2	GTPAse involved in membrane trafficking at the plasma membrane, trans-Golgi network, and clathrin-mediated endocytosis (Praefcke and McMahon, 2004; Bitoun *et al.*, 2004; Bitoun *et al.*, 2009)	Overexpressed in a subgroup with better prognosis in ALL with *MLL* gene rearrangement (Tsutsumi *et al.*, 2003)	Y
EXT1	A glycosyltransferase required for heparan sulfate chain elongation (Busse *et al.*, 2007) and its mutation confers multiple exostoses (Francannet *et al.*, 2001), common benign skeletal deformities	Promoter hypermethylation in AML, ALL and APL (Ropero *et al.*, 2004)	Y
FADD	A well-documented, key adaptor molecule facilitating receptor-induced cell death (reviewed by Tourneur *et al.*, 2005)	Induces apoptosis in HL (Dutton *et al.*, 2004), B-cell NHL (Lajmanovich *et al.*, 2004), ALCL (Oyarzo *et al.*, 2006), T-cell large granular lymphocyte (LGL) leukaemia (Yang *et al.*, 2008)	Y

HDAC5	A class II histone deacetylase that co-represses transcription via binding of MEF-2 (Lemercier *et al.*, 2000), its overexpression induces apoptosis and inhibits tumour growth (Huang *et al.*, 2002), *Hdac5*$^{-/-}$ mice shows histone acetylation dysregulation and hyperadaptation to chronic stress (Renthal *et al.*, 2007)	BCL6 represses TGF-β signalling achieved partially via recruitment of HDAC5 and subsequent complex-formation in BL cell lines (Wang *et al.*, 2008)	Y
KLHL21	Unknown function, deregulated in mental retardation (MR) patients with KDM5C mutations (Jensen *et al.*, 2010). Candidate TSG in neuroblastoma (Fujita *et al.*, 2008). Other proteins of KLHL family participate in Dishevelled degradation (Angers *et al.*, 2006). and oligodendrocytes elongation (Jiang *et al.*, 2007). Increased expression in curcumin-treated FL cell line (Skommer *et al.*, 2007)		N
MAFF	A basic leucine zipper (bZIP) transcription factor but lacks transactivation domain and forms heterodimer with Bach2 (Oyake *et al.*, 1996) that subsequently negatively regulates immunoglobulin heavy chain gene (Muto *et al.*, 1998). Also binds US2-DNA element in the promoter of oxytocin receptor (OTR) gene (Ye *et al.*, 2006)	MAFF is a HIF-1α target gene, and recently HIF-1α expression was found to be a favourable prognostic factor for DLBCL patients treated with R-CHOP (Evens *et al.*, 2010)	Y
MLLT6	Belongs to a small group of evolutionary conserved, putative transcription factors (BRD1, BRPF1 and MLLT10) containing an N-terminal PHD domain (McCullagh *et al.*, 1999)	Translocated in AML with fusion partner gene AF17 (Prasad *et al.*, 1994) and frequently involved in myeloid leukaemia-associated rearrangements (Meyer *et al.*, 2009)	Y
NHN1	Also known as zinc finger CCCH-type containing 18 (ZC3H18), and little is known. Associated with PUF60 that promotes intron splicing. (Hastings *et al.*, 2007) Not implicated in haematological malignancies		N
NUDT16	A nucleotide diphosphatase required for 5'-cap removal of RNA before RNA degradation by exonuclease (Peculis *et al.*, 2007). Maintains chromosome stability and cell growth (Abolhassani *et al.*, 2010)	None documented	N
NUMA1	A microtubule-binding protein that regulates mitotic spindle organisation (Yang and Snyder, 1992; Gaglio *et al.*, 1995)	Translocated in APL forming *NUMA1-RARα* fusion gene (Wells *et al.*, 1997). Expressed at high levels in AML (Neben *et al.*, 2004)	Y
P28ING5	A member of the inhibitor of growth family and a putative TSG, especially in squamous cell carcinoma (Cengiz *et al.*, 2010; Li *et al.*, 2010). Binds to p53 and enhances	P28ING5 is associated with the MOZ-MORF complex, and MOZ and MORF are frequently translocated in AML (Doyon *et al.*, 2006)	Y

	its activity (Shiseki *et al*, 2003)		
PGLS	A phosphogluconolactonase catalysing oxidative branch of pentose-phosphate pathway that generates NADPH (Miclet *et al.*, 2001)	Downregulated in PCNSL (Li *et al.*, 2008), highly-expressed in HL-60 cells treated with genistein, a natural protein tyrosine kinase inhibitor (Zhang *et al.*, 2007)	Y
PIP5K1C	PIP kinase required for neuronal development (Wang *et al.*,2007), involved in cell adhesion (Ling *et al.*, 2002) and inositol phosphate metabolism (Loijens and Anderson, 1996)	None documented	Y
POLE	A polymerase vital in replication of DNA and cell viability (Fuss and Linn, 2001; Hübscher *et al.*, 2002)	None documented	Y
PRAF2	A novel protein involved in regulation of intracellular protein transport and putative functions in vesicular trafficking (Fo *et al.*, 2006). Highly-expressed in the brain and synaptic vesicles (Koomoa *et al.*, 2008)	Its mammalian relative PRAF3 is involved in differentiation of myeloid leukaemia cells (Huang *et al.*, 2006a; Huang *et al.*, 2006b)	N
RBM5	A candidate TSG implicated in various malignancies: fibrosarcoma, (Edamatsu *et al.*, 2000) lung cancer, (Oh *et al*, 2006) downregulated in schwannomas (Welling *et al.*, 2002) and metastasis in multiple solid tumour types (Ramaswamy *et al.*, 2003). Upregulates proapoptotic caspase 2 alternative splicing (Fushimi *et al.*, 2008)	Suppresses CD95-mediated apoptosis in Jurkat (T-cell leukaemia) cell line (Sutherland *et al.*, 2001). Regulates expression of cell cycle and apoptosis genes in CEM (T-cell leukaemia) cell line (Mourtada-Maarabouni *et al.*, 2006)	Y
RPL4	A ribosomal protein of the 60S subunit and has been used as housekeeping gene in qRT-PCR analysis (Nairn *et al.*, 2007; Raval *et al.*, 2007). Overexpression of rat rpL4 induces apoptosis (Kajikawa *et al.*, 1998)	Overexpressed in asparaginase-resistant ALL (Holleman *et al.* 2004). Interacts with EBNA3A in lymphoblastoid cells that may regulate apoptosis (Calderwood *et al.*, 2007)	Y
RPL24	A riboprotein vital in protein synthesis and regulation of cell cycle (Oliver *et al.*, 2004)	Loss of one *Rpl24* allele decreases lymphoma incidence and delays tumour onset in *Eμ-Myc* mice, and the effects of one *Rpl24* allele deletion on tumourigenesis is specific to MYC-driven lymphomagenesis (Barna *et al.*, 2008; van Riggelen *et al.*, 2010)	Y

SAP30BP	A co-repressor of transcription and induces cell death, also interacts with SAP complex via SAP30, a component of the HDAC complex (Li *et al.*, 2004)	HDAC associated with SAP complex could mediate repression via PLZF protein, and *PLZF* rearrangement is implicated in APL (David *et al.*, 1998)	N
SEPT5	A septin mainly expressed in the nervous system (Beites *et al.*, 1999) and involved in exocytosis modulated by Cdk5 phosphorylation (Amin *et al.*, 2008)	Involved in MLL translocation in AML (Megonigal *et al.*, 1998)	Y
SPAG7	A sperm-associated antigen that plays a functional role in cytoskeleton, and upregulated in patients with symptomatic parvovirus B19 infection (Kerr *et al.*, 2005). Highly-expressed in both cancer and normal prostate cells. (Cho-Vega *et al.*, 2005)	Underexpressed in MCL with *p53* genomic deletions but not with *p53* point mutations (Greiner *et al.*, 2006)	Y
UBTF	A ribosomal transcription factor involved in pol I transcriptional activation of rDNA (Jantzen *et al.*, 1990) into pre-rRNA and maintains the pool of active rRNA genes during differentiation (Sanij *et al.*, 2008)	Expression is absent in Hodgkin and Reed-Sternberg cells compared to small reactive lymphocytes (Torres-Montaner *et al.*, 2000)	Y
ZNF133	KRAB-zinc finger family protein with its KRAB domain reported to repress transcription (Vissing *et al.*,1995), and was upregulated by INFγ stimulation (Andersen *et al.*, 2003). Its zinc finger motif also repressed transcription by interacting with PIAS1 and this required histone deacetylase (HDAC) activity (Lee *et al.*, 2007)	Upregulated in CML (Li *et al.*, 2002)	Y
ZNF154	Isolated and chromosomally mapped by Tommerup and Vissing (1995), but little is documented thereafter. Induced in stromal cells treated with oestradiol, tamoxifen or raloxifene (Pole *et al.*, 2004). Predicted as one of 77 discriminator of wild-type and mutated PTPN11 and RAS B-cell ALL at mRNA levels (Molteni *et al.*, 2009)		N
ZNF579	Unknown function and not implicated in haematological malignancies. Based on Gene Ontology categorisation, it participates in zinc ion and DNA binding, and regulation of transcription (www.geneontology.org). It represented one of the BAC clones used to differentiate patients in the recurrence from non-recurrence group of estrogen receptor-positive breast cancer (Han *et al.*, 2006)		N

ZNF638	A nucleoplasmic protein that binds cytidine-rich sequences of double-stranded DNA (Inagaki *et al.*, 1996)	A SEREX-identified cutaneous T-cell lymphoma (CTCL) antigen (Eichmüller *et al.*, 2001). Expressed in DT40 cells, a chicken lymphoma cell line, but ZNF638 gene disruption does not impede the growth of DT40 cells (Matsushima *et al.*, 2000)	Y
ZNF768	Like several other Krüppel-type zinc finger family genes, the specific function of ZNF768 is little known and has not been implicated in haematological malignancies. One of several genes downregulated in ovarian cancer in response to chemotherapy (L'Espérance *et al.*, 2008) and identified as a colorectal cancer antigen (Kijanka *et al*, 2010)		N

Supplementary Table 2

Normal tissue-derived MTC™ cDNA Panel I and Panel II (Clontech, Takara BioEurope)

Tissue	Pooled from (number of individuals)	Age range	Gender
Heart	3	24-41	Male
Brain	8	43-65	Male
Placenta	11	19-39	Female
Lung	1	50	Male
Liver	1	35	Male
Skeletal muscle	4	18-42	Male
Kidney	4	28-48	Male/Female
Pancreas	15	22-69	Male/Female
Spleen	3	49-54	Male/Female
Thymus	9	20-40	Male/Female
Prostate	98	15-70	Male
Testis	45	14-64	Male
Ovary	15	20-60	Female
Small intestine	32	15-57	Male/Female
Colon	5	27-61	Male/Female
Leukocytes	550	18-40	Male/Female